This is to certify that the
dissertation entitled

SYNTHESIS OF AROMATICS AND HYDROAROMATICS FROM D-GLUCOSE VIA A NATIVE AND A VARIANT OF THE SHIKIMATE PATHWAY

presented by

NINGQING RAN

has been accepted towards fulfillment
of the requirements for the

Ph.D. degree in CHEMISTRY

John W. Frost
Major Professor's Signature

8/20/04
Date

SYNTHESIS OF AROMATICS AND HYDROAROMATICS FROM D-GLUCOSE VIA A NATIVE AND A VARIANT OF THE SHIKIMATE PATHWAY

By

Ningqing Ran

A DISSERTATION

Submitted to
Michigan State University
in partial fulfillment of the requirements
for the degree of

DOCTOR OF PHILOSOPHY

Department of Chemistry

2004

ABSTRACT

SYNTHESIS OF AROMATICS AND HYDROAROMATICS FROM D-GLUCOSE VIA A NATIVE AND A VARIANT OF THE SHIKIMATE PATHWAY

By

Ningqing Ran

Microbial synthesis of aromatic chemicals from non-toxic D-glucose constitutes an intriguing alternative to current use of toxic benzene as a starting material. In addition, D-glucose is derived from renewable feedstocks such as starch and cellulose while benzene is derived from nonrenewable petroleum. As a case study of the challenges presented by the microbial toxicity of many aromatic chemicals, the synthesis of hydroquinone from D-glucose is examined. Construction and fermentor-controlled cultivation of an *Escherichia coli* catalyst is detailed for the conversion of D-glucose into the nontoxic hydroaromatic quinic acid via reduction of the shikimate pathway intermediate 3-dehydroquinic acid. Chemical oxidation of quinic acid in clarified, decolorized, ammonia-free culture supernatant then affords hydroquinone in high yield. By interfacing microbial synthesis with chemical synthesis, the toxicity of hydroquinone towards *E. coli* is circumvented.

Another value-added aromatic chemical that can be synthesized by way of the shikimate pathway is gallic acid. However, key aspects of the biosynthesis of gallic acid have not previously been elaborated. Gallic acid has been hypothesized to be derived via oxidation of 3-dehydroshikimic acid or alternatively, by hydroxylation of protocatechuic acid. 3-Dehydroshikimic acid is an intermediate in the shikimate pathway. Dehydration

of 3-dehydroshikimic acid leads to gallic acid. In this thesis, biosynthesis of gallic acid in *E. coli* is examined with chemically synthesized [5-^{18}O]-3-dehydroshikimic acid. Analysis by mass spectrometry of the ^{18}O labeling in gallic acid synthesized by *E. coli* from [5-^{18}O]-3-dehydroshikimic acid revealed full retention of the ^{18}O-labeling. These results suggest that oxidation of 3-dehydroshikimic acid is the primary biosynthetic route to gallic acid.

In addition to target-oriented biosynthesis of aromatics, a new strategy is examined to increase the concentration and yield of natural products biosynthesized via the shikimate pathway in *E. coli* by increasing phosphoenolpyruvate availability. A pyruvate-based shikimate pathway is created by the directed evolution of 2-keto-3-deoxy-6-phosphogalactonate (KDPGal) aldolase. The result is an enzyme that catalyzes the condensation of pyruvic acid with D-erythrose 4-phosphate to produce 3-deoxy-D-*arabino*-heptluosonic acid 7-phosphate (DAHP), which is the first committed intermediate in the shikimate pathway. By contrast, DAHP in the native shikimate pathway is formed by the condensation of phosphoenolpyruvate with D-erythrose 4-phosphate catalyzed by DAHP synthase. The ability of the created pyruvate-based shikimate pathway to support microbial growth and synthesize 3-dehydroshikimic acid is examined in *E. coli* constructs that lack phosphoenolpyruvate-based DAHP synthase activity.

To my parents,

for their love and support.

ACKNOWLEDGMENTS

It is with great pleasure that I take the opportunity to thank all the people that I am indebted to for their help. First and foremost, I want to thank my research advisor Prof. John Frost for his guidance and encouragement throughout the the course of my graduate career. His enthusiasm, intergral view on research and excellent writing skill have made a deep impression on me. I owe him lots of gratitute for showing me the way of research. In addition, I would like to thank the members of my graduate committee, Prof. Babak Borhan, Prof. John McCracken and Prof. Merlin Bruening for their intellectual input during the preparation of this dissertation.

I am grateful to Dr. Karen Draths for her inspiration, technique guidance and support to my research, particularly for the many stimulating and instructive discussions we had and for the arduous task of critic and proof reading of my dissertation. I also wish to thank all of the Frost group members, both past and present, Dr. Chad Hansen, Dr. Dave Knop, Dr. Spiros Kambourakis, Dr. Kai Li, Dr. Feng Tian, Dr. Jessica Barker, Dr. Sunil Chandran, Dr. Padmesh Venkitasubramanian, Dr. Jian Yi, Dr. Jiantao Guo, Dr. Wei Niu, Dr. Dongming Xie, Dr. Jihane Achkar, Dr. Mo Xian, Ms. Mapitso Molefe, Ms. Heather Stueben, Mr. Xiaofei Jia, Mr. Wensheng Li, Mr. Justus Jancauskas, Mr. Man-Kit Lau, Mr. Jingsong Yang and Mr. Kin Sing Lee for their assistant and friendship during the progression of this research.

This thesis is dedicated to my parents Quanyin Ran and Su Ye and my brother Ningyu Ran for their love and support.

TABLE OF CONTENTS

LIST OF TABLES

LIST OF FIGURES

LIST OF ABBREVIATIONS

Ac	acetyl
ADP	adenosine diphosphate
ATP	adenosine triphosphate
Ap	ampicillin
Ap^R	ampicillin resistance gene
bp	base pair
CA	chorismic acid
CIAP	calf intestinal alkaline phosphatase
Cm	chloramphenicol
Cm^R	chloramphenicol resistance gene
DAHP	3-deoxy-D-*arabino*-heptulosonic acid 7-phosphate
DCU	digital control unit
DEAD	diethyl azodicarboxylate
DEAE	diethylaminoethyl
DHQ	3-dehydroquinic acid
DHS	3-dehydroshikimic acid
D.O.	dissolved oxygen
DTT	dithiothreitol
E4P	D-erythrose 4-phosphate
EPSP	5-enolpyruvoylshikimate 3-phosphate
FBR	feedback resistant
GA	gallic acid
h	hour
HPLC	high pressure liquid chromatography

IPTG	isopropyl β-D-thiogalactopyranoside
Kan	kanamycin
Kan^R	kanamycin resistance gene
kb	kilobase
KDPG	2-keto-3-deoxy-6-phosphogluconate
KDPGal	2-keto-3-deoxy-6-phosphogalactonate
kg	kilogram
K_m	Michaelis constant
LB	Luria-Bertani
M	molar
M9	minimal salts
min	minute
mL	milliliter
μL	microliter
mM	millimolar
μM	micromolar
NAD	nicotinamide adenine dinucleotide, oxidized form
NADH	nicotinamide adenine dinucleotide, reduced form
NADP	nicotinamide adenine dinucleotide phosphate, oxidized form
NADPH	nicotinamide adenine dinucleotide phosphate, reduced form
NMR	nuclear magnetic resonance spectroscopy
OD	optical density
ORF	open reading frame
PCA	protocatechuic acid
PEP	phosphoenolpyruvic acid
PHB	*p*-hydroxybenzoic acid

PID	proportional-integral-derivative
PCR	polymerase chain reaction
Phe	L-phenylalanine
Pyr	pyruvate
Tyr	L-tyrosine
Trp	L-tryptophan
psi	pounds per square inch
PTS	phosphotransferase system
QA	quinic acid
rpm	rotations per minute
SA	shikimic acid
SDS	sodium dodecyl sulfate
S3P	shikimate 3-phosphate
Tc	tetracycline
TCA	tricarboxylic acid
TSP	sodium 3-(trimethylsilyl)propionate-*2,2,3,3-d*$_4$
TsOH	*p*-toluenesulfonic acid
UDP	Uridine 5'-diphosphate
UV	ultraviolet

CHAPTER ONE

Introduction

Today the chemical industry is dominated by technologies that rely on starting materials derived from petroleum and natural gas. The increasing scarcity and cost of petroleum and natural gas[1] are contributing to a growing interest in the use of renewable feedstocks to improve long-term sustainability. Carbohydrates such as D-glucose derived from plant-derived starch and cellulose represent a promising renewable starting material that could serve as an alternative to starting materials derived from fossil fuels. Consequently, biocatalysis has now emerged as a promising and fast-developing tool to harvest the energy and chemical building blocks locked in the carbon and oxygen atoms of carbohydrates.

Starch from corn serves as the primary feedstock for today's bioproducts industry.[2] The starch generated by corn wet milling is hydrolyzed to yield D-glucose that is then converted via microbial synthesis into products ranging from fuel ethanol to amino acids such as L-lysine as well as an emerging new product polylactide polymer. Cellulose is likely to serve as a valuable source of D-glucose in the future when cost-efficient depolymerization technology is available.[3] With the vast amount of carbon available from the glucose in cellulose, microbial synthesis holds great potential for the manufacturing of many new industrial chemicals.

In Chapter 2 of this dissertation, the synthesis of hydroquinone from D-glucose via a combination of microbial and chemical synthesis is described. Previous work in the Frost group explored microbial synthesis of quinic acid via the shikimate pathway in a

genetically modified *Escherichia coli* strain followed by chemical conversion of quinic acid to hydroquinone.[4] The overall yield of hydroquinone synthesized from D-glucose was 3%. Chapter 2 details the further improvement of microbial synthesis of quinic acid and the elaboration of a high-yielding chemical conversion of quinic acid into hydroquinone. Chapter 3 investigates the biosynthetic pathway responsible for the formation of gallic acid in *Escherichia coli.* This study begins with the chemical synthesis of [5-^{18}O]-3-dehydroshikimic acid. The ^{18}O labeling in gallic acid synthesized by *E. coli* from [5-^{18}O]-3-dehydroshikimic acid is then determined. Examination of the extent of ^{18}O labeling in product gallic acid excludes the involvement of protocatechuic acid as an intermediate and favors the direct oxidation of 3-dehydroshikimic acid as the primary biosynthetic route to gallic acid in *E. coli*. Chapter 4 presents the creation of a pyruvate-based shikimate pathway variant. In this novel shikimate pathway, the first catalytic step entails the condensation of pyruvate with D-erythrose 4-phosphate catalyzed by 2-keto-3-deoxy-6-phosphogalactonate (KDPGal) aldolase mutants created by directed evolution. By contrast, the first committed step in the native shikimate pathway is the condensation of phosphoenolpyruvate with D-erythrose 4-phosphate. The pyruvate-based shikimate pathway establishes a completely new strategy for increasing phosphoenolpyruvate availability in microbes.

Biosyntheses of value-added chemicals from D-glucose

Interestingly, only one hundred years ago biomass-derived carbohydrates played a significant role in the US economy. In the late 1800's, the largest selling chemicals were alcohols made from wood and grain, and the first man-made plastics, parkesine and

celluloid (cellulose nitrate), were derived from cellulose.[2,5] By the 1970's, hydrocarbon resources were established as the world's primary feedstock for chemical manufacture. In many cases, it is still more economical to produce chemicals from petroleum or natural gas than from plant-derived carbohydrates. Today the advances in biocatalysis and bioprocessing are beginning to make an impact on reducing the cost of producing industrial chemicals from renewable carbohydrates and making them more competitive with those products derived from petroleum (Figure 1).

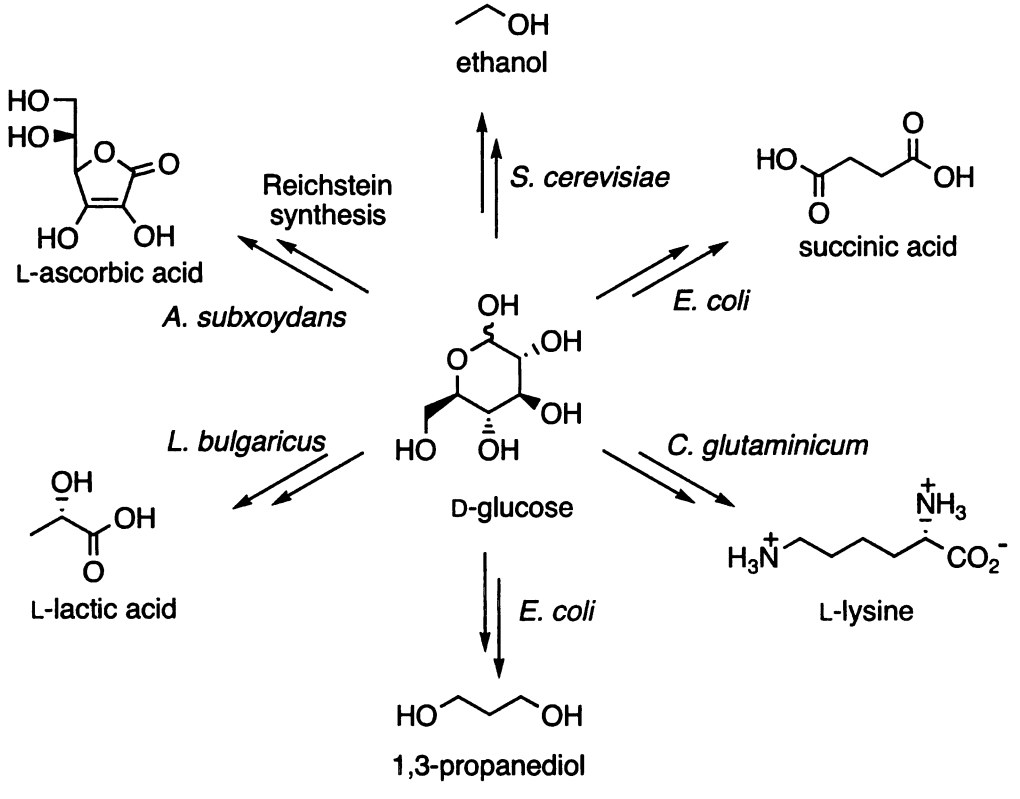

Figure 1. Selected fermentation products derived from D-glucose.

One example is the microbial synthesis of L-lactic acid from corn starch for use in production of polylactides. L-Lactic acid is primarily used as an acidulant in food and beverages, an electroplating bath additive, and a textile and leather additive.[6] It is estimated that 33×10^6 kg/year of L-lactic acid are used in the food industry alone. Homofermentative production of L-lactic acid by microbes like *Lactobacillus bulgaricus* is accomplished at titers of 100 g/L and in yields of 95% from starch by an enzymatic saccharification/fermentation process.[7] Polylactide is a biodegradable thermoplastic polymer produced from L-lactic acid through condensation and ring-opening polymerization performed using a solvent–free melt process.[8] Polylactides exhibit several desirable properties including high-stiffness, clarity and gloss, grease resistance and flavor barrier properties suitable for use in the packaging industry.[9] A joint venture between Cargill and Dow Chemical started up their first large-scale polylactide plant in Blair, Nebraska, with a 140×10^6 kg/year capacity.[10] Cargill Dow projects a possible market of 3.6×10^9 kg/year by 2020.[11] Ethyl lactate is another L-lactic acid derivative that has recently been commercialized. It's an environmentally benign solvent with properties superior to many conventional petroleum-based solvents. The use of ethyl lactate has been limited due to high production costs leading to high selling prices ($3.30~4.40/kg). Ethyl lactate is currently being used by Vertec Biosolvents Inc. in soy oil-solvent blends.[12] Acrylic acid, pyruvic acid, L-propylene glycol and 2,5-dimethyl-1,4-dioxane are other potential L-lactic acid derivatives which are currently produced from petroleum (Figure 2).[2]

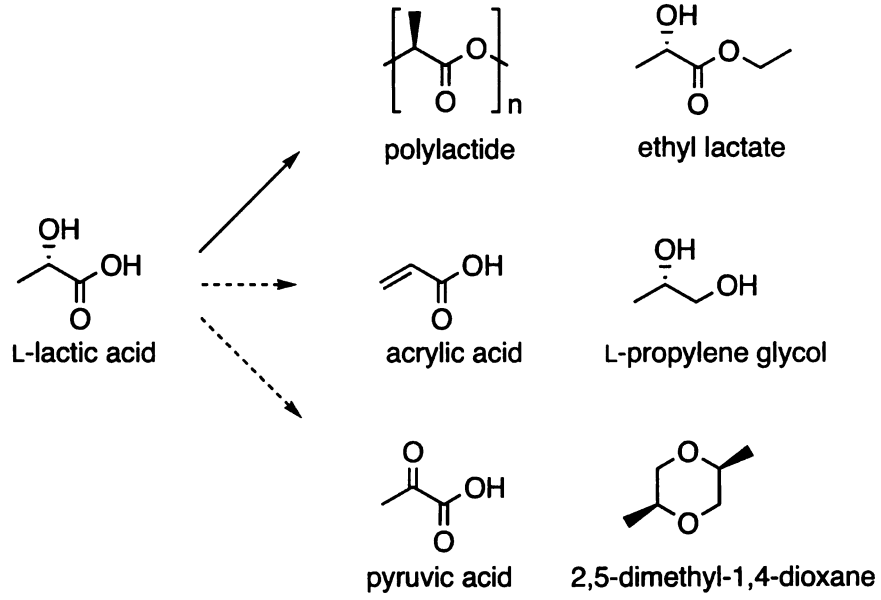

Figure 2. Commercially available and potential derivatives of L-lactic acid.

Recent advances in biotechnology also made an inroad in manufacturing of 1,3-propanediol. 1,3-Propanediol, together with terephthalic acid, is used to produce polytrimethylene terephthalate (PTT, Figure 3). PTT is a polymer with properties such as good resilience, stain resistance and low static generation relative to its competitors PET (polyethylene terephthalate) and nylon in fiber and textile applications. PTT is currently manufactured by Shell Chemical and Dupont. Shell developed a petrochemical route to 1,3-propanediol by the reaction of ethylene oxide with carbon monoxide and hydrogen.[13] Dupont currently makes 1,3-propanediol from propylene via acrolein. Genecor International and Dupont have been collaborating to develop the metabolic pathway in *E. coli* to produce 1,3-propanediol from D-glucose at a lower cost. In 2002, a pilot-scale 1,3-propanediol operation was built in Decatur, Illinois.[14] It is estimated that 1,3-propanediol has a potential 2020 market of 220×10^6 kg.

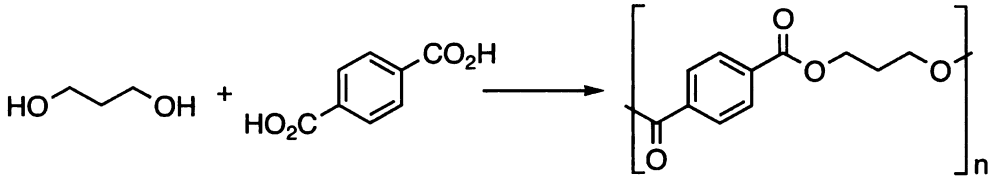

Figure 3. Synthesis of polytrimethylene terephthalate.

Succinic acid, with an annual production at 15×10^6 kg, is used as a surfactant and ion chelator in electropolating, food and pharmaceuticals. Industrial succinic acid is currently produced from butane via intermediacy of maleic anhydride.[15] Food-grade succinic acid could be produced through fermentation of glucose. Over the past 5-10 years, advances in fermentation and especially separation technology have reduced the potential production cost of microbial synthesized succinic acid from \$3.30 - \$4.40/kg in 1992 to about \$1.10/kg today. Further advances could significant reduce the cost of the bio-based succinic acid that would expend the current market and open up new applications. Succinic acid forms a platform from which many chemicals can be produced. Routes from succinic acid to chemicals including tetrahydrofuran (THF), 1,4-butanediol, γ-butyrolactone and succinate salts are nearly cost-competitive with their fossil fuel-based counterparts. Current production of 1,4-butanediol is based on the Reppe process in which acetylene is reacted with formaldehyde to butynediol followed by catalytic hydrogenation to 1,4-butanediol.[16] It can also be produced via acetoxylation of butadiene or hydroformation of allyl alcohol.[16] THF is an important solvent and is also used in the manufacture of polytetramethylene glycol. It is currently manufactured by the cyclodehydration of 1,4-butanediol and accounts for 48% of total 1,4-butanediol consumption.

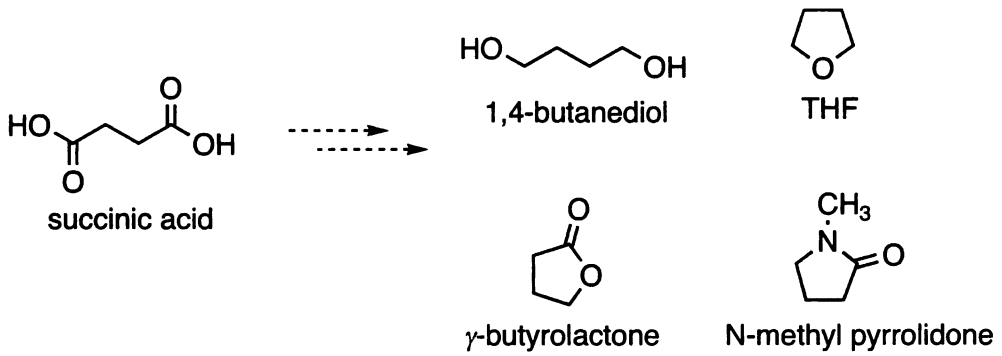

Figure 4. Potential derivatives of succinic acid.

Amino acids. Microbial production of amino acids has long been exploited in industry. The largest volume amino acids produced are L-glutamate, L-lysine and D,L-methionine. For instance, about 1×10^9 kg of L-glutamate are produced annually as a flavoring agent, and more than 4.4×10^8 kg/year of L-lysine are produced worldwide which is mainly used as an animal feed additive.[17] Both L-glutamate and L-lysine are produced industrially using *Corynebacterium glutamicum*, which is a L-glutamate accumulating soil bacterium discovered in 1957, from molasses (cane or sugar-beet) or starch hydrosylates. Microbe-synthesized L-lysine can reach a titer of 170 g/L with 54% yield based on carbohydrate starting material.[17]

Compared to the bulk production of L-glutamate and L-lysine, the aromatic amino acids L-phenylalanine, L-tyrosine and L-tryptophan are produced at significantly smaller volumes. L-Phenylalanine is produced predominantly for the production of the low-calorie sweeter aspartame using the NutraSweet process.[18] The worldwide production for L-phenylalanine is 1.2×10^7 kg/year. Fermentation processes for L-phenylalanine synthesis have been developed for genetically engineered strains of *C. glutamicum*,

Brevibacterium lactofermentum, *Bacillus sublitis* and *E. coli*.[19,20] L-Tyrosine is produced in an even smaller volume (1.5×10^5 kg/year) and is used for the production of the anti-Parkinson's drug L-DOPA and as a dietary supplement.[21] Microbial synthesis of L-tyrosine mainly employs strains of *E. coli, Bacillus substilis* or various forms of coryneform bacteria.[22] L-Tryptophan is produced at about 6×10^5 kg/year as a feed additive. Introduction of naphthalene dioxygenase into a tryptophan-synthesizing microbe that also expresses tryptophanase results in biocatalytic synthesis of indigo,[23] the vat dye that gives blue jeans the faded-blue coloration. Microbial engineering for production of L-tryptophan, has primarily been carried out in *E. coli*,[24] *Corynebacterium glutamicum*[25] and *Bacillus subtilis*.[26]

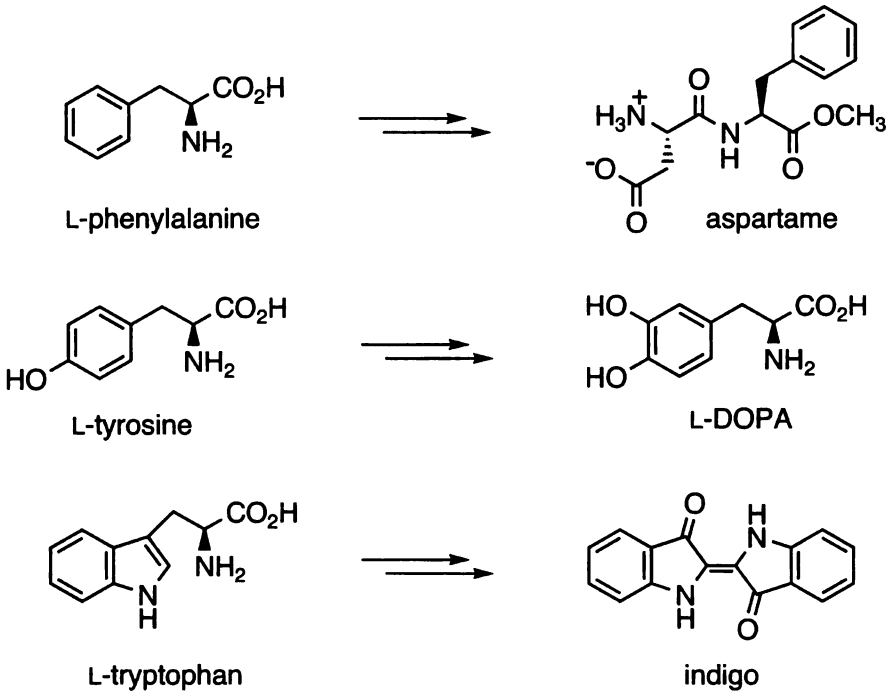

Figure 5. Chemicals synthesized from L-phenylalanine, L-tyrosine and L-tryptophan.

The shikimate pathway. The shikimate pathway, also referred to as the common pathway of aromatic amino acid biosynthesis, is essential for the transformation of simple carbohydrate precursors into the aromatic amino acids L-phenylalanine, L-tyrosine and L-tryptophan in plants, bacteria and fungi.[27] Mammals are incapable of *de novo* biosynthesis of aromatic amino acids. Therefore L-phenylalanine and L-tryptophan are essential components of animal diet, while animals can synthesize L-tyrosine in a single step from L-phenylalanine.

The substrates and products of the seven enzymatic reactions that convert phosphoenolpyruvate (PEP) and D-erythrose 4-phosphate (E4P) into chorismic acid (Figure 6) were identified by the early 1960's from studies of auxotrophs of *Escherichia coli* and *Klebsiella aerogenes*. The first committed step catalyzed by DAHP synthase involves condensation of PEP and E4P to form 3-deoxy-D-*arabino*-heptulosonic acid 7-phosphate (DAHP). Three isozymes of DAHP synthase exist in *E. coli*, each of which is sensitive to feedback inhibition by one of the three aromatic amino acids. The genes *aroF*, *aroG* and *aroH* encode for L-tyrosine-sensitive, L-phenylalanine-sensitive, and L-tryptophan-sensitive isozymes of DAHP synthase, respectively. DAHP is converted into 3-dehydroquinic acid (DHQ) by DHQ synthase which is encoded by *aroB*[28] in a complex reaction involving an intramolecular oxidation-reduction at C-5 of DAHP with a very tightly bound NAD^+ cofactor, a *syn* elimination of phosphate, and an intramolecular cyclization.[29] A *syn* elimination of water from DHQ affords 3-dehydroshikimic acid (DHS).[30] This reaction is catalyzed by 3-dehydroquinate dehydratase, which is a type I enzyme encoded by *aroD*.

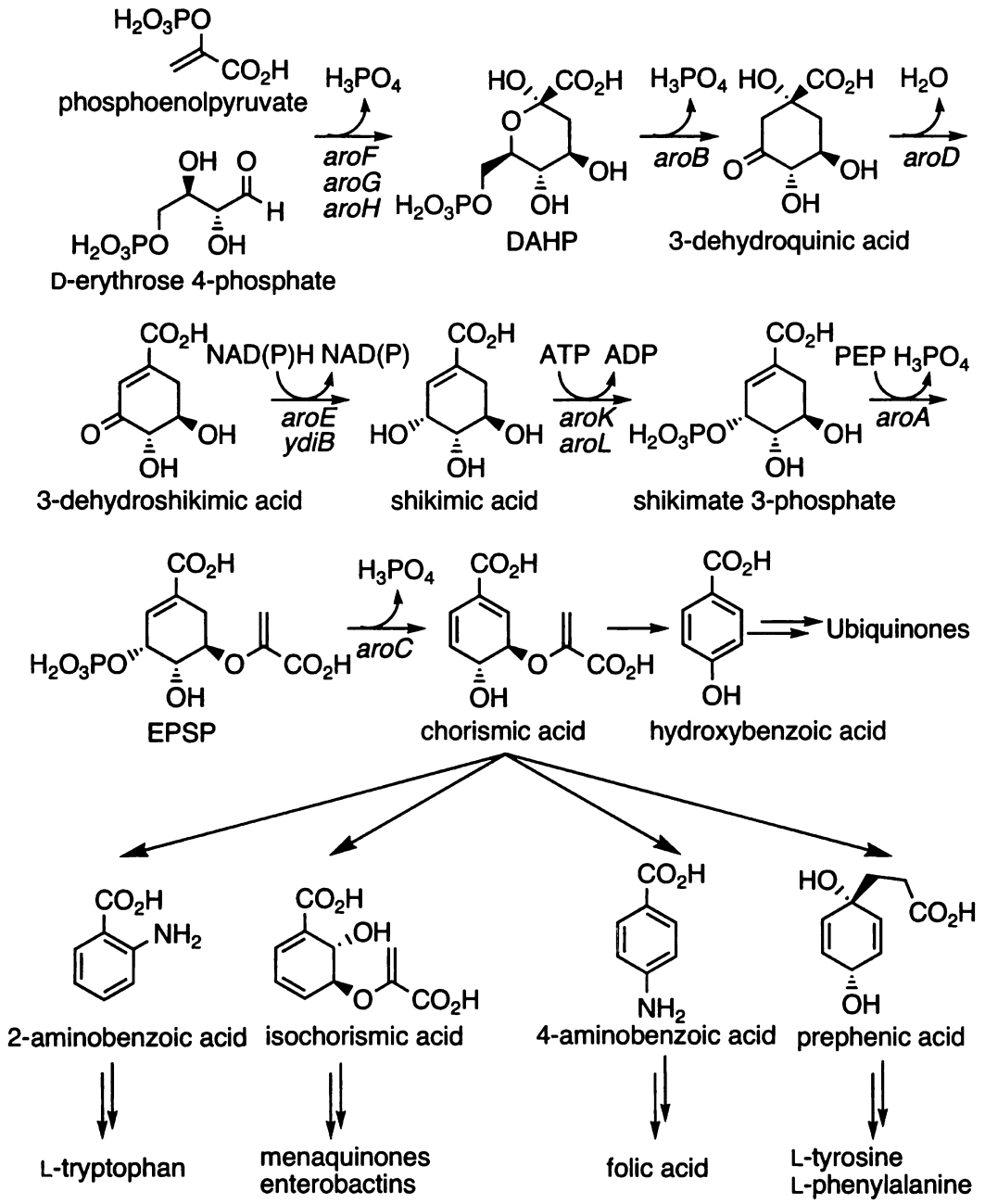

Figure 6. The common pathway of aromatic amino acid biosynthesis and pathways beyond chorismate. Intermediates (abbreviations): 3-deoxy-D-*arabino*-heptulosonic acid 7-phosphate (DAHP), 5-enolpyruvylshikimate-3-phosphate (EPSP). Genes, enzymes: *aroF*, DAHP synthase (tyrosine); *aroG*, DAHP synthase (phenylalanine); *aroH*, DAHP synthase (tryptophan); *aroB*, DHQ synthase; *aroD*, DHQ dehydratase; *aroE*, shikimate dehydrogenase; *ydiB*, shikimate dehydrogenase; *aroK*, shikimate kinase I; *aroL*, shikimate kinase II; *aroA*, EPSP synthase; *aroC*, chorismate synthase.

Reduction of 3-dehydroshikimic acid to shikimic acid in the presence of NADPH is catalyzed by *aroE*-encoded shikimate dehydrogenase.[31] Recently, a NADH-dependent shikimate dehydrogenase isozyme YdiB[32] was identified in *E. coli*. Shikimic acid is further converted to shikimate 3-phosphate by phosphoryl group transfer from ATP catalyzed by shikimate kinase. *E. coli* K12 carries two isozymes of shikimate kinase encoded by the loci *aroL*[33] and *aroK*.[34] 5-Enolpyruvoylshikimate 3-phosphate (EPSP) synthase, encoded by *aroA*,[35] catalyzes the reversible formation of 5-enolpyruvoylshikimate 3-phosphate and inorganic phosphate from shikimate 3-phosphate and phosphoenolpyruvate. The last enzyme of the common pathway is chorismate synthase,[36] encoded by *aroC*. It catalyzes the concerted 1,4-*trans* elimination of phosphate from 5-enolpyruvylshikimate-3-phosphate to afford chorismic acid, the precursor for biosynthesis of three aromatic amino acids L-tryptophan, L-tyrosine, and L-phenylalanine (Figure 6). In addition, biosynthetic pathways leading to ubiquinone, folic acid and enterochelin also branch away from the common pathway at chorismic acid (Figure 6). Folic acid-derived coenzymes are frequently involved in the biosynthetic transfer of one carbon fragments, ubiquinones are involved in electron transport, and enterochelin is an iron chelator responsible for iron uptake in numerous microorganisms.

Regulation of the shikimate pathway in prokaryotes such as *E. coli* involves both feedback inhibition and transcriptional control. DAHP synthase isozymes are sensitive to feedback inhibition by the respective aromatic amino acids. Transcription of genes encoding the L-tyrosine-and L-phenylalanine-sensitive isozymes are regulated by the *tyrR* repressor and transcription of the L-tryptophan-sensitive isozyme is regulated by the *trpR* repressor.[37] Shikimate kinase may represent a secondary control in the shikimate

pathway. *E. coli* shikimate kinase encoded by *aroK* is synthesized constitutively, but the synthesis of the other shikimate kinase encode by *aroL,* which provides the major activity *in vivo,* is under control of the *tyrR* and *trpR* proteins.[37]

The essential role of the shikimate pathway in bacteria, plants, fungi and parasites but its absence in mammals makes the enzymes involved in this pathway appealing targets for the development of broad-spectrum antibiotic drugs and herbicides. The widely used herbicide glyphosate, marketed under the trade name Roundup®,[38] inhibits the sixth enzyme in the pathway, 5-enolpyruvylshikimate-3-phosphate (EPSP) synthase. In addition to herbicidal activity, glyphosate also displayed antiparasite activity towards apicomplexan parasites including *Toxoplasma gondii*, which causes toxoplasmosis.[39]

Biocatalytic syntheses of aromatics by manipulating the shikimate pathway. The shikimate pathway has provided convenient access to a variety of aromatic chemicals including catechol,[40] vanillin,[41] benzoquinone and hydroquinone,[42] gallic acid,[43] pyrogallol,[43] *p*-hydroxybenzoic acid,[44] and phenol[45] in addition to various non-aromatic compounds such as shikimic acid,[4] 3-dehydroshikimic acid,[46] quinic acid[4] and adipic acid.[47] The benzene-free synthesis of aromatic molecules from carbohydrates constitutes a different path from conventional organic synthesis used by the chemical industry. Use of non-toxic and non-volatile carbohydrate feedstocks avoids the health problems and expenses associated with the use of carcinogenic and volatile benzene and its derivatives.

Biocatalytic conversion of a shikimate pathway metabolite into an aromatic molecule represents a straightforward approach to harness the potential of this pathway. Examples include the microbial conversion of D-glucose into catechol, gallic acid,

pyrogallol, vanillic acid and *p*-hydroxybenzoic acid by a genetically-modified microbial host. 3-Dehydroshikimic acid serves as a branch point for the biosyntheses of these aromatics via the common pathway (Figure 7).

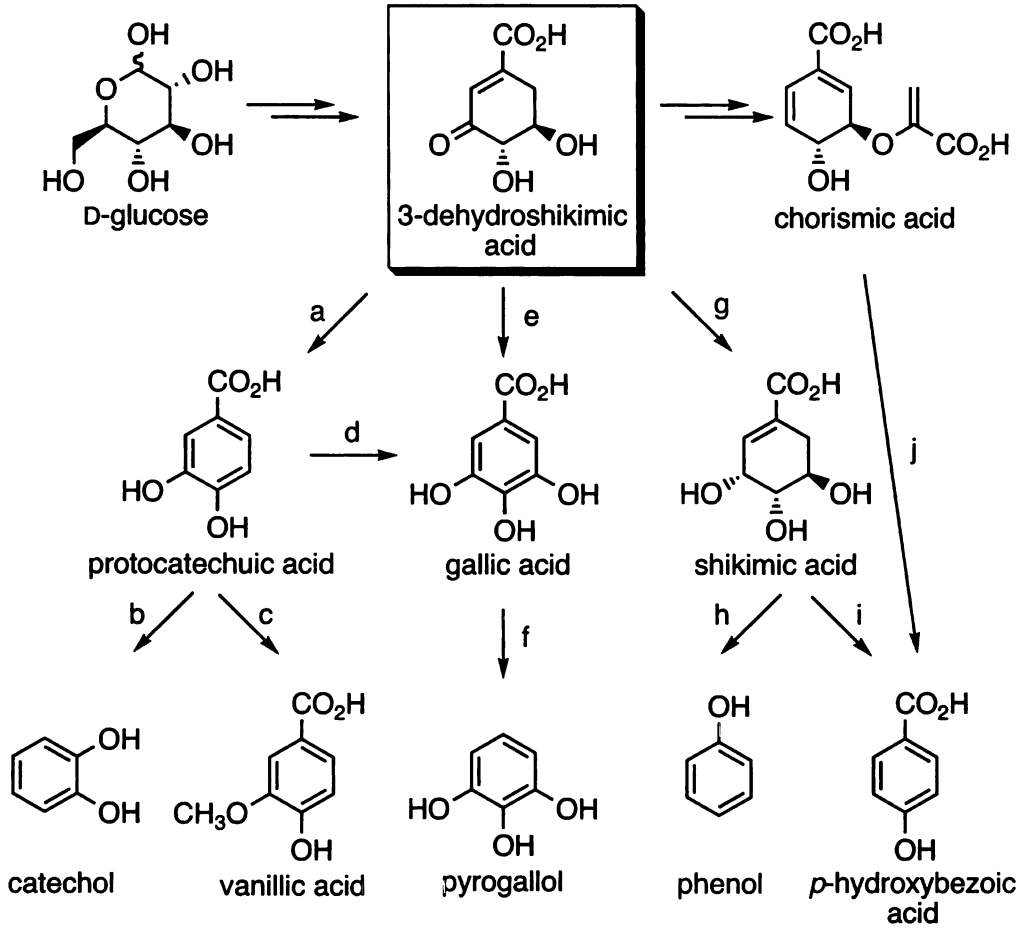

Figure 7. Value-added aromatic compounds synthesized from D-glucose via 3-dehydroshikimic acid intermediacy. Keys: (a) *aroZ*, 3-dehydroshikimate dehydratase; (b) *aroY*, protocatechuate decarboxylase; (c) (i) *COMT*, catechol-*O*-methyltransferase, (ii) aryl aldehyde dehydrogenase; (d) *pobA**, *p*-hydroxybenzoate hydroxylase; (e) O_2, Cu^{2+}, Zn^{2+}, AcOH; (f) *aroY*, PCA decarboxylase; (g) *aroE*, shikimate dehydrogenase; (h) H_2O, 350 °C; (i) 1 M H_2SO_4 in AcOH; (j) *ubiC*, chorismate-pyruvate lyase.

Li et al. developed *E. coli* KL3/pKL4.130B to convert D-glucose into 3-dehydroshikimic acid.[46] *E. coli* KL3 contains a mutation in the *aroE* gene encoding shikimate dehydrogenase, which renders *E. coli* KL3 incapable of converting 3-dehydroshikimic acid into shikimic acid. Enhancing the production of 3-dehydroshikimic acid requires transforming *E. coli* KL3 with a multicopy plasmid pKL*4*.130B containing $P_{aroF}aroF^{FBR}$, which encodes a feedback-insensitive isozyme of DAHP synthase, and a copy of *tktA*[48] to increase the activity of transketolase. Overexpression of $AroF^{FBR}$ and transketolase increase carbon flow into the shikimate pathway. *E. coli* KL3/pKL4.130B synthesized 69 g/L of 3-dehydroshikimic acid in 30% (mol/mol) yield from D-glucose under fed-batch fermentor conditions. The yield was further improved to 35% (mol/mol) by overexpression of a *ppsA*-encoded phosphoenolpyruvate synthase in a similar construct developed by Yi et al.[49]

Catechol and adipic acid. 3-Dehydroshikimic acid can be converted into catechol by introducing DHS dehydratase and PCA decarboxylase activities into a DHS-synthesizing strain. Catechol is an important chemical building block used in synthesis of a variety of flavors (vanillin, eugenol, isoeugenol), pharmaceuticals (L-DOPA, adrenaline, papaverine), agrochemicals (carbofuran, propoxur) and polymerization inhibitors and antioxidants (4-*tert*-butylcatechol, veratrol). Global production of catechol is estimated at 2.5×10^7 kg/year.[50] Most catechol production begins with Friedel-Crafts alkylation of benzene to afford cumene followed by Hock-type air oxidation of cumene to acetone and phenol (Figure 8). The phenol is then oxidized to a mixture of catechol and hydroquinone using 70% hydrogen peroxide either in the presence of transition metal catalysts or in formic acid solution where performic acid is the actual oxidant. Catechol

and hydroquinone are separated by distillation.[51] As an alternative to benzene as a starting material, D-glucose can be converted in an *aroE* auxotroph to 3-dehydroshikimic acid by plasmid-based expression of $AroF^{FBR}$, AroB, and TktA. A second plasmid incorporates a copy of *aroZ* and *aroY* isolated from *Klebsiella pneumoniae*. 3-Dehydroshikimic acid is aromatized to protocatechuic acid by *aroZ*-encoded 3-dehydroshikimic acid dehydratase, which then undergoes an enzymatic decarboxylation to catechol by the *aroY*-encoded PCA decarboxylase. Biocatalytic production with the pre-grown cells of AB2834/pKD136/pKD9.069A afforded catechol at concentrations of 2 g/L and 33% yield in minimal salts medium containing D-glucose.[40]

Although the toxicity of catechol towards *E. coli* hindered significant accumulation of catechol, inclusion of a *catA* encoding catechol 1,2-dioxygenase in the catechol producing strain converted catechol into *cis,cis*-muconic acid. The *catA*-encoded catechol 1,2-dioxygenase was isolated from *Acinetobacter calcoaceticus*.[52] Catalytic hydrogenation of *cis,cis*-muconic acid under mild conditions afforded adipic acid (Figure 8),[47a] a monomer for synthesis of nylon-6,6.[53] The global demand for adipic acid exceeds 1.9×10^9 kg/yr. Manufacture of adipic acid starts with hydrogenation of benzene to cyclohexane followed by air oxidation to cyclohexanol and cyclohexanone (Figure 8). Exhaustive oxidation of the cyclohexyl intermediates with 60 per cent nitric acid in the presence of copper and vanadium catalysts yields adipic acid.[53] Nitrous oxide is produced as a major byproduct of this process. Adipic acid production was estimated to account for 10% of the atmospheric nitrous oxide level which contributes to ozone depletion and global warming.[54] The process also requires use of elevated temperatures and pressures.

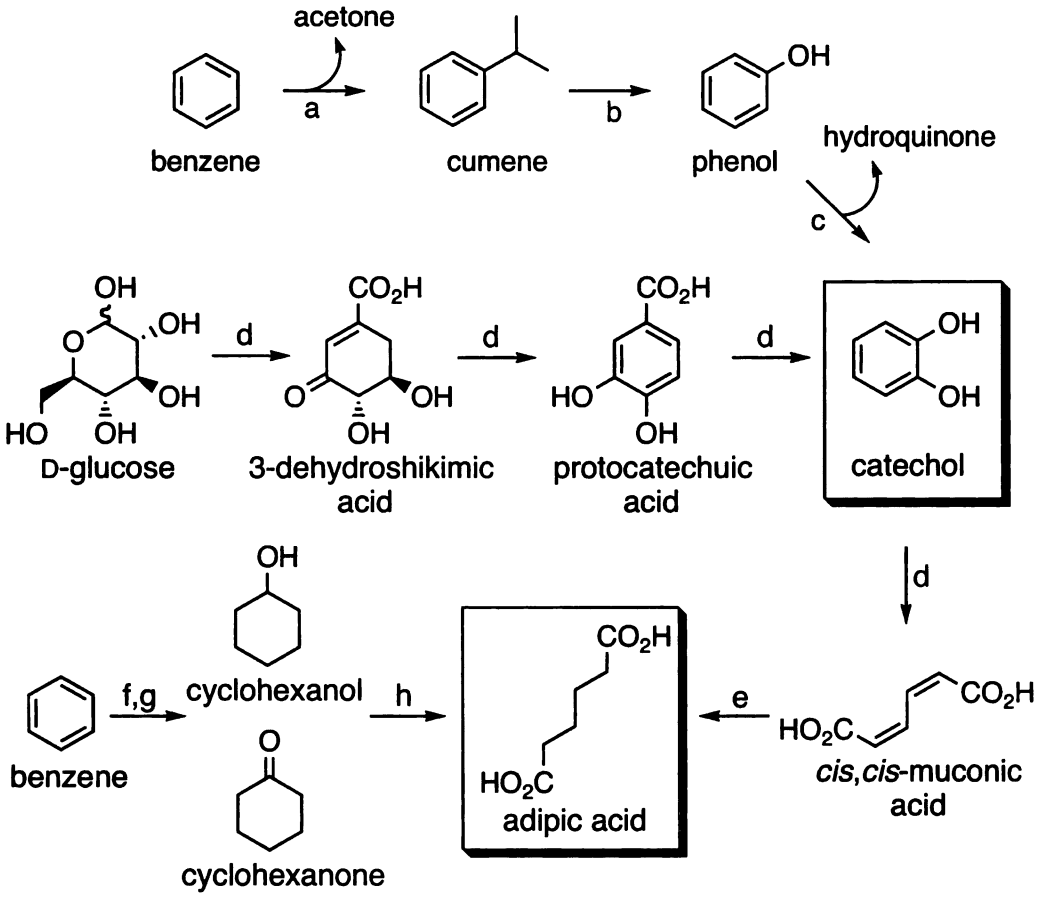

Figure 8. Conventional synthesis and biosynthesis of catechol and adipic acid. Keys: (a) propylene, 400-600 psi., solid H_3PO_4 catalyst, 200-260°C; (b) O_2, 80-130 °C, SO_2, 60-100 °C; (c) 70% H_2O_2, EDTA, Fe^{2+} or Co^{2+}, 70-80 °C; (d) *E. coli* WN1/pWN2.248; (e) H_2, 50 psi., 10% Pt/C; (f) Ni-Al_2O_3, H_2, 370-800 psi., 150-250 °C; (g) Co, O_2, 120-140 psi., 150-160 °C; (h) Cu, NH_4VO_3, 60% HNO_3, 60-80 °C.

The microbial-based route to adipic acid via catechol intermediacy has been improved from the previously reported synthesis under shake-flask conditions. The microbial synthesis utilized an *aroE* auxotroph *E. coli* WN1 expressing *aroZ*-encoded DHS dehydratase for the conversion of DHS to protocatechuic acid, *aroY*-encoded PCA decarboxylase for the conversion of PCA to catechol, and *catA*-encoded catechol 1,2-dioxygenase for the conversion of catechol to *cis,cis*-muconic acid. The construct *E. coli*

WN1/pWN2.248 synthesized 37 g/L *cis,cis*-muconic acid from D-glucose in 23% yield (mol/mol) (Figure 8). Hydrogenation of clarified cell broth with 10% Pt/C (5% mol/mol) and 50 psi H_2 afforded adipic acid in 97% yield from *cis,cis*-muconic acid. The interface of biocatalysis and catalytic hydrogenation allows adipic acid to be produced without formation of large amounts of nitrous oxide.

Vanillin. Vanillin is one of the most important aromatic flavor compounds used in the food and beverage industry and also finds use in formulations for perfumes.[55] Natural vanillin obtained from the vanilla beans of the orchid *Vanilla planifolia* accounts for only 2 x 10^4 kg/yr of the world's 1.2 x 10^7 kg/yr demand for vanillin.[56] The difference is made up by synthetic vanillin starting from petroleum-derived guaiacol. Condensation of guaiacol with glyoxylic acid affords mandelic acid (Figure 9). Oxidation of mandelic acid and subsequent decarboxylation results in vanillin. Synthetic vanillin sells for $12/kg while natural vanilla flavoring extracted from vanilla bean containing 2% vanillin sells for $30-120/kg.[57] The high price for natural vanilla flavoring reflects the labor-intensive cultivation, pollination, harvesting and curing of vanilla beans. The demand for natural flavorings has, in turn, prompted the development of biocatalytic routes to vanillin.

Biocatalytic conversion of D-glucose to vanillin passes through the intermediacy of 3-dehydroshikimic acid. Heterologous expression of the *aroZ* locus in *E. coli aroE* auxotroph KL7 leads to protocatechuic acid as previously discussed. Expression of rat-liver *COMT*-encoded catechol-*O*-methyltransferase in KL7 afforded 4.9 g/L of vanillic acid by fed-batch fermentation from D-glucose when the construct was supplemented with L-methionine (Figure 9). COMT catalyzes the methylation of protocatechuic acid to

a mixture of vanillic acid and isovanillic acid. The *in vitro* reduction of vanillic acid to vanillin was carried out by aryl aldehyde dehydrogenase purified from the fungus *Neurospora crassa* in 66% yield.[58] This two-step biocatalytic synthesis of vanillin is the only biocatalytic synthesis of vanillin using a carbohydrate as a starting material.[57]

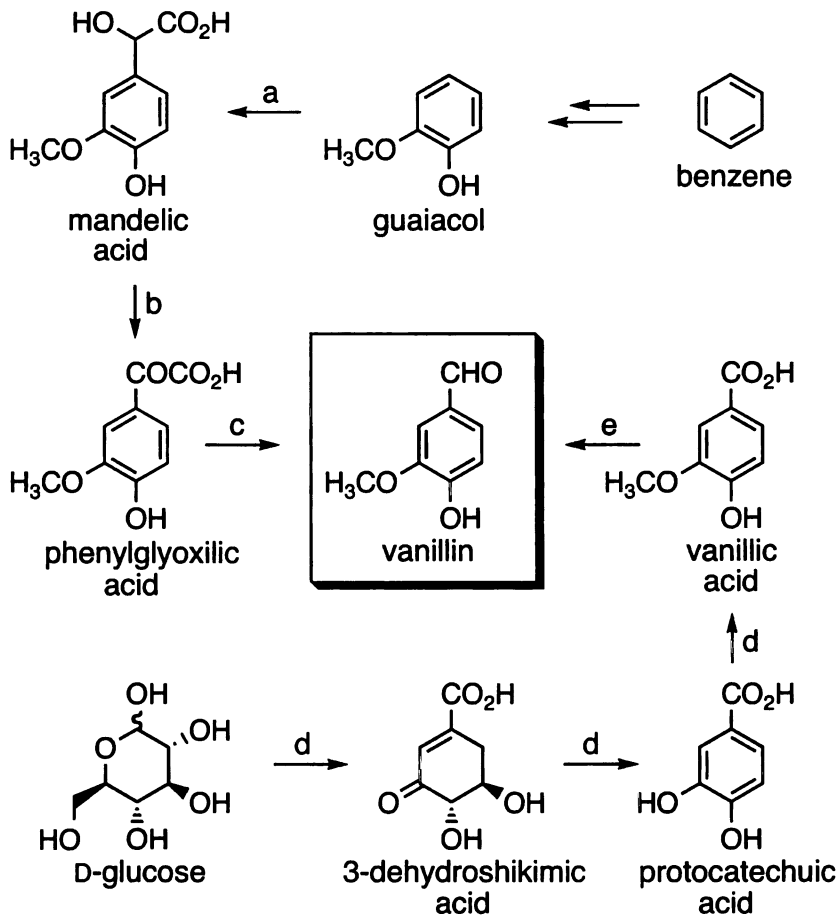

Figure 9. Synthesis of vanillin via benzene or D-glucose. Keys: (a) $HCOCO_2H$; (b) O_2; (c) H^+; (d) KL7/pKL5.26A; (e) *N. crassa* aryl aldehyde dehydrogenase.

***p*-Hydroxybenzoic acid.** *p*-Hydroxybenzoic acid is a component of liquid crystal polymers such as Xydar,[59] which have attracted considerable attention because of their

use in high-performance applications. Esters of *p*-hydroxybenzoic acid are also widely used as food preservatives.[60] *p*-Hydroxybenzoic acid is currently manufactured by Kolbe-Schmitt reaction of dried potassium phenoxide with 20 atm dry CO_2 at 180-250 °C. Product potassium *p*-hydroxybenzoate is converted to its free acid upon addition of mineral acid (Figure 11). Besides the required temperatures and pressures, *p*-hydroxybenzoic acid manufacture has to contend with handling of phenol which is a highly toxic, corrosive chemical.[61]

Chorismic acid can also be converted directly into *p*-hydroxybenzoic acid in a reaction catalyzed by *ubiC*-encoded[62] chorismate-pyruvate lyase. A genetically-modified *E. coli* biocatalyst that synthesizes elevated concentrations of chorismic acid and overexpresses the *ubiC*-encoded chorismate-pyruvate lyase afforded 12 g/L of *p*-hydroxybenzoic acid in 13% yield from glucose under fermentor-controlled conditions.[44]

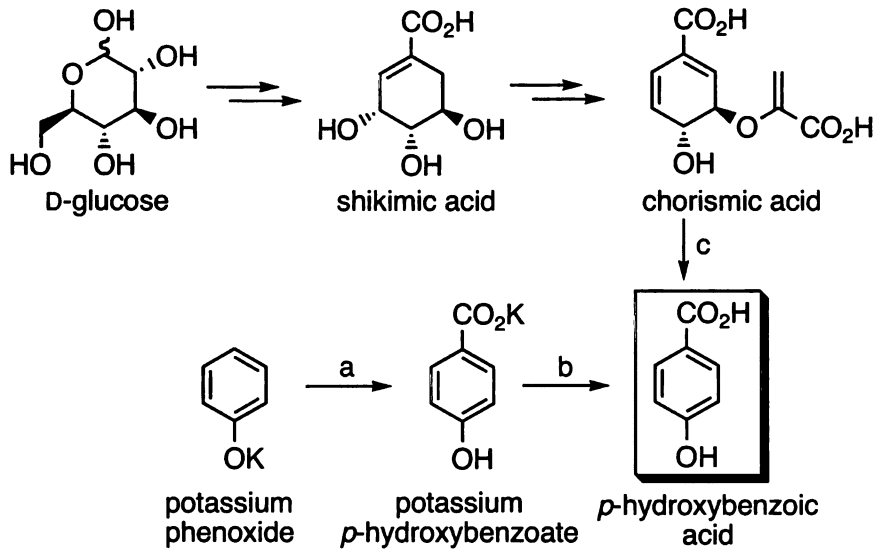

Figure 11. Synthesis of *p*-hydroxybenzoic acid from glucose and potassium phenoxide. Keys: (a) 20 atm CO_2, 180-250 °C; (b) H^+; (c) *ubiC*, chorismate-pyruvate lyase.

Gallic acid and pyrogallol. The biosynthesis of another molecule that stems from 3-dehydroshikimic acid is 3,4,5-trihydroxybenzoic acid, which is commonly known as gallic acid. This polyhydroxylated aromatic is currently isolated from gall nuts or from seed pods of *Coulteria tinctoria* trees found in Peru.[63] Thermal decarboxylation of gallic acid in copper autoclaves affords pyrogallol.[63] Two biocatalytic routes were developed with the aim to supplant isolation of gallic acid and pyrogallol from scarce natural resources. In one way, 3-dehydroshikimic acid in acetic acid solution can be oxidized by O_2 in the presence of catalytic amounts of Cu^{2+} and Zn^{2+} to afford gallic acid in 67% yield.[64] Alternatively, gallic acid can be obtained directly from D-glucose via protocatechuic acid intermediary (Figure 10).[43] *E. coli* KL7/pSK6.161 expresses a plasmids-localized mutant isozyme of *p*-hydroxybenzoate hydroxylase encoded by plasmid-localized *pobA**,[65] DHS dehydratase encoded by a genomic copy of *aroZ* and feedback-insensitive DAHP synthase encoded by plasmid-localized $aroF^{FBR}$. *E. coli* KL7/pSK6.161 afforded 20 g/L of gallic acid in 12% (mol/mol) yield from D-glucose under fermentor-controlled conditions.[43] Decarboxylation of gallic acid to pyrogallol was conducted by *E. coli* RB791*serA*::*aroB*/pSK6.234 expressing *aroY*-encoded PCA decarboxylase. Addition of gallic acid to a batch culture of *E. coli* RB791*serA*::*aroB*/pSK6.234 during its stationary phase of growth afforded pyrogallol in a concentration of 14 g/L in 97% (mol/mol) yield. The high-yielding biocatalytic decarboxylation of gallic acid to pyrogallol provides an attractive alternative to currently employed chemical decarboxylation process. The toxicity of pyrogallol towards growing *E. coli* cells precluded the direct synthesis of pyrogallol from D-glucose using a single microbial construct.

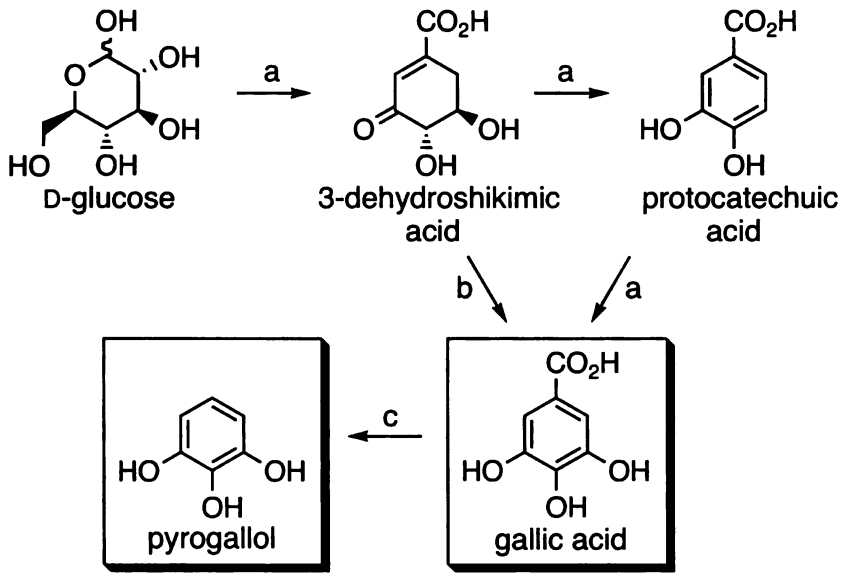

Figure 10. Synthesis of gallic acid and pyrogallol from D-glucose. Keys: (a) *E. coli* KL7/pSK6.161, 12%; (b) O_2, Cu^{2+}, Zn^{2+}, AcOH, 67%; (c) *E. coli* RB791*serA*::*aroB*/pSK6.234, 97%.

Syntheses of aromatics via a combination of biocatalytic and chemical conversions. The direct conversion approaches for biosynthesis of aromatics must contend with toxicity of the aromatic products towards the microbial biocatalysts. For example, it only takes 2.5 mM catechol to completely inhibit growth of *E. coli*.[40] Cells already in stationary phase can tolerate higher concentrations of catechol. As a result, the direct conversion of D-glucose to catechol was carried out by initial growth of the microbial biocatalyst to stationary phase followed by resuspension and culturing in minimal salts medium where synthesis of catechol occurred. Synthesis of pyrogallol also entailed addition of microbially synthesized gallic acid to pre-grown cells.[43] Although it is possible to continuously remove the toxic aromatics during the biocatalytic conversions, an alternative strategy has been developed to avoid the toxicity of aromatics to biocatalysts. This strategy involves employing microbial catalysis to synthesize an

intermediate, which is not toxic to the microbe, followed by chemical conversion of the intermediate to the desired aromatic product. Examples include the syntheses of phenol, *p*-hydroxybenzoic acid, 1,2,3,4-tetrahydroxybenzene and hydroxyhydroquinone from D-glucose.

Phenol and *p*-hydroxybenzoic acid. Phenol is used to make synthetic resins, dyes, pharmaceuticals, pesticides, perfumes, lubricating oils and solvents.[66] The Hock oxidation of benzene-derived cumene is currently the predominant method used in the production of phenol with an annual production of 5×10^9 kg (Figure 8). It is estimated that 20% of the global benzene production is directed to the manufacture of phenol.[67]

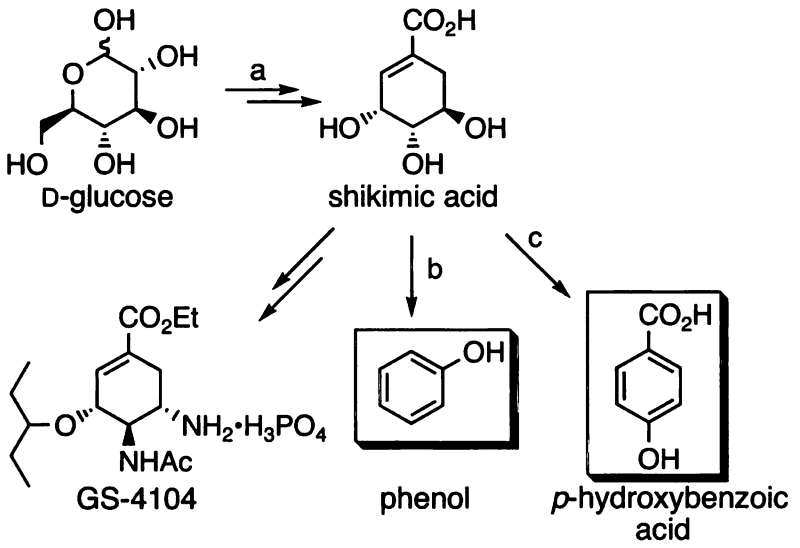

Figure 12. Synthesis of phenol and *p*-hydroxybenzoic acid via intermediacy of shikimic acid. Keys: (a) *E. coli* SP1.1/pKD12.138 or SP1.1*pts*/pSC6.090; (b) H_2O, 350 °C; (c) 1 M H_2SO_4 in AcOH.

Commercially available shikimic acid is isolated from fruits of *Illicium* plant at a cost of approximately $10,000/kg.[27a] *E. coli* SP1.1/pKD12.138[4] was constructed for

microbial production of shikimic acid from glucose, and a further improved construct SP1.1*pts*/pSC6.090 has achieved a titer to 87 g/L and 36% (mol/mol) yield.[68] The shikimate-producing biocatalyst has been licensed by Roche for the synthesis of neuraminidase inhibitor GS-4104, an anti-influenza drug sold under the name Tamiflu™.[69] *E. coli* synthesis of shikimic acid results from disruption of the genomic *aroL* and *aroK* loci, overexpression of feedback-insensitive, $aroF^{FBR}$-encoded DAHP synthase, *aroE*-encoded shikimate dehydrogenase and *tktA*-encoded transketolase to channel more carbon into the shikimate pathway.[4] Shikimic acid can also be used as an intermediate in the synthesis of phenol. A benzene-free route to phenol was achieved by aromatization and decarboxylation of microbes synthesized shikimic acid in near-critical water to afford phenol in an overall 14% yield from D-glucose (Figure 12).[45] Conversion of shikimic acid to phenol in near-critical water circumvents the potent antimicrobial activity of phenol and avoids the use of strong acids. *p*-Hydroxybenzoic acid can also be synthesized from shikimic acid by refluxing shikimic acid in acetic acid containing1 M sulfuric acid in an overall 15% yield from D-glucose.[45]

Polyhydroxybenzenes. The strategy of combining biocatalysis and chemical catalysis has also been used in the synthesis of 1,2,3,4-tetrahydroxybenzene from D-glucose (Figure 13). D-Glucose was converted into *myo*-inositol in 11% yield by an *E. coli* strain expressing *myo*-inositol 1-phosphate synthase from *Saccharomyces cerevisiae*. Oxidation of the biosynthesized *myo*-inositol to *myo*-inosose was carried out by *Gluconobacter oxidans* ATCC 621 in 95% yield. *myo*-Inosose underwent aromatization under acidic conditions to afford 1,2,3,4-tetrahydroxybenzene in 66% yield. In a similar approach, Katinuma et al.[70] synthesized 2-deoxy-*scyllo*-inosose from D-glucose with an

enzymatic reaction catalyzed by 2-deoxy-*scyllo*-inosose synthase from *Bacillus circulans* in 38% yield. Treatment of the 2-deoxy-*scyllo*-inosose with HI in acetic acid afforded catechol in 59% yield. Hansen et al. converted the 2-deoxy-*scyllo*-inosose into hydroxyhydroquinone in 39% yield by acid-catalyzed dehydration.[71]

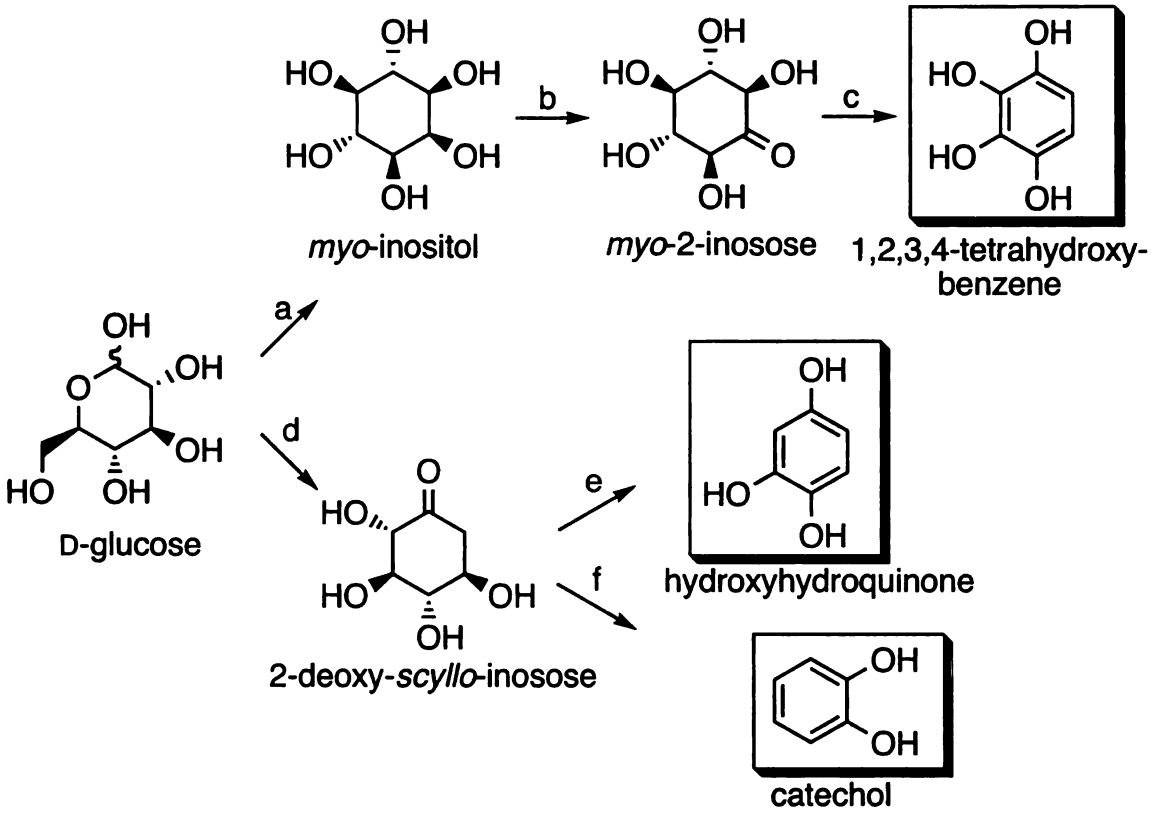

Figure 13. Syntheses of polyhydroxybenzenes from D-glucose. Keys: (a) JWF1/pAD1.88A (b) *Gluconobacter oxidans*; (c) 0.5 M H_2SO_4, reflux; (d) (i) hexokinase, ATP, Mg^{2+}, (ii) 2-deoxy-*scyllo*-inosose synthase, NAD^+; (e) 0.5 M H_3PO_4, reflux; (f) HI, HOAc.

In Chapter 2 of this thesis, a synthetic route to hydroquinone from glucose that utilized this hybrid synthesis strategy will be presented. A genetically engineered *E. coli* construct produces quinic acid as a non-toxic intermediate which is then chemically converted into hydroquinone. This synthesis was accomplished by manipulation of the

shikimate pathway for the synthesis of quinic acid and the development of high-yielding methodologies for conversion of quinic acid into hydroquinone in purified fermentation broth. As seen from the syntheses of phenol and polyhydroxybenzenes, utilization of this strategy enables glucose to replace benzene as the starting material for synthesis of hydroquinone and also avoids the microbial toxicity of hydroquinone.

Directed evolution

Continuously expanding applications of enzymes and whole cells as biocatalysts for the chemical, pharmaceutical and food industries create a growing demand for enzymes that exhibit superior properties including higher operational stability, higher activities with unnatural substrates and higher enantioselectivity. Traditionally, enzymes used in industry were isolated for these purposes by the screening of microorganisms from culture collections or from extreme environments.[72] Over the past few years, rapidly increasing availability of entire genome-sequences together with development of bioinformatic tools have significantly broadened the possible range of enzymes that could be used in industry. However, the performance of wild-type enzymes that evolved over billions of years for highly specific and controlled reactions in the context of living organisms are not always suited for specific industrial applications. In this respect, directed evolution has emerged as a powerful tool for improving the characteristics of enzymes in a targeted manner. Previously, enzymes catalysis was modified using mutation and selection with approaches such as UV and chemical mutagenesis, mutator strains and modeling-based point mutagenesis. Directed evolution[73,74] combines random mutagenesis and/or *in vitro* recombination together with screening or selection for the

rapid evolution of individual proteins, biosynthetic pathways, and bacterial genomes.[75] Contrary to traditional random and directed mutagenesis, which are slow processes in general, directed evolution can accelerate the improvement of desired properties. The first step in directed evolution is to generate genetic diversity starting from a single gene or a family of related genes by random mutagenesis or gene recombination, the resulting gene library is cloned back into an expression vector and transformed into a suitable microorganism for protein expression. Clones expressing improved proteins are identified by selection or screening, and those genes encoding improved proteins are isolated and used as parents for the next round of directed evolution. This process of improvement is repeated until the goal is achieved (Figure 14).[76]

Error-prone polymerase chain reaction (EP-PCR) is a commonly used method to generate random point mutations within a gene sequence.[77] Error-prone PCR utilizes a low-fidelity polymerase such as *Thermus aquaticus* (*Taq*) polymerase in combination with reaction conditions such as adding Mn^{2+} and lowering annealing temperature which further decrease the fidelity of the polymerase. In contrast to the point mutations generated by error-prone PCR, gene recombination involves the recombination of multiple DNA sequences to create a library of chimeras. DNA shuffling, the first developed and still the most widely used technique for *in vitro* gene recombination, was reported by Stemmer in 1994.[73] In this method, parental genes are first randomly fragmented with DNase I, and the purified fragments are then reassembled into full-length gene products by repeated cycles of overlap extension reactions. Recombinogenic events occur when fragments derived from different parental genes prime on each other.

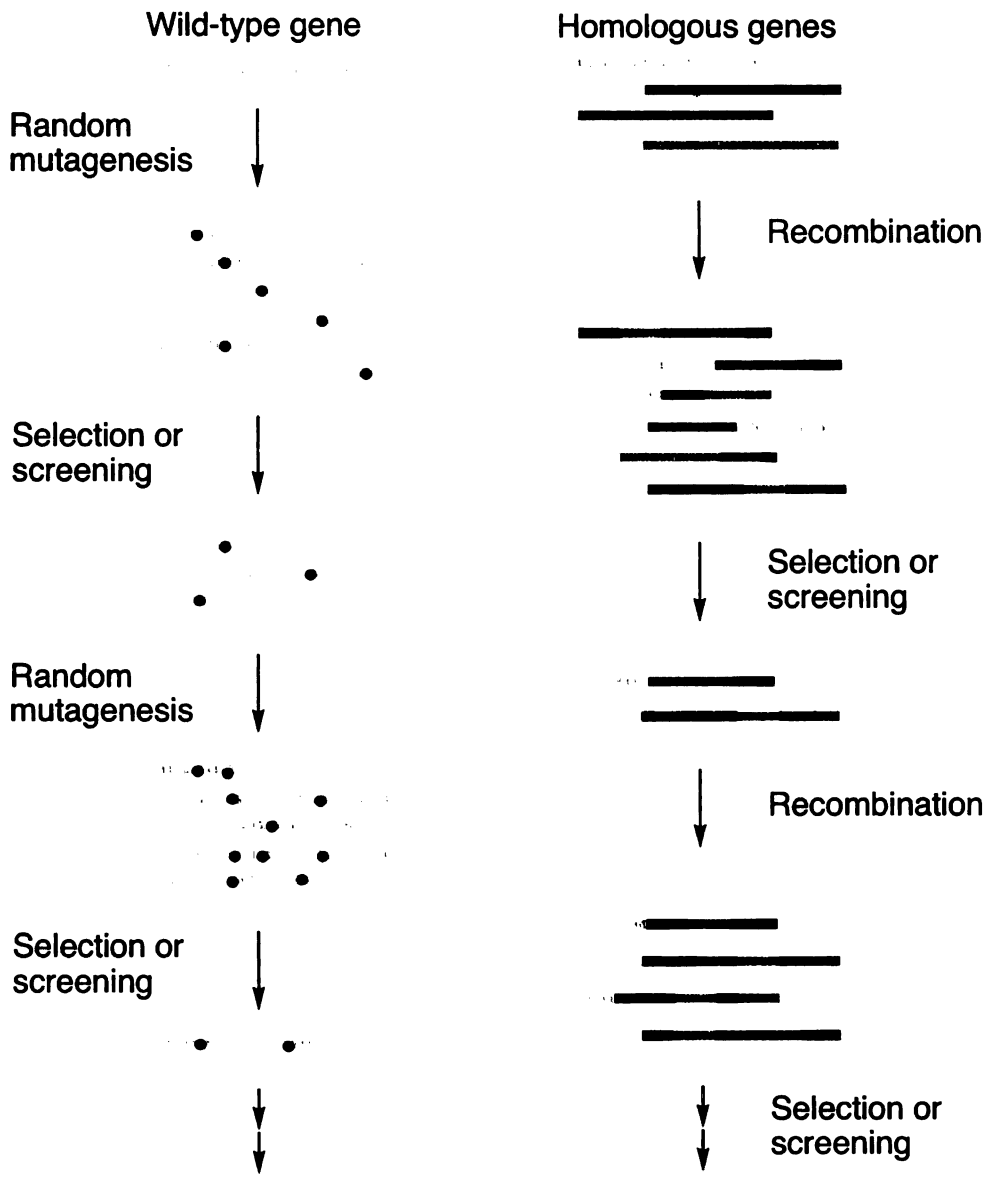

Figure 14. Conventional approach and DNA shuffling for protein evolution.

The end products of gene recombination are chimeric genes containing pieces of DNA from different parental genes.[78] Following the pioneer work of Stemmer, new tools were developed that enhance existing methods of mutation and screening, such as single-strand DNA shuffling,[79] random chimeragenesis on transient template (RACHITT),[80] incremental truncation for the creation of hybrid enzymes (ITCHY),[81] random priming

recombination, (RPR),[82] staggered extension process (StEP),[83] sequence homology-independent protein recombinantion (SHIPREC)[84] and synthetic ligation assembly.[85]

The crucial point and also the most challenging step in the directed evolution is development of an efficient and sensitive method for the identification and isolation of desired mutants out of a library of 10^4-10^6 variants.[76] This is performed either by selection or by screening using high-throughput technologies. Selection might be applicable[86] in cases when the desired protein function is essential for the survival or growth of the host organism. This is often achieved by genetic complementation of host organisms that are deficient in a certain pathway or activity.[87] Using high-throughput selection, large libraries of enzyme variants can be assayed and the size of the library is only limited by the cell transformation efficiency. Unfortunately, devising a selection method for a given enzyme can be quite difficult. Screening is the process in which every library member is assayed individually using biochemical or biophysical analysis such as colorimetry, high-pressure liquid chromatography (HPLC) or gas chromatography-mass spectrometry (GC-MS). This is commonly done in either a 96-well or 384-well microtiter plate using a detectable signal developed on the basis of the targeted catalytic activity. These high-throughput screens can be done with whole cells, cell lysates, or partially purified enzymes. Screening often limits the size of library that can be assayed to $10^4 - 10^6$, even when robotic hardware is employed. On the other hand, screening assays are flexible since experimental conditions can be tailored to meet a specific requirement.[78] Other screening methods were also developed for *in vitro* or *in vivo* screening or selection. These include compartmentalization and selection based on an *in vitro* selection system confined with a water-in-oil emulsion,[88] phage display

coupled with substrate co-immobilization onto the phage surface, leading to modified indentifiable phages carrying the desired activity,[89] and a three-hybrid system to detect desired enzymatic activity *in vivo*.[90]

Improving activity. Directed evolution is frequently used to improve enzyme fitness for a given industrial and biotechnology application. For example, Arnold and coworkers reported the use of random mutagenesis and saturation mutagenesis to improve the thermal stability of protease subtilisin E.[91] Gray et al. improved the thermal stability of haloalkane dehalogenase from *Rhodococcus rhodochrous* for the hydrolysis of 1,2,3-trichloropropane to the corresponding alcohol 2,3-dichloropropanol, which can be further converted to epoxides, by saturation mutagenesis.[92] A recent example is the generation of red fluorescent protein suitable for living cell imaging.[93] The red fluorescent protein (DsRed) from *Discosoma* coral holds great potential for a spectrally distinct companion of the widely used green fluorescent protein (GFP) from *Aequorea* jellyfish as a reporter for gene expression and regulation. However, the potential of the red fluorescent protein to be a generally accepted tool is hampered by its slow chromophore maturation and obligate tetramerization. Although directed evolution has been applied successfully to green fluorescent protein to improve the fluorescent signal to 45-fold greater than commercially available GFP,[94] engineering of the red fluorescent protein has proven to be difficult. Bevis et al.[93a] used several rounds of directed and random mutagenesis with library sizes ranging from 10^3 to 10^5 variants to create red fluorescent protein variants that mature 15 times faster than the wild-type protein. Tsien et al. further evolved this DsRed variant to be monomeric using a combination of structure-based design and directed evolution.[93b]

Altering stereoselectivity. DNA shuffling has also been applied successfully to changing the stereoselectivity of an enzyme. For instance, Arnold and coworkers improved the hydantoinase process for production of L-methionine in *E. coli* by inverting the enantioselectivity of the D-selective hydantoinase (40% enantiomeric excess) from *Arthrobacter sp.* DSM 9771 into an L-selective enzyme (20% enantiomeric excess) and increasing its total activity by five-fold.[95] These engineered mutants were licensed to Degussa Fine Chemicals, which is currently developing a biocatalytic process for the synthesis of various L-amino acids.[78] Reetz and coworkers[96] reported the inversion of the stereoselectivity of a lipase from *Pseudomonas aeruginosa* by carrying out successive rounds of error-prone PCR combined with DNA shuffling. One mutant showed pronounced *R*-selectivity (E=30) compared with the wild-type enzyme that only showed modest *S*-selectivity.

Modifying substrate specificity. Modifying an enzyme for new substrate recognition and regio- and stereospecificity has been a long-standing goal. In general, modifying the substrate selectivity of an enzyme is more difficult than improving the activity of an enzyme in a different environment due to the complex relationship between the enzyme structure and its substrate.[97]

There have been some impressive advances in this arena. For example, Yano et al.[98] reported successful reengineering of an aspartate aminotransferase to a β-branched aminotransferase using random mutagenesis and selection for complementation of an engineered deficiency in the endogenous β-branched aminotransferase. After five cycles of mutation and selection with 10^6-10^7 variants in each cycle, an aspartate aminotransferase variant was generated that utilized 2-oxo acids 10^5 times more

efficiently than the wild-type enzyme. Recent efforts on modifying the substrate selectivity by directed evolution include 2-hydroxybiphenyl 3-monooxygenase and biphenol dioxygenase.[99] A particularly successful example is the directed evolution of an orthogal aminoacyl-tRNA synthase suitable for incorporating synthetic amino acids into proteins via an amber suppressor tRNA *in vivo*. Tyrosyl-tRNA synthetase from *Methanococcus jannaschii* was evolved to an efficient *O*-methyl-L-tyrosine tRNA synthetase.[100] Based on those literature examples, it seems that a large library size and a powerful *in vivo* selection method were the key to the successful enzyme evolution.

Chapter 3 of this thesis details the creation of a pyruvate-based shikimate pathway. The centerpiece of this successful creation lies on modifying substrate specificity of the *dgoA*-encoded 2-keto-3-deoxy-6-phosphogalactonate aldolase. Wild-type 2-keto-3-deoxy-6-phosphogalactonate aldolase catalyzes the reversible condensation of pyruvate and D-glyceradehyde 3-phosphate. After 4-5 rounds of PCR mutagenesis and DNA shuffling, the evolved 2-keto-3-deoxy-6-phosphogalactonate aldolase exhibits a 25-fold increase in K_m/k_{cat} towards the catalyzed condensation of pyruvate and D-erythrose 4-phosphate to form 3-deoxy-D-*arabino*-heptulosonic acid 7-phosphate.

Reference

[1]http://www.eia.doe.gov/emeu/steo/pub/contents.html *Short-term energy outlook*- February 2004.

[2] Paster, M.; Pellegrino, J. L.; Carole, T. M. *Industrial Bioproducts: Today and Tomorrow*; U. S. Department of Energy, Office of Energy Efficiency and Renewable Energy, Office of the Biomass Program, 2003. From http://www.bioproducts-bioenergy.gov.

[3] (a) Bozell, J. J.; Landucci, R. *Alternate Feedstocks Program Technical and Economic Assessment*; U. S. Department of Energy, Office of Industrial Technologies, 1993. (b) Lynd, L. R.; Cushman, J. H.; Nichols, R. J.; Wyman, C. E. Fuel ethanol from cellulose biomass. *Science* **1991**, *251*, 1318-1323. (c) Zaldivar, J.; Nielson, J.; Olsson, L. Fuel ethanol production from lignocellulose: a challenge for metabolic engineering and process integration. *Appl. Microbiol. Biotechnol.* **2001**, *56*, 17-34.

[4] Draths, K. M.; Knop, D. R.; Frost, K. M. Shikimic acid and quinic acid: replacing isolation from plant sources with recombinant biocatalysis. *J. Am Chem. Soc.* **1999**, *121*, 1603-1604.

[5] *The History of Plastics*, http://inventors.about.com/library/inventors/blplastic.htm

[6] Datta, R. In *Kirk-Othmer Encyclopedia of Chemical Technology*, 4th ed.; Kroschwitz, J. I.; Howe-Grant, M. Eds.; Wiley: New York, 1997; Vol. 13, p. 1042-1062.

[7] Datta, R.; Tsai, S-H.; Bonsignore, P.; Moon, S-H.; Frank, J. R. Technological and economic potential of poly(lactic acid) and lactic acid derivatives. *FEMS Microbiol. Rev.* **1995**, *16*, 221-231.

[8] Garlotta, D. A literature review of poly(lactic acid). *J. Polym. Environ.* **2001**, *9*, 63-84.

[9] New food service alternative from annually renewable resources unveiled for use in major avenues. Cargill Dow LLC press release, March 5, 2001. http://www.cargilldow.com.

[10] Cargill Dow's world-scale manufacturing facility comes on line. Cargill Dow LLC press release, April 4, 2002. http://www.cargilldow.com.

[11] Fahey, J. Forbes Magazine, November 26, 2001, 206.

[12] Chang, J. Vertec biosolvents on verge of breaking out with new replacement applications, *Chemical Market Reporter*, September 2, 2002.

[13] Stinson, S. C. Fine and intermediate chemical makers emphasize new projects and processes. *Chem. Eng. News.* **1995**, *17*, 10-14.

[14] http://www.dupont.com/biotech/resources

[15] Fumagalli, C. In *Kirk-Othmer Encyclopedia of Chemical Technology*, 4th ed.; Kroschwitz, J. I.; Howe-Grant, M. Eds.; Wiley: New York, 1997; Vol. 22, p. 1074-1102.

[16] Hort, E. V.; Taylor, P. In *Kirk-Othmer Encyclopedia of Chemical Technology*, 4th ed.; Kroschwitz, J. I.; Howe-Grant, M., Eds.; Wiley: New York, 1997; Vol. 1, p. 210-211.

[17] (a) Salm, H.; Eggeling, L.; de Graaf, A. A. Pathway analysis and metabolic engineering in *Corynebacterium glutamicum. Biol. Chem.* **2000**, *381*, 899-910. (b) Eggling, L.; Sahm, H. L-Glutamate and L-lysine: traditional products with impetuous developments. *Appl. Microbiol. Biotechnol.* **1999**, *52*, 146-153.

[18] McCann, J. E. *Sweet Success: How NutraSweet Created a Billion Dollar Business*; Business One Irwin: Homewood, IL, 1990.

[19] De Boer, L.; Dijkhuizen, L. Microbial and enzymatic processes for L-phenylalanine production. *Adv. Biochem. Eng./Biotechnol.* **1990**, *41*, 1-27.

[20] Grinter, N. J. Developing an L-phenylalanine process. *Chemtech* **1998**, *7*, 33-37.

[21] Bongaerts, J.; Kramer, M.; Muller, U.; Raeven, L.; Wubbolts, M. Metabolic engineering for microbial production of aromatic amino acids and derived compounds. *Metab. Eng.* **2001**, *3*, 289-300.

[22] Maiti, T. K.; Roy, A.; Mukherjee, S. K. Chatterjee, S. P. Microbial production of L-tyrosine: a review. *Hindustan Antibiot. Bull.* **1995**, *37*, 51-65.

[23] (a) Murdock, D.; Ensley, B. D.; Serdar, C.; Thalen, M. Construction of metabolic operons catalyzing the *de novo* biosynthesis of indigo in *Escherichia coli. Biotechnology* **1993**, *11*, 381-386. (b) Berry, A.; Battist, S.; Chotani, G.; Dodge, T. C.; Peck, S.; Power, S.; Weyler, W. Biosynthesis of indigo using recombinant *E. coli*: development of a biological system for the cost-effective production of a large volume chemical. Proceedings-Biomass Conference Americas: Energy, Environment, Agriculture and Industry, 2nd, Portland, Oreg. Aut. 21-24, 1995, p. 1121-1129. (c) Berry, A.; Dodge, T. C.; Pepsin, M.; Weyler, W. Application of metabolic engineering to improve both the production and use of biotech indigo. *Indust. Microbiol. Biotech.* **2002**, *28*, 127-133.

[24] Berry, A. Improving production of aromatic compounds in *Escherichia coli* by metabolic engineering. *Trends Biotechnol.* **1996**, *14*, 250-256.

[25] Katsumata, R.; Ikeda, M. Hyperproduction of tryptophan in *Corynebacterium glutamicum* by pathway engineering. *Biotechnology* **1993**, *11*, 921-925.

[26] Kurahashi, O.; Tsuchida, T.; Kawashima, N.; Ei, H.; Yamane, K. L-Tryptophan production by transformed *Bacillus subtilis*. JP 61096990, 1984.

[27] (a) Haslam, E. In *Shikimic Acid: Metabolism and Metabolites*; Wiley: New York, 1993. (b) Bentley, R. The shikimate pathway - a metabolic tree with many branches. *Crit. Rev. Biochem. Mol. Biol.* **1990**, *25*, 307-384. (c) Herrmann, K. M. In *Amino Acids: Biosynthesis and Genetic Regulation*; Herrmann, K. M., Somerville, R. L., Ed.; Addison-Wesley: Reading, 1983: p. 301.

[28] Frost, J. W.; Bender, J. L.; Kadonaga, J. T.; Knowles, J. R. Dehydroquinate synthase from *Escherichia coli*: purification, cloning, and construction of overproducers of the enzyme. *Biochemistry* **1984**, *23*, 4470-4475.

[29] Carpenter, E. P.; Hawkins, A. R.; Frost, J. W.; Brown, K. A. Structure of dehydroquinate synthase reveals an active site capable of multistep catalysis. *Nature* **1998**, *394*, 299-302.

[30] (a) Smith, B. W.; Turner, M. J.; Haslam, E. Shikimate pathway. 4. Stereochemistry of 3-dehydroquinate dehydratase reaction and observations on 3-dehydroquinate synthetase. *J. Chem. Soc., Perkins Trans. 1* **1975**, *1*, 52-55. (b) Duncan, K.; Chaudhuri, S.; Campbell, M. S.; Coggins, J. R. The overexpression and complete amino-acid-sequence of *Escherichia coli* 3-dehydroquinase. *Biochem. J.* **1986**, *238*, 475-483.

[31] (a) Anton, I. A.; Coggins, J. R. Sequencing and overexpression of the *Escherichia coli aroE* gene encoding shikimate dehydrogenase. *Biochem. J.* **1988**, *249*, 319-326. (b) Chaudhuri, S.; Coggins, J. R. The purification of shikimate dehydrogenase from *Escherichia coli*. *Biochem. J.* **1985**, *226*, 217-223.

[32] Benach, J.; Lee, I.; Edstrom, W.; Kuzin, A. P.; Chiang, Y. W.; Acton, T. B.; Montelione, G. T.; Hunt, J. F. The 2.3-angstrom crystal structure of the shikimate 5-dehydrogenase orthologue YdiB from *Escherichia coli* suggests a novel catalytic environment for an NAD-dependent dehydrogenase. *J. Biol. Chem.* **2003**, *278*, 19176-19182.

[33] (a) DeFeyter, R. C.; Pittard, J. Genetic and molecular analysis of AroL, the gene for shikimate kinase-II in *Escherichia coli* K-12. *J. Bacteriol.* **1986**, *165*, 226-232. (b) DeFeyter, R. C.; Pittard, J. Purification and properties of shikimate kinase-II from *Escherichia coli* K-12. *J. Bacteriol.* **1986**, *165*, 331-333.

[34] LØbner-Olesen, A.; Marinus, M. G. Identification of the gene (Arok) encoding shikimic acid kinase-I of *Escherichia coli*. *J. Bacteriol.* **1992**, *174*, 525-529.

[35] Duncan, K.; Coggins, J. R. The Serc-AroA operon of *Escherichia coli*: a mixed function operon encoding enzymes from 2 different amino-acid biosynthetic pathways. *Biochem. J.* **1986**, *234*, 49-57. (b) Duncan, K.; Lewendon, A.; Coggins. J. R. The purification of 5-enolpyruvylshikimate 3-phosphate synthase from an overproducing strain of *Escherichia coli*. *FEBS Lett.* **1984**, *165*, 121-127.

[36] White, P. J.; Millar, G.; Coggins, J. The overexpression, purification and complete amino-acid sequence of chorismate synthase from *Escherichia coli* K12 and its comparison with the enzyme from *Neurospora crassa*. *Biochem. J.* **1988**, *251*, 313-322.

[37] Pittard, A. J. Biosynthesis of the aromatic amino acids. In *Escherichia coli and Salmonella typhimurium: Cellular and Molecular Biology*. Neidhardt, F. C. ed. ASM Press (Washington, DC: American Society for Microbiology) 1996, p. 458-484.

[38] Kishore, G. M.; Shah, D. M. Amino acid biosynthesis inhibitors as herbicides. *Annu. Rev. Biochem.* **1988**, *57*, 627-663.

[39] Roberts, F.; Roberts, C. W.; Johnson, J. J.; Kyle, D. E.; Krell, T.; Coggins, J. R.; Coombs, G. H.; Milhous, W. K.; Tzipori, S.; Ferguson, D. J. P.; Chakrabarti, D.; McLeod, R. Evidence for the shikimate pathway in apicomplexan parasites. *Nature* **1998**, *393*, 801-805.

[40] Draths, K. M.; Frost, J. W. Environmentally compatible synthesis of catechol from D-glucose. *J. Am. Chem. Soc.* **1995**, *117*, 2395-2400.

[41] Li, K.; Frost, J. W. Synthesis of vanillin from glucose. *J. Am. Chem. Soc.* **1998**, *120*, 10545-10546.

[42] Draths, K. M.; Ward, T. L.; Frost, J. W. Biocatalysis and nineteenth century organic chemistry: conversion of D-glucose into quinoid organics. *J. Am. Chem. Soc.* **1992**, *114*, 9725-9726.

[43] Kambourakis, S.; Draths, K. M.; Frost, J. W. Synthesis of gallic acid and pyrogallol from glucose: replacing natural product isolation with microbial catalysis. *J. Am. Chem. Soc.* **2000**, *122*, 9042-9043.

[44] Barker, J. L.; Frost, J. W. Microbial synthesis of *p*-hydroxybenzoic acid from glucose. *Biotechnol. Bioeng.* **2001**, *76*, 376-390.

[45] Gibson, J. M.; Thomas, P. S.; Thomas, J. D.; Barker, J. L.; Chandran, S. S.; Harrup, M. K.; Draths, K. M.; Frost, J. W. Benzene-free synthesis of phenol. *Angew. Chem., Intl. Ed.* **2001**, *40*, 1945-1948.

[46] Li, K.; Mikola, M. R.; Draths, K. M.; Worden, R. M.; Frost, J. W. Fed-batch fermentor synthesis of 3-dehydroshikimic acid using recombinant *Escherichia coli*. *Biotechnol. Bioeng.* **1999**, *64*, 61-73.

[47] (a) Draths, K. M.; Frost, J. W. Environmentally compatible synthesis of adipic acid from D-glucose. *J. Am. Chem. Soc.* **1994**, *116*, 399-400. (b) Niu, W.; Draths, K. M.; Frost, J. W. Benzene-free synthesis of adipic acid. *Biotechnol. Prog.* **2002**, *18*, 201-211.

[48] Draths, K. M.; Pompliano, D. L.; Conley, D. L.; Frost, J. W.; Berry, A.; Disbrow, G. L.; Staversky, R. J.; Lievense, J. C. Biocatalytic synthesis of aromatics from D-glucose: the role of transketolase. *J. Am. Chem. Soc.* **1992**, *114*, 3956-3962.

[49] Yi, J.; Li, K.; Draths, K. M.; Frost, J. W. Modulation of phosphoenolpyruvate synthase expression increases shikimate pathway product yields in *E. coli*. *Biotechnol. Prog.* **2002**, *18*, 1141-1148.

[50] Krumenacker, L.; Costantini, M.; Pontal, P.; Sentenac, J. In *Kirt-Othmer Encyclopedia of Chemical Technology*, 4th ed.; Kroschwitz, J. I., Howe-Grant, M., Eds.; Wiley, New York, 1995, Vol 13, p. 996.

[51] (a) Franck, H.-G.; Stadelhofer, J. W. *Industrial Aromatic Chemistry*; Springer-Verlag: New York, 1988; p. 183-190. (b) Szmant, H. H. In *Organic Building Blocks of the Chemical Industry*; New York: Wiley, 1989, p. 512-519.

[52] Neidle, E. L.; Ornston, L. N. Cloning and expression of *Acinetobacter calcoaceticus* catechol 1,2-dioxygenase structural gene *catA* in *Escherichia coli*. *J. Bacteriol.* **1986**, *168*, 815-820.

[53] Davis, D. D.; Kemp, D. R. In *Kirk-Othmer Encyclopedia of Chemical Technology*, 4th ed.; Kroschwitz, J. I.; Howe-Grant, M., Eds.; Wiley: New York, 1997; Vol. 1, p. 466-493.

[54] (a) Thiemens, M. H.; Trogler, W. C. Nylon production – an unknown source of atmospheric nitrous oxide. *Science* **1991**, *251*, 932. (b) Dickinson, R. E.; Cicerone, R. J. Future global warming from atmosphere trace gases. *Nature* **1986**, *319*, 109-115.

[55] Esposito, L.; Formanek, K.; Kientz, G.; Mauger, F.; Maureux, V.; Robert, G.; Truchet, F. In *Kirk-Othmer Encyclopedia of Chemical Technology*, 4th ed.; Kroschwitz, J. I., Howe-Grant, M., Eds.; Wiley: New York, 1997; Vol. 24, p. 812.

[56] Clark, G. S. Vanillin. *Perf. Flavor.* **1990**, *15*, 45-54.

[57] Priefert, H.; Rabenhorst, J.; Steinbuchel, A. Biotechnological production of vanillin. *Appl. Microbiol. Biotechnol.* **2001**, *56*, 296-314.

[58] (a) Gross, G. G.; Bolkart, K. H.; Zenk, M. H. Reduction of cinnamic acid to cinnamaldehyde and alcohol. *Biochem. Biophys. Res. Commun.* **1968**, *32*, 173-178. (b) Gross, G. G.; Zenk, M. H. Reduction of aromatic acids to aldehydes and alcohols in a cell-free system. I. Purification and properties of aryl aldehyde: NADP oxidoreductase from *Neurospora crassa*. *Eur. J. Biochem.* **1969**, *8*, 413-419. (c) Gross, G. G. Formation and reduction of intermediate acyladenylate by aryl-aldehyde. NADP oxidoreductase from *Neurospora crassa*. *Eur. J. Biochem.* **1972**, *11*, 585-592. (d) Zenk, M. H.; Gross, G. G. Enzymatic reduction of cinnamic acids. *Recent Adv. Phytochem.* **1972**, *4*, 87-106.

[59] Kirsch, M. A.; Williams, D. J. Understanding the thermoplastic polyester business. *Chemtech* **1994**, *24*, 40-49.

[60] Szmant, H. H. In *Organic Building Blocks of the Chemical Industry*, New York: Wiley, 1989, p. 467.

[61] Lenga, R. E.; Votoupal, K. L. *The Sigma-Aldrich Library of Regulatory and Safety Data*; Sigma-Aldrich: Milwaukee, WI, 1993.

[62] Siebert, M.; Berchthold, A.; Melzer, M.; May, U. Berger, U. Ubiquinone biosynthesis - cloning of the genes coding for chorismate pyruvate-lyase and 4-hydroxybenzoate octaprenyl transferase from *Escherichia coli*. *FEBS Lett.* **1992**, *307*, 347-350.

[63] Leston, G. In *Kirk-Othmer Encyclopedia of Chemical Technology*; 4th ed.; Kroschwitz, J. I., Howe-Grand, M., Eds.; New York, 1997; Vol. 19, p. 778.

[64] Kambourakis, S.; Frost, J. W. Synthesis of gallic acid: Cu^{2+}-mediated oxidation of 3-dehydroshikimic acid. *J. Org. Chem.* **2000**, 6904-6909.

[65] (a) Entsch, B.; Palfey, B. A.; Ballou, D. P.; Massey, V. Catalytic function of tyrosine residues in para-hydroxybenzoate hydroxylase as determined by the study of site-directed mutants. *J. Biol. Chem.* **1991**, *266*, 17341-17349. (b) Eschrich, K.; van der Bolt, F. J. T.; de Kok, A.; van Berkel, W. J. H. Role of Tyr201 and Tyr385 in substrate activation by *p*-hydroxybenzoate hydroxylase from *Pseudomonas fluorescens*. *Eur. J. Biochem.* **1993**, *216*, 137-146.

[66] Wallace, J. In *Kirk-Othmer Encyclopedia of Chemical Technology*, 4th ed., Vol. 18; Kroschwitz, J. I.; Howe-Grant, M., eds.; Wiley: New York, 1998, p. 592-602.

[67] Szmant, H. H. In *Organic Building Blocks of the Chemical Industry*; Wiley: New York, 1989, p. 434.

[68] Chandran, S. C.; Yi, J.; Draths, K. M.; von Daeniken, R.; Weber, W.; Frost, J. W. Phosphoenolpyruvate availability and the biosynthesis of shikimic acid. *Biotechnol. Prog.* **2003**, *19*, 808-814.

[69] (a) Federspiel, M.; Fischer, R.; Henning, M.; Mair, H.-J.; Oberhauser, T.; Rimmler, G.; Albiez, T.; Bruhin, J.; Estermann, H.; Gandert, C.; Gockel, V.; Gotzo, S.; Hoffmann, U.; Huber, G.; Janatsch, G.; Lauper, S.; Odette, T.-S.; Trussardi, R.; Zwahlen, A. G. Industrial synthesis of the key precursor in the synthesis of the anti-influenza drug Oseltamivir phosphate (Ro 64-0796/002, GS-4104-02): ethyl (3*R*,4*S*,5*S*)-4,5-epoxy-3-(1-ethyl-propoxy)-cyclohex-1-ene-1-carboxylate. *Org. Process Res. Dev.* **1999**, *3*, 266-274. (b) Kim, C. U.; Lew, W.; Williams, M. A.; Liu, H.; Zhang, L.; Swaminathan, S.; Bischofberger, N.; Chen, M. S.; Mendel, D. B.; Tai, C. Y.; Laver, W. G.; Stevens, R. C. Influenza neuraminidase inhibitors possessing a novel hydrophobic interaction in the enzyme active site: design, synthesis, and structural analysis of carbocyclic sialic acid analogues with potent anti-influenza activity. *J. Am. Chem. Soc.* **1997**, *119*, 681-690. (c) Rohloff, J. C.; Kent, K. M.; Postich, M. J.; Becker, M. W.; Chapman, H. H.; Kelly, D. E.; Lew, W.; Louie, M. S.; McGee, L. R.; Prisbe, E. J.; Schultze, L. M.; Yu, R. H.; Zhang, L. Practical total synthesis of the anti-influenza drug GS-4104. *J. Org. Chem.* **1998**, *63*, 4545-4550.

[70] Kakinuma, K.; Nango, E.; Kudo, F.; Matsushima, Y.; Eguchi, T. An expeditious chemo-enzymatic route from glucose to catechol by the use of 2-deoxy-*scyllo*-inosose synthase. *Tetrahedron Lett.* **2000**, *41*, 1935-1938.

[71] Hansen, C.; Frost, J. W. Deoxygenation of polyhydroxybenzene: an alternative strategy for the benzene-free synthesis of aromatic chemicals. *J. Am. Chem. Soc.* **2001**, *124*, 5926-5927.

[72] (a) Cheetham, P. S. J. Screening for novel biocatlysts. *Enzyme Microb. Technol.* **1987**, *9*, 194-213. (b) Ogawa, J.; Shimizu, S. Microbial enzymes: new industrial applications from traditional screening methods. *Trends Biotechnol.* **1999**, *17*, 13-20.

[73] (a) Stemmer, W. P. C. DNA shuffling by random fragmentation and reassembly: *in vitro* recombination for molecular evolution. *Proc. Natl. Acad. Sci. USA* **1994**, *91*, 10747-10751. (b) Stemmer, W. P. C. Rapid evolution of a protein *in vitro* by DNA shuffling. *Nature* **1994**, *370*, 389-391.

[74] Crameri, A.; Raillard, S-A.; Bermudez, E.; Stemmer, W. P. C. DNA shuffling of a family of genes from diverse species accelerates directed evolution. *Nature* **1998**, *391*, 288-291.

[75] Zhang, Y-X.; Perry, K.; Vinci, V. A.; Powell, K.; Stemmer, W. P. C.; del Cardayre, S. B. Genome shuffling leads to rapid phenotypic improvement in bacteria. *Nature* **2002**, *415*, 644-646.

[76] Schmidt-Dannert, C. Directed evolution of single proteins, metabolic pathways and viruses. *Biochemistry* **2001**, *44*, 13125-13136.

[77] Cadwell, R. C.; Joyce, G. F. Randomization of genes by PCR mutagenesis. *PCR Methods Appl.* **1992**, *2*, 28-33.

[78] Woodyer, R.; Chen, W.; Zhao, H. Outrunning nature: directed evolution of superior biocatalysts. *J. Chem. Edu.* **2004**, *81*, 126-133.

[79] Zha, W.; Zhu, T.; Zhao, H. Family shuffling with single-stranded DNA. In *Methods in Molecular Biology* (Totowa, NJ, United States) **2003**, *231*(Directed Evolution Library Creation), 91-97.

[80] Coco, W. M.; Levinson, W. E.; Crist, M. J.; Hektor, H. J.; Darzins, A.; Pienkos, P. T.; Squires, C. H.; Monticello, D. J. DNA shuffling method for generating highly recombined genes and evolved enzymes. *Nat. Biotechnol.* **2001**, *19*, 354-359.

[81] Ostermeier, M.; Shim, J. H.; Benkovic, S. J. A combinatorial approach to hybrid enzymes independent of DNA homology. *Nat. Biotechnol.* **1999**, *17*, 1205-1209.

[82] Shao, Z.; Zhao, H.; Giver, L.; Arnold, F. H. Random-priming in vitro recombination: an effective tool for directed evolution. *Nucleic Acids Res.* **1998**, *26*, 681-683.

[83] Zhao, H.; Giver, L.; Shao, Z.; Affholter, J. A.; Arnold, F. H. Molecular evolution by staggered extension process (StEP) in vitro recombination. *Nat. Biotechnol.* **1998**, *16*, 258-261.

[84] Sieber, V.; Martinez C. A.; Arnold F. H. Libraries of hybrid proteins from distantly related sequences. *Nat. Biotechnol.* **2001**, *19*, 456-60.

[85] Short, J. M. Diversa Corporation, Synthetic ligation assembly in directed evolution. US Patent 6,605,449 B1, 2003.

[86] Fastrez, J. *In vivo* versus *in vitro* screening or selection for catalytic activity in enzymes and abzymes. *Mol. Biotechnol.* **1997**, *7*, 37-55.

[87] Naki, D.; Paech, C., Ganshaw, G., Schellenberger, V. Selection of a subtilisin-hyperproducing *Bacillus* in a highly structured environment. *Appl. Environ. Microbiol.* **1998**, *49*, 290-294.

[88] Tawfik, D. S.; Griffins, A. D. Man-made cell-like compartments for molecular evolution. *Nat. Biotechnol.* **1998**, *16*, 652-656.

[89] (a) Pedersen, H.; Holder, S.; Sutherlin, D. P.; Schwitter, U.; King, D. S.; Schultz, P. G. A method for directed evolution and functional cloning of enzymes. *Proc. Natl. Acad. Sci. USA* **1998**, *95*, 10523-10528. (b) Demartis, S.; Huber, A.; Viti, F.; Lozzi, L.; Giovannoni, L.; Neri, P.; Winter, G.; Neri, D. A strategy for the isolation of catalytic activities from repertoires of enzymes displayed on phage. *J. Mol. Biol.* **1999**, *286*, 617-

633.

[90] Firestine, S. M.; Salinas, F.; Nixon, A. E.; Baker, S. J.; Benkovic, S. J. Using an AraC-based three-hybrid system to detect biocatalysts *in vivo*. *Nat. Biotechnol.* **2000**, *18*, 544-547.

[91] Miyazaki, K.; Arnold, F. H. Exploring nonnatural evolutionary pathway by saturation mutagenesis: rapid improvement of protein function. *J. Mol. Evol.* **1999**, *49*, 716-720.

[92] Gray, K. A.; Richardson, T. H.; Kretz, K.; Short, J. M.; Bartnek, F.; Knowles, R.; Kan, L.; Swanson, P. E.; Robertson, D. E. Rapid evolution of reversible denaturation and elevated melting temperature in a microbial haloalkane dehalogenase. *Adv. Synth. Catal.* **2001**, *343*, 607-617.

[93] (a) Bevis, B. J.; Glick, B. S. Rapidly maturing variants of the *Discosoma* red fluorescent protein (DsRed). *Nat. Biotechnol.* **2002,** *20*, 83-87. (b) Campbell, R. E.; Tour, O.; Palmer, A. E.; Steinbach, P. A.; Baird, G. S.; Zacharias, D. A.; Tsien, R. Y. A monomeric red fluorescent protein. *Proc. Natl. Acad. Sci. USA* **2002**, *99*, 7877-7882.

[94] Crameri, A.; Whitehorn, E. A.; Tate, E.; Stemmer, W. P. C. Improved green fluorescent protein by molecular evolution using DNA shuffling. *Nat. Biotechnol.* **1996**, *14*, 315-319.

[95] May, O.; Nguyen, P. T.; Arnold, F. H. Inverting enantioselectivity by directed evolution of hydantoinase for improved production of L-methionine. *Nat. Biotechnol.* **2000**, *18*, 317-320.

[96] Zha, D.; Wilensek, S.; Hermes, M.; Jaeger, K. A.; Reetz, M. T. Complete reversal of enantioselectivity of an enzyme-catalyzed reaction by directed devolution. *Chem. Commun.* **2001**, 2664-2665.

[97] Tao, H.; Cornish, V. W. Milestones in directed enzyme evolution. *Curr. Opin. Chem. Biol.* **2002**, *6*, 858-864.

[98] Yano, T.; Oue, S.; Kagamiyama, H. Directed evolution of an aspartate aminotransferase with new substrate specificities. *Proc. Natl. Acad. Sci. USA* **1998**, *95*, 5511-5515.

[99] (a) Meyer, A.; Schmid, A.; Held, M.; Westphal, A. H.; Rothlisberger, M.; Kohler, H. P.; van Berkel, W. J.; Witholt, B. Changing the substrate reactivity of 2-hydroxybiphenyl 3-monooxygenase from *Pseudomonas azeleica* HBP1 by directed evolution. *J. Biol. Chem.* **2002**, *277*, 5575-5582. (b) Barriault, D.; Plante, M. M.; Sylvestre, M. Family shuffling of a targeted bphA region to engineer biphenyl dioxygenase. *J. Bacterial.* **2002**, *184*, 3794-3800.

[100] Wang, L.; Brock, A.; Herberich, B.; Schultz, P. G. Expanding the genetic code of *Escherichia coli*. *Science* **2001**, *292*, 498-500.

CHAPTER TWO

Benzene-Free Synthesis of Hydroquinone

Introduction

Hydroquinone is a pseudocommodity chemical used in photographic developer and in the synthesis of polymerization inhibitors and rubber antioxidants.[1] Global demand for hydroquinone was estimated at 42×10^6 kg/year in 1997, with a projected annual growth rate of 3-5%.[2] Previously synthesized by a route employing stoichiometric amounts of MnO_2 to oxidize aniline, manufacture of hydroquinone is now dominated by Hock oxidation of 1,4-diisopropylbenzene and peroxide hydroxylation of phenol by homogeneous or heterogeneous catalysis (Figure 15). In addition to chemical synthesis, microbial hydroxylation of benzene and phenol to hydroquinone has also been achieved in low yield. All these syntheses have the common feature that volatile and carcinogenic benzene and its derivatives are the starting material.

Synthesis of hydroquinone via intermediacy of aniline and nitrobenzene generates large quantities of salt stream including $MnSO_4$, $(NH_4)_2SO_4$, and iron oxide salts.[1] Both Hock-type and peroxide oxidations constitute improvements in the synthesis of hydroquinone by virtue of reducing the number of required synthetic steps and eliminating byproduct salt streams. Manufacture of hydroquinone by Hock oxidation of 1,4-diisopropylbenzene and peroxide hydroxylation of phenol (Figure 15) accounts for about 60% and 30% of global hydroquinone production, respectively.[1] The 1,4-diisopropylbenzene is synthesized by Freidel-Crafts reaction of benzene or cumene with propylene or 2-propanol. Catalyzed air oxidation of 1,4-diisopropylbenzene produces

dihydroperoxide, hydroxyhydroperoxide, and dicarbinol products. The hydroxyhydroperoxide and dicarbinol are converted into the dihydroperoxide upon treatment with H_2O_2. Acid-catalyzed cleavage of the dihydroperoxide produces acetone and hydroquinone. One drawback in this route is the formation of explosive acetone hydroperoxides during the acid-catalyzed cleavage reactions (Figure 15).[1] Reaction of phenol with H_2O_2 in the presence of acid catalysts leads to a mixture of hydroquinone and catechol (Figure 8, Chapter 1). The acid catalyst employed such as formic, sulfuric, trifluoromethanesulfonic acids and synthetic zeolites during reaction of phenol with H_2O_2 significantly controls the ratio of hydroquinone to catechol.[1]

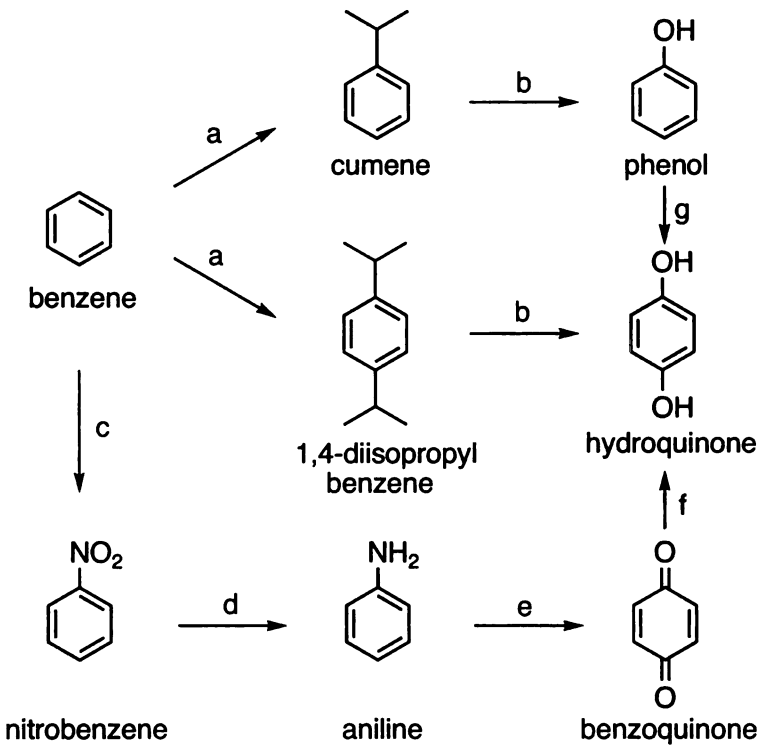

Figure 15. Chemical synthesis of hydroquinone from benzene. Keys: (a) 2-propene, HZSM-12; (b) i) O_2, NaOH, ii) H_2SO_4; (c) HNO_3, H_2SO_4; (d) Cu/SiO_2, H_2; (e) MnO_2, H_2SO_4; (f) Fe^0; (g) HCO_2H, HCO_3H.

Similar to the chemical synthesis of hydroquinone from benzene and phenol, microbe-catalyzed routes to hydroquinone have included the synthesis from phenol by butane-catabolizing bacterium *Mycobacterium* sp. HB50, and the conversion from benzene by the methane-catabolizing *Methylosinus trichosporium* OB3b (Figure 16).[3] Phenol, hydroquinone, and benzoquinone are all toxic toward microbes.[3a] To reduce the toxicity of hydroquinone toward the microbial catalyst, a continuous reaction system was developed for *Mycobacterium* sp. HB50 allowing phenol to be converted into hydroquinone with a specific volumetric productivity of 2-3 g/L/h. *Methylosinus trichosporium* OB3b synthesized approximately 1 g/L of hydroquinone from benzene with use of a chemostat to control reaction conditions. The major advantage of using *Mycobacterium* sp. HB50 was its greater resilience toward hydroquinone and benzoquinone toxicity relative to *Methylosinus trichosporium*.[3a]

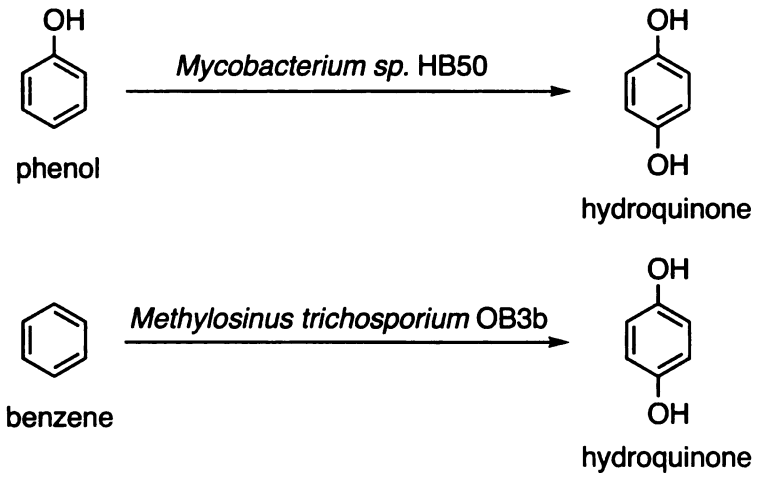

Figure 16. Microbial routes to hydroquinone from phenol and benzene.

Conversion of phenol to hydroquinone catalyzed by *Mycobacterium* sp. HB50 and conversion of benzene to hydroquinone catalyzed by *Methylosinus trichosporium* OB3b share with the aforementioned (Figure 15) chemical routes the feature of directly or indirectly using fossil fuel-derived benzene as the starting material. A biocatalytic synthesis of hydroquinone from glucose would provide a fundamentally different access to the aromatic molecule. The use of carcinogenic benzene and its derivatives would be completely avoided in this route. In theory, glucose can be converted into hydroquinone via a biocatalytic route involving intermediacy of *p*-hydroxybenzoic acid (Figure 17). Glucose can be converted into *p*-hydroxybenzoic acid at a concentration of 12 g/L in 13% (mol/mol) yield using recombinant *Escherichia coli* constructs.[4] Conversion of *p*-hydroxybenzoic acid into hydroquinone would be catalyzed by *p*-hydroxybenzoate 1-hydroxylase, an enzyme found in *Candida parapsilosis*.[5] To construct a single microbe capable of catalyzing the conversion of glucose into hydroquinone, the *C. parapsilosis* gene encoding *p*-hydroxybenzoate 1-hydroxylase would likely have to be isolated and then expressed in a *p*-hydroxybenzoate-synthesizing microbial host.

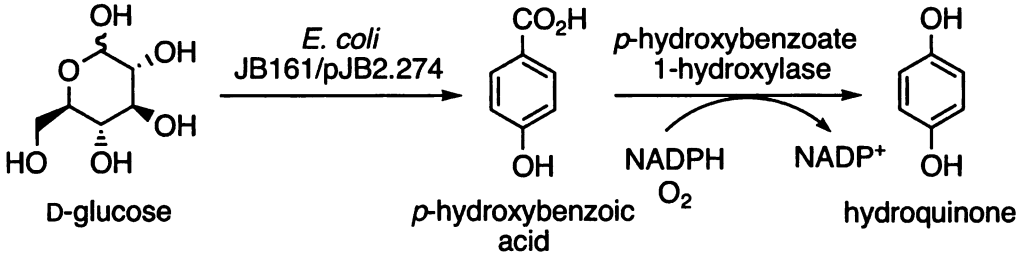

Figure 17. Proposed biocatalytic synthesis of hydroquinone from D-glucose.

The proposed microbial synthesis of hydroquinone from glucose via intermediacy of *p*-hydroxybenzoic acid, although avoiding use of benzene as starting material, still must contend with the microbial toxicity of product hydroquinone. To circumvent the toxicity of the aromatic product, a two-step synthesis that involves biocatalytic conversion of glucose to quinic acid followed by chemical conversion of quinic acid to hydroquinone was examined. Draths et al.[6] constructed *E. coli* AB2848/pKD136/pTW8090A, which synthesized 4.8 g/L of quinic acid in 31% yield from glucose by expression of the *qad*-encoded quinate dehydrogenase from *Klebsiella pneumoniae*. Oxidation of the biosynthesized quinic acid with 100 equivalents of MnO_2 afforded 10% yield of hydroquinone upon heating at 100°C for 18 h.[6] Microbial synthesis of quinic acid by the heterologous *E. coli* strain provided a relatively inexpensive source of the hydroaromatic for conversion to the pseudocommodity chemical hydroquinone. The key distinction between the chemical oxidation of microbe-synthesized quinic acid as a route to hydroquinone relative to all reported or theoretical biocatalytic syntheses of hydroquinone is that the microbial catalyst never comes into contact with a toxic aromatic starting material, aromatic intermediate or aromatic product. Quinic acid at neutral pH does not adversely affect either growth or metabolism of *E. coli*.

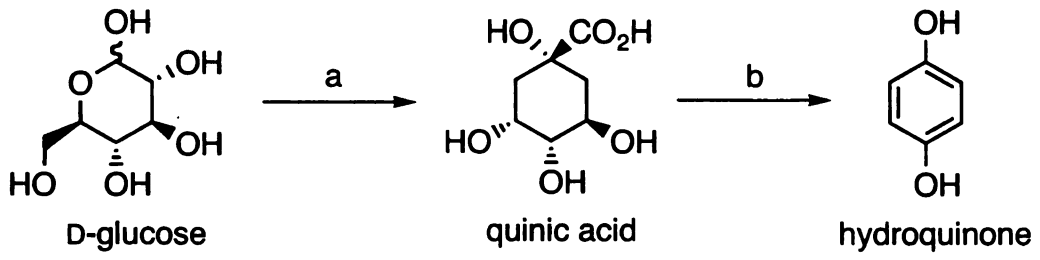

Figure 18. Previously examined synthesis of hydroquinone from D-glucose. Keys: (a) *E. coli* AB3248/pKD136/pTW8090A, 31%; (b) MnO_2 (100 equiv.), 100 °C, 10%.

In order to be cost-competitive with the commercial chemical process for hydroquinone, both the microbial synthesis of quinic acid and the chemical conversion of quinic acid to hydroquinone need to be high yielding and low cost. In the reported biocatalytic synthesis of hydroquinone, the *E. coli* AB3248/pKD136/pTW8090A was cultured under shake-flask conditions. It is generally difficult to control oxygenation and pH during growth of microbes in shake flasks. Microbes cultured under shake-flask conditions are also under physiological stress due to the glucose-rich environment present immediately after inoculation that changes to a glucose-limited environment as the cultures grow. The two-plasmid system and the heterologous expression of quinate dehydrogenase from *K. pneumoniae* also hindered cultivation of the biocatalyst under fed-batch fermentation conditions. The finding that *E. coli aroE*-encoded shikimate dehydrogenase also catalyzes the reduction of 3-dehydroquinate to quinic acid opens a new avenue to biosynthesis of quinic acid with a homogeneous *E. coli* construct.[7] The first part of this chapter will discuss the construction and strategies to improve microbial synthesis of quinic acid.

The reported chemical conversion of quinic acid to hydroquinone utilized manganese dioxide, which has the same environmental problem associated with the commercial route to hydroquinone where stoichiometric amounts of MnO_2 are used to oxidize aniline. To reduce the environmental pollution and improve the yield of this conversion, chemical conversion of quinic acid into hydroquinone requires the development of high-yielding reactions using inexpensive reagents. Due to the potentially high cost of isolating quinic acid from fermentation broth. the developed methodology should be appropriate for use in aqueous medium. The second part of the

chapter will deliberate the high-yielding chemical conversions developed for synthesis of hydroquinone from quinic acid.

Microbial synthesis of quinic acid from D-glucose.

(-)-Quinic acid is found in a variety of plant materials ranging from *Cinchona* bark to tobacco leaves to cranberries.[8] Its isolation from crude quinine (an anti-malaria drug isolated from *Cinchona* bark) dated back to 1790,[9] although its structure and stereochemistry were assigned more than a hundred years later by Fisher and Dangschzt.[10] As a chiral synthon with its highly-functionalized, six-membered carbocyclic ring and multiple asymmetric centers, quinic acid has garnered attention for combinatorial synthesis[11] and natural products syntheses. Numerous biologically active molecules have been constructed in whole, or in part, from quinic acid. The diversity of these molecules encompasses the anti-influenza drug GS4104,[12] (-)-sugiresinol dimethyl ether, a derivative of (-)-sugiresinol isolated from *Cryptomeria japonica*,[13] the epoxycyclohexenone core of scyphostatin, a powerful inhibitor of neutral sphongomyelinase,[14] (+)-eutypoxide B, a secondary metabolite of fungus *Eutypa lata* responsible for pathogenic vineyard die-back disease,[15] the A ring of 1α,25-dihydroxyvitamin D_3 derivatives as potential drugs for treatment of osteoporosis and psoriasis,[16] the 2-iodocyclohexenone acetal portion of anticancer drug taxol,[17] and the bicyclic core structure of the potent enediyne antitumoral agent esperimicin-A_1[18] (Figure 19). Quinic acid has also been used to prepare a chiral ketone for generation of chiral dioxirane used in asymmetric epoxidation of prochiral olefins (Figure 19).[19]

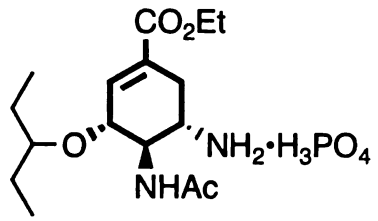

GS-4104

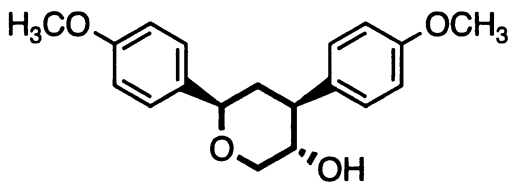

(-)-sugiresinol dimethyl ether

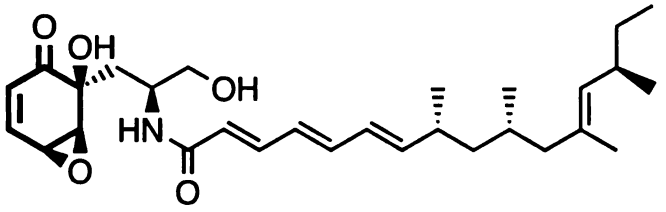

scyphostatin

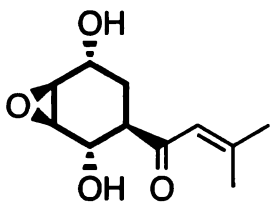

(+)-eutypoxide B

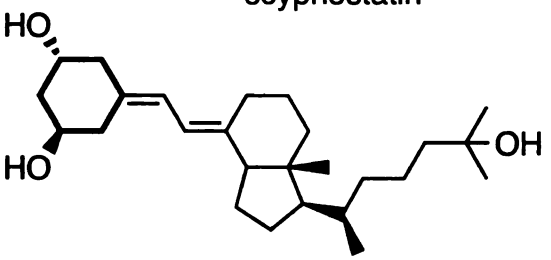

1α,25-dihydroxy-19-norvitamin D_3

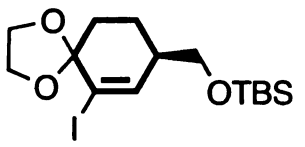

2-Iodocyclohexenone acetal

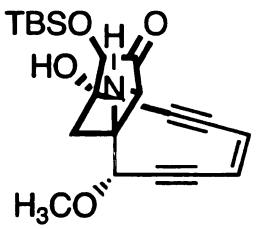

bicyclic core of esperamicin-A_1

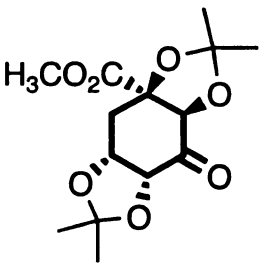

chiral ketone for
asymmetric epoxidation

Figure 19. Selected molecules synthesized from quinic acid. The portions from quinic acid are indicated in bold.

Commercially available quinic acid is isolated from *Cinchona* bark.[20] Two stereospecific syntheses of quinic acid from D-arabinose[21] and ketol silyl ether **1**,[22] respectively have been reported in the literature. D-Arabinose was reduced by catalytic hydrogenation to D-arabitol followed by several protection steps to 1,5-*O*-dityrityl-2,3,4-*O*-benzyl-D-arabitol, which was then converted 5-methylene-1,2,3-cyclohexanetriol. Oxidative cleavage of the methylene compound by $OsO_4/NaIO_4$ afforded a cyclohexanone compound, which was further converted to a cyanohydrin followed by hydrolysis and de-protection of the acetyl groups to yield quinic acid (Figure 20).[21]

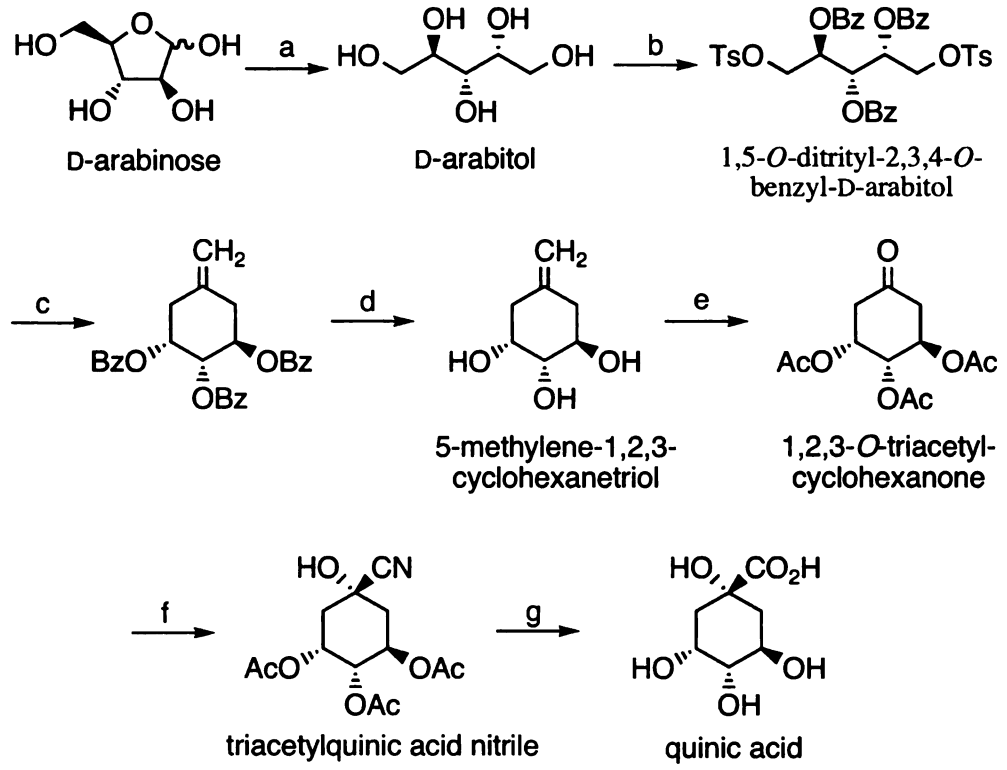

Figure 20. Chemical synthesis of quinic acid from D-arabinose. Keys: (a) Ni, H_2, 96%; (b) i) triphenylmethyl chloride, pyridine, 75%; ii) benzyl chloride, KOH, 80%; iii) 70% AcOH, 69%; iv) *p*-TsCl, pyridine, 76%; (c) i) methylenetriphenylphosphorane, ii) CH_2O, 82%; (d) Na, liquid NH_3, 80%; (e) i) Ac_2O, pyridine, 82%, ii) cat. OsO_4, $NaIO_4$, 92%; f) HCN, 86%; (g) i) Ac_2O, pyridine, 65%; ii) HBr/AcOH; iii) H_2O, 78%; iv) NaOH, H_2O, 95%.

Synthesis of quinic acid from ketol silyl ether **1** proceeded through a hydroxylation reaction followed by a retro-Diels-Alder reaction to give the cyclohexenone **3**. Dihydroxylation of **3** by OsO_4/NMO afforded a *cis*-diol as major product. Reduction of the ketone **4** by $NaBH_4$ followed by deoxygenation reaction to give fully protected quinic acid. Removal of the three alcohol protecting groups by refluxing with CBr_4 and hydrolysis of the methyl ester with NaOH afforded quinic acid (Figure 21).

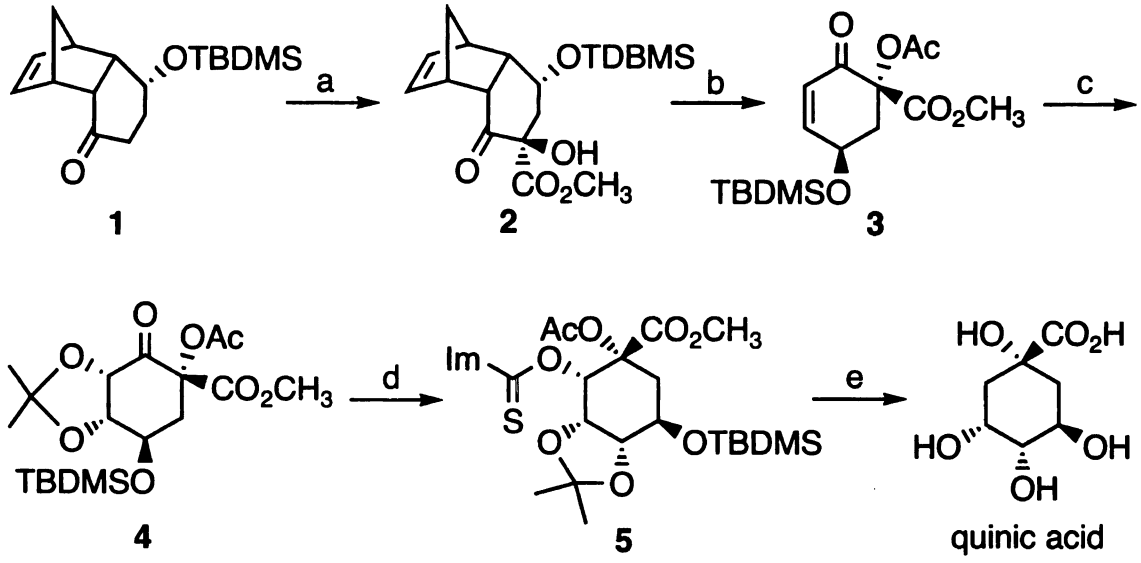

Figure 21. Chemical synthesis of quinic acid from ketol silyl ether 1. Keys: (a) i) NaH, $OC(OCH_3)_2$, THF, rt., 86%; ii) O_2, KF, $P(OEt)_3$, DMSO, rt., 90%; (b) i) Ac_2O, pyridine, rt., 100%; ii) Ph_2O, reflux, 100%; (c) i) OsO_4, NMO, THF-H_2O (2:1), 0°C, 86%; ii) $(CH_3)_2C(OCH_3)_2$, PPTS; (d) i) $NaBH_4$, CH_3OH, -78 °C, 85%; ii) thiocarbonyl-1,1'-diimidazole, 50 °C, 100%; (e) i) Bu_3SnH, toluene, reflux, 80%; ii) CBr_4, CH_3OH, reflux, 86%; iii) NaOH, H_2O, rt. 100%.

In 1992, Draths et al. established a microbial route to quinic acid from D-glucose with a transgenic *E. coli* strain that expressed quinate dehydrogenase encoded by the *qad* locus from *Klebsiella pneumoniae*.[6] The finding that *E. coli* shikimate dehydrogenase

catalyzes reduction of 3-dehydroquinic acid to quinic acid led to a redesign of *E. coli* biocatalyst for synthesis of quinic acid in 1999.[7] Synthesis of quinic acid then employed an *E. coli* host strain lacking *aroD*-encoded 3-dehydroquinate dehydratase activity. Carbon flow directed into the common pathway of aromatic amino acid biosynthesis led to formation of 3-dehydroquinic acid. Rather than catalyzing the reduction of 3-dehydroshikimic acid in the microbial synthesis of shikimic acid, overexpressed, *aroE*-encoded shikimate dehydrogenase catalyzed the reduction of 3-dehydroquinic acid to afford product quinic acid (Figure 22).

E. coli host QP1.1 was constructed by the site-specific insertion of *aroB* into the *serA* locus of *E. coli* AB2848, which lacks 3-dehydroquinate dehydratase activity due to a mutation in its *aroD* locus.[23] As a result of an inability to biosynthesize aromatic amino acids and vitamins, L-phenylalanine, L-tyrosine, L-tryptophan, *p*-hydroxybenzoic acid, *p*-aminobenzoic acid, and 2,3-dihydroxybenzoic acid were added to cultures of quinate-synthesizing *E. coli* QP1.1 constructs. Increasing the flow of carbon into the common pathway of aromatic amino acid biosynthesis was then accomplished with plasmid-localized $aroF^{FBR}$,[24] which encodes a mutant isozyme of DAHP synthase insensitive to feedback inhibition by the aromatic amino acids supplements required for growth of *E. coli* QP1.1 constructs. The two genomic *aroB* loci in *E. coli* QP1.1 increase the specific activity of 3-dehydroquinate synthase to a level where this enzyme is no longer an impediment to the flow of carbon through the common pathway of aromatic amino acid biosynthesis.[25] Disruption of the genomic *serA* locus attendant with insertion of the second *aroB* locus also provides the basis for plasmid maintenance. The *serA* locus encodes 3-phosphoglycerate dehydrogenase, which is an enzyme required for L-serine

biosynthesis. Growth of *E. coli* QP1.1 in minimal salts medium without supplementation with L-serine required maintenance and expression of plasmid-localized *serA*.

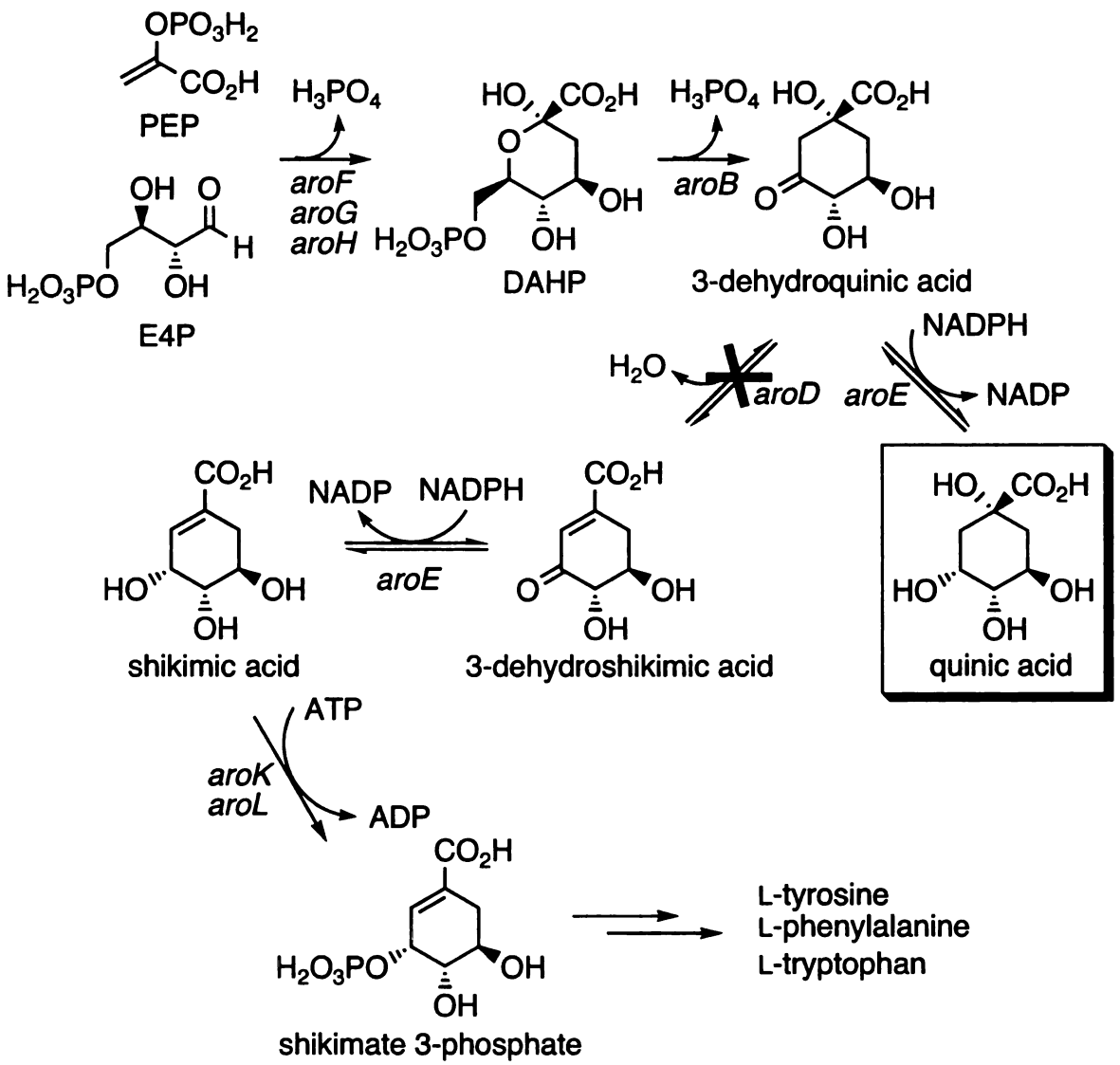

Figure 22. The truncated aromatic amino acid biosynthetic pathway with quinic acid biosynthesis. Intermediates (abbreviations): phosphoenolpyruvate (PEP), D-erythrose 4-phosphate (E4P), 3-deoxy-D-*arabino*-heptulosonic acid 7-phosphate (DAHP). Genes (enzymes): *aroF*, *aroG*, *aroH*, DAHP synthase; *aroB*, 3-dehydroquinate synthase; *aroD*, 3-dehydroquinate dehydratase; *aroE*, shikimate dehydrogenase; *aroK*, *aroL*, shikimate kinase.

Along with *serA* and the aforementioned *aroF*^{FBR}, *aroE* and *tktA* were included on plasmid pKD12.138 (Figure 23).[26] Overexpression of *aroE*-encoded shikimate dehydrogenase reduces 3-dehydroquinic acid into quinic acid. Utilization of *E. coli* *aroE*-encoded shikimate dehydrogenase instead of *K. pneumoniae qad*-encoded quinate dehydrogenase avoided the common difficulty associated with heterologous expression. This meant that promoter compatibility and codon usage were completely avoided as factors requiring consideration in route to achieving adequate overexpression of the enzyme that reduced 3-dehydroquinic acid to quinic acid. The construction of plasmid pKD12.138 began with PCR amplification of a 1.2-kb $P_{tac}P_{aroE}aroE$ fragment from pIA321.[27] The *aroE* with its own promoter P_{aroE} was under the transcriptional control of a *tac* promoter in pIA321. Cloning the $P_{tac}P_{aroE}aroE$ into pKL4.20B[24a] which already bears an *aroF*^{FBR} locus on a pSU18 vector afforded the 4.8-kb plasmid pKD12.036A. The orientation of the $P_{tac}P_{aroE}aroE$ locus is in the opposite direction as that of *aroF*^{FBR}. The 1.9-kb *serA* locus was excised from pD2625[28] and subsequently cloned into pKD12.036A to afford pKD12.047A. The orienation of the *serA* locus is in the same direction as that of $P_{tac}P_{aroE}aroE$. The *β-lac* gene was PCR amplified from pSU18 and inserted into pKD12.047A resulting in the 7.7-kb plasmid pKD12.112.[7] A 2.2-kb *tktA* fragment excised from pMF51A[29] was ligated into pKD12.112 using T4 ligase afforded the 9.9-kb plasmid pKD12.138. The *tktA* gene is transcribed in the same direction as that of *serA* gene.[26] Overexpression of *tktA*-encoded transketolase is hypothesized to increase the availability of D-erythrose 4-phosphate.[30]

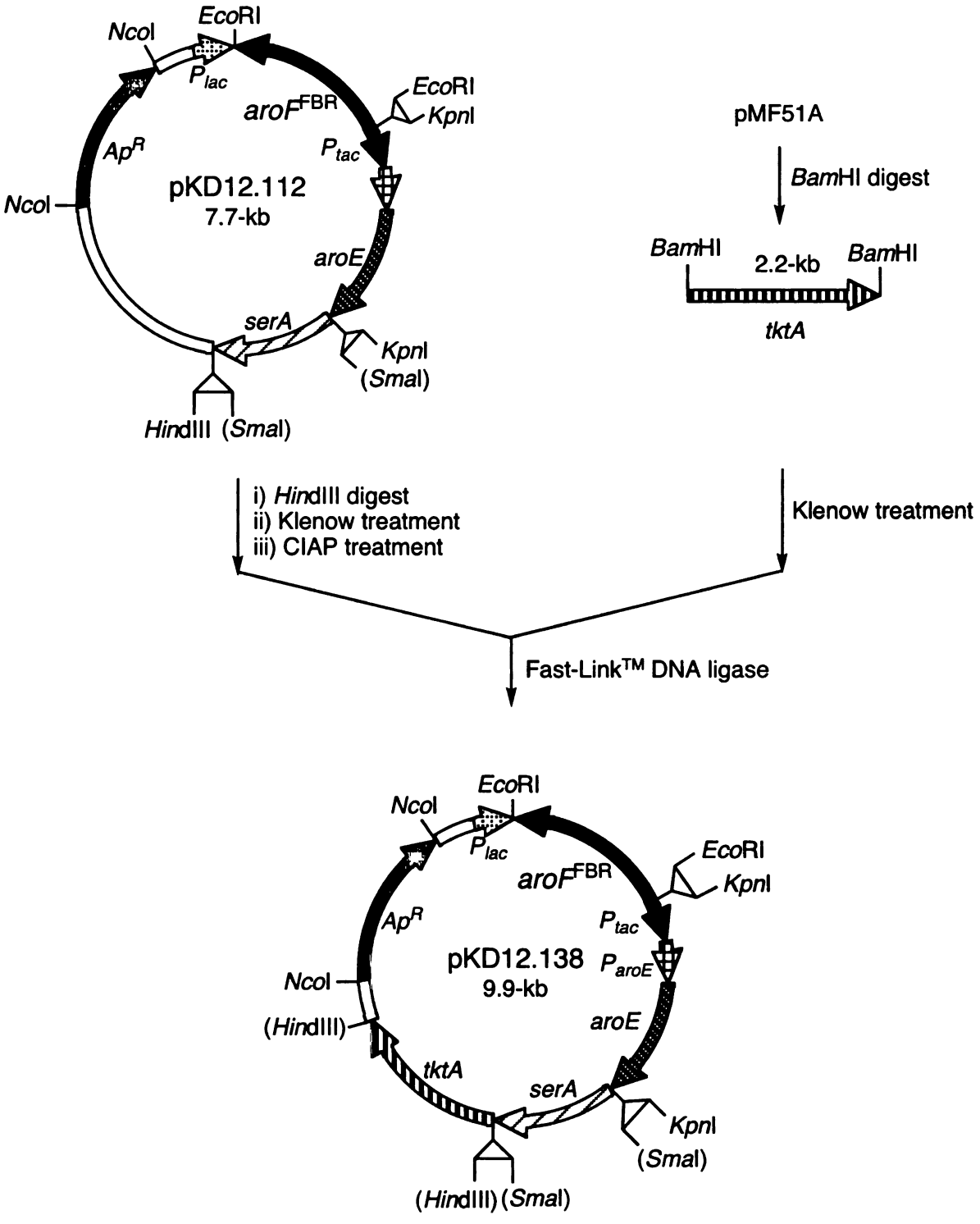

Figure 23. Construction of plasmid pKD12.138.

Biosynthesis of quinic acid by glucose-limited fed-batch fermentation. The quinate-synthesizing *E. coli* QP1.1/pKD12.138 were cultured under fermentor-controlled conditions at 33 °C, pH 7.0, with dissolved oxygen maintained at a set point of 10% air saturation. Plasmid maintenance relied on nutritional pressure as opposed to resistance to antibiotics. Glucose addition was controlled by dissolved O_2 concentration with the rate of glucose addition dictated by a proportional-integral-derivative (PID) control loop. When dissolved oxygen levels exceeded the set point value indicating decreased microbial metabolism, the rate of glucose addition was increased and conversely the rate of glucose addition was decreased when dissolved oxygen levels declined below the set point value indicating increased microbial metabolism. A proportional gain (K_c) on the glucose PID control loop of 0.1 was used for culturing *E. coli* QP1.1/pKD12.138. These conditions maintained a steady-state concentration of glucose of approximately 0.2 mM.[26]

Fed-batch fermentations of *E. coli* QP1.1/pKD12.138 synthesized 49 g/L of quinic acid in 20% (mol/mol) yield in 48 h (Figure 24). The titer is more than a 10-fold increase relative to the account of quinic acid production by *E. coli* AB2848/pKD136/pTW8090A, and required neither heterologous gene expression nor a multiple plasmid expression system. In addition to quinic acid, 3-dehydroquinic acid was accumulated at low levels in fermentation supernatant. Concentrations of 3-dehydroquinic acid steadily increased in the culture supernatant of *E. coli* QP1.1/pKD12.138 reaching a maximum concentration of 11.2 g/L at 24 h followed by a steadily decline to 5.5 g/L at 48 h.

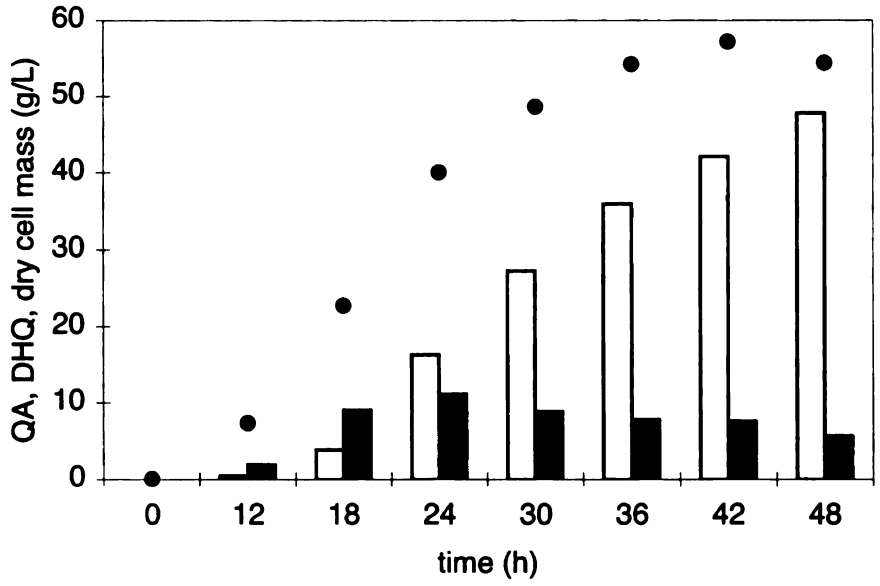

Figure 24. *E. coli* QP1.1/pKD12.138 cultured under glucose-limited, fermentor-controlled conditions. Quinic acid (□), DHQ (■), dry cell mass (●) in g/L.

The yield (entry 1, Table 2) of quinic acid synthesized by *E. coli* QP1.1/pKD12.138 reflects both the amount of glucose consumed to form biomass as well as the amount of glucose consumed to synthesize quinic acid. The theoretical maximum yield for synthesis of quinic acid from glucose with *E. coli* using phosphoenolpyruvate:carbohydrate phosphotransferase system (PTS) for glucose transport is 43% (mol/mol).[24a] The detailed analysis of theoretical maximum yield is deferred to Chapter 3.

Cultures of *E. coli* QP1.1/pKD12.138 needed to be supplemented with aromatic amino acids and aromatic vitamins due to the *aroD* mutation rendering 3-dehydroquinate dehydratase catalytically inactive. *E. coli* QP1.1/pKD12.138 supplemented with partially purified shikimic acid produced 45 g/L of quinic acid in 23% molar yield.[31]

The accumulation of substantial concentrations of 3-dehydroquinic acid during the fermentation raised a question whether the shikimate dehydrogenase activity was sufficient in *E. coli* QP1.1/pKD12.138 to channel all the 3-dehydroquinic acid forward to quinic acid. Shikimate dehydrogenase specific activities were measured in the reverse direction at 25 °C with the oxidation of shikimic acid to 3-dehydroshikimic acid by monitoring the reduction of $NADP^+$ at 340 nm ($\varepsilon = 6.18 \times 10^{-3}\ M^{-1}\ cm^{-1}$).[32] Table 2 shows the shikimate dehydrogenase activities increased linearly from 9.2 units/mg to 19 units/mg during the fermentation runs (entry 1, Table 2). The steady decrease of 3-dehydroquinic acid concentration from 24 h to 48 h also raised an intriguing possibility that 3-dehydroquinic acid previously synthesized and exported into the culture medium could be transported back into the cytoplasm and subsequently be reduced to quinic acid.

Table 1. Concentrations and yields of quinic acid and 3-dehydroquinic acid synthesized by various *E. coli* strains under different culture conditions.

entry	construct	[QA][c] g/L	QA yield[e]	[DHQ][d] g/L	DHQ yield[f]	Total yield[g]
1	QP1.1/pKD12.138[a]	49	20%	5.5	2.2%	22%
2	QP1.1/pNR4.230[a]	46	20%	4.8	2.0%	22%
3	QP1.1/pKD15.071[a]	49	18%	11	4.1%	22%
4	QP1.1/pNR4.272[a]	56	20%	7.7	2.8%	23%
5	QP1.1/pKD12.138[b]	25	8.2%	46	16%	24%
6	QP1.1/pNR4.230[b]	39	12%	31	9.3%	21%
7	QP1.1*ptsG*/pKD12.138[b]	26	9.8%	36	14%	24%

[a]glucose-limited fermentor-controlled conditions. [b]glucose-rich fermentor-controlled conditions. [c]QA: quinic acid. [d]DHQ: 3-dehydroquinic acid. [e](mol QA)/(mol glucose consumed) [f](mol DHQ)/(mol glucose consumed) [g](mol QA + mol DHQ)/(mol glucose consumed)

Table 2. Shikimate dehydrogenase specific activities for various strains cultured under different conditions.

entry	constructs	shikimate dehydrogenase (U/mg)			
		12 h	24 h	36 h	48 h
1	QP1.1/pKD12.138[a]	9.2	10	15	19
2	QP1.1/pNR4.230[a]	22	27	32	46
3	QP1.1/pKD15.071[a]	9.5	12	14	17
4	QP1.1/pNR4.272[a]	23	32	45	51
5	QP1.1/pKD12.138[b]	8.5	11	10	11
6	QP1.1/pNR4.230[b]	19	22	22	23

[a]glucose-limited fermentor-controlled conditions. [b]glucose-rich fermentor-controlled conditions.

Table 3. DAHP synthase specific activities for various strains cultured under different conditions.

entry	constructs	DAHP synthase (U/mg)			
		12 h	24 h	36 h	48 h
1	QP1.1/pKD12.138[a]	0.40	0.33	0.22	0.16
2	QP1.1/pNR4.230[a]	0.71	0.29	0.20	0.10
3	QP1.1/pKD15.071[a]	0.65	0.73	0.43	0.30
4	QP1.1/pNR4.272[a]	0.94	1.29	0.80	0.44
5	QP1.1/pKD12.138[b]	0.46	1.05	0.90	0.74
6	QP1.1/pNR4.230[b]	0.44	1.73	1.57	0.73

[a]glucose-limited fermentor-controlled conditions. [b]glucose-rich fermentor-controlled conditions.

Increasing *aroE*-encoded shikimate dehydrogenase activity seems to be essential to increase quinic acid production. In plasmid pKD12.138, the $P_{tac}P_{aroE}aroE$ gene was derived from plasmid pIA321,[27] where the transcription of *aroE* is under the control of P_{aroE} and P_{tac} tandom promoters. Plasmid pLZ1.169[33] contained the same set of gene as that of pKD12.112 except pLZ1.169 expressed the *aroE* open reading frame directly under the control of a P_{tac} promoter. Plasmid pNR4.230 was then constructed by cloning a 2.2-kb *tktA* gene excised from plasmid pSK4.203 into pLZ1.169 (Figure 25).

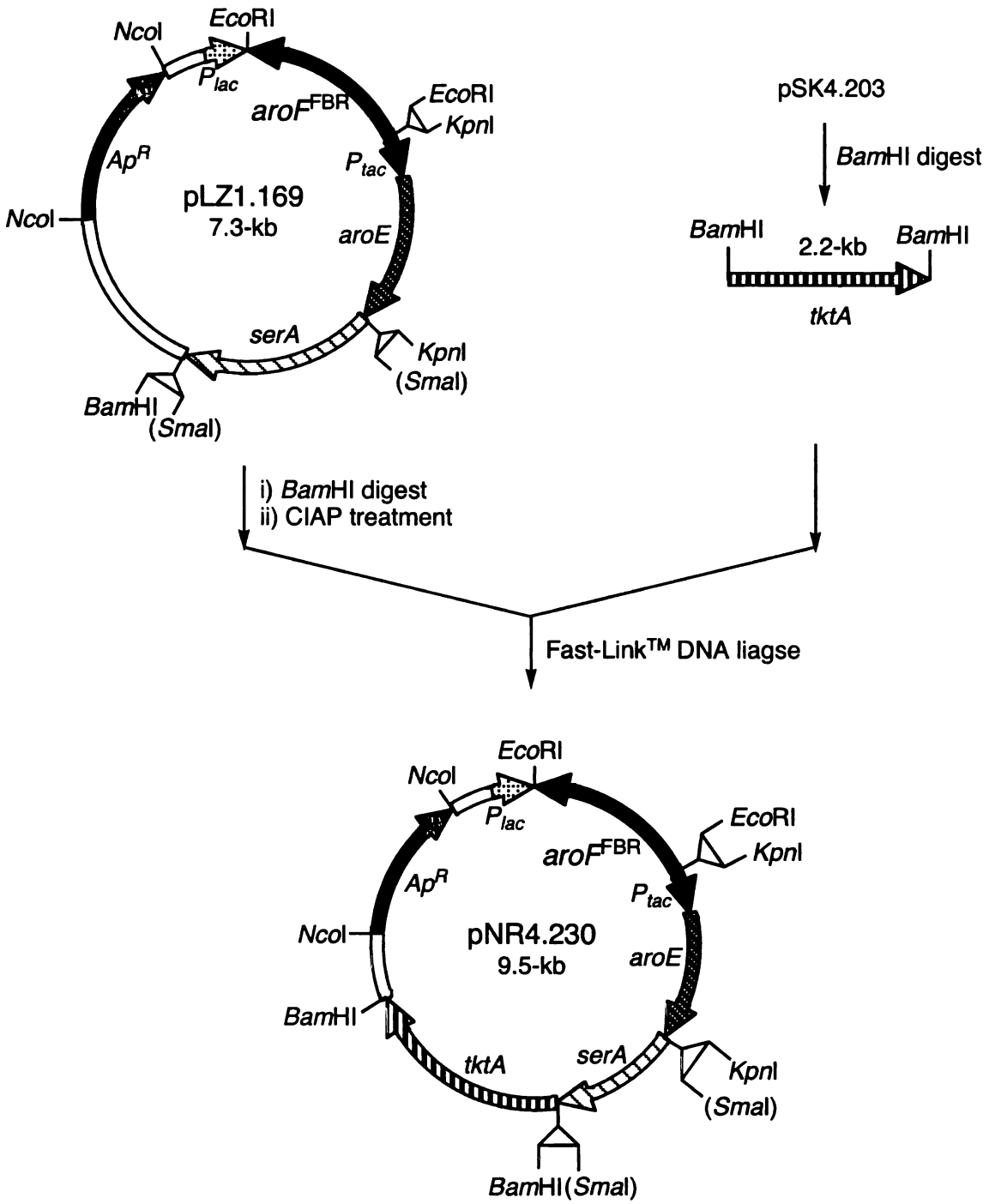

Figure 25. Construction of plasmid pNR4.230.

Culturing *E. coli* QP1.1/pNR4.230 under same conditions synthesized 46 g/L of quinic acid and 4.8 g/L of 3-dehydroquinic acid at 48 h (entry 2, Table 1). The maximum concentration of 3-dehydroquinic acid was 7 g/L at 24 h (Figure 26). Comparison of the specific activities obtained for QP1.1/pKD12.138 and QP1.1/pNR4.230 revealed that changing from $P_{tac}P_{aroE}aroE$ to $P_{tac}aroE$ resulted in more than a two-fold increase in shikimate dehydrogenase activity under the same fermentation conditions (entres 1 and 2, Table 2). DAHP synthase specific activities were also about the same in these two constructs (entries 1 and 2, Table 3). The slight decrease in quinic acid concentration synthesized by QP1.1/pNR4.230 compared to QP1.1/pKD12.138 may reflect the metabolic burden caused by the higher expression level of shikimate dehydogenase.

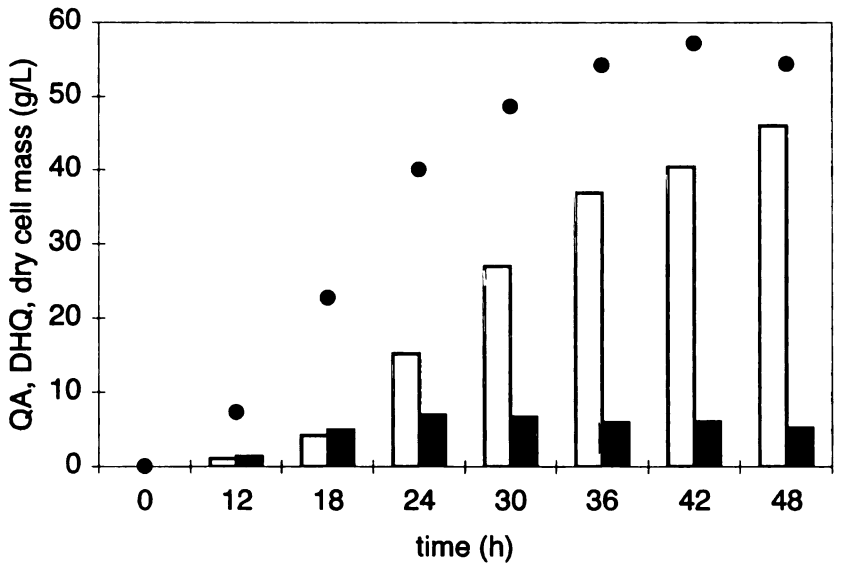

Figure 26. *E. coli* QP1.1/pNR4.230 cultured under glucose-limited, fermentor-controlled conditions. Quinic acid (□), DHQ (■), dry cell mass (●) in g/L.

Circumvent phosphoenolpyruvate consumption by PTS-mediated glucose transport. Microbes such as *E. coli* employ the phosphoenolpyruvate:carbohydrate phosphotransferase (PTS) system for glucose transport with the expenditure of one molecule of phosphoenolpyruvate for one molecule of glucose transported into the cytoplasm.[34] The PTS system is composed of general PTS proteins and carbohydrate-specific proteins. The general PTS proteins include soluble cytoplastic enzyme I (EI) encoded by *ptsI* gene and histidine protein (HPr) encoded by *ptsH* gene that participate in transferring a phospho group from phosphoenolpyruvate to carbohydrates-specific PTS proteins. The glucose specific PTS proteins are composed of soluble *crr*-encoded IIA^{Glc} and *ptsG*-encoded membrane-bound permease $IICB^{Glc}$ (Figure 27).

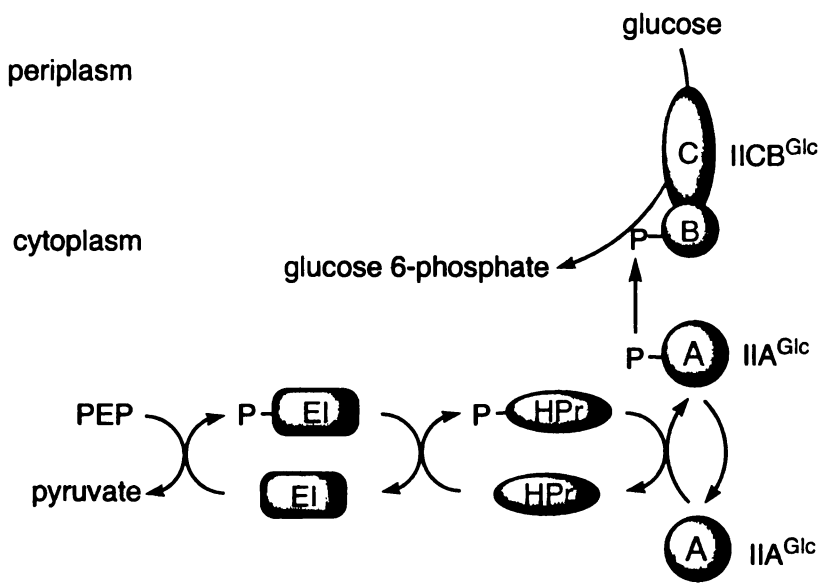

Figure 27. Schematic of glucose transport and phosphorylation using PTS system. Abbreviations: PEP, phosphoenolpyeuvate; EI, PTS enzyme I; HPr, PTS HPr protein; IIA^{Glc}, glucose-specific PTS soluble component; $IICB^{Glc}$, glucose-specific PTS membrane component.

As shown in Figure 27, the phosphoryl group is transferred from phosphoenolpyruvate to EI, then to HPr, and finally to IIA^{Glc}. Phosphorylated IIA^{Glc}

phosphorylates the membrane-bound $IICB^{Glc}$ that subsequently catalyzes the transport and phosphorylation of glucose. Utilization of phosphoenolpyruvate by PTS for glucose transport has been known to limit the yields of biosynthesis of shikimate pathway metabolites.[35] The PTS-generated pyruvate is further metabolized and not recycled to phosphoenolpyruvate under normal aerobic culture conditions.

Phosphoenolpyruvate synthase-mediated pyruvate recycling to alleviate phosphoenolpyruvate limitation, first demonstrated by Patnaik et al,[36] has been successively exploited to improve the titers and yields of shikimate pathway products such as DAHP,[36] 3-dehydroshikimic acid,[37] and shikimic acid.[38] *E. coli ppsA*-encoded phosphoenolpyruvate synthase catalyzes the conversion of pyruvate with adenosine triphosphate (ATP) to form phosphoenolpyruvate, adenosine monophosphate (AMP) and inorganic phosphate.[36] When phosphoenolpyruvate synthase fully recycles PTS-generated pyruvate to phosphoenolpyruvate, the theoretical maximum yield for the synthesis of 3-dehydroquinic acid from glucose will be doubled to 86% (mol/mol). The detailed analysis of this yield enhancement is deferred to Chapter 4.

In an effort to increase the intercellular availability of phosphoenolpyruvate, plasmid pKD15.071 was constructed by plasmid localization of the *ppsA* gene into pKD12.138 (Figure 30).[31] The transcription of *ppsA* was under the control of its own promoter. *E. coli* QP1.1 transformed with pKD15.071 was cultivated under fed-batch fermentation conditions for 48 h (Figure 28). The resulting 49 g/L quinic acid that was synthesized was identical to that observed in *E. coli* QP1.1/pKD12.138 (entry 3 vs. entry 1, Table 1). The final 3-dehydroquinic acid concentration increased to 11 g/L, resulting in a final QA:DHQ molar ratio of 4.5. Although the total production of quinic acid and

3-dehydroquinic acid was increased, the improvement was not reflected in the concentration of quinic acid synthesized, but in the accumulation of more 3-dehydroquinic acid in culture supernatant. The total yield of quinic acid and 3-dehydroquinic acid remained unchanged relative to that achieved with *E. coli* QP1.1/pKD12.138 (entry 3 vs. entry 1, Table 1).

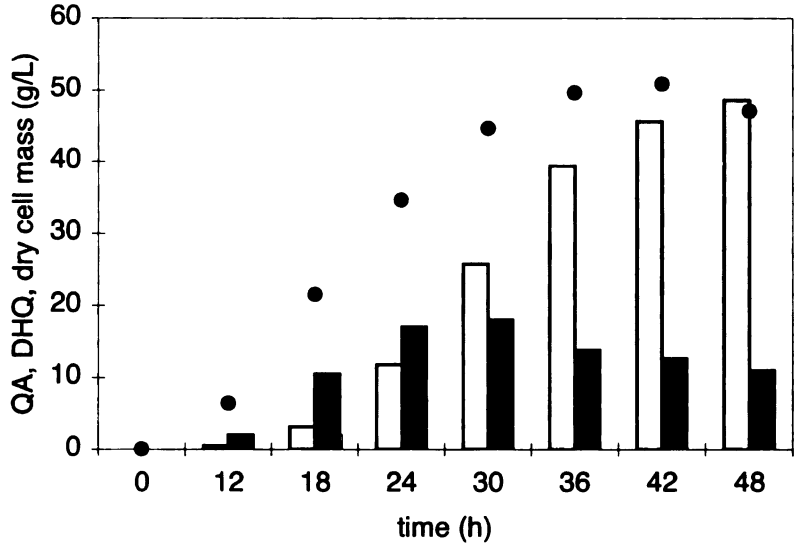

Figure 28. *E. coli* QP1.1/pKD15.071 cultured under glucose-limited, fermentor-controlled conditions. Quinic acid (□), DHQ (■), dry cell mass (●) in g/L.

The increased 3-dehydroquinic acid accumulation observed in fermentations of *E. coli* QP1.1/pKD15.071 prompted examination of the impact of phosphoenolpyruvate synthase overexpression in *E. coli* construct QP1.1/pNR4.230 which showed a 2-fold higher shikimate dehydrogenase activity (entry 2 vs. entry 1, Table 2). The 3.0-kb *ppsA* gene was cloned into pNR4.230 in the same fashion as in pKD15.071 (Figure 31). Culturing QP1.1/pNR4.272 under the same conditions resulted in 56 g/L of quinic acid in 20% (mol/mol) yield and 7.7 g/L of 3-dehydroquinic acid in 2.8% (mol/mol) yield (Figure 29 and entry 4, Table 1).

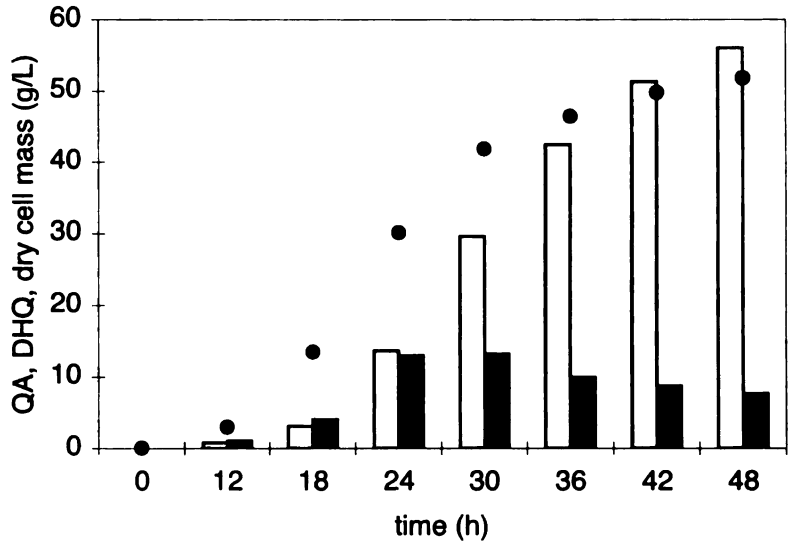

Figure 29. *E. coli* QP1.1/pNR4.272 cultured under glucose-limited, fermentor-controlled conditions. Quinic acid (□), DHQ (■), dry cell mass (●) in g/L.

The increase in the concentration of quinic acid and the increase in yield achieved by *E. coli* QP1.1/pNR4.272 relative to *E. coli* QP1.1/pKD12.138 represent a modest improvement attendant with doubling the shikimate dehydrogenase activity and overexpression of phosphoenolpyruvate synthase. Increased shikimate dehydrohenase expression level also has a negative impact on phosphoenolpyruvate synthase activity. The measured phosphoenolpyruvate synthase activity is lower in construct *E. coli* QP1.1/pNR4.272 than that in *E. coli* QP1.1/pKD15.071 (entry 1 vs. 2, Table 4).

Table 4. Phosphoenolpyruvate synthase specific activity during fermentation runs.

entry	constructs[a]	PEP synthase (U/mg)			
		12 h	24 h	36 h	48 h
1	QP1.1/pKD15.071	0.05	0.05	0.04	0.06
2	QP1.1/pNR4.272	0.03	0.04	0.02	0.01

[a]glucose-limited fermentor-controlled conditions.

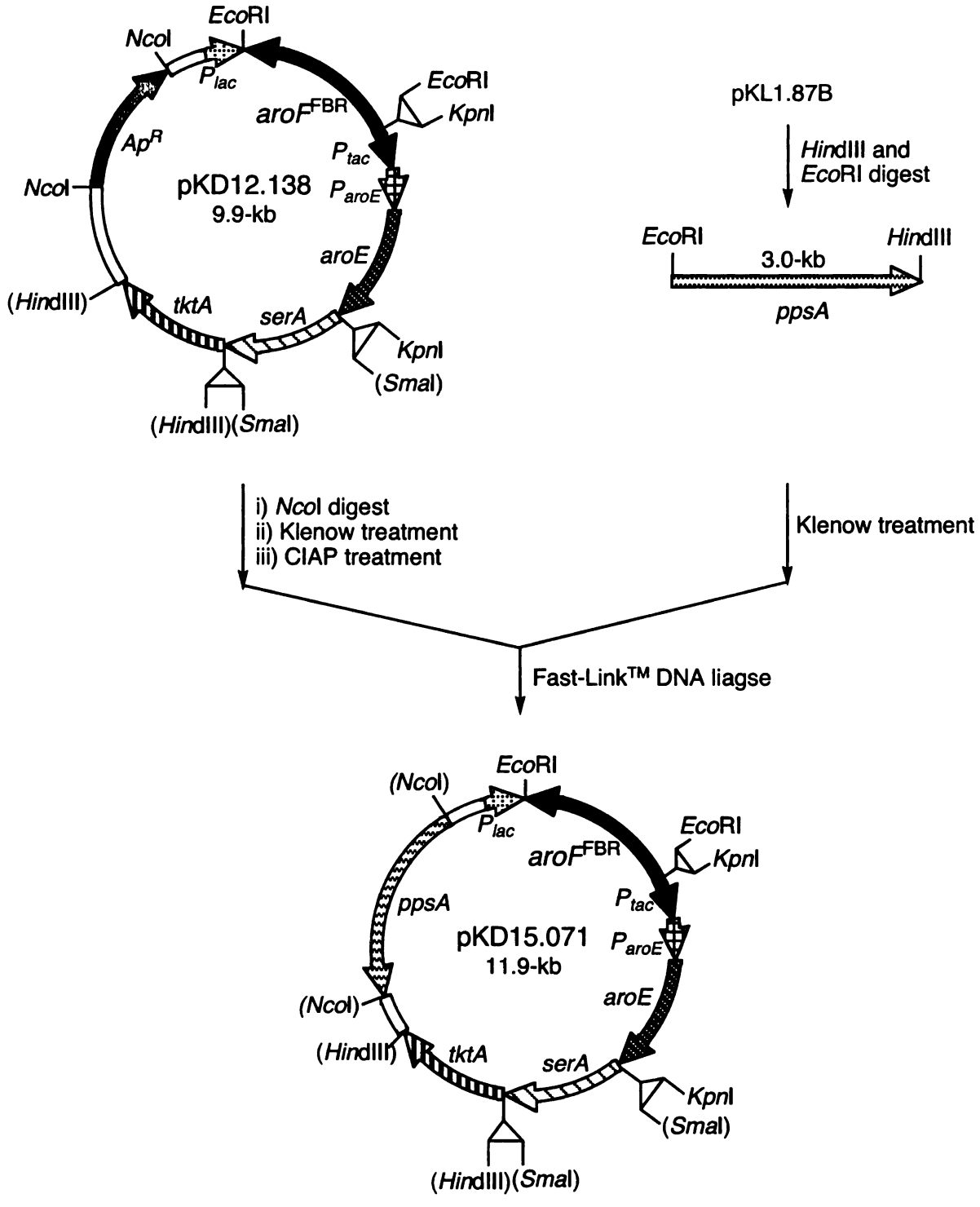

Figure 30. Construction of plasmid pKD15.071.

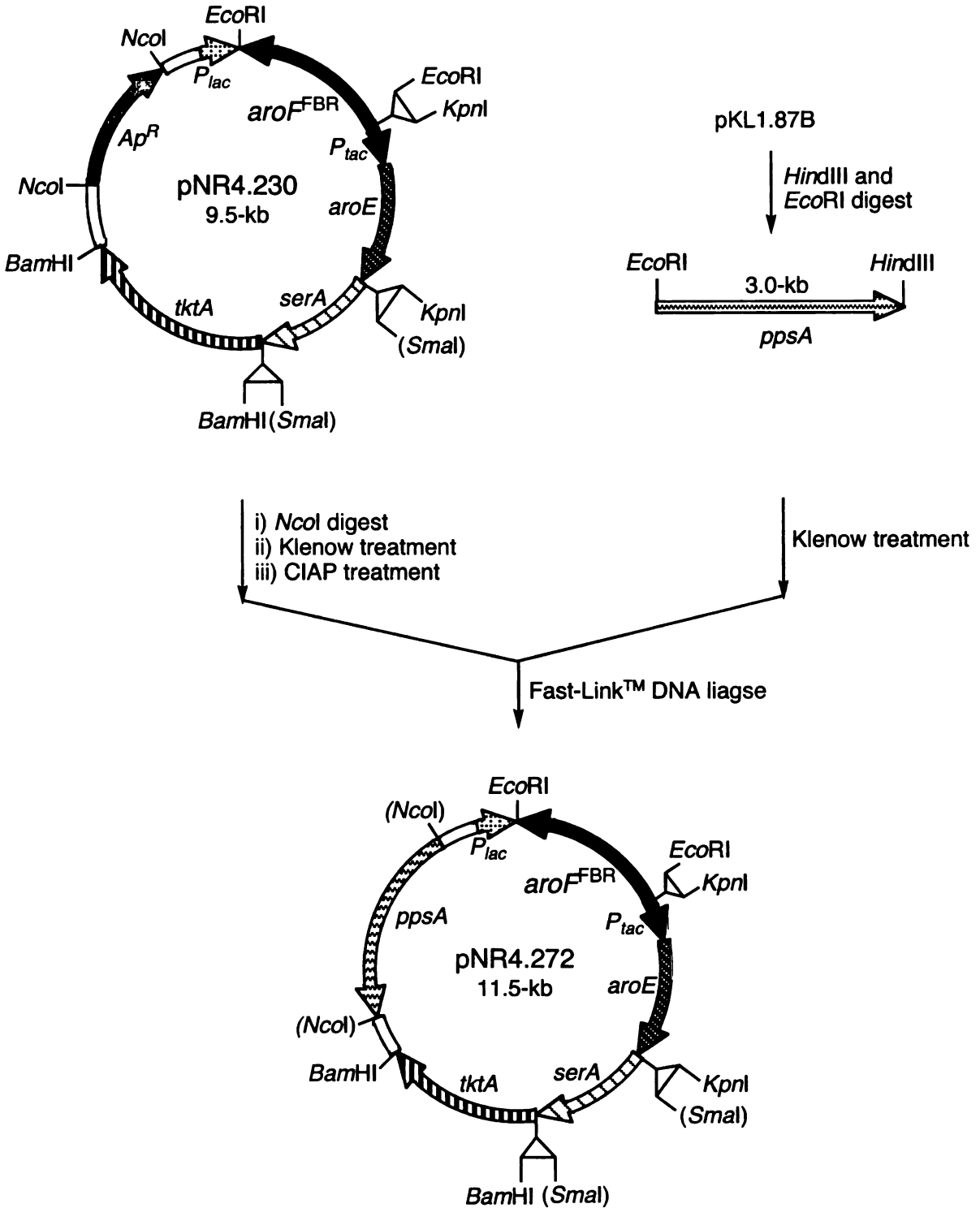

Figure 31. Construction of plasmid pNR4.272.

Another reported strategy to avoid expenditure of phosphoenolpyruvate by PTS is utilization of a non-PTS system for glucose transport. Non-PTS glucose transport includes *Zymomonas mobilis glf*-encoded glucose facilitator[39] and *E. coli galP*-encoded galactose-proton symport.[40] After entry, glucose is phosphorylated by *Z. mobilis* or *E. coli glk*-encoded glucokinase to produce glucose 6-phosphate (Figure 32). It has been demonstrated that the *Z. mobilis* glucose facilitator and glucokinase can complement glucose transport and phosphorylation in *E. coli* strain lacking a functional native PTS system.[39]

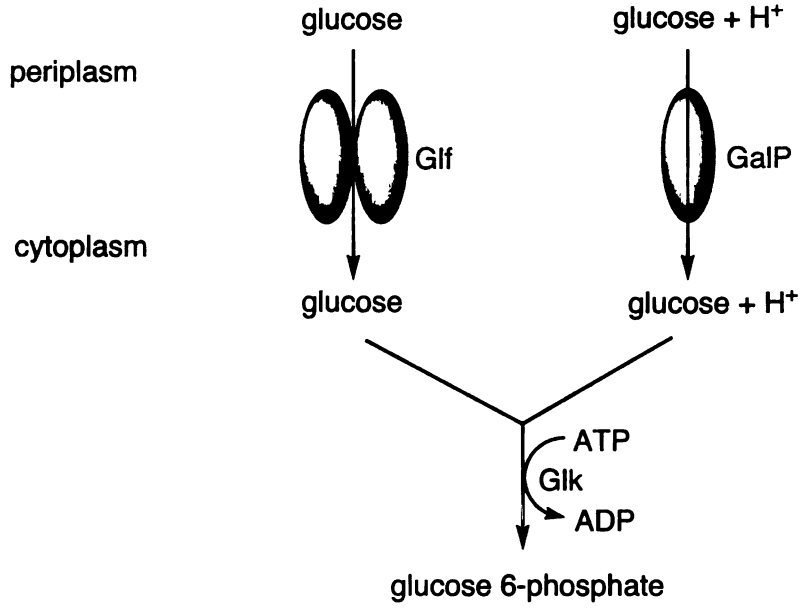

Figure 32. Schematic of non-PTS glucose transport and phosphorylation.

The effect of expression of *Z. mobilis glf* and *glk* genes in a non-PTS *E. coli* host for the production of quinic acid was evaluated. *E. coli* QP1.1*pts* was constructed by disruption of the *ptsH*, *ptsI* and *crr* genes involved in the PTS-mediated glucose transport system by P1 phage transduction of *E. coli* QP1.1 using *E. coli* TP2811[41] (*Δ(ptsH, ptsI,*

crr)::Kan^R) as the donor strain. Plasmid pSC6.090[38] that was prepared by inserting a *glfglk* cassette under the transcriptional control of a P_{tac} promoter into plasmid pKD12.138 was then transformed into *E. coli* QP1.1*pts*. However, *E. coli* QP1.1*pts*/pSC6.090 cultivated under glucose-rich fermentor-controlled conditions grew slowly and failed to reach the stationary phase of growth. This is in contrast with a previously examined shikimate-synthesizing *E. coli* SP1.1*pts*/pSC6.090 which synthesized 71 g/L of shikimic acid in 27% (mol/mol) yield from glucose.[38]

3-Dehydroquinic acid recapture under glucose-limited conditions. The profile of 3-dehydroquinic acid synthesized under glucose-limited, fermentor-controlled conditions suggested an intriguing possibility that *E. coli* QP1.1 could transport 3-dehydroquinic acid previously synthesized and exported into the culture medium back into the cytoplasm and subsequently reduce it to quinic acid. To verify this hypothesis, *E. coli* QP1.1/pNR4.276, a construct incapable of *de novo* synthesizing quinic acid from glucose, was constructed. The *aroF*^{FBR} gene in the plasmid pNR4.230 was inactivated by a four-nucleotide frame shift to create the plasmid pNR4.276 (Figure 33). As a result, *E. coli* QP1.1/pNR4.276 expressed DAHP synthase only from its chromosomal *aroF*, *aroG*, and *aroH* loci. All of the DAHP synthase activity expressed in *E. coli* QP1.1/pNR4.276 was then sensitive to feedback inhibition by L-tyrosine, L-phenylalanine, and L-tryptophan added into the fermentation medium.

E. coli QP1.1/pNR4.276 was cultured under glucose-limited conditions with the addition of L-tyrosine (0.35 g), L-phenylalanine (0.35 g), and L-tryptophan (0.175 g) every 6 h staring from 12 h and continuing until 36 h to inhibit native DAHP synthase

activities. The absence of quinic acid and 3-dehydroquinic acid in a control experiment indicated an effective inhibition of DAHP synthase under this condition.

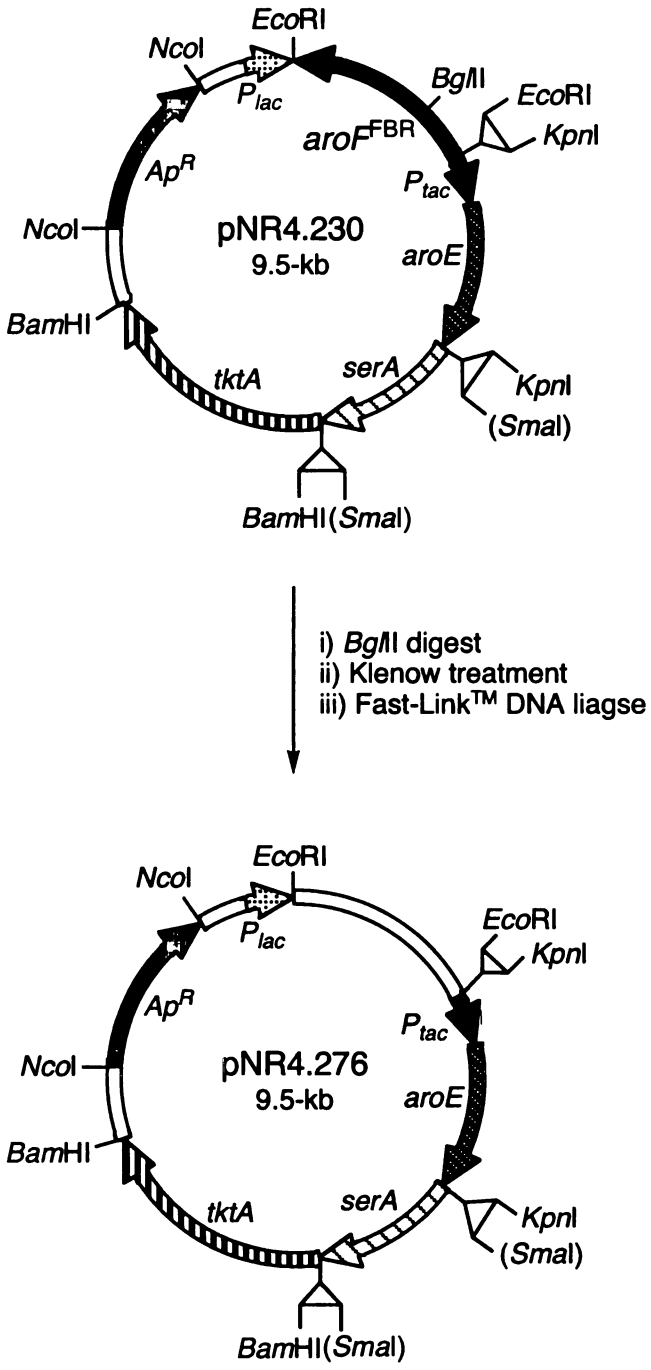

Figure 33. Construction of plasmid pNR4.276.

3-Dehydroquinic acid was synthesized from quinic acid in 5 steps according to a method described previously (Figure 34).[42] The *trans*-diol of methyl quinate was selectively protected with 2,3-butane bisacetal[43] followed by transesterification to afford the benzyl ester of protected quinate **7**. Oxidation of compound **7** with KIO_3 in the presence of a catalytic amount of $RuCl_3$ gave fully protected dehydroquinate **8**. Acid hydrolysis of the 2,3-butane bisacetal protecting group followed by catalytic hydrogenation of the benzyl ester **9** afforded 3-dehydroquinic acid in 36% total yield from quinic acid. A recently reported synthesis of 3-dehydroquinic acid utilized the similar reaction sequence for conversion of quinic acid to 3-dehydroquinic acid.[44]

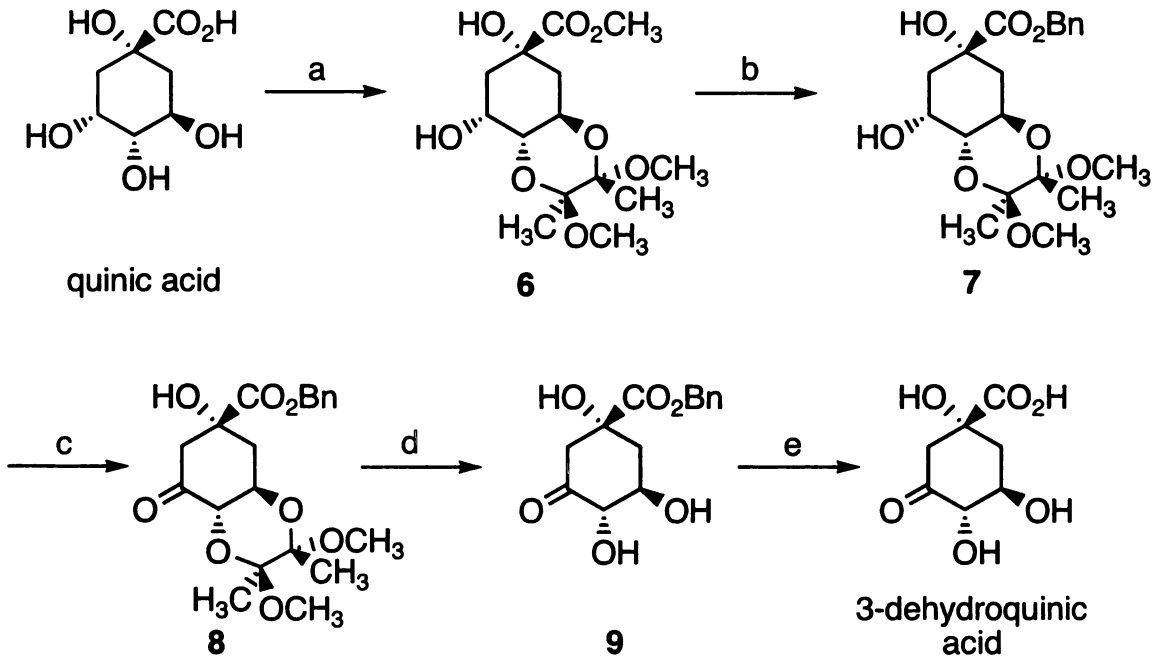

Figure 34. Synthesis of 3-dehydroquinic acid from quinic acid. Keys: (a) i) Dowex-50 (H^+), MeOH, reflux; ii) trimethylorthoformate, 2,3-butanedione, (±)-10-camphosulfornic acid, 66%; (b) $(Bu_2SnCl)O(Bu_2SnOH)$ (0.05 equiv.), BnOH (2 equiv.), toluene, reflux; (c) $RuCl_3$ (0.03 equiv.), KIO_3 (3 equiv.), benzyltrimethyl ammonium chloride (0.02 equiv.), room temperature, 67%; (d) CF_3CO_2H/H_2O (20:1, v/v), CH_2Cl_2, 0 °C, 2 h, 82%; (e) Pd/C (0.05 equiv.), H_2, 50 psi, THF/H_2O (1:1, v/v), 97%.

The synthesized 3-dehydroquinic acid (5.0 g) was added into *E. coli* QP1.1/pNR4.276 culture medium at 18 h again with the same aromatic amino acid supplements as in the control experiment to inhibit *E. coli* native DAHP synthase activities. Formation of quinic acid was observed 6 h after the addition of 3-dehydroquinic acid (Figure 35). At 48 h, 2.5 g/L of quinic acid and 2.1 g/L of 3-dehydroquinic acid were present in the culture supernatant. This result indicates that recapture of 3-dehydroquinic acid from culture medium into *E. coli* cytoplasm and subsequent reduction by shikimate dehydrogenase operate in this construct under glucose-limited fermentor-controlled condition.

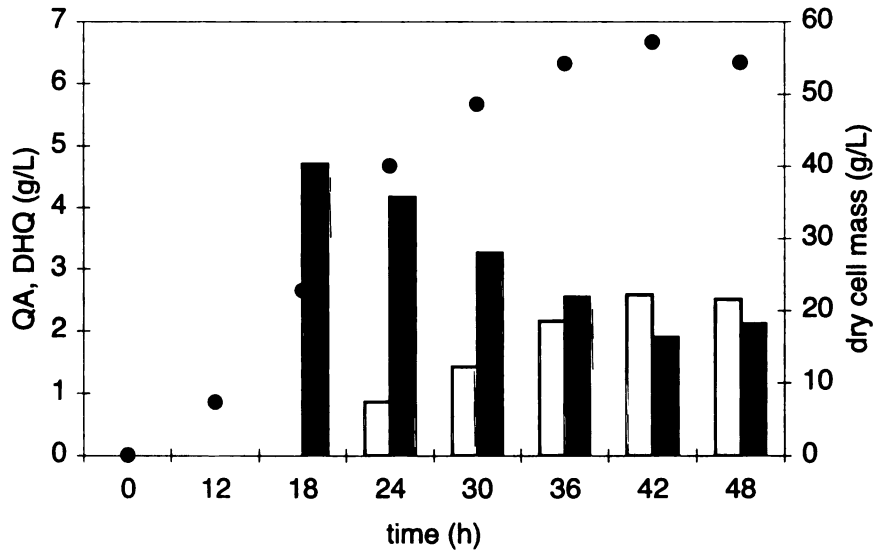

Figure 35. Biosynthesis of quinic acid from the added 3-dehydroquinic acid by *E. coli* QP1.1/pNR4.276 under glucose-limited, fermentor-controlled conditions. Quinic acid (□), DHQ (■), dry cell mass (●) in g/L.

Biosynthesis of quinic acid under glucose-rich, fermentor-controlled conditions. Glucose-rich fermentation where glucose is constantly added to the fermentation vessel at a rate sufficient to maintain a glucose concentration between 50 mM and 160 mM is an effective method for increasing the flow of carbon directed into the shikimate pathway.[45] However, culturing *E. coli* QP1.1/pKD12.138 at 33°C, pH 7.0, D.O. 10% under the glucose-rich conditions, only led to the formation of 25 g/L of quinic acid and 46 g/L of 3-dehydroquinic acid by 48 h (Figure 36). Examination of the DAHP synthase specific activities under this condition revealed higher activities compared to that of the same construct cultivated under glucose-limited condition (entry 5 vs. entry 1, Table 3). However, the shikimate dehydrogenase activities declined significantly. It remained at a stable level of approximately 10 units/mg throughout the fermentation run under glucose-rich condition, as compared to a gradual increase from 9 to 19 units/mg under glucose-limited condition (entries 5 and 1, Table 2).

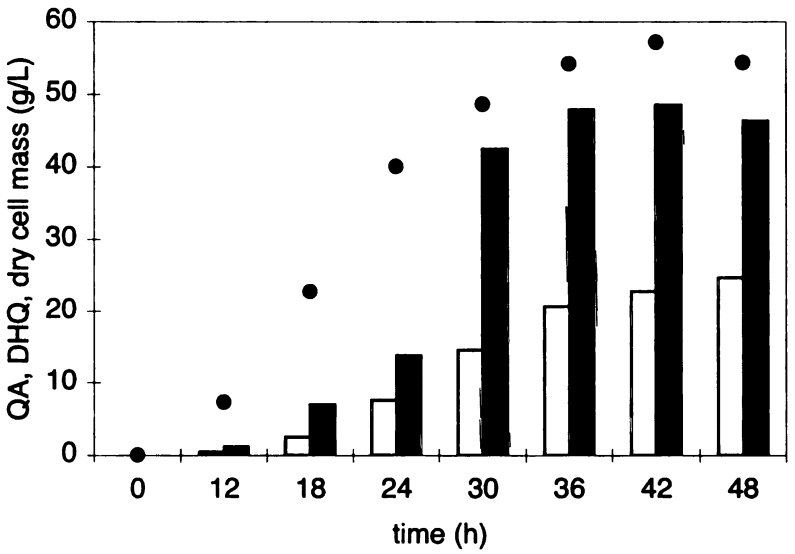

Figure 36. *E. coli* QP1.1/pKD12.138 cultured under glucose-rich, fermentor-controlled conditions. Quinic acid (□), DHQ (■), dry cell mass (●) in g/L.

Cultivation of *E. coli* QP1.1/pNR4.230 (Figure 37) under glucose-rich, fed-batch conditions synthesized 39 g/L of quinic acid in 12% (mol/mol) yield and 31 g/L of 3-dehydroquinic acid in 9.3% (mol/mol) yield (entry 6, Table 2) by 48 h. The increase of 14 g/L of quinic acid relative to QP1.1/pKD12.138 corresponded to a decline of 15 g/L of 3-dehydroquinic acid. Comparison of the enzyme activities revealed a two-fold increase in shikimate dehydrogenase activities (entry 6 vs. entry 5, Table 2) and similar DAHP synthase activities (entry 6 vs. entry 5, Table 3). The two-fold increased expression of shikimate dehydrogenase increased the concentration of synthesized quinic acid significantly under glucose-rich conditions.

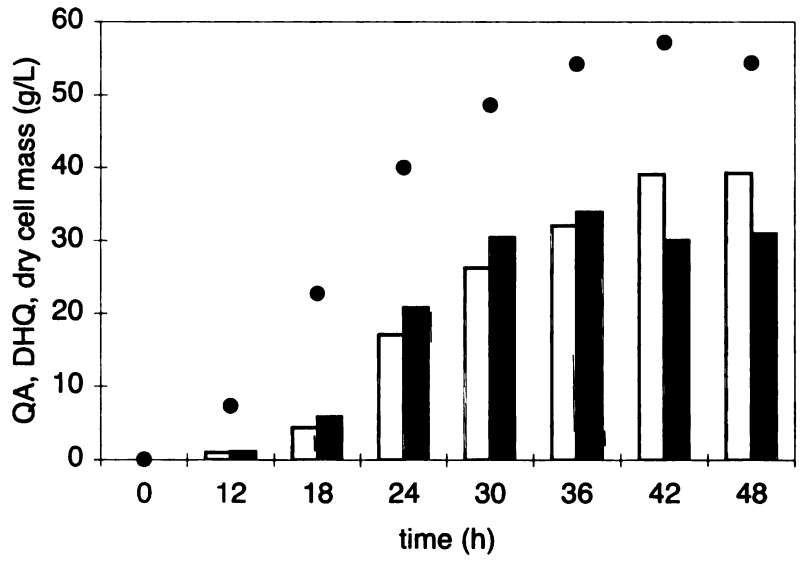

Figure 37. *E. coli* QP1.1/pNR4.230 cultured under glucose-rich, fermentor-controlled conditions. Quinic acid (□), DHQ (■), dry cell mass (●) in g/L.

Biosynthesis of quinic acid in a *E. coli* QP1.1 mutant devoid of catabolite repression by glucose. The accumulation of substantial concentrations of 3-dehydroquinic acid under glucose-rich fermentation conditions can not be solely

attributed to the lower expression of shikimate dehydrogenase since the shikimate dehydrogenase activities of QP1.1/pNR4.230 under glucose-rich fermentation conditions were even higher than those of OP1.1/pKD12.138 under glucose-limited conditions (entry 6 vs. entry 1, Table 2). One possibility is that *E. coli* can not transport back and reduce 3-dehydroquinic acid previously synthesized and exported into the fermentation medium due to catabolite repression by glucose that is present in high concentrations under glucose-rich condition.

In addition to its role in carbohydrate transport, the PTS system is also known to be involved in the regulation of catabolite repression.[34] In an attempt to disrupt catabolite repression in *E. coli* QP1.1 strain by glucose, a mutation in *E. coli ptsG* locus was introduced into *E. coli* QP1.1 by P1-phage mediated transduction of *ptsG::Tn5* from *E. coli* IT1168.[46] As described previously, *ptsG* encodes a transmembrane $IICB^{GLC}$ protein in the *E. coli* phosphoenolpyruvate-dependent glucose phosphotransferase (PTS) system for transport and phosphorylation of glucose to glucose 6-phosphate (Figure 26).[47] The $IICB^{GLC}$ protein is phosphorylated by phosphorylated IIA^{GLC} protein. In the presence of high glucose concentration, the IIA^{GLC} protein is subsequently dephosphorylated. The dephosphorylated IIA^{GLC} protein binds to and inactivates a number of non-PTS carbohydrates permeases.[34] Disruption of the *ptsG* gene has been shown to result in a loss of catabolite repression by glucose.[48] *E. coli* QP1.1*ptsG* formed blue colonies on X-gal indicator plate containing glucose and lactose. The formation of blue colonies indicated expression of β–galactosidase in the presence of glucose due to the inactivation of catabolite repression. The effect of introducing the *ptsG* mutation on quinic acid production was tested on *E. coli* QP1.1*ptsG*/pKD12.138, which was cultivated under

glucose-rich fed-batch fermentation conditions. Over a period of 48 h, *E. coli* QP1.1*ptsG*/pKD12.138 synthesized 36 g/L of 3-dehydroquinic acid and 26 g/L of quinic acid (Figure 38). The concentration and yield of quinic acid synthesized by *E. coli* QP1.1/pKD12.138 and *E. coli* QP1.1*ptsG*/pKD12.138 were essentially the same (entry 5 vs. entry 7, Table 1). The decline in total production relative to *E. coli* QP1.1/pKD12.138 may reflect a slower rate of glucose transport by inactivating the major glucose transport protein. Glucose transport in *E. coli* QP1.1*ptsG* could occur less efficiently via one or more of the receptors belonging to the glucose, mannitol or mannose family of proteins that are not specific for glucose transport.[34]

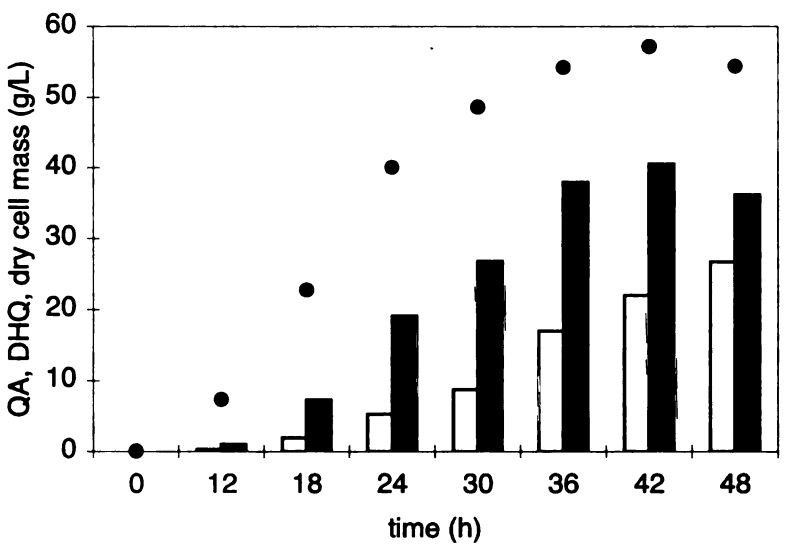

Figure 38. *E. coli* QP1.1*ptsG*/pKD12.138 cultured under glucose-rich, fermentor-controlled conditions. Quinic acid (□), DHQ (■), dry cell mass (●) in g/L.

In summary, a microbial route to quinic acid by *E. coli* QP1.1/pNR4.272 has achieved a titer of 56 g/L and 20% (mol/mol) yield from glucose under glucose-limited, fermentor-controlled condition.

co

pe

m

or

co

pl

tr

de

E

ac

Q

Q

ie

th

by

al

3

m

ac

sy

ac

Hydroquinone Toxicity. The toxicity of hydroquinone toward ethanologenic *E. coli* cultured on xylose under fermentative conditions has been analyzed from the perspective of hydroquinone's inhibition of sugar catabolism and damage to the plasma membrane.[49] To gauge the toxicity of hydroquinone toward *E. coli* cultured aerobically on glucose, a 3-dehydroquinic acid-synthesizing *E. coli* QP1.1/pKL4.33[24a] was used. *E. coli* QP1.1/pKL4.33 differs from *E. coli* QP1.1/pKD12.138 only in the absence of plasmid-localized *aroE* encoding shikimate dehydrogenase and *tktA* encoding transketolase. Utilization of *E. coli* QP1.1/pKL4.33 that only synthesizes 3-dehydroquinic acid for analysis of hydroquinone's toxicity avoided the complication with *E. coli* QP1.1/pKD12.138 that synthesized a mixture of quinic acid and 3-dehydroquinic acid. The fermentor conditions used to culture 3-dehydroquinate-synthesizing *E. coli* QP1.1/pKL4.33 were based on the parameters used to culture quinate-synthesizing *E. coli* QP1.1/pKD12.138. A sterile, aqueous solution of hydroquinone was added to the fermentor run to a final concentration of 2 g/L at 12 h.

E. coli QP1.1/pKL4.33 was able to grow and synthesize 3-dehydroquinic acid in the presence of added hydroquinone. However, 3-dehydroquinic acid synthesis dropped by approximately 50% upon addition of hydroquinone (Figure 39a). Less cell mass was also formed (Figure 39a) and increased amounts of acetic acid were produced (Figure 39b) in the presence of added hydroquinone. The specific activity of DAHP synthase did not significantly change over the course of the fermentor run when hydroquinone was added. As the first enzyme in the common pathway, the specific activity of DAHP synthase significantly determines carbon flow directed into synthesis of 3-dehydroquinic acid.[50] The reduced concentration of synthesized 3-dehydroquinic acid, reduction in cell

mass, and increased production of acetic acid observed for *E. coli* QP1.1/pKL4.33 indicate that hydroquinone concentrations as low as 2 g/L are toxic to *E. coli* growth and metabolism.

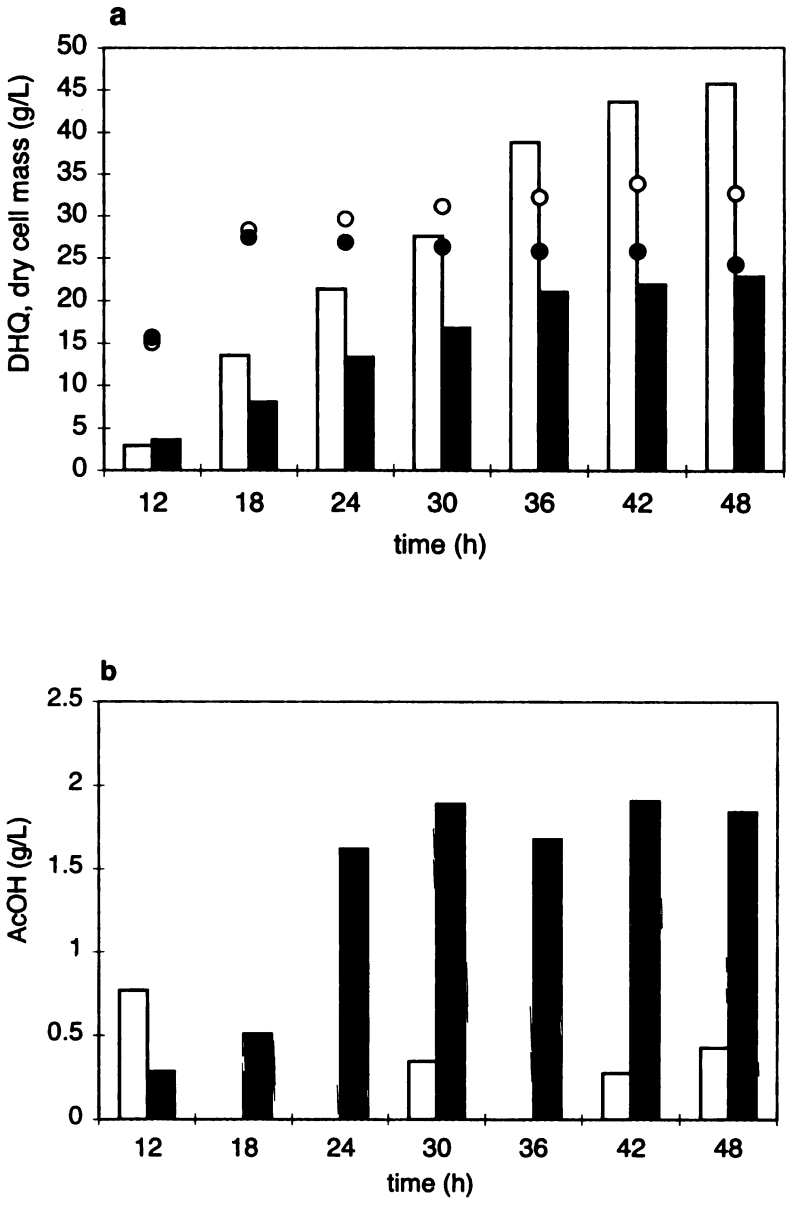

Figure 39. 3-Dehydroquinate-synthesizing *E. coli* QP1.1/pKL4.33. (a) 3-Dehydroquinic acid (DHQ) synthesis and *E. coli* cell mass in the absence (□) vs. presence (■) of added hydroquinone; (b) Acetic acid formation in the absence (□) vs. presence (■) of added hydroquinone.

Chemical synthesis of hydroquinone from quinic acid.

The literature method that used magnesium (IV) dioxide for oxidation of quinic acid to hydroquinone[6,51] resulted in a low yield and formation of salts as byproducts. New chemical methodology was needed to significantly increase the yield and eliminate the byproducts. Reagents were needed that were sufficiently robust for use in fermentation broths while being mild enough to avoid overoxidation of hydroquinone to benzoquinone.

The conversion of quinic acid to hydroquinone can be viewed to proceed via an oxidative decarboxylation followed by dehydration and subsequent aromatization to hydroquinone. Chemical methods for oxidative decarboxylation of α-hydroxycarboxylic acids involves the use of a variety of oxidants including periodate,[52] permanganate,[53] chromic acid,[54] lead acetate[55] and hypochlorite.[56] Among these, hypochlorite is easily available, cheap and an environmentally acceptable chemical (bleaching agent). Hypochlorite has been well established as a versatile oxidant in organic chemistry. Diols, diones and α-hydroxyketones are easily cleaved oxidatively with hypochlorites.[57] Hypochlorite-induced oxidative decarboxylation of α-hydroxycarboxylic acids and α-keto acids have been reported in the literature. Nwaukwa et al.[58] reported conversions of α-hydroxy carboxylic acids into lower carboxylic acid homologs with calcium hypochlorite in aqueous acetonitrile-acetic acid solutions. Carlsen[56] reported oxidation of α-hydroxyacids exclusively to the corresponding aldehydes with sodium hypochlorite in a two-phase ether-water solvent system without the addition of acetic acid. Elmore et al.[59] extended the hypochlorite-induced oxidative decarboxylation to trisubstituted acetic acid compounds.

Hypochlorite oxidations of quinic acid. A typical fermentation broth of *E. coli* QP1.1/pNR4.272 contains 290 mM ammonium quinate, 44 mM ammonium 3-dehydroquinate, approximately 1 M ammonium salts, 43 mM potassium phosphate and around 50 g/L of cell mass. Ammonium hydroxide along with 1 M H_2SO_4 were added to the culture medium to maintain the pH at 7 during fermentation runs.

The quinic acid fermentation broth was partially purified to remove *E. coli* cells, proteins and ammonium salts. *E. coli* cells were removed by centrifugation. Heating the culture supernatant to reflux followed by acidification resulted in precipitation of proteins, which were removed by centrifugation. The clarified fermentation broth was then decolorized with activated charcoal. 3-Dehydroquinic acid could be removed from quinic acid broth by converting it into protocatechuic acid upon reflux with acid and was subsequently removed during the charcoal decolorization step. Initial attempts at oxidative decarboxylation of quinic acid with sodium hypochlorite (commercial bleach) were carried out in the decolorized fermentation broth. However, hypochlorite oxidation of quinic acid was not observed in lieu of ammonium ion removal. Hence, clarified, decolorized fermentation broth was passed through a strong cation-exchange resin (Dowex 50 H^+) to remove ammonium ion prior to hypochlorite oxidation.

Sodium hypochlorite (3 equivalents) was added to clarified, decolorized, ammonium ion-free fermentation broth. The reaction was then acidified to pH 1.5 – 2 with simultaneous addition of H_2SO_4 (2 M, 1.25 equivalents) and reacted at room temperature to give 3(*R*),5(*R*)-trihydroxycyclohexanone (**10**, Figure 40) based on ^1H NMR analysis of the crude reaction solution. Excess hypochlorite was then quenched with 2-propanol. Without purification, the resulting solution was refluxed under an inert

atmosphere for 10 h. The concentration of cyclohexanone **10** decreased rapidly, the concentration of hydroquinone increased, and α,β-unsaturated enones **11** and **12** accumulated as intermediates (Figure 41).

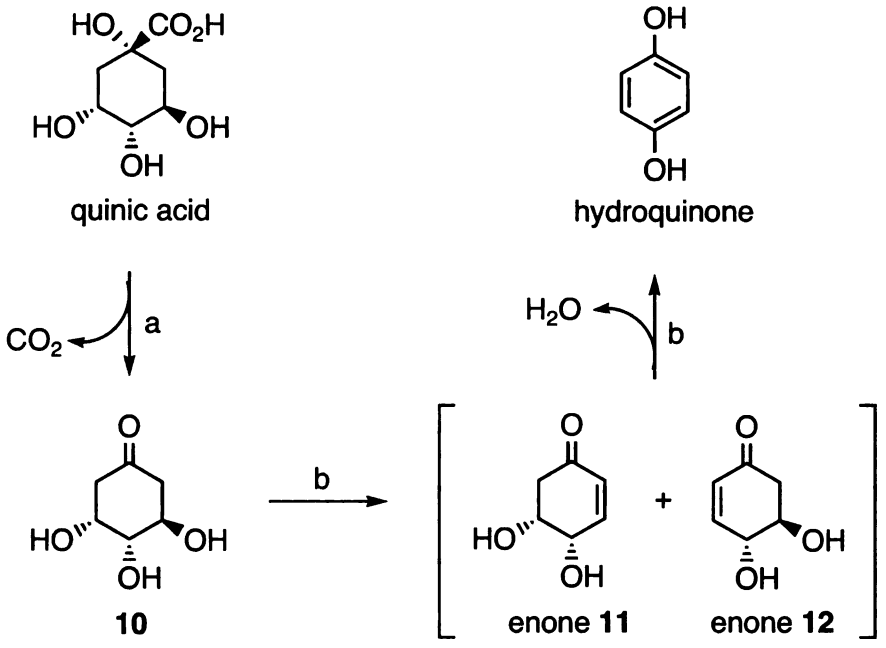

Figure 40. Conversion of quinic acid to hydroquinone. Keys: (a) i) NaOCl, room temperature, ii) 2-propanol, room temperature; (b) reflux.

Identification and quantification of enone intermediates **11** and **12** was accomplished by ^{1}H NMR analysis of aliquots withdrawn from the reaction solution and comparison with the ^{1}H NMR spectra of enones **11** and **12** independently synthesized from 3(*R*),5(*R*)-trihydroxycyclohexanone (**10**) and butane 2,3-bisacetal-protected methyl quinate, respectively (Figure 42). Extraction of the dehydration/aromatization reaction solution with *tert*-butylmethyl ether followed by sublimation afforded hydroquinone in 87% overall isolated yield from quinic acid.

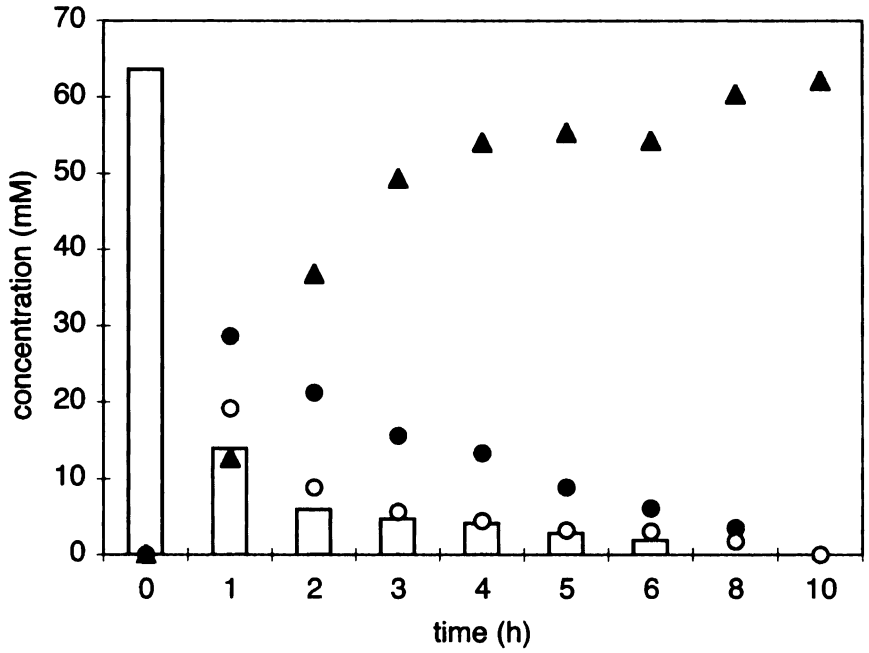

Figure 41. Dehydration and aromatization of 3(*R*),5(*R*)-trihydroxycyclohexanone (10) to hydroquinone. 3(*R*),5(*R*)-trihydroxycyclohexanone (10) (□), 4(*S*),5(*R*)-dihydroxy-2-cyclohexen-1-one (11) (●), 4(*R*),5(*R*)-dihydroxy-2-cyclohex-1-one (12) (○), hydroquinone (▲).

The enone **11** was obtained in a three-step synthesis from quinic acid. The intermediate **13** has been used as a chiral building block in a number of natural product syntheses.[13a,b,60] Synthesis of compound **13** via the 3(*R*),5(*R*)-trihydroxycyclohexanone **10** provided a shorter route compared to the reported synthesis from quinic acid.[61] Removal of the acetonide protecting group of **13** gave *cis*-diol **11** in 23% total yield from quinic acid. Synthesis of enone intermediate **12** utilized selective protection of the *trans*-diol of the methyl quinate with the butane 2,3-bisacetal protecting group.[43] Reduction of the methyl ester with lithium aluminum hydride followed by cleavage of the resulting vicinal diol by $NaIO_4$ afforded the β-hydroxyketone **16**. The hydroxy group was eliminated by acetylation followed by treatment with diisopropylethylamine. Removal of

the butane 2,3-bisacetal protecting group with trifluoroacetic acid afforded *trans*-diol **12** in 40% overall yield from quinic acid.

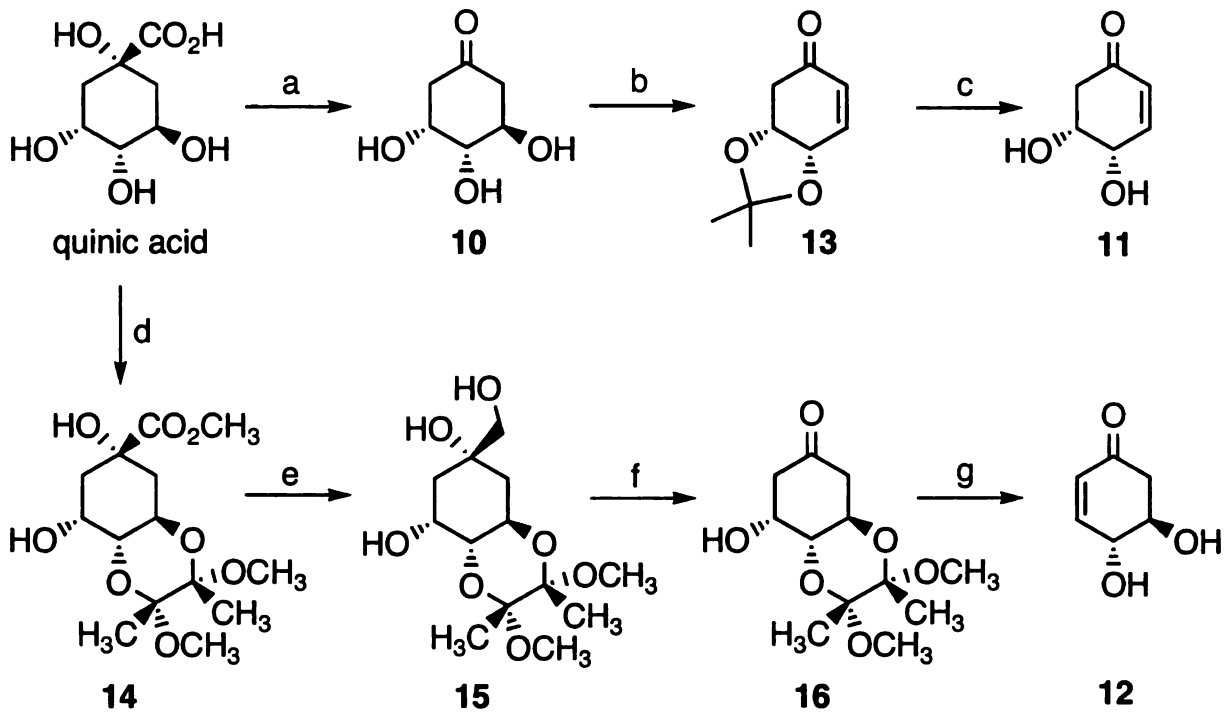

Figure 42. Syntheses of enone intermediates 11 and 12 from quinic acid. Keys: (a) NaOCl, H_2SO_4, rt., 76%; (b) i) acetone, TsOH, rt., 79%; ii) Ac_2O, (i-Pr)$_2$NEt, DMAP, CH_2Cl_2, 0 °C, 91%; (c) CF_3CO_2H/H_2O (2:1, v/v), 0 °C, 43%; (d) i) CH_3OH, Dowex 50(H^+), reflux; ii) 2,3-butanedione, $CH(OCH_3)_3$, CH_3OH, CSA, reflux, 79% (e) $LiAlH_4$, THF, 0 °C, rt., 93% (f) $NaIO_4$, phosphate buffer (pH 7), 0 °C, room temp., 72%; (g) i) Ac_2O, (i-Pr)$_2$NEt, DMAP, CH_2Cl_2, 0 °C, 100%; ii) $CF_3CO_2H/CH_2Cl_2/H_2O$ (9:1:1, v/v/v), 0 °C, 75%.

Electrochemical oxidation. Quinic acid was also converted into 3(*R*),5(*R*)-trihydroxycyclohexanone (**10**, Figure 40) by electrochemical oxidation.[62] The electrolysis was performed at room temperature in a 50 cm^3 electrolysis cell (Figure 43) fitted with a pair of Pt electrodes (2 × 1.35 cm^2). Clarified, decolorized, ammonium ion-free quinic acid fermentation broth was adjusted to pH 10 by addition of 1 N aqueous

NaOH prior to electrolysis. Electrolysis at a current density of 400 mA/cm^2 for 4 h afforded 3(*R*),5(*R*)-trihydroxycyclohexanone **10** in 24% yield along with an 8% yield of formic acid. A total of 25% of unreacted quinic acid remained in the solution. The rest of the quinic acid was likely to be oxidized to CO_2 during the electrolysis. Electrolysis at a higher current density (600 mA/cm^2) or electrolysis for a longer period of time resulted in increased formation of formic acid without increased yields of ketone **10**.

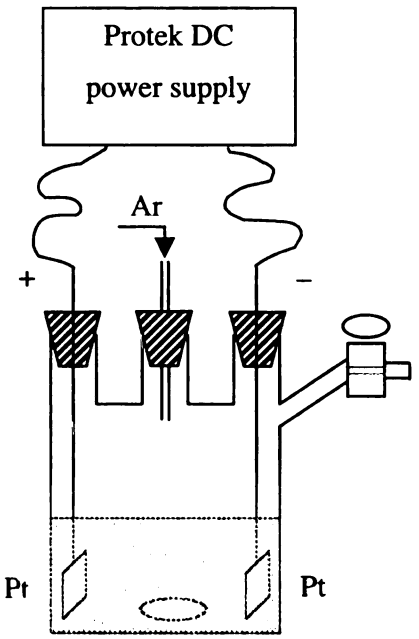

Figure 43. Diagram of electrochemical oxidation apparatus.

Transition metal-mediated oxidation. High-yielding conversion of quinic acid to hydroquinone by transition metal-mediated oxidative decarboxylation was achieved using stoichiometric amounts of Ce^{4+} and V^{5+} salts (Table 1). Oxidation of quinic acid in clarified, decolorized, ammonium ion-free fermentation broth at room temperature with

ceric ammonium sulfate ($(NH_4)_2Ce(SO_4)_3$) followed by refluxing the reaction solution for 10 h afforded hydroquinone in 91% isolated yield (entry 1, Table 5). Addition of vanadium pentoxide (V_2O_5) and H_2SO_4 to quinate-containing fermentation broth, which had been clarified, decolorized, and rendered ammonium ion-free led to an 85% isolated yield of hydroquinone (entry 2, Table 5) after heating the reaction solution to 50 °C and final reaction at reflux for 8 h. The oxidations and associated reaction conditions summarized in Table 5 are noteworthy in the absence of benzoquinone formation resulting from oxidation of the initially formed hydroquinone.

Catalytic oxidative decarboxylation. O_2 is an environmental-friendly oxidant in organic chemistry. Catalytic aerobic oxidative decarboxylation of α-hydroxyacids by a Co(III) *ortho*-phenylene-bis-(*N'*-methyloxamidate) complex in the presence of pivalaldehyde has been reported.[63] However, this reaction was performed in organic solvent and required use of a stoichiometric amount of pivalaldehyde.

In route to identification of metals that could be used in catalytic amounts, CuCl with O_2 as a cooxidant and $FeSO_4$ or $RuCl_3$ with H_2O_2 as the cooxidant were examined.[64] No oxidative decarboxylation of quinic acid in clarified, decolorized, ammonium ion-free fermentation broth was observed. However, use of substoichiometric, catalytic amounts of Ag_3PO_4 along with potassium persulfate ($K_2S_2O_8$) as the cooxidant did lead to oxidative decarboxylation. For these Ag_3PO_4-catalyzed oxidations, removal of ammonium ions was critical. The presence of ammonium ions led to formation of a silver mirror and an absence of hydroquinone formation. Oxidation of quinic acid in partially purified culture supernatant with a catalytic amount of Ag_3PO_4 (10 mol %) and cooxidant $K_2S_2O_8$ heated initially at 50 °C followed by heating of the reaction solution at

reflux afforded an 85% yield of hydroquinone (entry 3, Table 5). Quantities of Ag_3PO_4 catalyst as low as 2 mol % and 1 mol % relative to quinic acid could be used (entries 4 and 5, Table 5) although significant decreases in the yield of hydroquinone obtained were observed.

Table 5. Reaction conditions and yields for chlorine-free oxidation of quinic acid.

entry	oxidant/catalyst (equiv.)[a]	conditions	Hydroquinone yield,[b] %
1	$(NH_4)_2Ce(SO_4)_3$ (2.4)	rt., 30 min; reflux, 10 h	91
2	V_2O_5 (1.1)	50 °C, 4 h; reflux, 8 h	85
3	$K_2S_2O_8$ (1.2)/Ag_3PO_4 (0.10)	50 °C, 4 h; reflux, 8 h	85
4	$K_2S_2O_8$ (1.2)/Ag_3PO_4 (0.02)	50 °C, 4 h; reflux, 8 h	74
5	$K_2S_2O_8$ (1.2)/Ag_3PO_4 (0.01)	50 °C, 4 h; reflux, 8 h	51

[a] Units: mol oxidant/mol quinic acid. [b] reported yields are based on isolated, purified hydroquinone.

Discussion

Microbial synthesis of quinic acid from glucose. The first reported microbial synthesis of quinic acid relied on heterogeneous expression of the *Klebsiella pneumoniae qad* gene encoding NAD^+-requiring quinate dehydrogenase.[6] Synthesis of quinic acid utilizing the *E. coli aroE*-encoding $NADP^+$-dependent shikimate dehydrogenase is noteworthy given that 3-dehydroquinic acid is not its native substrate. Overexpression of the *E. coli aroE* gene instead of the *K. pneumoniae qad* gene in *E. coli* constructs avoids the difference in codon usage and protein folding between these two organisms. The shikimate dehydrogenase activity in this study was measured using oxidation of shikimic acid as the substrate.[65] The Michaelis constant (K_m = 1.2 mM) for the unnatural substrate 3-dehydroquinic acid by shikimate dehydrogenase is roughly ten times higher than for 3-

dehydroshikimic acid (K_m = 0.11 mM), and the v_{max} is slightly lower for shikimate dehydrogenase-catalyzed reduction of 3-dehydroquinic acid than 3-dehydroshikimic acid (0.096 mmol/L/min vs. 0.11 mmol/L/min).[7] Therefore, the specific activities determined during fermentation runs do not represent the *in vivo* activities with 3-dehydroquinic acid as substrate.

A two-fold increase in shikimate dehydrogenase activity resulted from replacing the $P_{tac}P_{aroE}$ tandom promoter in *E. coli* QP1.1/pKD12.138 with a single P_{tac} promoter for *aroE* in *E. coli* QP1.1/pNR4.230 but did not lead to an increase in either the concentration or yield of biosynthesized quinic acid. The approximately 5 g/L of 3-dehydroquinic acid accumulated in fermentation broth of *E. coli* QP1.1/pKD12.138 at 48 h under the glucose-limited conditions could be attributed to feedback inhibition of shikimate dehydrogenase by quinic acid in light of the precedent that shikimate dehydrogenase is feedback-inhibited by shikimic acid.[28] When *ppsA*-encoding phosphoenolpyruvate synthase was co-expressed with *tktA*-encoding transketolase in *E. coli* QP1.1/pKD15.071 and *E. coli* QP1.1/pNR4.272, the flow of carbon into the common pathway was elevated. *E. coli* QP1.1/pKD15.071 synthesized the same amount of quinic acid (49 g/L) as *E. coli* QP1.1/pKD12.138, which possibly reflects a limitation imposed by inadequate shikimate dehydrogenase activity. Accordingly, increasing shikimate dehydrogenase specific activity by two-fold in *E. coli* QP1.1/pNR4.272 led to an increase in synthesized quinic acid.

The steady decrease from 24~48 h of 3-dehydroquinic acid, which initially increased in concentration over the first 24 h during fermentor-controlled cultivation, raised an intriguing possibility that *E. coli* was capable of recapturing 3-dehydroquinic

acid in the culture medium and subsequently reducing it to quinic acid under glucose-limited conditions. A putative quinate transport protein has been found in *Aspergillus nidulans*.[66] However, a quinate transport protein has not been identified in *E. coli*. To establish the recapture of initially exported 3-dehydroshikimic acid, chemically synthesized 3-dehydroquinic acid was added into fermentation medium of *E. coli* QP1.1/pNR4.276, which lacks an active feedback-insensitive DAHP synthase. The three native DAHP synthase isozymes encoded by *aroF*, *aroG* and *aroH* in the *E. coli* QP1.1 genome are subjected to the feedback inhibition by three aromatic amino acids, L-tyrosine, L-phenylalanine and L-tryptophan. Addition of three aromatic amino acids into the fermentation medium effectively blocked the biosynthesis of shikimate pathway metabolites. *E. coli* QP1.1/pNR4.276 catalyzed the conversion of 3-dehydroquinic acid added to its culture medium into a 1.2:1 molar ratio of quinic acid:3-dehydroquinic acid within 36 h. Formation of quinic acid supports the hypothesis that *E. coli* is capable of recapturing 3-dehydroquinic acid in the culture medium and reducing it to quinic acid.

The importance of recapturing 3-dehydroquinic acid was demonstrated when *E. coli* biocatalysts were cultured under fermentor-controlled, glucose-rich conditions. Culturing *E. coli* QP1.1/pNR4.230 under glucose-rich condition resulted in the synthesis of 39 g/L of quinic acid and 31 g/L of 3-dehydroquinic acid. By contrast, *E. coli* QP1.1/pKD12.138 under glucose-limited condition synthesized 49 g/L of quinic acid and 5.5 g/L of 3-dehydroquinic acid, although the latter construct possessed lower shikimate dehydrogenase specific activities (entry 6 vs. entry 1, Table 2).

Catabolite repression by glucose likely contributed to the dramatic shift in product profile under glucose-rich culture conditions. Excess glucose present in the fermentation

medium may inhibit the transport of 3-dehydroquinic acid synthesized and exported into the culture medium back into the *E. coli* cytoplasm. For *E. coli* QP1.1/pKD12.138 and *E. coli* QP1.1/pNR4.230, shikimate dehydrogenase specific activities were significant lower under glucose-rich conditions relative to the activities observed under glucose-limited conditions. Meanwhile, DAHP synthase activity is generally higher under glucose-rich condition than that under glucose-limited condition. The combination of these effects resulted in the accumulation of significant concentrations of 3-dehydroquinic acid byproduct in the culture medium.

Inactivating catabolite repression by glucose could enable *E. coli* to transport 3-dehydroquinate into the cytoplasm in the presence of glucose. One such catabolite repression-insensitive mutant, *E. coli* QP1.1*ptsG*/pKD12.138, was constructed and examined under glucose-rich culture conditions but did not result in an increase in quinic acid synthesis. One straightforward way to increase quinic acid synthesis without reestablishing the 3-dehydroquinic acid recapture mechanism under glucose-rich culture conditions is to further increase the shikimate dehydrogenase activity to compete with 3-dehydroquinate export. *E. coli* QP1.1/pNR4.230 synthesized a higher concentration of quinic acid relative to *E. coli* QP1.1/pKD12.138, which possessed lower shikimate dehydrogenase specific activities under glucose-rich, fermentor-controlled conditions (entry 5 vs. 6, Table 1). However, further increasing shikimate dehydrogenase activities by expressing *aroE* from a stronger promoter such as *T7* promoter might not be beneficial to quinic acid production due to the metabolic burden associated with high levels of protein expression.

One possible solution to this problem is to increase the catalytic efficiency of the *aroE*-encoding shikimate dehydrogenase toward the unnatural substrate 3-dehydroquinic acid by directed evolution or site-directed mutagenesis. After completion of this work, a *ydiB*-encoded shikimate dehydrogenase isozyme in *E. coli* was reported and characterized.[67,68] The YdiB is a dual specificity quinate/shikimate dehydrogenase using either NAD^+ or $NADP^+$ as a cofactor. The K_m for quinate with NAD^+ as cofactor is 41 μM which is 10 times lower than with $NADP^+$ as cofactor (K_m = 555 μM). The K_m value for shikimate is 20 μM with NAD^+ and 120 μM with $NADP^+$ as cofactor. By contrast, *aroE*-encoded shikimate dehydrogenase isozyme uses $NADP^+$ exclusively with a K_m value of 65 μM for shikimate.[67] However, the catalytic efficiency of *aroE*-encoded shikimate dehydrogenase (k_{cat} = 14,200 min^{-1}) is 2000-4000 fold higher than the *ydiB*-encoded dual-substrate dehydrogenase (k_{cat} = 3-7 min^{-1}). YdiB shares a 50% similarity with the AroE counterpart. Both enzymes display a similar architecture with two α/β domains separated by a wide cleft.

Replacing *aroE*-encoded shikimate dehydrogenase with *ydiB*-encoded quinate/shikimate dehydrogenase in the quinate-synthesizing *E. coli* constructs may not be able to achieve high-titer synthesis of quinic acid due to its low k_{cat} value. However, site-specific mutagenesis or directed evolution of the *aroE*-encoded shikimate dehydrogenase isozyme could be utilized to create a mutant dehydrogenase that exhibits both high catalytic efficiency and high specificity toward 3-dehydroquinic acid. The availability of X-ray crystal structures for both AroE and YdiB potentially could simplify and accelerate the mutagenesis and evolution process. Since the structures of AroE and YdiB are similar, comparison of their substrate-binding motif may provide valuable

information to guide the site-directed mutagenesis or saturation mutagenesis in *aroE*-encoded shikimate dehydrogenase. Screening methods based on measuring dehydrogenase activity toward reduction of 3-dehydroquinic acid can be exploited to identify the mutants with improved activity. Alternatively, a selection strategy can be envisioned to take advantage of the reversibility of these dehydrogenase-catalyzed conversions by selecting mutants capable of using quinic acid as a sole aromatic amino acids supplement in an *E. coli* strain lacking DAHP synthase. An improved quinate dehydrogenase is expected to eliminate the 3-dehydroquinate accumulation mentioned above and channel all of the carbon directed into the shikimate pathway into quinic acid.

Chemical synthesis of hydroquinone from quinic acid. With the improvements achieved in the biocatalytic methodology for conversion of glucose into quinic acid, improving the companion chemical methodology for conversion of quinic acid into hydroquinone becomes critical to make this route practical. Reaction methodology previously employed for the chemical conversion of quinic acid to hydroquinone (Figure 18) by refluxing purified quinic acid in an aqueous solution with MnO_2 synthesized hydroquinone in 10% yield.[6] Utilization of MnO_2 has the same problem associated with the commercial route to hydroquinone where stoichiometric amounts of MnO_2 are used to oxidize aniline (Figure 15).[1]

Oxidative decarboxylation of quinic acid by reactions with hypochlorite afforded 3(*R*),5(*R*)-trihydroxycyclohexanone (**10**, Figure 40) rapidly and quantitatively at room temperature. The mild reaction conditions and the stability of 3(*R*),5(*R*)-trihydroxycyclohexanone under these conditions are critical for a high-yielding conversion of quinic acid into hydroquinone. Dehydration and aromatization of ketone

10 to hydroquinone during oxidative decarboxylation of quinic acid would likely result in overoxidation of hydroquinone to benzoquinone or chlorination of hydroquinone.

Of all the methods developed for chlorine-free oxidative decarboxylation of quinic acid, electrochemical oxidation of quinic acid was the simplest and most environmental-friendly method. However, this method suffered from overoxidation of either quinic acid or its decarboxylation product **10** as suggested by the formation of formic acid. Only approximately 50% of the mass balance could be accounted for after partial electrochemical oxidation of quinic acid. The lack of improved 3(*R*),5(*R*)-trihydroxycyclohexanone (**10**) yields realized with use of electrochemical oxidation led to the examination of oxidative decarboxylation of quinic acid with Ce^{4+} and V^{5+}. Oxidative decarboxylation of α-hydroxycarboxylic acids with Ce^{4+} and V^{+5} has been reported.[69] The metal-mediated oxidation of the α-hydroxycarboxylate quinic acid afforded favorable yields (Table 5) of hydroquinone formed with $(NH_4)_2Ce(SO_4)_3$ and V_2O_5 as oxidants.

Moving from use of stoichiometric to catalytic amounts of metal for oxidation of quinic acid took advantage of the reported ability of Ag^{2+} formed from peroxydisulfate oxidation of Ag^{1+} to accelerate the oxidation of carboxylic acids.[70] Use of insoluble Ag_3PO_4 as catalyst followed from inorganic phosphate being the dominant oxyanion present in fermentation broth. Overoxidation of hydroquinone to benzoquinone was not observed when only a small molar excess of $K_2S_2O_8$ relative to quinic acid was used.

Benzene-free synthesis of hydroquinone. Exposure to benzene, which has been linked to both acute myeloid leukemia and non-Hodgkin's lymphoma,[71] continues to create challenges to the chemical industry. Besides the fact that benzene is derived from

nonrenewable resources, high costs have been cited by the U.S. chemical industry to be a major impediment to reducing exposure limits for benzene.[72] Ultimately, the most effective way of addressing benzene's human health risk may be the development of fundamentally new syntheses for aromatic chemicals and products from non-toxic, non-volatile and renewable starting materials to replace the existing synthetic routes from benzene and its derivatives. The synthesis of hydroquinone via chemical oxidation of microbe-synthesized quinic acid can be viewed as being part of this process.

E. coli QP1.1/pNR4.272 synthesizes 56 g/L of quinic acid in 20% yield from glucose. Fermentor-controlled conditions for this conversion are amenable to scale-up for larger volume cultivation. Nonetheless, significant improvement in the yield and concentration of quinic acid microbially synthesized from glucose is needed. Oxidation of quinic acid with NaOCl or $Ag_3PO_4/K_2S_2O_8$ allows quinic acid to be converted into hydroquinone in high yield and without overoxidation to benzoquinone. Synthesis of hydroquinone from glucose clearly has aspects that need to be further improved before this route can be used on an industrial scale. However, the microbial synthesis of quinic acid and chemical oxidation of glucose-derived quinic acid described in this chapter moves the synthesis of hydroquinone from glucose from a proof-of-concept conversion to a route that may ultimately supplant currently employed syntheses of hydroquinone where benzene serves as the starting material.

There is also an economic opportunity associated with producing chemicals from glucose and other carbohydrates. As declining reserves and increasing consumption lead to continuing increases in the price of petroleum,[73] the costs of using petroleum-derived benzene will likewise increase. By contrast, the increasing availability of glucose derived

from corn starch and the development of corn fiber and lignocellulose as carbohydrate feedstocks suggest that glucose and other carbohydrates will become an increasingly valuable source of carbon for synthesis of chemicals. As the world moves to national CO_2 budgets set by international treaty, hydroquinone synthesized from carbohydrates such as glucose may also be important CO_2 credits, given the consideration that the glucose used as a starting material is essentially an immobilized form of CO_2.

Reference

[1] Krumenacker, L.; Costantini, M.; Pontal, P.; Sentenac, J. In *Kirk-Othmer Encyclopedia of Chemical Technology, 4th ed.*; Wiley: New York, 1995, Vol. 13, p. 996-1014.

[2] Brand, T. Hydroquinone set to expand as new uses push demand. *Chemical Market Reporter* **1997**, *251*, 5.

[3] (a) Yoshikawa, A.; Yoshida, S.; Terao, I. Microbial preparation of hydroquinone. *Bioprocess Technol.* **1993**, *16*, 149-161. (b) Hall, M. C. Microbiological preparation of hydoquinone. European Patent 0 073 134 A2, 1982. (c) Higgins, I. J.; Hammond, R. C.; Sariaslani, F. S.; Best, D.; Davies, M. M.; Tryhorn, S. E.; Taylor, F. Biotransformation of hydrocarbons and related compounds by whole organism suspensions of methane-grown *Methylosinus trichosporium* OB 3b. *Biochem. Biophys. Res. Commun.* **1979**, *89*, 671-677.

[4] (a) Barker, J. L.; Frost, J. W. Microbial synthesis of *p*-hydroxybenzoic acid from glucose. *Biotechnol. Bioeng.* **2001**, 76, 376-390. (b) Amaratunga, M.; Lobos, J. H.; Johnson, B. F.; Williams, D. U.S. Patent 6030819, 2000.

[5] (a) van Berkel, W. J. H.; Eppink, M. H. M.; Middelhoven, W. J.; Vervoort, J.; Rietjens, I. M. Catabolism of 4-hydroxybenzoate in *Candida parasilosis* proceeds through initial oxidative decarboxylation by a FAD-dependent 4-hydroxybenzoate 1-hydroxylase. *FEMS Microbiol. Lett.* **1994**, *121*, 207-215. (b) Eppink, M. H. M.; Boeren, S. A.; Vervoort, J.; van Berkel, W. J. H. Purification and properties of 4-hydroxybenzoate 1-hydroxylase (decarboxylating), a novel flavin adenine dinucleotide-dependent monooxygenase from Candida parapsilosis CBS604. *J. Bacteriol.* **1997**, *179*, 6680-6687. (c) Eppink, M. H.; Cammaart, E.; Van, Wassenaar. D.; Middelhoven, W. J.; van Berkel, W. J. Purification and properties of hydroquinone hydroxylase, a FAD-dependent monooxygenase involved in the catabolism of 4-hydroxybenzoate in *Candida parapsilosis* CBS604. *Eur. J. Biochem.* **2000**, *267*, 6832-6840.

[6] Draths, K. M.; Ward, T. L.; Frost, J. W. Biocatalysis and nineteenth century organic chemistry: conversion of D-glucose into quinoid organics. *J. Am. Chem. Soc.* **1992**, *114*, 9725-9726.

[7] Draths, K. M.; Knop, D. R.; Frost, J. W. Shikimic acid and quinic acid: replacing isolation from plant sources with recombinant biocatalysis. *J. Am. Chem. Soc.* **1999**, *121*, 1603-1604.

[8] Eliel, E. L.; Ramirez, M. B. (-)-Quinic acid: configurational (stereochemical) descriptors. *Tetrahedron: Asymmetr.* **1997**, *8*, 3551-3554.

[9] Hofmann, F. C. *Crell's Chemische Annalen*, **1790**, *2* 314.

[10] Fisher, H. O., L.; Dangschat, G. *Ber. Dtsch. Chem. Gas.* **1932**, *65*, 1009.

[11] Phoon, C. W.; Abell, C. Use of quinic acid as template in solid-phase combinatorial synthesis. *J. Comb. Chem.* **1999**, *1*, 485-492.

[12] Federspiel, M.; Fischer, R.; Hennig, M.; Mair, H.-J.; Oberhauser, T.; Rimmler, G.; Albiez, T.; Bruhin, J.; Estermann, H.; Gandert, C.; Goeckel, V.; Goetzoe, S.; Hoffmann, U.; Huber, G.; Janatsch, G.; Lauper, S.; Roeckel-Staebler, O.; Trussardi, R.; Zwahlen, A. G. Industrial synthesis of the key precursor in the synthesis of the anti-influenza drug Oseltamivir phosphate (Ro 64-0796/002, GS-4104-02): Ethyl (3*R*,4*S*,5*S*)-4,5-epoxy-3-(1-ethyl-propoxy)-1-cyclohexene-1-carboxylate. *Org. Proc. Res. Develop.* **1999**, *3*, 266-274.

[13] Matsuo, K.; Sugimura, W.; Shimizu, Y.; Nishiwaki, K.; Kuwajima, H. Synthesis of (-)-sugiresinol dimethyl ether utilizing (-)-quinic acid. *Heterocycles* **2000**, *53*, 1505-1513.

[14] Murray, L. M.; O'Brien, P.; Taylor, R. J. K. Stereoselective reactions of a (-)-quinic acid-derived enone: application to the synthesis of the core of scyphostatin. *Org. Lett.* **2003**, *5*, 1943-1946.

[15] Barros, M. T.; Maycock, C. D.; Ventura, M. R. Enantioselective total synthesis of (+)-Eutypoxide B. *J. Org. Chem.* **1997**, *62*, 3984-3988.

[16] Ono, K.; Yoshida, A.; Saito, N.; Fujishima, T.; Honzawa, S.; Suhara, Y.; Kishimoto, S.; Sugiura, T.; Waku, K.; Takayama, H.; Kittaka, A. Efficient synthesis of 2-modified 1α,25-dihydroxy-19-norvitamin D_3 with Julia olefination: high potency in induction of differentiation on HL-60 cells. *J. Org. Chem.* **2003**, 68, 7407-7415.

[17] Su, Z.; Paquette, L. A. Conversion of D-(-)-quinic acid into an enantiopure C-4 functionalized 2-iodocyclohexenone acetal. *J. Org. Chem.* **1995**, *60*, 764-766.

[18] Ulibarri, G.; Nadler, W.; Skrydstrup, T.; Audrain, H.; Chiaroni, A.; Riche, C.; Grierison, D. S. Construction of the bicyclic core structure of the enediyne antibiotic esperamicin-A_1 in either enantiomeric form from (-)-quinic acid. *J. Org. Chem.* **1995**, *60*, 2753-2761.

[19] Wang, Z.-X.; Shi. Y. A new type of ketone catalyst for asymmetric epoxidation. *J. Org. Chem.* **1997**, *62*, 8622-8623.

[20] Haslam, E. In *Shikimic Acid: Metabolism and Metabolites*; Wiley & Sons: New York, 1993, p. 56.

[21] Bestmann, H. J.; Heid, H. A. Stereospecific synthesis of optically pure quinic acid and shikimic acid from D-arabinose. *Angew. Chem., Int. Ed. Engl,.* **1971**, *10*, 336-337.

[22] Hiroya, K.; Ogasawara, K. A concise enantio- and diastereo-controlled synthesis of (-)-quinic acid and (-)-shikimic acid. *Chem. Commun.* **1998**, 2033-2034.

[23] Pittard, J.; Wallace, B. J. Distribution and function of genes concerned with aromatic biosynthesis in *Escherichia coli*. *J. Bacteriol.* **1966**, *91*, 1494-1508.

[24] (a) Li, K.; Mikola, M. R.; Draths, K. M.; Worden, R. M.; Frost, J. W. Fed-batch fermentor synthesis of 3-dehydroshikimic acid using recombinant *Escherichia coli*. *Biotechnol. Bioeng.* **1999**, *64*, 61-73. (b) Weaver, L. M.; Hermann, K. M. Cloning of an *aroF* allele encoding a tyrosine-insensitive 3-deoxy-D-*arabino*-heptulosonate 7-phosphate synthase. *J. Bacteriol.* **1990**, *172*, 6581-6584.

[25] Snell, K. D.; Draths, K. M.; Frost, J. W. Synthetic modification of the *Escherichia coli* chromosome: enhancing the biocatalytic conversion of glucose into aromatic chemicals. *J. Am. Chem. Soc.* **1996**, *118*, 5605-5614.

[26] Ran, N.; Knop, D. R.; Draths, K. M.; Frost, J. W. Benzene-free synthesis of hydroquinone. *J. Am. Chem. Soc.* **2001**, *123*, 10927-10934.

[27] Anton, I. A.; Coggins. J. R. Sequencing and overexpression of the *Escherichia coli aroE* gene encoding shikimate dehydrogenase. *Biochem. J.* **1988**, *249*, 319-326.

[28] Dell, K. A.; Frost, J. W. Identification and removal of impediments to biocatalytic synthesis of aromatics from D-glucose: rate-limiting enzymes in the common pathway of aromatic amino acid biosynthesis. *J. Am. Chem. Soc.* **1993**, *115*, 11581-11589.

[29] Farabaugh, M. M. S. Thesis, Michigan State University, 1996.

[30] (a) Draths, K. M.; Pompliano, D. L.; Frost, J. W.; Berry, A.; Disbrow, G. L.; Staversky, R. J.; Lievense, J. C. Biocatalytic synthesis of aromatics from D-glucose: the role of transketolase. *J. Am. Chem. Soc.* **1992**, *114*, 3956-3962. (b) Patnaik, R.; Liao, J. C. Engineering of *Escherichia coli* central metabolism for aromatic metabolite production with near theoretical yield. *Appl. Environ. Microbiol.* **1994**, *60*, 3903-3908.

[31] Knop, D. R. Doctorate Dissertation, Michigan State University, 2002.

[32] Chaudhuri, S.; Anton, I. A.; Coggins, J. R. Shikimate dehydrogenase from *Escherichia coli*. *Methods Enzymol.* **1987**, *142*, 315-320.

[33] Zhu, L. Y.; Frost, J. W. Unpublished result.

[34] Postma, P. W.; Lengeler, J. W.; Jacobson, G. R. Phosphoenolpyruvate:carbohydrate phosphotransferase systems. In *Escherichia coli and Salmonella: Cellular and Molecular Biology*, 2nd ed.; Neidhardt, F. C., Ed.; ASM press: Washinfton, DC, 1996: p. 1149-1174.

[35] (a) Forberg, C.; Eliaeson, T.; Haggstrom, L. Correlation of theoretical and experimental yields of phenylalanine from non-growing cells of a *rec Escherichia coli* strain. *J. Biotech.* **1988**, *7*, 319-322. (b) Frost, J. W.; Draths, K. M. Biocatalytic syntheses of aromatics from D-glucose: renewable microbial sources of aromatic compounds. *Ann. Rev. Microbial.* **1995**, *49*, 557-579.

[36] Patnaik, R.; Spitzer, R. G.; Liao, J. C. Pathway engineering for production of aromatics in *Escherichia coli*: confirmation of stoichiometric analysis by independent modulation of AroG, TktA, and Pps activities. *Biotechnol. Bioeng.* **1995**, *46*, 361-370.

[37] Yi, J.; Li, K.; Draths, K. M.; Frost, J. W. Modulation of phosphoenolpyruvate synthase expression increases shikimate pathway product yields in *E. coli*. *Biotechnol. Prog.* **2002**, *18*, 1141-1148.

[38] Chandran, S. C.; Yi, J.; Draths, K. M.; von Daeniken, R.; Weber, W.; Frost, J. W. Phosphoenolpyruvate availability and the biosynthesis of shikimic acid. *Biotechnol. Prog.* **2003**, *19*, 808-814.

[39] Parker, C.; Barnell, W. O.; Snoep, J. L.; Ingram, L. O.; Conway, T. Characterization of the *Zymomonas mobilis* glucose facilitator gene product (*glf*) in recombinant *Escherichia coli*: examination of transport mechanism, kinetics and the role of glucokinase in glucose transport. *Mol. Microbiol.* **1995**, *15*, 795-802.

[40] (a) Saier, M. H. Jr.; Bromberg, F. G.; Roseman, S. Characterization of constitutive galactose permease mutants in *Salmonella typhimurium*. *J. Bacteriol.* **1973**, *113*, 512-514. (b) Flores, N.; Xiao, J.; Berry, A.; Bolivar, F.; Valle, F. Pathway engineering for the production of aromatic compounds in *Escherichia coli*. *Nat. Biotechnol.* **1996**, *14*, 620-623.

[41] Levy, S.; Zeng, G.; Danchin, A. Cyclic AMP synthesis in *Escherichia coli* strains bearing known deletions in the *pts* phosphotransferase operon. *Gene* **1990**, *86*, 27-33.

[42] Tian, F. Doctorate Dissertation, Michigan State University, 1998.

[43] Montchamp, J.-L.; Tian, F.; Hart, M. E.; Frost, J. W. 2,3-Butane bisacetal protection of vicinal diequatorial diols. *J. Org. Chem.* **1996**, *61*, 3897-3899.

[44] Sann, C. L.; Abell, C.; Abell, A. D. A conventient method for the synthesis of dehydroquinic acid. *Synth. Commun.* **2003**, *33*, 527-533.

[45] Knop, D. R.; Draths, K. M.; Chandran, S. S.; Barker, J. L.; von Daeniken, R.; Weber, W.; Frost, J. W. Hydroaromatic equilibration during biosynthesis of shikimic acid. *J. Am. Chem. Soc.* **2001**, *123*, 10173-10182.

[46] Kimata, K.; Takahashi, H.; Inada, T.; Postma, P.; Aiba, H. cAMP receptor protein-cAMP plays a crucial role in glucose-lactose diauxie by activating the major glucose transporter gene in *E. coli*. *Proc. Natl. Acad. Sci. USA* **1997**, *94*, 12914-12919.

[47] (a) Erni, B.; Zanolari, B. Glucose-permease of the bacterial phosphotransferase system. Gene cloning, overproduction, and amino acid sequence of enzyme II^{Glc}. *J. Biol. Chem.* **1986**, *261*, 16398-16403. (b) Bouma, C. L.; Meadow, N. D.; Stover, E. W.; Roseman, S. II-B^{Glc}, a glucose receptor of the bacterial phosphotransferase system: Molecular cloning of *ptsG* and purification of the receptor from an overproducing strain of *Escherichia coli*. *Proc. Natl. Acad. Sci. USA* **1987**, *84*, 930-934.

[48] (a) Donnelly, M. I.; Sanville-Millard, C.; Chatterjee, R. US Patent, 6,159,738, 2000. (b) Nichols, N. N.; Dien, B. S.; Bothast, R. J. Use of catabolite repression mutants for fermentation of sugar mixtures to ethanol. *Appl. Microbiol. Biotechnol.* **2001**, *56*, 120-125.

[49] Zaldivar, J.; Martinez, A.; Ingram, L. O. Effect of alcohol compounds found in hemicellulose hydrolysate on the growth and fermentation of ethanologenic *Escherichia coli*. *Biotechnol. Bioeng.* **2000**, *68*, 524-530.

[50] Ogino, T.; Garner, C.; Markley, J. L.; Herrmann, K. M. Biosynthesis of aromatic compounds: ^{13}C NMR spectroscopy of whole *Escherichia coli* cells. *Proc. Natl. Acad. Sci. USA.* **1982**, *79*, 5828-5832.

[51] Woskresensky, A. *Justus Liebiegs Ann. Chem.* **1838**, *27*, 257.

[52] Yahuka, Y.; Katz, R.; Sarel, S. Bile acid chemistry. III. Stepwise side-chain shortening by way of sodium per-iodate oxidation of α-hydroxy bile acids into corresponding aldehydes. *Tetrahedron Lett.* **1968**, 1725-1728.

[53] Bhale, V. M.; Sant, P. G.; Bafna, S. L. Acid permanganate oxidation of tartaric acid. *J. Sci. Ind. Res.* **1956**, *15B*, 45-46.

[54] Bakore, G. V.; Narian, S. Kinetic investigation of the oxidation of some α-hydroxy-carboxylic acids by chromic acid. *J. Chem. Soc.* **1963**, 3419-3424.

[55] Sheldon, R. A.; Kochi, J. K. Oxidative decarboxylation of acids by lead tetraacetate. *Org. React.* **1972**, *19*, 279-421.

[56] Carlsen, P. H. J. Oxidation of α-hydroxy carboxylic acid with sodium hypochlorite. *Acta Chem. Scand. B.* **1984**, *38*, 343-344.

[57] (a) Carlsen, P. H. J.; Misund, K.; Roe, J. Synthesis of optical active glyceric acid derivatives from ascorbic acids. *Acta Chem. Scand.* **1995**, *49*, 297-300. (b) Stevens, R.

V.; Chapman, K. T.; Stubbs, C. A.; Tam, W. W.; Albizati, K. F. Further studies on the utility of sodium hypochlorite in organic synthesis. Selective oxidation of diols and directed conversion of aldehydes to esters. *Tetrahedron Lett.* **1982**, *23*, 4647-4650.

[58] Nwaukwa, S. O.; Keehn, P. M. Oxidative cleavage of α-diols, α-diones, α-hydroxyketones and α-hydroxy- and α-keto acids with calcium hypochlorite [$Ca(OCl)_2$]. *Tetrahedron Lett.* **1982**, *23*, 3135-3138.

[59] Elmore, P. R.; Reed, R. T.; Terkle-Huslig, T.; Welch, J. S.; Young, S. M.; Landolt, R. G. Hypochlorite-induced oxidative decarboxylation of trisustituted acetic acids. *J. Org. Chem.* **1989**, *54*, 970-972.

[60] (a) Barros, M. T.; Maycock, C. D.; Ventura, M. R. The effect of DMSO on the borohydride reduction of a cyclohexanone: a formal enantioselective synthesis of (+)-epibatidine. *Tetrahedron Lett.* **1999**, *40*, 557-560. (b) Kamenecka, T. M.; Overman, L. E. An enantioselective approach to the synthesis of manzamine A. *Tetrahedron Lett.* **1994**, *35*, 4279-4282.

[61] (a) Audia, J. E.; Boisvert, L.; Patten, A. D.; Villalobos, A.; Danishefsky, S. J. Synthesis of two useful, enantiomerically pure derivatives of (*S*)-4-hydroxy-2-cyclohexenone. *J. Org. Chem.* **1989**, *54*, 3738-3340. (b) Trost, B. M.; Romero, A. G. Synthesis of optically active isoquinuclidines utilizing a diastereoselectivity control element. *J. Org. Chem.* **1986**, *51*, 2332-2342.

[62] (a) Renaud, P.; Hurzeler, M.; Seebach, D. Electrochemical oxidation of (*S*)-malic-acid-derivatives: a route to enantiomerically pure alkylmalonaldehydic esters. *Helv. Chim. Acta* **1987**, *70*, 292-298. (b) Baizer, M. M. Recent developments in organic synthesis by electrolysis. *Tetrahedron* **1984**, *40*, 935-969.

[63] Blay, G.; Fernández, I.; Formentin, P.; Pedro, J. R.; Roselló, A. L.; Ruiz, R.; Journaux, Y. Catalytic aerobic oxidative decarboxylation of α-hydroxy-acids. Methyl mandelate as a benzoyl anion equivalent. *Tetrahedron Lett.* **1998**, *39*, 3327-3330.

[64] (a) Toussaint, O.; Capdevielle, P.; Maumy, M. Oxidative decarboxylation of aliphatic carboxylic acids by the copper(I)/oxygen system. *Tetrahedron Lett.* **1984**, *25*, 3819-3822. (b) Barak, G.; Dakka, J.; Sasson, Y. Selective oxidation of alcohols by a H_2O_2-$RuCl_3$ under phase-transfer conditions. *J. Org. Chem.* **1988**, *53*, 3553-3555. (c) Goebel, W. F. Derivatives of citraconic acid: I. the synthesis of methyltartaic acid and the decomposition of the dihydroxymaleic acid. *J. Am. Chem. Soc.* **1925**, *47*, 1990-1998.

[65] Chaudhuri, S.; Coggins, J. R. The purification of shikimate dehydrogenase from *Escherichia coli*. *Biochem. J.* **1985**, *226*, 217-223.

[66] Whittington, H. A.; Grant, S.; Roberts, C. F.; Lamb, H.; Hawkins, A. R. Identification

and isolation of a putative permease gene in the quinic acid utilization (QUT) gene cluster of *Aspergillus nidulans*. *Curr. Genet.* **1987**, *12*, 135-139.

[67] Michel, G.; Roszak, A. W.; Sauve, V.; Maclean, J.; Matte, A.; Coggins, J. R.; Cygler, M.; Lapthorn, A. J. Structure of shikimate dehydrogenase AroE and its paralog YdiB. *J. Biol. Chem.* **2003**, *278*, 19463-19472.

[68] Benach, J.; Lee, I.; Edstrom, W.; Kuzin, A. P.; Chiang, Y.; Acton, T. B.; Montelione, G. T.; Hunt, J. F. The 2.3-Å crystal structure of the shikimate 5-dehydrogenase orthologue YdiB from *Escherichia coli* suggests a novel catalytic environment for a NAD-dependent dehydrogenase. *J. Biol. Chem.* **2003**, *278*, 19176-19182.

[69] (a) Ho, T.-L. Ceric ion oxidation in organic chemistry. *Synthesis* **1973**, 347-354. (b) Amjad, Z.; McAuley, A.; Gomwalk, U. D. Metal-ion oxidations in solution. Part 16. The oxidation of α-hydroxycarboxylic acids by cerium(IV) in perchloric acid media. *Chem. Soc. Dalton Trans.* **1977**, 82-88. (c) Jones, J. R.; Waters, W. A.; Littler, J. S. Oxidation of organic compounds with quinquevalent vanadium. VII. The kinetic resemblance between oxidations of some α-hydroxy acids and that of pinacol and of its monomethyl ether. *J. Chem. Soc.* **1961**, 630-633. (d) Kalidoss, P.; Srinivasan, V. S. Estimated distribution between one- and two-equivalent reaction paths in vanadium(V)-induced electron transfer. *Chem. Soc. Dalton Trans.* **1984**, 2631-2635.

[70] (a) Anderson, J. M.; Kochi, J. K. Silver(I)-catalyzed oxidative decarboxylation of acids by peroxydisulfate. Role of silver(II). *J. Am. Chem. Soc.* **1970**, *92*, 1651-1659. (b) Walling, C.; Camaioni, D. M. Role of silver(II) in silver-catalyzed oxidations by peroxydisulfate. *J. Org. Chem.* **1978**, *43*, 3266-3271. (c) Kumar, A.; Neta, P. Complexation and oxidation of glycine and related compounds by Ag (II). *J. Am. Chem. Soc.* **1980**, *102*, 7284. (d) Minisci, F.; Citterio, A.; Giordano, C. Electron-transfer processes: peroxydisulfate, a useful and versatile reagent in organic chemistry. *Acc. Chem. Res.* **1983**, *16*, 27-32.

[71] (a) O'Connor, S. R.; Farmer, P. B.; Lauder, I. Benzene and non-Hodgkin's lymphoma. *J. Pathol.* **1999**, *189*, 448-453. (b) Farris, G. M.; Everitt, J. I.; Irons, R.; Popp, J. A. Carcinogenicity of inhaled benzene in CBA mice. *Fundam. Appl. Toxicol.* **1993**, *20*, 503-507. (c) Huff, J. E.; Haseman, J. K.; DeMarini, D. M. Multiple-site carcinogenecity of benzene in Fischer 344 rats and B6C3F1 mice. *Environ. Health Perspect.* **1989**, *82*, 125-163.

[72] *Trade Secrets, A Moyers Report.* http://www.pbs.org/tradesecrets/transcript.html.

[73] http://www.eia.doe.gov/emeu/steo/pub/contents.html *Short-term energy outlook*-February 2004.

CHAPTER THREE

Analysis of Gallic Acid Biosynthetic Pathway in *Escherichia coli* with [5-^{18}O]-3-Dehydroshikimic Acid

Introduction

Gallic acid (3,4,5-trihydroxybenzoic acid) is a central precursor for hydrolysable tannins, the abundant secondary metabolites in higher plants. Commercial availability of gallic acid relies on its isolation and hydrolysis of tannins from insect carapices (gall nuts) harvested in China, and from the seed pods of *Coulteria tinctoria* tree found in Peru.[1] Gallic acid and its esters have found a diverse range of industrial uses, such as antioxidants in food and cosmetics, and used as a material for inks and paints.[1] In the pharmaceutical industry, gallic acid is used for the synthesis of antibiotic trimethoprim (Figure 44).[1] Thermal decarboxylation of gallic acid in copper autoclaves afforded pyrogallol (1,2,3-trihydroxybenzene, Figure 44), which is used in the production of dyes and photographic developers and also in laboratories for absorbing oxygen.[1]

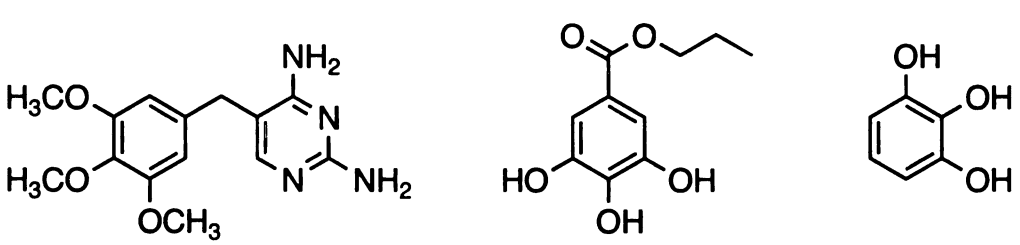

trimethoprim propyl gallate pyrogallol

Figure 44. Industrial chemicals derived from gallic acid.

Tannins, together with lignins, are the most widespread and abundant polyphenols in plants.[2] The involvement of tannins in the protection of plants against insert and mammalian herbivores is well established.[3] Tannins can form insoluble complexes with proteins that subsequently reduce the feeding value of the plant. Similarly, commercial uses of tannins in the leather industry are also based on their binding with proteins.[4] Plant tannins are classified as condensed tannins and hydrolysable tannins. The latter is characterized by a central β-D-glucose moiety whose hydroxyl groups are esterified with one to five gallic acid molecules. The fully galloylated glucose derivative, 1,2,3,4,6-*O*-pentagalloylglucose, is regarded as an immediate precursor to gallotannins and ellagitannins, two subclasses of hydrolysable tannins.[2b]

The initial steps in enzymatic synthesis of a wide range of complex gallotannins and ellagitannins are comprised of series of reactions from gallic acid and UDP-glucose to 1,2,3,4,6-*O*-pentagalloyglucose via 1-*O*-galloylglucose **4** (Figure 45).[2b,5] 1,2,3,4,6-*O*-Pentagalloylglucose can be converted to gallotannins by the addition of as many as 10-12 additional galloyl residues to the 1,2,3,4,6-*O*-pentagalloylglucose core by using 1-*O*-galloylglucose **4** as galloyl donor. Ellagitannins are formed by oxidative processes that yield C-C linkages between adjacent galloyl groups of the 1,2,3,4,6-*O*-pentagalloylglucose, followed by subsequent formation of dimeric and oligomeric derivatives that are connected via C-C or C-O-C bonds between the galloyl residues.[2b,5]

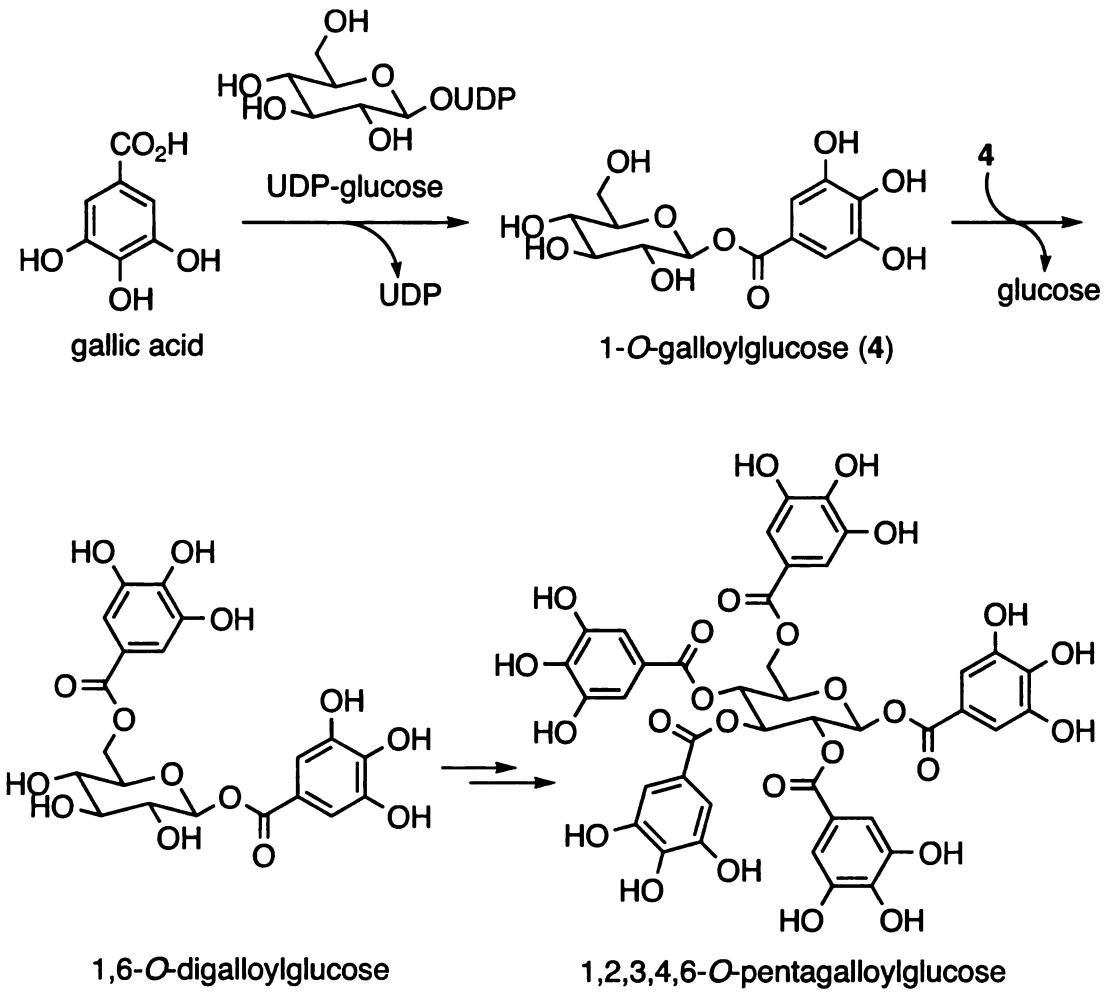

Figure 45. Biosynthesis of 1,2,3,4,6-*O*-pentagalloylglucose.

Biosynthesis of gallic acid, the principle phenolic unit of hydrolysable tannins, is not yet fully clarified. In addition to higher plants, gallic acid is also observed in cultures of *Phycomyces blakesleeanus*,[6] *Pseudomonas fluorescens*,[7] *Entorobacter cloacae*,[7] *Aspergillus terreus*[8] and recombined *E. coli*.[9] Three alternative pathways leading to gallic acid have been proposed as illustrated in Figure 46.[10]

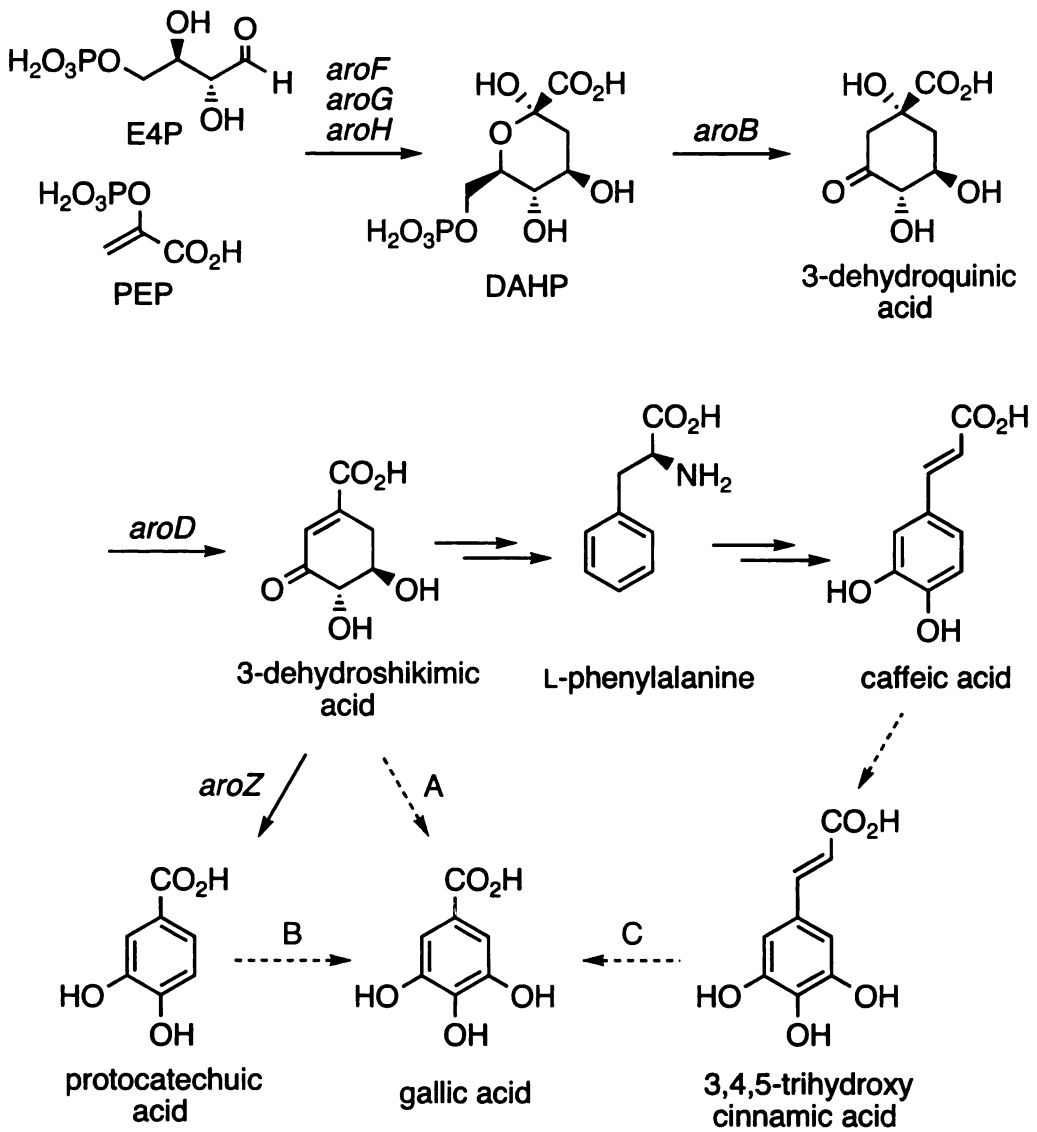

Figure 46. Three proposed pathways for biosynthesis of gallic acid. Pathway A, via 3-dehydroshikimic acid; Pathway B, via protocatechuic acid; Pathway C, via caffeic acid derived from L-phenylalanine.

In the proposed pathways A and B, gallic acid is biosynthesized from 3-dehydroshikimic acid. 3-Dehydroshikimic acid could be enzymatically converted into gallic acid by oxidoreductase-catalyzed dehydrogenation followed by subsequent aromatization (Pathway A) or dehydratase-catalyzed conversion to protocatechuic acid (PCA) followed by hydroxylation of the protocatchuic acid to form gallic acid (Pathway

B). On the other hand, gallic acid could be derived from L-phenylalanine via caffeic acid intermediacy involving side-chain degradation of 3,4,5-trihydroxycinnamic acid (Pathway C), since it is generally accepted that benzoic acids are produced in higher plants by side-chain degradation of cinnamic acids.[11]

Ambiguous results regarding these alternative pathways were obtained after feeding carboxyl-^{14}C-labeled shikimic acid to *Rhus* and *Acer* leaves.[10c] Experimental evidence that favored the directed biosynthesis of gallic acid from 3-dehydroshikimic acid in higher plants came from induction experiments with the herbicide glyphosate[12] (*N*-(phosphonomethyl)glycine). Glyphosate inhibits a shikimate pathway enzyme, 5-enolpyruvylshikimate-3-phosphate synthase, and causes a reduction in the synthesis of aromatic amino acids and phenylpropanoids. However, the level of gallic acid was higher in higher plants treated with glyphosate, which indicated that gallic acid was derived from a shikimate pathway intermediate before shikimate 3-phosphate, the substrate for 5-enolpyruvylshikimate-3-phosphate synthase. Strong evidence supporting this view has been obtained by feeding ^{13}C-glucose to cultures of fungus *Phycomyces blakesleeanus* and to young leaves of dicotyloneous tree *Rhus typhina*, followed by NMR spectroscopic analyses of isotope distributions of the isolated gallic acid and aromatic amino acids.[13]

Cultures of *P. blakesleeanus* were grown in medium containing [1-^{13}C]-glucose (99.5% ^{13}C enrichment) as carbon source. Gallic acid and aromatic amino acids L-phenylalanine, L-tyrosine and L-tryptophan were isolated from culture media and cell mass. Figure 47 showed the abbreviated conversions of glucose to L-phenylalanine, L-tyrosine and L-tryptophan and their respective ^{13}C-enrichment on each carbon atom. Due

to the symmetry of the aromatic rings of gallic acid, L-phenylalanine and L-tyrosine, the ring carbon atom at 2/6 and 3/5 yielded average ^{13}C abundances, although they had different biosynthetic origins. The ^{13}C-labeling pattern of the aliphatic side-chain that was derived from phosphoenolpyruvate was used to reconstruct the labeling pattern of phosphoenolpyruvate. On the other hand, L-tryptophan reflected the ^{13}C distributions of the original shikimate ring system, and the labeling pattern of D-erythrose 4-phosphate can be reconstructed based on the L-tryptophan biosynthetic pathway.

The labeling patterns of phosphoenolpyruvate, D-erythrose 4-phosphate and L-phenylalanine were used to predict the labeling patterns of gallic acids biosynthesized via intermediacy of cafferic acid, 3-dehydroshikimic acid, or protoctechuic acid. As shown in Figure 48, the observed gallic acid labeling pattern of gallic acid closely agreed with the predictedlabeling patterns for biosynthesis involving intermediacy of 3-dehydroshikimic acid or protocatechuic acid, but not with the predicted labeling patterns for biosynthesis proceeding via the phenylpropanoid pathway.[14] Labeling experiments with a mixture of [U-^{13}C]-glucose and unlabeled glucose on young leaves of *R. typhina* also agreed with the hypothesis that gallic acid was derived from 3-dehydroshikimic acid or protocatchuic acid.[13] This ruled out L-phenylanine as major precursor for gallic acid biosynthesis. However, the intermediacy of protocatechuic acid still remained an open question due to the fact that protocatechuic acid had the same carbon skeleton as 3-dehydroshikimic acid. Earlier work with cell-free systems from mung bean seedlings[15] and leaves from *Pelagonium inquinan*[16] suggested the involvement of the protocatechuic acid in biosynthesis of gallic acid, but these preliminary results were never corroborated by detailed investigations.

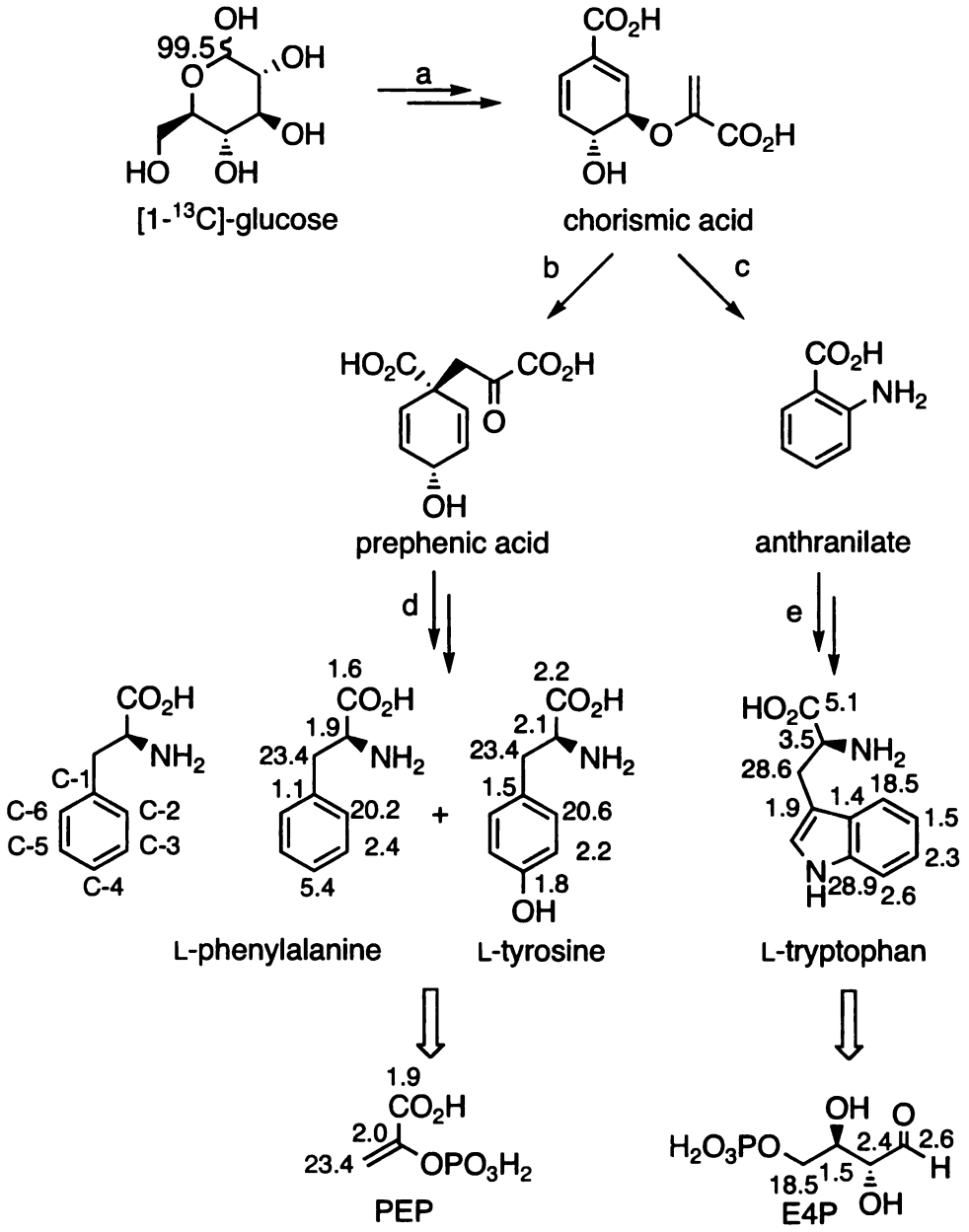

Figure 47. ^{13}C-Abundance (in percentage) of L-phenylalanine, L-tyrosine and L-tryptophan from *P. blakesleeanus* cultured with [1-^{13}C]-glucose. Keys: (a) see Figure 7, Chapter 2; (b) chorismate mutase (*pheA*); (c) anthranilate synthase (*trpD*, *trpE*); (d) L-phenylalanine and L-tyrosine biosynthesis enzymes;[17] (e) L-tryptophan biosynthesis enzymes.[17] The labeling pattern of phosphoenolpyruvate (PEP) and D-erythrose 4-phosphate (E4P) were reconstructed from aromatic amino acids based on established mechanisms of the shikimate pathway.

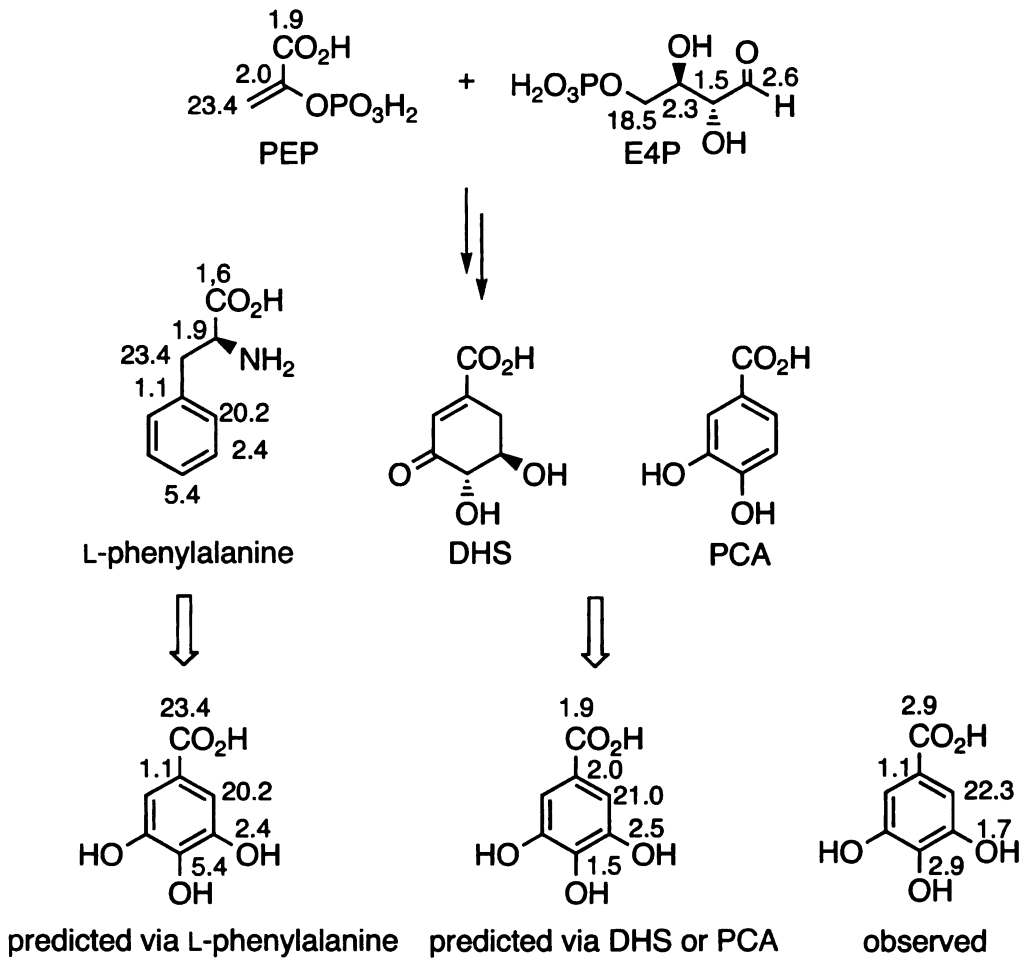

Figure 48. Predicted and observed labeling patterns of gallic acid synthesized by *P. blakesleeanus* cultured with [1-^{13}C]-glucose.

Distinguishing the two pathways can be achieved using [5-^{18}O]-3-dehydroshikimic acid (Figure 49). If gallic acid was biosynthesized via the dehydrogenation of 3-dehydroshikimic acid, the resulting gallic acid would contain an ^{18}O-labeled oxygen atom, which can be determined by mass spectrometry. If gallic acid was formed via dehydration to protocatechuic acid followed by hydroxylation of protocatechuic acid with O_2, the product gallic acid would not contain ^{18}O-labeled hydroxyl group (Figure 49).

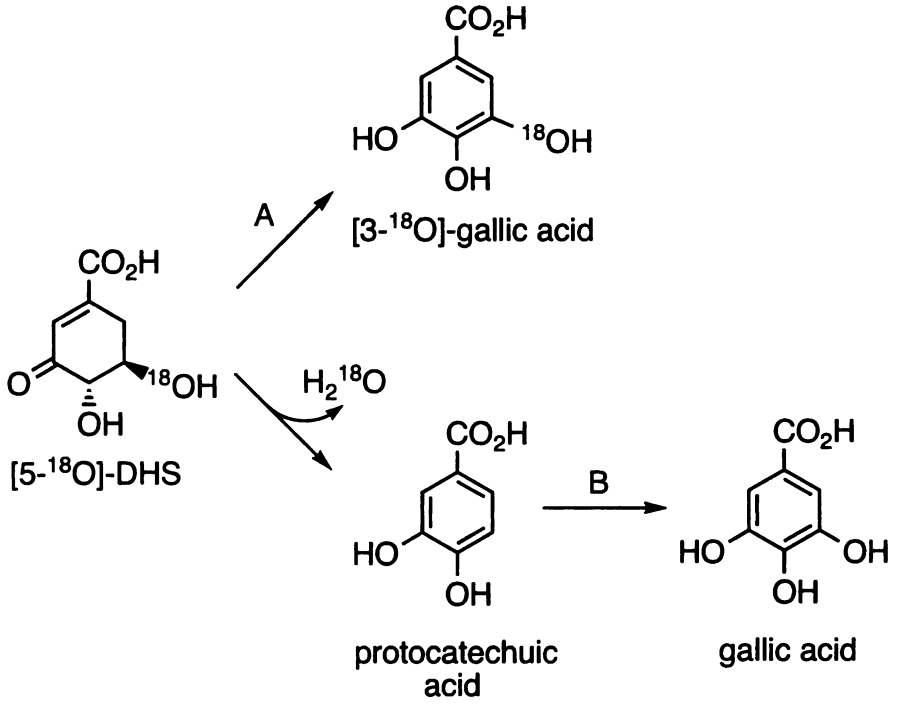

Figure 49. Strategy for distinguishing proposed gallic acid biosynthetic pathways with [5-^{18}O]-3-dehydroshikimic acid. A. Oxidoreductase-catalyzed oxidation of 3-dehydroshikimic acid; B. Hydroxylase-catalyzed hydroxylation of protocatechuic acid.

Synthesis of [5-^{18}O]-3-dehydroshikimic acid.

The [5-^{18}O]-3-dehydroshikimic acid was synthesized from shikimic acid via a chemoenzymatic route (Figure 50). Berchtold's procedure was adapted for the synthesis of the hydroxyl epoxide **21.**[18] Acid catalyzed epoxide opening[19] with 2 equivalents $H_2{}^{18}O$ provided the [5-^{18}O]-shikimate methyl ester **22**, which was purified by reverse phase HPLC method in 37% yield. Base-catalyzed hydrolysis converted **22** to [5-^{18}O]-shikimic acid. Conversion of [5-^{18}O]-shikimic acid to [5-^{18}O]-3-dehydroshikimic acid was carried out by an enzymatic oxidation using shikimate dehydrogenase and $NADP^+$.

Shikimate dehydrogenase was purified from *E. coli* strain AB2834/pIA321 that contained a plasmid-localized *aroE* encoding shikimate dehydrogenase as previously described.[20] To reduce the cost of the cofactor, the $NADP^+$ required for oxidation of

[5-^{18}O]-shikimic acid was regenerated by reductive amination of α-ketoglutarate with NADPH and ammonia catalyzed by L-glutamate dehydrogenase.[21] Excess amounts of α-ketoglutarate and L-glutamate dehydrogenase were used to drive the reaction to completion. Subsequent purification of the reaction mixture using an anion exchange column (Bio-Rad AG-1-X8, acetic form) gave the [5-^{18}O]-3-dehydroshikimic acid in 84% yield (Figure 50).

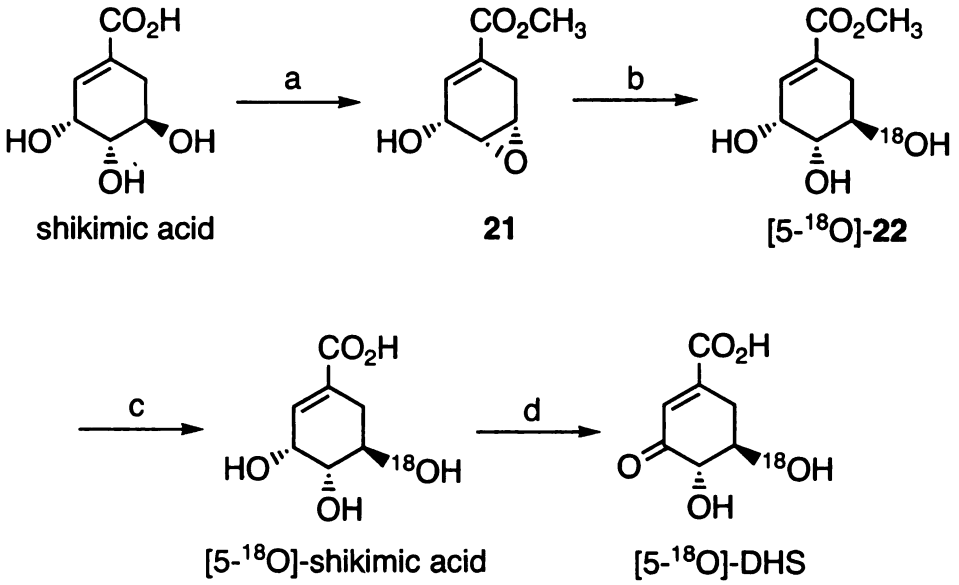

Figure 50. Synthesis of [5-^{18}O]-3-dehydroshikimic acid from shikimic acid. Keys: (a) i) CH_3OH, Amberlite IR120 (H^+), reflux, 24 h, 100%; ii) PPh_3, DEAD, THF, 0 °C–rt., 1.5 h, 80%; (b) $H_2{}^{18}O$ (2 equiv.), CF_3SO_3H (0.1 equiv.), CH_3CN, 0 °C–rt. 48 h, 37%; (c) NaOH, THF/H_2O (1:1, v/v), rt., 5 h, 100%; (d) shikimate dehydogenase, $NADP^+$, α-ketoglutaric acid, NH_4Cl, L-glutamate dehydrogenase, potassium phosphate buffer (pH 8.0), rt., 5 h, 84%.

Biosynthesis of gallic acid in *E. coli*.

In addition to higher plants and fungi, recombinant *E. coli* constructs are capable of biosynthesis of gallic acid under fermentor-controlled conditions.[9] Gallate-synthesizing *E. coli* KL3 was constructed from *E. coli* AB2834*aroE* by homologous

recombination of an *aroB* gene into the chromosomal *serA* locus.[9a] The absence of *aroE*-encoded shikimic dehydrogenase activity that catalyzes the conversion of 3-dehydroshikimate to shikimate resulted in the accumulation of 3-dehydroshikimate in culture supernatant. *E. coli* KL3 expressing plasmid-localized $aroF^{FBR}$, which encodes a feedback-insensitive isozyme of DAHP synthase, biosynthesized gallic acid along with 3-dehydroshikimic acid during fermentation runs in a ratio of around 1:6 - 1:11 (mol gallic acid/mol 3-dehydroshikimic acid). However, no enzyme activity that catalyzed the conversion of 3-dehydroshikimic acid to gallic acid was detected in *E. coli* crude cell extracts.[22] The lack of assayable activity might suggest that the responsible enzyme was labile or 3-dehydroshikimic acid was not the immediate precursor. [5-^{18}O]-3-Dehydroshikimic acid was then used to determine unequivocally whether the gallic acid biosynthetic pathway proceeded directly from 3-dehydroshikimic acid or via protocatechuic acid intermediacy.

[5-^{18}O]-3-Dehydroshikimic acid (0.75 g) was mixed with unlabeled 3-dehydroshikimic acid (10.25 g) to prepare [5-^{18}O]-enriched 3-dehydroshikimic acid. The levels of ^{18}O-enrichment in the [5-^{18}O]-3-dehydroshikimic acid and the isolated product gallic acid were determined by fast atom bombardment (FAB) mass spectrometry. Although ^{13}C NMR analysis of ^{18}O incorporation is common in natural product biosynthesis studies,[23] the relatively low ^{18}O-enrichment levels used in this study and difficulties encountered on quantitative interpretation prevented its utility in this study. Mass spectrometry permited direct observation and quantitative determination of the ^{18}O-labeling in gallic acid. However, direct measurement of ^{18}O-enrichment level in 3-dehydroshikimic acid using FAB(-) mass spectrometry was unsuccessful. Converting 3-

dehydroshikimic acid to shikimic acid alleviated the interferance but still gave an unsatisfactory mass spectrum due to a weak molecular ion signal. To circumvent this problem, 3-dehydroshikimic acid was first chemically oxidized to gallic acid by $Cu(OAc)_2$ using a previously established method,[24] and then its ^{18}O-enrichment was measured by FAB(-) mass spectrometry to represent the ^{18}O-enrichment level in 3-dehydroshikimic acid.

Entry 2 in Table 6 shows ion abundances at *m/z* 169, *m/z* 170, and *m/z* 171 from the FAB(-) mass spectrometry data (100:12.00:8.65). The ion signal at *m/z* 169 was the molecular ion peak ($C_7H_5O_5$, $M\text{-}H^+$), which was set to 100. The ion signal at *m/z* 170, ($M\text{-}H^+$+1), corresponds to ions containing one ^{13}C atom ($C_6{}^{13}CH_5O_5$). The ion peak at *m/z* 171, ($M\text{-}H^+$+2), is contributed by ions containing either one ^{18}O atom or ions bearing two ^{13}C atoms ($C_7H_5O_4{}^{18}O$ and $C_5{}^{13}C_2H_5O_5$). For unlabeled gallic acid, its ratios of the abundance of the molecular ion ($M\text{-}H^+$) at *m/z* 169 to ($M\text{-}H^+$+1) peak at *m/z* 170 to ($M\text{-}H^+$+2) signal at *m/z* 171 were 100:11.74:2.21 (entry 1, Table 6) and was used as background. To calculate ^{18}O-enrichment in gallic acid, the background contributions due to naturally occurring ^{18}O atoms and ions bearing two ^{13}C atoms were subtracted from isotope peaks at *m/z* 171. The excess ^{18}O-derived portion at *m/z* 171 relative to the total (sum of ion intensities at *m/z* 169, 170 and 171) was calculated as the ^{18}O-enrichment. Therefore, the ^{18}O-enrichment in the gallic acid corresponding to the prepared [5-^{18}O]-enriched 3-dehydroshikimic acid was 5.34% ((8.65-2.21)/(100+12.9+8.65)).

Table 6. ^{18}O-Enrichment determined by FAB(-) mass spectrometry.

entry	compound	Ion distribution (average of three)			^{18}O enrichment	^{18}O incorporation
		m/z 169	*m/z* 170	*m/z* 171		
1	GA (unlabeled)	100	11.74	2.21	-	-
2	DHS added (^{18}O-enriched)	100	12.00	8.65	5.34%	100%
3	GA (*E. coli* KL3/pRC1.55B)	100	12.92	8.96	5.54%	104%
4	GA (*E. coli* KL7/pSK6.76)	100	11.76	2.32	0.10%	1.9%
5	GA (air oxidation)	100	12.02	7.47	4.40%	82.4%
6	DHS recovered (*E. coli* KL3/pRC1.55B)	100	11.71	8.46	5.20%	97.4%

Abbreviations: 3-dehydroshikimic acid (DHS); galic acid (GA).

The [5-^{18}O]-enriched 3-dehydroshikimic acid was then added to a culture medium of *E. coli* KL3/pRC1.55B with glucose addition under fermentor-controlled conditions. Plasmid pRC1.55B contained a *serA* gene encoding 3-phosphoglycerate dehydrogenase, a critical enzyme for biosynthesis of L-serine. Incorporation of a *serA* gene complemented the chromosomal *serA* inactivation and thus enabled *E. coli* KL3/pRC1.55B to grow in minimal salts medium without L-serine supplementation. Disruption of the *aroE* gene also interrupted the biosyntheses of aromatic amino acids and aromatic vitamins. Therefore, growth of *E. coli* KL3/pRC1.55B required supplementation with L-tyrosine, L-tryptophan, L-phenylalanine, *p*-hydroxybenzoic acid, *p*-aminobenzoic acid and 2,3-dihydroxybenzoic acid in culture medium. Another purpose of adding aromatic amino acids into the culture medium was to inhibit native DAHP synthases encoded by *aroF, aroG* and *aroH* loci in the *E. coli* KL3/pRC1.55B

genome. The effective inhibition of DAHP synthases was critical in this study due to interference from newly synthesized unlabeled 3-dehydroshikimic acid from glucose. A *shiA*-encoded transport protein responsible for transporting 3-dehydroshikimate and shikimate in *E. coli* has been identified.[25] Expression of the *shiA* gene is not regulated by TyrR repressor protein. Therefore, the [5-^{18}O]-enriched 3-dehydroshikimate could be transported into the cytoplasm in the presence of aromatic amino acids in the culture medium.

E. coli KL3/pRC1.55B was cultivated in 100 mL of M9 medium supplemented with aromatic amino acids and aromatic vitamins for 10-12 h at 37°C with agitation at 250 rpm and then transferred to a fermentor which contained 700 mL of culture medium when its OD_{600} reached 2-3. Cultivation under fermentor-controlled conditions was performed in a 2.0 L capacity Biostat MD B-Braun fermentor. The temperature was maintained at 36°C, and the pH at 7.0 by addition of concentrated NH_4OH or 2 *N* H_2SO_4. Dissolved oxygen was maintained at 20% air saturation throughout the fermentation process. [5-^{18}O]-Enriched 3-dehydroshikimic acid (5.0 g) was added to the culture at 20 h when the fermentation culture entered the stationary growth phase of its growth. Aromatic amino acids L-tyrosine (0.7 g), L-phenylalanine (0.7 g) and L-tryptophan (0.35 g) were added at the beginning of the fermentation as required for growth and at 18 h and 30 h to inhibit the native DAHP synthase activity. The effective inhibition of native DAHP synthase by supplementing aromatic amino acids was confirmed by the absence of shikimate pathway metabolites in *E. coli* KL3/pRC1.55B culture medium in a separate experiment without addition of 3-dehydroshikimic acid under fermentor-controlled conditions.

During the fermentation, the concentration of 3-dehydroshikimic acid slowly decreased, gallic acid (0.39 g/L) and 3-dehydroquinic acid (DHQ, 0.89 g/L) were produced at 42 h (Figure 51). After removal of cells and proteins, the supernatant (450 mL) was extraction with ethyl acetate, the organic phase was dried and gallic acid (0.0462 g) and a small amount of protocatechuic acid (0.0082 g) were isolated by a separation employing reverse phase HPLC. Compared with the ^{18}O-enrichment (5.34%) in the added 3-dehydroshikimic acid (entry 2, Table 6), the level of ^{18}O-enrichment (5.54%) in the isolated gallic acid (entry 3, Table 6) clearly indicates that the resulting 3-dehydroshikimic acid was converted into gallic acid with retention of ^{18}O-labeled oxygen.

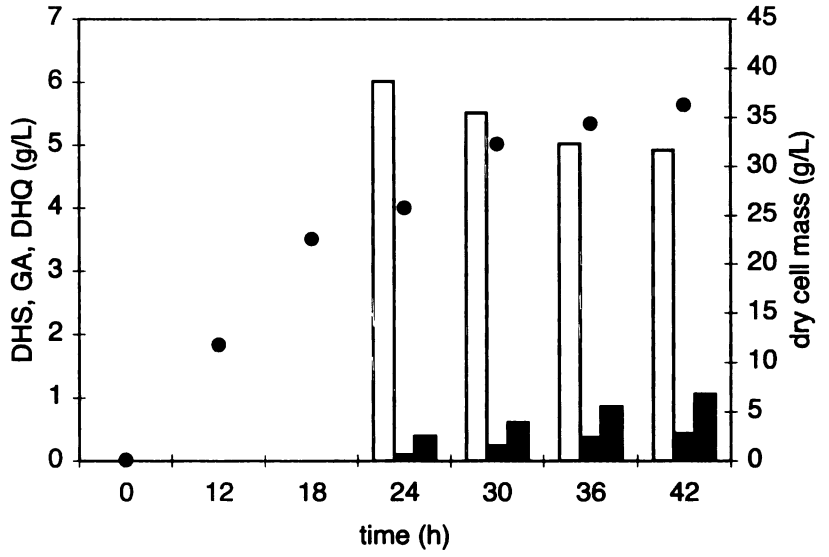

Figure 51. Gallic acid and 3-dehydroquinic acid production upon addition of [5-^{18}O]-enriched 3-dehydroshikimic acid by *E. coli* KL3/pRC1.55B. 3-Dehydroshikimic acid (DHS, open bar), gallic acid (GA, black bar), 3-dehydroquinic acid (DHQ, gray bar), dry cell mass (●).

The remaining 3-dehydroshikimic acid in fermentation broth was also extracted with ethyl acetate from fermentation supernatant using a continuous liquid-liquid extraction apparatus. The ^{18}O-enrichment of 5.20% (entry 6, Table 6) indicated that the ^{18}O-labeling in 3-dehydroshikimic acid was stable during the fermentation.

An alternative biocatalytic route for converting glucose to gallic acid has been reported that utilized the *K. pneumoniae aroZ*-encoded DHS dehydratase[26] to dehydrate 3-dehydroshikimic acid to protocatechuic acid followed by hydroxylation of protocatechuic acid by the *P. aeruginosa pobA**-encoded *p*-hydroxybenzoate hydroxylase (Figure 52).[27] *E. coli* KL7/pSK6.161 synthesized 20 g/L of gallic acid in 12% yield from glucose under fermentor-controlled conditions. *E. coli* KL7 was constructed by homologous recombination of an *aroBaroZ* insert into chromosomal *serA* locus in the *aroE* strain AB3248. Plasmid pSK6.161 contained *pobA**, $aroF^{FBR}$ and *serA* genes required for biosynthesis of gallic acid.[24]

DHS dehydratase is present in *Neurospora crassa*[28] and other microorganisms as well.[29] Isotopic labeling studies showed that DHS dehydratase from *N. crassa* catalyzed the *syn* elimination of water from C-5 hydroxyl group of 3-dehydroshikimic acid in which the hydroxyl oxygen atom at C-5 was lost.[30] Mutagenesis of the *pobA* gene, which encodes *p*-hydroxybenzoate hydroxylase in *Pseudomonas aeruginosa,* produced a mutant *p*-hydroxybenzoate hydroxylase encoded by *pobA**, which was capable of hydroxylating protocatechuic acid to form gallic acid.[31]

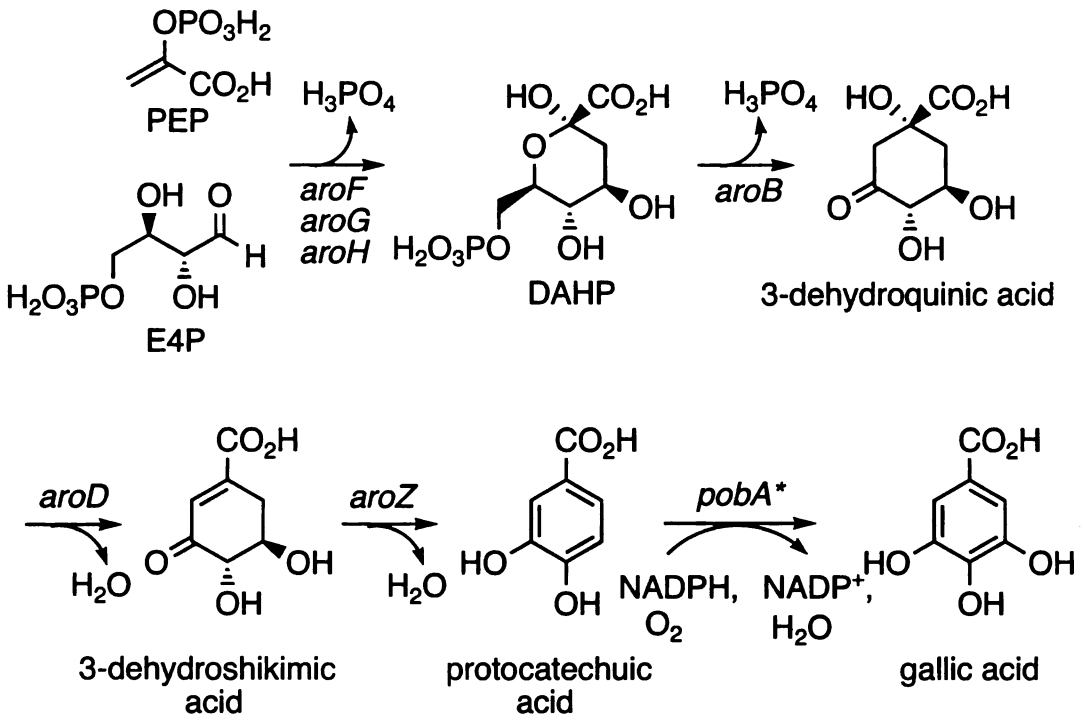

Figure 52. Microbial synthesis of gallic acid by exploiting *pobA activity.** Intermediates (abbreviations): phosphoenolpyruvate (PEP), D-erythrose 4-phosphate (E4P), 3-deoxy-D-*arabino*-heptulosonic acid 7-phosphate (DAHP). Genes (enzymes): *aroF*, *aroG*, *aroH*, DAHP synthase; *aroB*, 3-dehydroquinate synthase; *aroD*, 3-dehydroquinate dehydratase; *aroZ*, 3-dehydroshikimate dehydratase; *pobA**, *p*-hydroxybenzoate hydroxylase.

Plasmid pSK6.76 contained *aroZ, serA* and *pobA** genes. *E. coli* KL7/pSK6.76 was capable of converting 3-dehydroshikimic acid into gallic acid by a mechanism that represented the proposed gallic acid biosynthetic pathway via protocatechuic acid. Therefore, *E. coli* KL7/pSK6.76 was used as model for the alternate pathway to gallic acid that proceeds via 3-dehydroshikimic acid intermediacy. Due to the absence of a feedback-insensitive DAHP synthase, *E. coli* KL7/pSK6.76 was incapable of *de novo* biosynthesis of shikimate pathway metabolites when aromatic amino acids were added into the fermentation medium to inhibit the native, genome-encoded DAHP synthases.

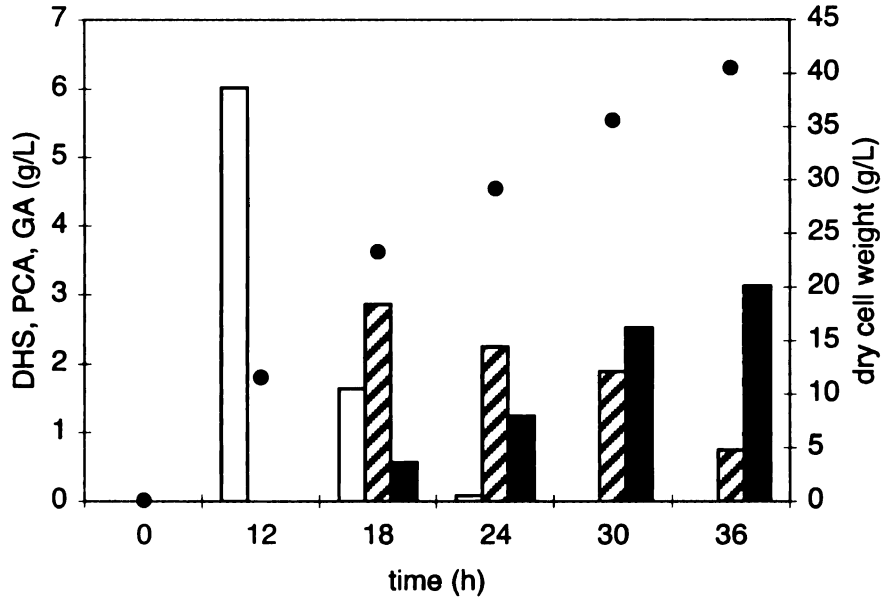

Figure 53. Gallic acid and 3-dehydroquinic acid production upon addition of [5-^{18}O]-enriched 3-dehydroshikimic acid by *E. coli* KL7/pSK6.76. 3-Dehydroshikimic acid (DHS, □), protocatechuic acid (PCA, stripped bar), gallic acid (GA, ■), dry cell mass (●).

KL7/pSK6.76 was cultured under fermentor-controlled conditions where the temperature was maintained at 36 °C, pH was maintained at 7 and dissolved oxygen was controlled at 20% of air saturation. [5-^{18}O]-Enriched 3-dehydroshikimic acid (5.0 g) was added at 12 h, aromatic amino acids, L-tyrosine (0.7 g), L-phenylalanine (0.7 g) and L-tryptophan (0.35 g) was added at the beginning of fermentation and again at 18 h. Although the *lacI* repressor gene was not present in the plasmid, isopropyl β-D-thiogalactopyranoside (IPTG, 15 mg) was added every 6 h after 12 h. Consumption of 3-dehydroshikimic acid and accumulation of protocatechuic acid were observed simultaneously during the first 12 h after addition of 3-dehydroshikimic acid. Complete consumption of 3-dehydroshikimic acid resulted in synthesis of 2.3 g/L of protocatechuic acid and 1.2 g/L of gallic acid at 12 h after addition (Figure 53). Protocatechuic acid

concentration was then decreased from 2.3 g/L at 24 h to a final concentration at 0.75 g/L at 36 h, while the concentration of gallic acid concentration increased from 1.24 g/L at 24 h to a final concentration of 3.1 g/L at 36 h. This profile was consistent with the biocatalytic route to gallic acid via protocatechuic acid as an intermediate.

The gallic acid produced by *E. coli* KL7/pSK6.76 was isolated from culture supernatant and analyzed using FAB(-) mass spectrometry. The ratio of the ^{18}O-labeled gallic acid signal (*m/z* 171) over its unlabeled counterpart (*m/z* 169, 170) was 2.32 to 111.76 (100+11.76), which meant the ^{18}O-enrichment in the gallic acid was 0.10% (entry 4, Table 6). The very low incorporation (1.9%) of ^{18}O atom in the final product gallic acid indicates the ^{18}O-labeled hydroxyl group of 3-dehydroshikimic acid was lost and the newly added hydroxyl group was from $^{16}O_2$ as predicted by the reaction mechanism. For comparison, gallic acid synthesized by *E. coli* KL3/pRC1.55B fully retained the ^{18}O labeling (entry 3, Table 6) and clearly was not biosynthesized via protocatechuic acid intermediacy.

Kambourakis et al.[24] reported a Cu^{2+}/Zn^{2+} mediated air oxidation of 3-dehydroshikimic acid in acetic acid solution to afford gallic acid in 70% yield. Air-oxidation of 3-dehydroshikimic acid in phosphate-buffered water (1.0 M, pH 6.5) led to a mixture of gallic acid (14%), protocatechuic acid (12%), tricarballylic acid (14%) and pyrogallol (3%) at 40 °C after 50 h. A plausible mechanism[32] for air oxidation of 3-dehydroshikimic acid was also proposed that involved initial tautomerization to an enediol form **23**. Enediol **23** could either form protocatechuic acid by elimination of a water molecule or further react with O_2 to yield gallic acid, tricarballytic acid and pyrogallol (Figure 54). Evidence for the presence of enediol **23** intermediacy was

obtained after isolation of dihydrogallic acid from an anaerobic K_2HPO_4 (1 M) solution of 3-dehydroshikimic acid. Inorganic phosphate could function as a general base to catalyze the initial tautomerization of 3-dehydroshikimic acid in phosphate-buffered water.

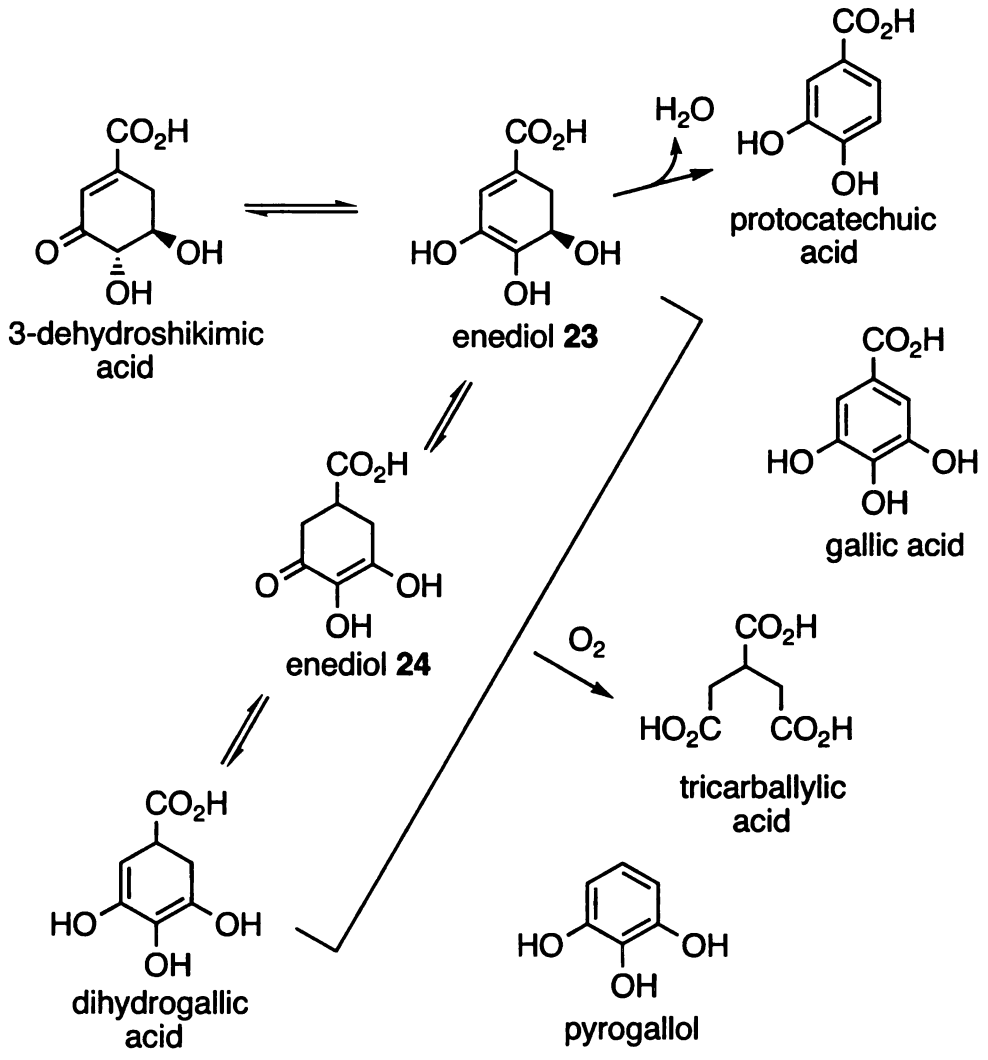

Figure 54. Mechanism for base-catalyzed air oxidation of 3-dehydroshikimic acid.

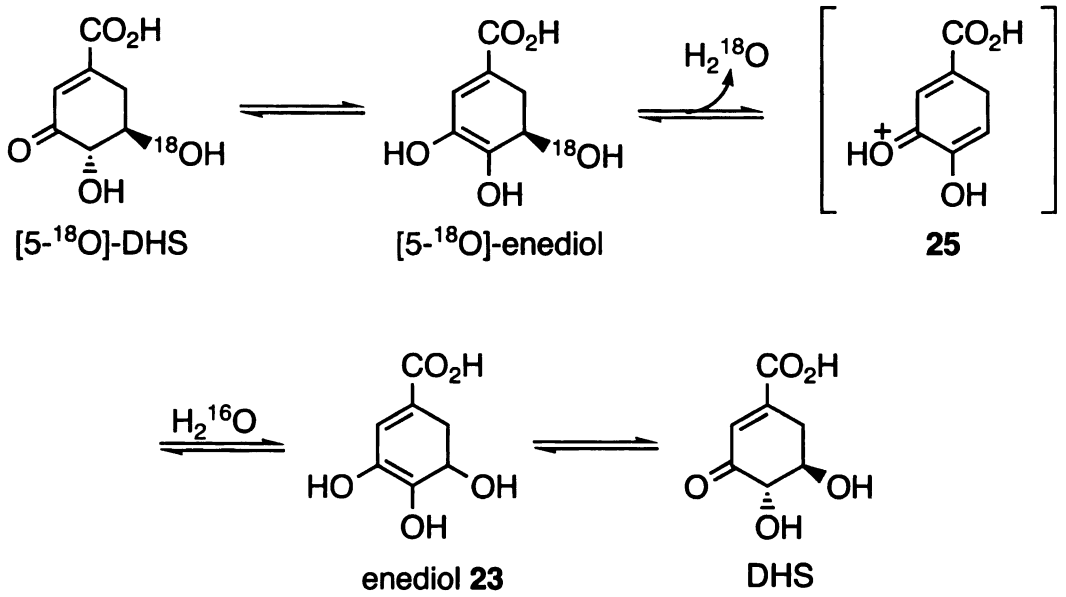

Figure 55. Proposed mechanism for ^{18}O-exchange of 3-dehydroshikimic acid in inorganic phosphate buffered water.

Although dilute inorganic phosphate buffer (43 mM) was used in the fermentation medium, the possibility that gallic acid formed in the *E. coli* fermentation was the result of air oxidation of biosynthesized 3-dehydroshikimate could not be ruled out. It was not clear whether the hydroxyl oxygen atom at C-5 was exchangable during tautomerization process. The air oxidation of [5-^{18}O]-enriched 3-dehydroshikimic acid was carried out in potassium phosphate buffer (1 M, pH 6.5) at room temperature. After 48 h, gallic acid (19.7%), PCA (22.7%) and tricarballylic acid (25.0%) were produced as reported previously. Gallic acid produced by air oxidation was purified and analyzed by mass spectrometry as mentioned before. Mass spectra data showed an ^{18}O-enrichment of 4.40% (entry 5, Table 6), which indicated only 82.4% of the ^{18}O-labeling in 3-dehydroshikimic acid was incorporated into gallic acid as a result of air oxidation catalyzed by inorganic phosphate. The loss of 17.6% ^{18}O atom during air oxidation might result from the [5-^{18}O]-hydroxyl exchange with $H_2{}^{16}O$ in inorganic phosphate buffer. A

possible mechanism for this exchange is proposed in Figure 55. The first step involves tautomerization of 3-dehydroshikimic acid to its enediol form, same as in the air oxidation process that leads to a mixture of gallic acid, protocatechuic acid, tricarballylic acid and pyrogallol. Elimination of the 5-hydroxy group leads to a α,β-unsaturated intermediate **25**. $H_2{}^{16}O$ could add to intermediate **25** through 1,4-addition reaction.

Discussion

Conversion of 3-dehydroshikimic acid into gallic acid has been narrowed to two pathways. 3-Dehydroshikimic acid could be directly oxidized to gallic acid which would be indicated by retention of C-5 hydroxyl group in 3-dehydroshikimic acid in the C-3 hydroxyl of gallic acid. Alternatively, 3-dehydroshikimic acid could undergo initial dehydration to protocatchuic acid involving elimination of the 5-hydroxy group, followed by hydroxylation to afford gallic acid. [5-^{18}O]-3-Dehydroshikimic acid was chemically synthesized and [this labeled 3-dehydroshikimic acid was added into a culture of *E. coli* KL3/pRC1.55B in which *in vivo* biosynthesis of shikimate pathway metabolites was inhibited. Gallic acid was produced along with 3-dehydroquinic acid. Since *E. coli* KL3/pRC1.55B is incapable of producing shikimate pathway metabolites under the fermentation conditions, the production of 3-dehydroquinic acid indicates the added 3-dehydroshikimic acid was transported into the *E. coli* cytoplasm presumably by a *shiA*-encoded shikimate transport protein and was converted to 3-dehydroquinic acid by the reversible, *aroD*-encoded 3-dehydroquinate dehydratase.

The gallic acid produced by *E. coli* KL3/pRC1.55B and the remaining 3-dehydroshikimic acid in the culture medium were isolated and analyzed by mass

spectrometry. The full ^{18}O-labeling retention in the gallic acid synthesized indicates that the 5-hydroxyl group in 3-dehydroshikimic acid was completely incorporated into gallic acid. By contrast, the ^{18}O-labeled 5-hydroxyl group in 3-dehydroshikimic acid was almost completely lost when protocatechuic acid is the intermediate in gallic acid synthesis by KL7/pSK6.76. These results clearly indicate indicated that 3-dehydroshikimic acid was directly oxidized to gallic acid without protocatechuic acid intermediacy in recombinant *E. coli* KL3.

In addition to *E. coli*, this methodology can also be applied to probe the gallic acid biosynthesis in higher plant and fungi, which might lead to the discovery of a 3-dehydroshikimate dehydrogenase. However, the reported inorganic phosphate-catalyzed aerobic oxidation of 3-dehydroshikimic acid needed to be examined carefully. Abiotic aerobic oxidation could also result in retention of ^{18}O atom in product gallic acid. The lack of assayable enzyme activity for conversion of 3-dehydroshikimic acid to gallic acid in cell-free extract adds more ambiguity to the existence of an oxidoreductase for 3-dehydroshikimate oxidation in nature.

Air oxidation of 3-dehydroshikimic acid is always accompanied by the formation of nearly equal quantities of protocatechuic acid and tricaballylic acid, which is not consistent with the much higher ratio of gallic acid to protocatechuic acid observed in the [5-^{18}O]-3-dehydroshikimate feeding experiment (6.2:1 by *E. coli* KL3/pRC55). Additional evidence that disfavors the abiotic aerobic oxidation of 3-dehydroshikimic acid comes from the results that the ^{18}O-labeling was partially washed out in gallic acid produced by aerobic oxidation of 3-dehydroshikimic acid in inorganic phosphate-buffered water. Therefore, examination of the extent of label washout in ^{18}O-enriched 3-

dehydroshikimic acid after fermentation could provide additional insights into the role of aerobic oxidation in the conversion of 3-dehydroshikimic acid to gallic acid. The remaining 3-dehdroshikimic acid was isolated from the *E. coli* KL3/pRC1.55B fermentation supernatant and analyzed by mass spectrometry. The data reveals a slightly decline in ^{18}O-incorporation in 3-dehydoshikimic acid after fermentation (97.4%) compared with the added 3-dehydroshikimic acid (100%). This result indicates that the exchange reaction occurred at a much slower rate in the fermentation medium possibly due to low concentration (43 mM) of inorganic phosphate and an oxygen level of 20% air saturation used in the fermentation conditions. These results suggest that abiotic, aerobic oxidation is unlikely to be the primary route for gallic acid formation although a small portion of gallic acid is possibly formed by this mechanism.

After the work was completed, Ossipov et al.[33] isolated the first 3-dehydroshikimate dehydrogenase that catalyzes the direct oxidation of 3-dehydroshikimic acid to gallic acid from leaves of mountain birch (*Betula pubescens ssp. Czerepanovii*). The 3-dehydroshikimate dehydrogenase was found to be a $NADP^+$-dependent enzyme with a K_m value of 0.008 mM for $NADP^+$ and a K_m value of 0.49 mM for 3-dehydroshikimate. The discovery of 3-dehydroshikimate dehydrogenase also raises an interesting question about the biosynthesis of its substrate, 3-dehydroshikimic acid in higher plants, since it is generally accepted that the third and fourth steps of the shikimate pathway are catalyzed by a bifunctional enzyme 3-dehydroquinate dehydratase-shikimate dehydrogenase in higher plants plastids.[34] The metabolite channeling mechanism prevents the accumulation of 3-dehydroshikimate, the immediate precursor to gallic acid.

Therefore, the biosynthesis of 3-dehydroshikimate is proposed to proceed by monofunctional enzymes.[35]

The protein sequence of the 3-dehydroshikimate dehydrogenase from birch was not obtained.[36] In theory, heterologous expression of the 3-dehydroshikimate dehydrogenase in a 3-dehydroshikimate producing *E. coli* strain could constitute a better biosynthesis of gallic acid than current synthesis by *E. coli* KL7/pSK6.161[27] via protocatechuic acid intermediacy. In *E. coli* KL7/pSK6.161, the conversion of protocatechuic acid to gallic acid catalyzed by the *pobA**-encoded *p*-hydroxybenzoate hydroxylase generates H_2O_2 as a byproduct. This H_2O_2 is capable of damaging *E. coli* cells and therefore reducing the yield and concentration of gallic acid synthesized by *E. coli*.

Reference

[1] Leston, G. In *Kirk-Othmer Encyclopedia of Chemical Technology*; Kroschwitz, J. I., Howe-Grant, M., Eds.; Wiley: New York, 1996; Vol. 19, p 778.

[2] (a) Scalbert, A.; Mila, I.; Expert, D.; Marmolle, F.; Albrecht, A.-M.; Hurrell, R.; Huneau, J.-F.; Tome, D. Polyphenols, metal ion complexation and biological consequences. *Basic Life Sci.* **1999**, *66*, 545-554. (b) Gross, G. G. Biosynthesis, biodegradation and cellular localization of hydrolysable tannins. *Recent Advances Phytochem.* **1998**, *33*, 185-213.

[3] Harborne, J. B.; Grayer, R. J.; Flavonoids and inserts. In *The Flavonoids-Advances in Research Since 1986*. Harborne, J. B. Ed., Chapman and Hall, London, 1994, p. 589.

[4] Haslam, E. In *Practical Polyphenolics: From Structure to Molecular Recognition and Physiology Action*. Cambridge University Press, Cambridge, 1998.

[5] Grundhofer, P.; Niemetz, R.; Schilling, G.; Gross, G. G. Biosynthesis and subcellular distribution of hydrolysable tannins. *Phytochem.* **2001**, *57*, 915-927.

[6] Haslam, E.; Haworth, R. D.; Knowles, P. F. Gallotannins. IV. The biosynthesis of gallic acid. *J. Chem. Soc.* **1961**, 1854-1859.

[7] Korth, H. Formation of gallic acid from quinic acid by *Enterobacter cloacae* and *Pseudomonas fluorescens*. *Arch. Microbiol.* **1973**, *89*, 67-72.

[8] Kawakubo, J.; Nishira, H.; Aoki, K.; Shinke, R. Studies on phenolic-compounds production by molds. 2. Isolation of a gallic acid-producing microorganism with sake cake medium and production of gallic acid. *Biosci. Biotech. Biochem.* **1993**, *57*, 1360-1361.

[9] (a) Li, K.; Mikola, M. R.; Draths, K. M.; Worden, R. M.; Frost, J. W. Fed-batch fermentor synthesis of 3-dehydroshikimic acid using recombinant *Escherichia coli*. *Biotechnol. Bioeng.* **1999**, *64*, 61-73. (b) Yi, J.; Li, K.; Draths, K. M.; Frost, J. W. Modulation of phosphoenolpyruvate synthase expression increases shikimate pathway product yields in *E. coli*. *Biotechnol. Prog.* **2002**, *18*, 1141-1148. (c) Yi, J.; Draths, K. M.; Li, K.; Frost, J. W. Altered glucose transport and shikimate pathway product yields in *E. coli*. *Biotechnol. Prog.* **2003**, *19*, 1450-1459.

[10] (a) Cornthwaite, D.; Haslam, E. Gallotannins. IX. Biosynthesis of gallic acid in *Rhus typhina*. *J. Chem. Soc.* **1965**, 3008-3011. (b) Saijo, R. Pathway of gallic acid biosynthesis and its esterification with catechins in young tea shoots. *Agric. Biol. Chem.* **1983**, *47*, 455-460. (c) Ishikura, N.; Hayashida, S.; Tazaki, K. Biosynthesis of gallic and ellagic acids with ^{14}C-labeled compounds in *Acer* and *Rhus* leaves. *Bot. Mag. Tokyo* **1984**, *97*, 355-367.

[11] Loscher, R.; Heide, L. Biosynthesis of *p*-hydroxybenzoate from *p*-coumarate and *p*-coumaroyl-coenzyme A in cell-free extracts of *Lithospermum erithrorhizon* cell cultures. *Plant Physiol.* **1994**, *106*, 271-279.

[12] (a) Lydon, J.; Duck, S. O. Glyphosate induction of elevated levels of hydroxybenzoic acids in higher plants. *Agric. Food Chem.* **1988**, *36*, 813-818. (b) Becerril, J.; Duke, S.; Lydon, J. Glyphosate effects on shikimate pathway products in leaves and flowers of velvetleaf. *Phytochem.* **1989**, *28*, 695-700.

[13] Werner, I.; Bacher, A.; Eisenreich W. Retrobiosynthetic NMR studies with ^{13}C-labeled glucose: formation of gallic acid in plants and fungi. *J. Biol. Chem.* **1997**, *272*, 25474-25482.

[14] Dixon, R. A.; Achnine, L.; Kota, P.; Liu, C.-J.; Reddy, M. S. S.; Wang, L. The phenylpropanoid pathway and plant defense: a genomics perspective. *Mol. Plant Pathol.* **2002**, *3*, 371-390.

[15] Tateoka, T. N. Formation of protocatechuic acid from 5-dehydroshikimic acid in the extract of mung bean seedlings. *Bot. Mag. Tokyo* **1968**, *81*, 103-104.

[16] Kato, N.; Shiroya, M.; Yoshida, S.; Hasegawa, M. Biosynthesis of gallic acid by a homogenate of the leaves of *Pelargonium inquinans*. *Bot. Mag. Tokyo* **1968**, *81*, 506-507.

[17] Pittard, A. J. Biosynthsis of aromatic amino acids. In *Escherichia coli and Salmonella: Cellular and Molecular Biology*, 2nd ed.; Neidhardt, F. C., Ed.; ASM press: Washinfton, DC, 1996: p. 458-484..

[18] (a) McGowan, D. A.; Berchtold, G. A. (-)-Methyl *cis*-3-hydroxy-4,5-oxycyclohex-1-enecarboxylate: stereospecific formation from and conversion to (-)-methyl shikimate; Complex formation with bis(carbomethoxy)hydrazine. *J. Org. Chem.* **1981**, *46*, 2381. (b) Tan, D. S.; Foley, M. A.; Stockwell, B. R.; Shair, M. D.; Schreiber, S. L. Synthesis and preliminary evaluation of a library of polycyclic small molecules for use in chemical genetic assays. *J. Am. Chem. Soc.* **1999**, *121*, 9073-9087.

[19] Gustin, D. J.; Hilvert, D. J. Chemoenzymatic synthesis of isotopically labeled chorismic acids. *J. Org. Chem.* **1999**, *64*, 4935-4938.

[20] Chaudhuri, S.; Anton, I. A.; Coggins, J. R. Shikimate dehydrogenase from *Escherichia coli*. *Methods Enzymol.* **1987**, *142*, 315-320.

[21] (a) Tolbert, T. J.; Williamson, J. R. Preparation of specifically deuterated and ^{13}C-labeled RNA for NMR studies using enzymatic synthesis. *J. Am. Chem. Soc.* **1997**, *119*, 12100-12106. (b) Carrea, G.; Bovara, R.; Cremonesi, P.; Lodi, R. Enzymatic preparation of 12-ketochenodeoxycholic acid with NADP regeneration. *Biotechnol. Bioeng.* **1984**, *26*,

560-563. (c) Wong, C.-H.; McCurry, S. D.; Whitesides, G. M. Practical enzymatic syntheses of ribulose 1,5-bisphosphate and ribose 5-phosphate. *J. Am. Chem. Soc.* **1980**, *102*, 7938-7939. (d) Chenault, H. K.; Whitesides, G. M. Regeneration of nicotinamide cofactors for use in organic synthesis. *Applied Biochem. Biotechnol.* **1987**, *14*, 147-197.

[22] Kambourakis, S. Doctorate Dissertation, Michigan State University, 2000.

[23] Vederas, J. C. Biosynthetic studies using oxygen-18 isotope shifts in carbon-13 nuclear magnetic resonance. *Can. J. Chem.* **1982**, *60*, 1637-1642.

[24] Kambourakis, S.; Frost, J. W. Synthesis of gallic acid: Cu^{2+} mediated oxidation of 3-dehydroshikimc acid. *J. Org. Chem.* **2000**, *65*, 6904-6909.

[25] Whipp, M. J.; Camakaris, H.; Pittard, A. J. Cloning and analysis of the *shiA* gene, which encodes the shikimate transport system of *Escherichia coli* K-12. *Gene* **1998**, *209*, 185-192.

[26] Draths, K. M.; Frost, J. W. Environmentally compatible synthesis of catechol from D-glucose. *J. Am. Chem. Soc.* **1995**, *117*, 2395-2400.

[27] Kambourakis, S.; Draths, K. M.; Frost, J. W. Synthesis of gallic acid and pyrogallol from glucose: replacing natural product isolation with microbial catalysis. *J. Am. Chem. Soc.* **2000**, *122*, 9042-9043.

[28] Schweizer, M.; Case, M. E.; Dykstra, C. C.; Giles, N. H.; Kushner, S. R. Cloning and quinic acid (*qa*) gene cluster from *Neurospora crassa*: Identification of recombinant plasmids containing both *qa-2+* and *qa-3+*. *Gene* **1981**, *14*, 23-32.

[29] Hawkins, A. R.; Francisco daSilva, A. J.; Roberts, C. F. Cloning and characterization of the three enzyme structural genes *QUTB*, *QUTC* and *QUTE* from the quinic acid utilization gene cluster in *Aspergillus nidulans*. *Curr. Genetics* **1985**, *9*, 305-311.

[30] (a) Gross, S. R. Enzymic conversion of 5-dehydroshikimic acid to protocatechuic acid. *J. Biol. Chem.* **1958**, *233*, 1146-1151. (b) Floss, H. G.; Scharf, K. H.; Zenk, M. H.; Onderka, D. F.; Carroll, M. Stereochemistry of the enzymic and nonenzymic conversion of 3-dehydroshikimate into protocatechuate. *J. Chem. Soc., Chem. Commun.* **1971**, *14*, 765-766.

[31] (a) Entsch, B.; Palfey, B. A.; Ballou, D. P.; Massey, V. Catalytic function of tyrosine residues in *para*-hydroxybenzoate hydroxylase as determined by the study of site-directed mutants. *J Biol. Chem.* **1991**, *266*, 17341-17349. (b) Eschrich, K.; van der Bolt, F. J. T.; de Kok, A.; van Berkel, W. J. H. Role of Tyr201 and Tyr385 in substrate activation by *p*-hydroxybenzoate hydroxylase from *Pseudomonas fluorescens*. *Eur. J. Biochem.* **1993**, *216*, 137-146.

[32] Richman, J. E.; Chang, Y.-C.; Kambourakis, S.; Draths, K. M.; Almy, E.; Snell, K. D.; Strasburg, G. M.; Frost, J. W. Reaction of 3-dehydroshikimic acid with molecular oxygen and hydrogen peroxide: products, mechanism, and associated antioxidant activity. *J. Am. Chem. Soc.* **1996**, *118*, 11587-11591.

[33] Ossipov, V.; Salminen, J.-P.; Ossipov, S.; Haukiojia, E.; Pihlaja, K. Gallic acid and hydrolysable tannins are formed in birch leaves from an intermediate compound of the shikimate pathway. *Biochem. System. Ecol.* **2003**, *31*, 3-16.

[34] Hermann, K. M.; Weaver, L. M. The shikimate pathway. *Ann. Rev. Plant. Physiol. Plant. Mol. Biol.* **1999**, *50*, 473-503.

[35] Mousdale, D.; Coggins, J. Subcellular localization of the common shikimate pathway enzymes in *Pisum sativum L. Planta* **1985**, *163*, 241-249.

[36] Ossipov, V. personal communication.

CHAPTER FOUR

Creation of a Pyruvate-Based Shikimate Pathway in *Escherichia coli*

Introduction

Improving the synthesis of hydroquinone from glucose discussed in Chapter 2 is part of a larger effort to improve microbial syntheses of shikimate pathway products. A variety of strategies have been employed for improving the yields of shikimate pathway metabolites in *E. coli*.[1,2] These strategies are primarily focused on expression of mutant isozymes of DAHP synthase that are insensitive to feedback inhibition by aromatic amino acids and increasing the availability of D-erythrose 4-phosphate (E4P) and phosphoenolpyruvate (PEP). E4P and PEP are the substrates of DAHP synthase, which is the first enzyme in the shikimate pathway.

In vivo activity of the first enzyme plays an essential role in directing carbon flow into the shikimate pathway.[3] Feedback inhibition of the DAHP synthase isozymes *in vivo* by aromatic amino acids constitutes the major regulatory control of aromatic amino acids biosynthesis.[3a] Several alleles that encode feedback-insensitive DAHP synthase have been obtained by mutation of *aroF*,[3b,1f] *aroG*[4] and *aroH*.[5] The use of DAHP synthase isozymes that are insensitive to feedback inhibition by aromatic amino acids has been a centerpiece of virtually all efforts to synthesize shikimate pathway products in high yield.

D-Erythrose 4-phosphate is derived from the non-oxidative pentose phosphate pathway. Draths et al.[6] demonstrated in 1990 that amplified expression of transketolase resulted in a two-fold increase in concentrations of biosynthesized shikimate pathway metabolites presumably by increasing the availability of D-erythrose 4-phosphate.

Transketolase catalyzes the conversion of D-fructose 6-phosphate into D-erythrose 4-phosphate. Transketolase also serves to generate the substrate D-sedoheptulose-7-phosphate for conversion to D-erythrose 4-phosphate catalyzed by *tal*-encoded transaldolase. Overexpression of transaldolase also relieves D-erythrose 4-phosphate limitation in the presence of overexpressed phosphoenolpyruvate synthase. No further improvements in the biosynthesis of shikimate pathway metabolites has been observed when both transketolase and transaldolase are overexpressed.[7]

Phosphoenolpyruvate is derived from the Embden-Meyerhof-Parnas glycolytic pathway. Besides being a substrate for the first enzyme in the shikimate pathway, phosphoenolpyruvate is also used as a phosphate donor in the phosphoenolpyruvate:carbohydrate phosphotransferase (PTS) system for microbial transport and phosphorylation of glucose, as a substrate in 3-deoxy-D-*manno*-octulosonate biosynthesis and peptidoglycan biosynthesis, and participates in ATP-generating reactions catalyzed by pyruvate kinase.[8] The resulting competition between the shikimate pathway and other enzymes for the cellular supplies of phosphoenolpyruvate limits the concentrations and yields of natural products synthesized by way of the shikimate pathway.

In wild-type *E. coli*, the major consumer of phosphoenolpyruvate is the glucose phosphotransferase system (PTS) for transport and phosphorylation of glucose.[9] PEP-mediated phosphoryl group transfer both energetically drives glucose transport and generates the glucose 6-phosphate. One molecule of phosphoenolpyruvate is converted into pyruvate for every molecule of glucose transported into the cytoplasm by the PTS system. PTS-generated pyruvate is oxidized through the tricarboxylic acid cycle (TCA

cycle) to carbon dioxide and is apparently not recycled to phosphoenolpyruvate under normal aerobic culture conditions. The theoretical maximum total yield for shikimate pathway products synthesized from glucose is 43% (mol/mol) based on theoretical flux analysis[1d] (Figure 56). The yield reflects the fundamental limitation imposed on microbial synthesis by the PTS-mediated glucose transport.

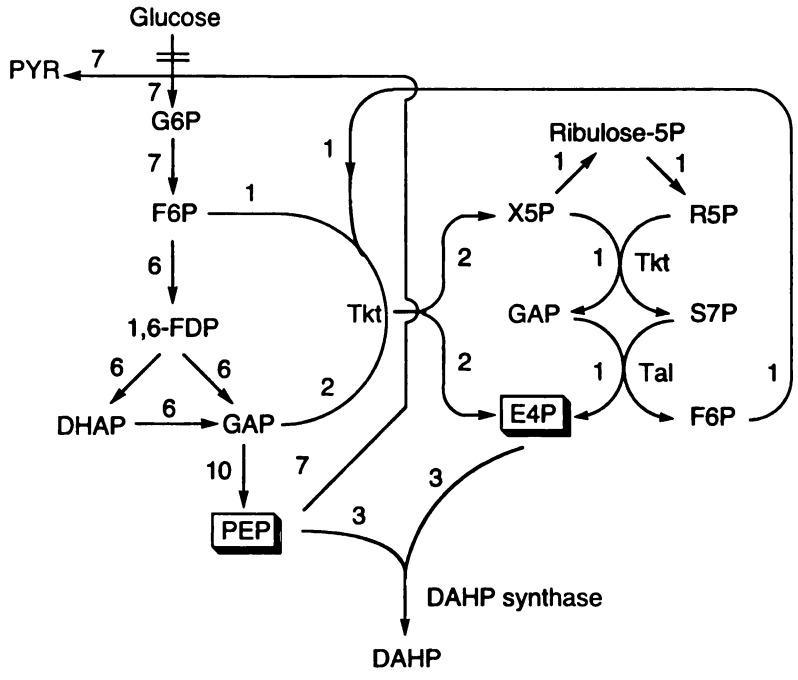

Figure 56. Reaction pathways for maximal conversion of glucose to DAHP for *E. coli* strains reliant on PTS for glucose transport. The numbers are the relative fluxes needed to convert 7 mol of glucose into DAHP. Enzymes: Pps, PEP synthase; Tkt, transketolase; Tal, transaldolase. Metabolites: G6P, glucose 6-phosphate; F6P, fructose 6-phosphate; 1,6-FDP, 1,6-fructose diphosphate; DHAP, dihydroxyacetone phosphate; GAP, glyceraldehyde 3-phosphate; R5P: ribose 5-phosphate; X5P, xylulose 5-phosphate; S7P, sedoheptulose 7-phosphate; PYR, pyruvate.

The theoretical maximum yield is calculated by assuming that the branching pathways are blocked and the carbon flow is directed by the most efficient pathways with minimal loss to carbon dioxide, other metabolites and biomass. Under these conditions,

the relative flux through each step at the steady state can be calculated by balancing the input (production) and output (consumption) fluxes from each metabolite pool. If *E. coli* transports glucose by PTS without recycling pyruvate to phosphoenolpyruvate, the input of 7 mol of glucose can produce 3 mol of DAHP (43% molar yield) and 7 mol of pyruvate (Figure 56), which is further metabolized to CO_2 and acetyl-CoA for the TCA cycle.

Different strategies have been described for increasing the cytoplasmic concentration of phosphoenolpyruvate by way of circumventing the expenditure of phosphoenolpyruvate by the PTS-mediated glucose transport employed by *E. coli* and many other microbes.[10] Those strategies comprised of recycling of the PTS-generated pyruvate back to phosphoenolpyruvate using amplified expression of *ppsA*-encoded phosphoenolpyruvate synthase[1d] and replacing PTS-driven glucose transport by facilitated diffusion mediated by the *Zymomonas mobilis glf*-encoded glucose facilitator[11] and galactose-proton symport mediated by *E. coli galP*-encoded galactose permease (Figure 57).[2a] In addition, employing a different source of carbon such as D-xylose and L-arabinose for microbial growth and shikimate pathway products production would circumvent the PTS-mediated glucose transport since the transport of these pentoses in *E. coli* are driven by a high affinity permease driven by the conversion of ATP to ADP.[1d,12] Unfortunately, commercial D-xylose and L-arabinose streams that are pure, abundant, and inexpensive are not currently available. An alternative strategy employs glucose adjuncts that can be readily converted to phosphoenolpyruvate. For example, equivmolar amounts of succinic acid can be added to glucose-limited cultures of *E. coli* KL3/pKL6.218A. This construct converted succinic acid by way of the TCA cycle into oxaloacetate.

Overexpressed phosphoenolpyruvate carboxylase then converted the oxaloacetate into PEP. Glucose-limited cultures of *E. coli* construct KL3/pKL6.218A overexpressing phosphoenolpyruvate carboxykinase in the presence of DAHP synthase and transketolase led to synthesis of 30% higher concentrations of 3-dehydroshikimic acid.[13] The yield (29%, mol/mol), however, was almost the same as using glucose as sole carbon source (28%, mol/mol).

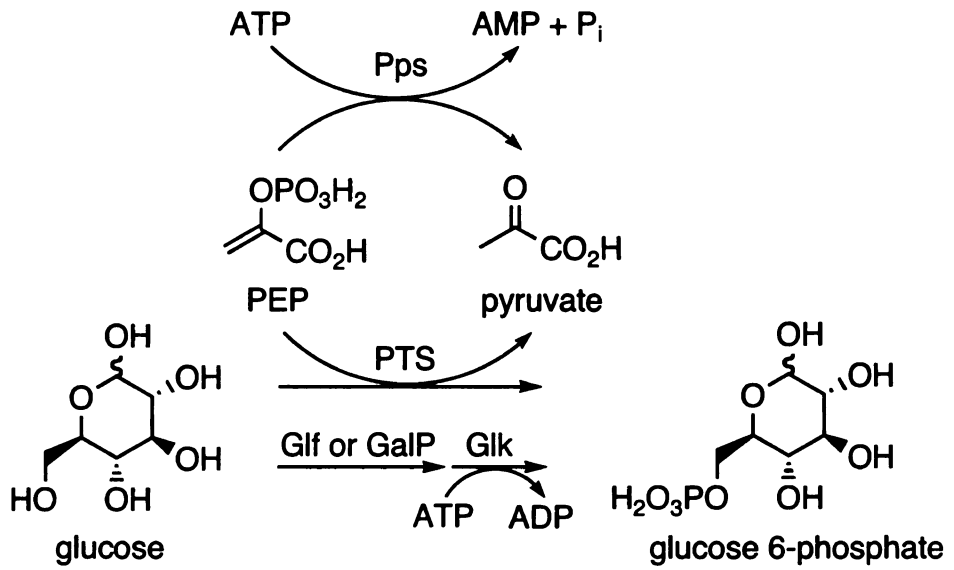

Figure 57. Previously examined strategies to increase phosphoenolpyruvate availability. Metabolite: PEP, phosphoenolpyruvate. Enzymes: Pps, phosphoenolpyruvate synthase; Glf, glucose facilitator; GalP, galactose permease; Glk, glucose kinase.

This work explores whether pyruvate can replace phosphoenolpyruvate in an enzyme-catalyzed condensation with D-erythrose 4-phosphate to form 3-deoxy-D-*arabino*-heptulosonate 7-phosphate (DAHP, Figure 58). The centerpiece of this created shikimate pathway variant is the directed evolution of 2-keto-3-deoxy-6-phosphogalactonate (KDPGal, Figure 58) aldolase.[14] This constitutes a fundamental departure from all previous strategies employed to increase phosphoenolpyruvate

availability in *E. coli*. The pyruvate-based shikimate pathway utilizes the pyruvate byproduct of PTS-mediated glucose transport instead of competing with PTS-mediated glucose transport for cellular supplies of phosphoenolpyruvate.

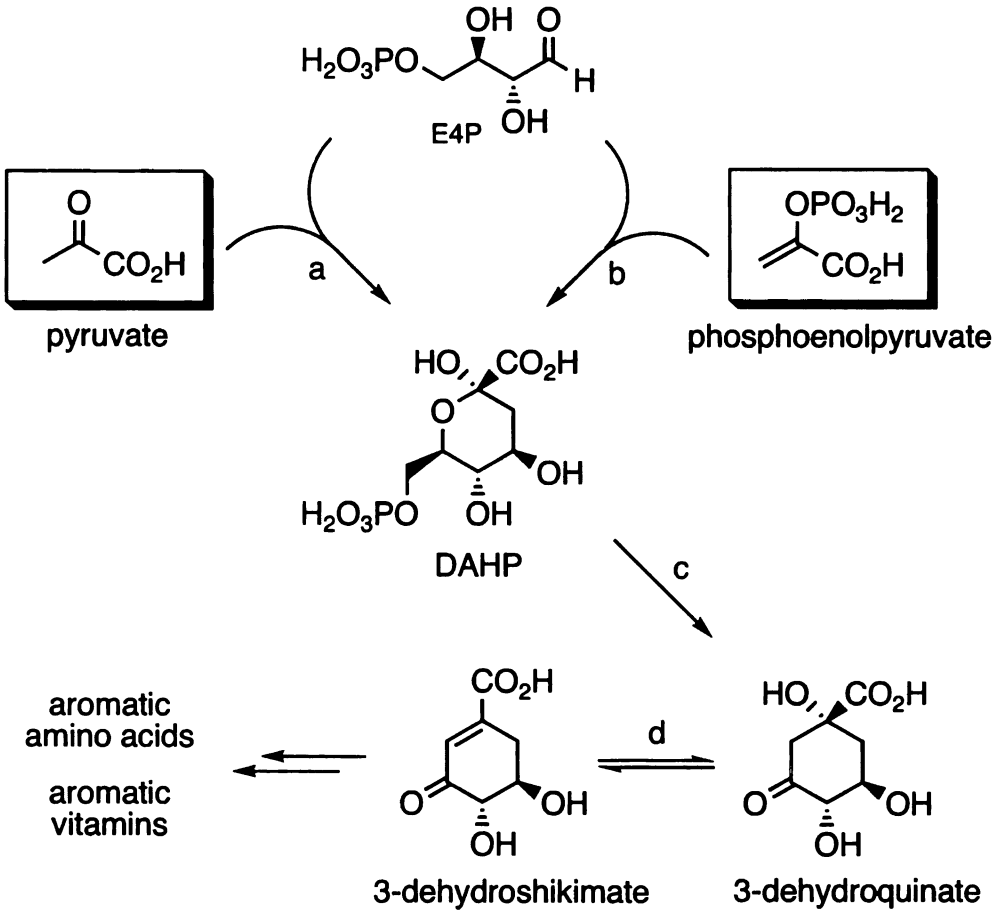

Figure 58. Proposed pyruvate-based shikimate pathway and the native phosphoenolpyruvate-based shikimate pathway. [a] Metabolites: E4P, D-erythrose 4-phosphate; DAHP, 3-deoxy-D-*arabino*-heptulosonic acid 7-phosphate. [b] Enzymes (genes): (a) KDPGal aldolase (*dgoA*); (b) DAHP synthase (*aroF, aroG, aroH*); (c) 3-dehydroquinate synthase (*aroB*); (d) 3-dehydroquinate dehydratase (*aroD*).

An input of 7 mol of glucose can thus produce 6 mol of DAHP under the condition where 1 mol of pyruvate generated by the PTS system is converted to phosphoenolpyruvate (Figure 59). This in theory can be accomplished by converting

pyruvate into oxalacetate by way of the TCA cycle followed by PEP carboxykinase-catalyzed conversion to phosphoenolpyruvate. The theoretical maximum yield for biosynthesis of a shikimate pathway metabolite such as 3-dehydroshikimic acid via a pyruvate-based shikimate pathway is 86% (mol/mol) as compared with 43% (mol/mol) using the phosphoenolpyruvate-based shikimate pathway with PTS-mediated glucose transport (Figure 59).

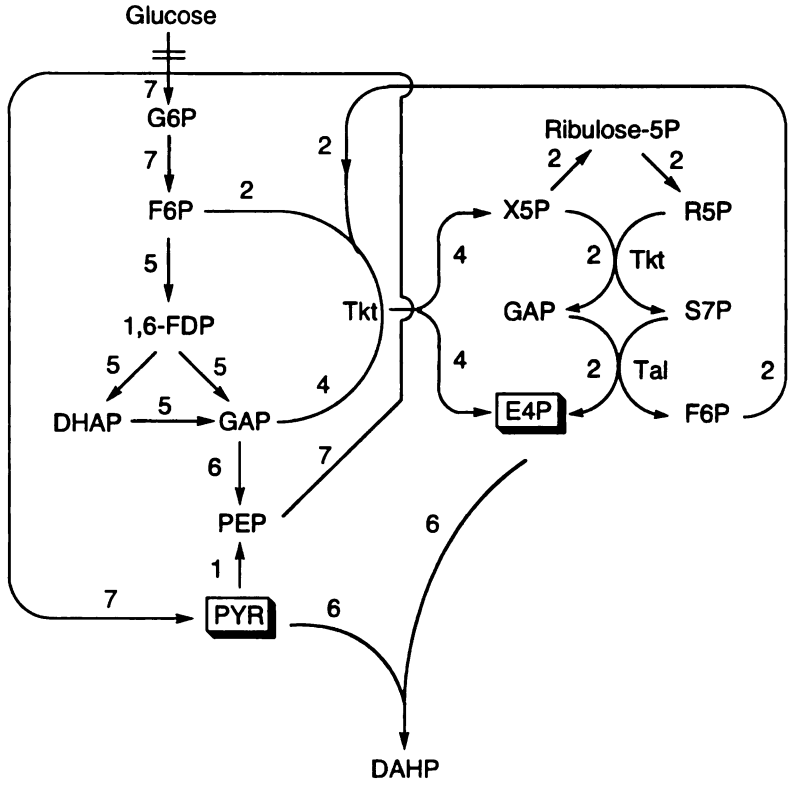

Figure 59. Reaction pathways for maximal conversion of glucose to DAHP for *E. coli* strains employing pyruvate-based shikimate pathway. The numbers are the relative fluxes needed to convert 7 mol of glucose into DAHP. Enzymes: Pps, PEP synthase; Tkt, transketolase; Tal, transaldolase. Metabolites: G6P, glucose 6-phosphate; F6P, fructose 6-phosphate; 1,6-FDP, 1,6-fructose diphosphate; DHAP, dihydroxyacetone phosphate; GAP, glyceraldehyde 3-phosphate; R5P: ribose 5-phosphate; X5P, xylulose 5-phosphate; S7P, sedoheptulose 7-phosphate; PYR, pyruvate.

According to Lowry et al.,[15] the concentration of pyruvate in *E. coli* cells grown on glucose is about 0.9 μmol/g (dry weight), while the phosphoenolpyruvate concentration is about 0.21 μmol/g (dry weight). Utilization of the more abundant pyruvate as the substrate for the first enzyme of the shikimate pathway instead of phosphoenolpyruvate might therefore lead to the synthesis of higher concentrations of shikimate pathway products. A pyruvate-based shikimate pathway is also potentially important form the standpoint of controlling fed-batch cultures. When glucose is added too rapidly to *E. coli* during fed-batch cultures under fermentor-controlled conditions, large amounts of pyruvate are generated by the microbe resulting in the export and accumulation of acetic acid in the culture supernatant.[16] To avoid the accumulation of acetic acid to toxic levels, the rate of glucose addition needs to be closely matched to the rate of glucose consumed by the microbe.[16] In a pyruvate-based shikimate pathway, the glucose addition rate may not need to be tightly controlled since the pyruvate generated during PTS-mediated glucose transport is being consumed to make shikimate pathway products.

Although relieved from feedback inhibition by aromatic amino acids, the $AroF^{FBR}$ and $AroG^{FBR}$ feedback-insensitive isozymes of DAHP synthase are prone to a decline in specific activity over the course of an *E. coli* culture. Tribe and Pittard reported a 7 h^{-1} half-life for the specific activity of AroG and a 5.5 h^{-1} half-life for the specific activity of AroF.[17] Unlike the native DAHP synthase isozymes which are feedback-inhibited by aromatic amino acids, KDPGal aldolase is unlikely to be subject to feedback inhibition by aromatic amino acids. Replacing the proteolysis-labile DAHP synthase with KDPGal

aldolase would be beneficial to the biosynthesis of shikimate pathway products by maintaining stable enzyme activity.

Beyond the attendant biocatalytic implications, a shikimate pathway variant based on condensation of pyruvate with D-erythrose 4-phosphate may be important as a theoretical construct. Minimizing expenditure of the high-energy phosphoenolpyruvate by the shikimate pathway might be a metabolic advantage under certain growth conditions. The shikimate pathway variant outlined in this chapter may thus serve as a model of a naturally occurring aromatic biosynthetic pathway that remains to be discovered.

Previously examined syntheses of shikimate pathway products by *E. coli* constructs with phosphoenolpyruvate synthase overexpression. Patnaik et al[1d] were the first to demonstrate the positive effect on shikimate pathway product yields attendant with recycling of pyruvate back to phosphoenolpyruvate by amplified expression of *ppsA*-encoded PEP synthase. PEP synthase catalyzes the generation of phosphoenolpyruvate from pyruvate with the expenditure of high-energy ATP to form AMP.[18] If one molecule of pyruvate generated from phosphoenolpyruvate for glucose transport and formation of glucose 6-phosphate is recycled back to phosphoenolpyruvate instead of being oxidized to CO_2, the maximum theoretical yield for shikimate pathway products synthesized from glucose would be 86% (mol/mol).

Figure 60 shows that if pyruvate is fully recycled to phosphoenolpyruvate by *ppsA*-encoded PEP synthase, a total of 6 mol of DAHP can be produced from 7 mol of glucose (86% molar yield). It is also noteworthy from the flux distribution in Figure 60 that 4 mol out of 6 mol input E4P is derived from the transketolase-catalyzed reaction by

coupling Embden-Meyerhof pathway intermediate fructose-6-phosphate and glyceraldehyde 3-phosphate. In reality, this is not likely to happen without amplified expression of transketolase.

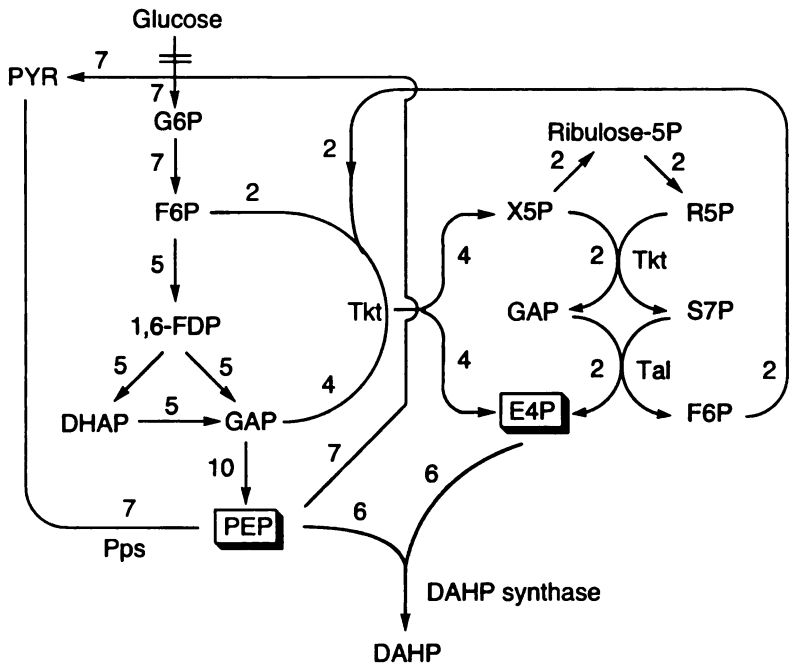

Figure 60. Reaction pathways for maximal conversion of glucose to DAHP for *E. coli* strains with fully recycling pyruvate to phosphoenolpyruvate. The numbers are the relative fluxes needed to convert 7 mol of glucose into DAHP. Enzymes: Pps, PEP synthase; Tkt, transketolase; Tal, transaldolase. Metabolites: G6P, glucose 6-phosphate; F6P, fructose 6-phosphate; 1,6-FDP, 1,6-fructose diphosphate; DHAP, dihydroxyacetone phosphate; GAP, glyceraldehyde 3-phosphate; R5P: ribose 5-phosphate; X5P, xylulose 5-phosphate; S7P, sedoheptulose 7-phosphate; PYR, pyruvate.

Using an *E. coli aroB* construct with overexpression of a feedback-insensitive isozyme of DAHP synthase ($AroG^{FBR}$), PEP synthase and transketolase, 3-deoxy-D-*arabino*-heptulosonic acid (DAH) was synthesized in 90% (mol/mol) yield from glucose as reported by Patnaik et al.[1d,1e] However, the yield likely overestimated the actual

conversion of glucose into DAH since the *aroB* construct was initially grown in rich medium followed by resuspension in minimal salts medium containing glucose.

Previously examined shikimate pathway synthesis by *E. coli* constructs employing non-PTS glucose transport. In another approach, expenditure of PEP during glucose transport was completely avoided by a non-PTS glucose transport mechanism. Non-PTS glucose transport includes facilitated diffusion mediated by the *Zymomonas mobilis glf*-encoded glucose facilitator[19] and galactose-proton symport mediated by the *E. coli galP*-encoded galactose permease.[20] Glf is a low-affinity glucose facilitator with an apparent K_m for glucose of approximately 1.1-2.9 mM.[19] GalP is a member of the major facilitator family (MFS).[21] *E. coli* constructs were assembled where PTS-mediated glucose transport was replaced with heterologous expression of the *Z. mobilis glf*-encoded glucose facilitator or the *E. coli galP*-encoded galactose permease. Genomic *E. coli glk*-encoded glucokinase alone or in combination with plasmid-localized *Z. mobilis glk*-encoded glucokinase phosphorylates glucose to glucose-6-phosphate using ATP as the phosphoryl group donor. On the basis of the flux analysis shown in Figure 61, the maximum theoretical yield for shikimate pathway products synthesized from glucose would also be 86% (mol/mol).

Ingram and coworkers[11] were the first to demonstrate that *E. coli* mutants lacking PTS-mediated glucose transport and phosphorylation can grow on glucose with heterologous expression of the *Z. mobilis glf*-encoded glucose facilitator protein and *Z. mobilis glk*-encoded glucokinase. Heterologous expression of the *Z. mobilis glf*-encoded glucose facilitator[22] increased the concentrations of L-phenylalanine synthesized by various *E. coli* constructs. The impact of expression of *Z. mobilis glf* and *Z. mobilis glk*

on synthesis of shikimic acid in *E. coli* SP1.1*pts*/pSC6.090B, which is deficient in PTS-mediated transport and phosphorylation of glucose, has been examined.[23] SP1.1*pts*/pSC6.090B synthesized 71 g/L of shikimic acid in 27% (mol/mol) yield which represented the highest yield achieved for shikimic acid synthesis with no supplement of yeast extract.

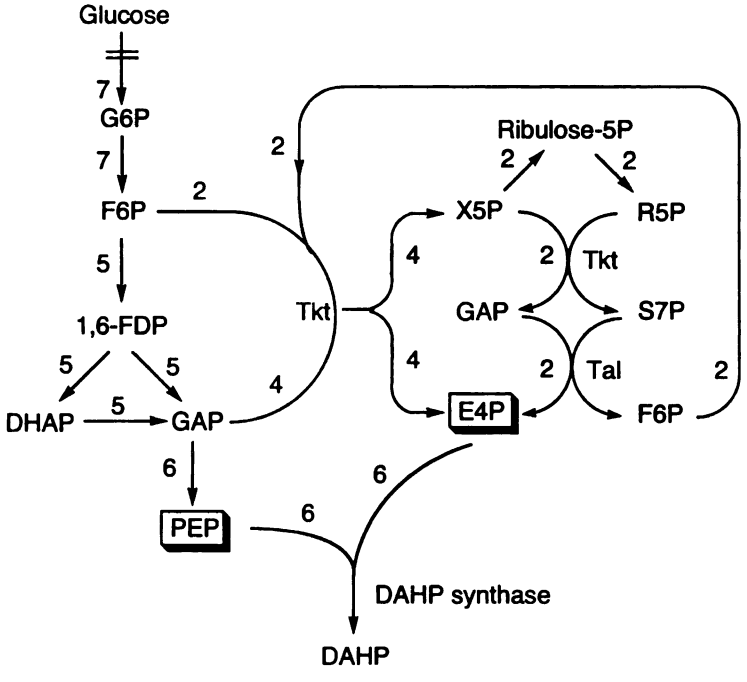

Figure 61. Reaction pathways for maximal conversion of glucose to DAHP for *E. coli* strains employing non-PTS glucose transport. The numbers are the relative fluxes needed to convert 7 mol of glucose into DAHP. Enzymes: Pps, PEP synthase; Tkt, transketolase; Tal, transaldolase. Metabolites: G6P, glucose 6-phosphate; F6P, fructose 6-phosphate; 1,6-FDP, 1,6-fructose diphosphate; DHAP, dihydroxyacetone phosphate; GAP, glyceraldehyde 3-phosphate; R5P: ribose 5-phosphate; X5P, xylulose 5-phosphate; S7P, sedoheptulose 7-phosphate; PYR, pyruvate.

Several research groups have studied the impact of shikimate pathway product yields in *E. coli* attendant with replacement of PTS-mediated glucose transport with glucose transport mediated with by the GalP galactose-proton symport system.[2] Valle

and coworkers examined DAHP production in *E. coli* NF9 which was devoid of PTS-mediated glucose transport and relied on GalP-mediated glucose transport.[2a] *E. coli* NF9/pRW5tkt synthesized 2.4-fold more DAHP under shake-flask culture conditions relative to *E. coli* PB103/pRW5tkt, which retained PTS-mediated glucose transport.[2a] Plasmid pRW5tkt contained *tktA* encoding transketolase and $aroG^{FBR}$ encoding feedback-insensitive DAHP synthase. Synthesis of DAHP in 71% (mol/mol) yield from glucose by *E. coli* NF9*aroB* harboring feedback-insensitive $aroG^{FBR}$ and *tktA* genes, and a detailed analysis of carbon metabolism have recently been reported[2d,2e] for *E. coli* constructs where GalP was recruited for glucose transport. In a contradictory report, Bailey and coworkers[2c] examined L-phenylalanine synthesis in *E. coli* PPA316/pSY130-14, which also relied on GalP-mediated glucose transport with inactivation of PTS-mediated glucose transport. Plasmid pSY130-14 carried $aroF^{FBR}$ encoding feedback-insensitive DAHP synthase and $pheA^{FBR}$ encoding chorismate mutase-prephenate dehydratase, which are the critical regulated steps in L-phenylalanine biosynthesis. In contrast to Valle's result, *E. coli* PPA316/pSY130-14 under fermentor-controlled culture conditions produced less L-phenylalanine in the range of 0 - 67% of that produced by the PTS strain PPA305/pSY130-14.[2c] The divergent impact of GalP-mediated glucose transport on the synthesis of L-phenylalanine relative to synthesis of DAHP may be the result of different *E. coli* strains and different cultivation conditions. The Bailey study also didn't amplify expression of either transketolase or transaldolase. Increased availability of phosphoenolpyruvate in *E. coli* is not reflected in increased shikimate pathway product yield until the availability of D-erythrose 4-phosphate is increased with amplified expression of transketolase.[1e]

DAHP synthase (3-deoxy-D-*arabino*-heptulosonate-7-phosphate synthase). DAHP synthase catalyzes the first committed step in the shikimate pathway. The two substrates, phosphoenolpyruvate and D-erythrose 4-phosphate, condense in a stereospecific aldol-like reaction to form a molecule of 3-deoxy-D-*arabino*-heptulosonate 7-phosphate (DAHP). Addition occurs to the *re*-face of the carbonyl group of D-erythrose 4-phosphate and to the *si*-face of the double bond in the phosphoenolpyruvate. In *E. coli*, there are three isozymes of DAHP synthase. Each isozyme is specifically feedback-regulated by one of the three aromatic amino acids end products. The crystal structure of the phenylalanine-regulated DAHP synthase from *E. coli* has been described and represents the first reported protein structure of this family.[24] The data show a tetrameric enzyme complex to be made of a dimer of two tight dimmers with the monomers each possessing a single $(\beta/\alpha)_8$-barrel domain. The active site of the enzyme is situated at the carboxy terminal end of the $(\beta/\alpha)_8$-barrel and possesses an overall net positive potential which complements the negatively charges substrates, phosphoenolpyruvate and D-erythrose 4-phosphate. The crystal structure of the phenylalanine-regulated DAHP synthase complexed with its inhibitor L-phenylalanine, phosphoenolpyruvate and its metal cofactor Mn^{2+} has been determined recently to elucidate the allosteric inhibition mechanism by L-phenylalanine.[25] L-Phenylalanine is bound in a cavity located on the outer side of the DAHP synthase $(\beta/\alpha)_8$-barrel near its N-amino terminus in each of the four monomers and about 20 Å from the closet active site. Upon binding with L-phenylalanine. the enzyme loses the ability to bind D-erythrose 4-phosphate and binds phosphoenolpyruvate in a flipped orientation.

KDPGal aldolase (2-keto-3-deoxy-6-phosphogalactonate aldolase). The key enzyme in the proposed pyruvate-based shikimate pathway is *dgoA*-encoded KDPGal aldolase. By catalyzing the reversible cleavage of KDPGal to pyruvate and D-glyceraldehyde 3-phosphate (GAP, Figure 62), KDPGal aldolase enables *E. coli* to use D-galactonate as a sole carbon and energy source. D-Galactonate is transported into the *E. coli* cytoplasm by the *dgoT*-encoded transport protein. D-Galactonate catabolism in *E. coli* cytoplasm involves the conversion of D-galactonate into pyruvate and glyceraldehydes 3-phosphate by the sequential actions of *dgoD*-encoded galactonate dehydratase, *dgoK*-encoded 2-keto-3-deoxygalactonate kinase and *dgoA*-encoded 2-keto-3-deoxy-6-phosphogalactonate aldolase (KDPGal aldolase, Figure 62).[26] The D-galactonate catabolic enzymes are tightly regulated and only expressed in the presence of D-galactonate. The absence of these enzyme activities in *E. coli* grown on galactose suggests that D-galactonate catabolic enzymes do not participate in galactose catabolism in *E. coli*.

Galactose is metabolized in enteric bacteria including *E. coli* by the conversion of galactose to glucose 6-phosphate. The catabolism is initiated by phosphorylation of galactose to galactose-1-phosphate catalyzed by *galK*-encoded galactokinase, followed by conversion to UDP-galactose catalyzed by *galT*-encoded galactose-1-phosphate uridylyltransferase, then to UDP-glucose catalyzed by *galE*-encoded UDP-galactose-4-epimerase. UDP-glucose is converted into glucose-6-phosphate by *galU*-encoded glucose-1-phosphate uridylytransferase and *pgm*-encoded phosphoglucomutase. On the other hand, the catabolism of galactose in *Pseudomonas* is via an Entner-Doudoroff pathway[27] in which galactose is oxidized to D-galactonate by a galactose dehydrogenase.

D-Glactonate is then converted to pyruvate and glyceraldehydes 3-phosphate following the same catalytic route as in the *E. coli* galactonate catabolic pathway (Figure 62). This galactose catabolic pathway is also found in *Caulobacter cresentus*,[28] *Azotobacter vinelandii*,[29] *Rhizobium meliloti*,[30] *Gluconobacter liquefaciens*[31] and nonpathogenic *Mycobacteria*.[32] Consequently, KDPGal aldolase activity has been detected in all the microbes mentioned above. In all instances, KDPGal aldolase is an inducible enzyme, expressed only when cells are grown on galactose or galactonate as the sole carbon source.

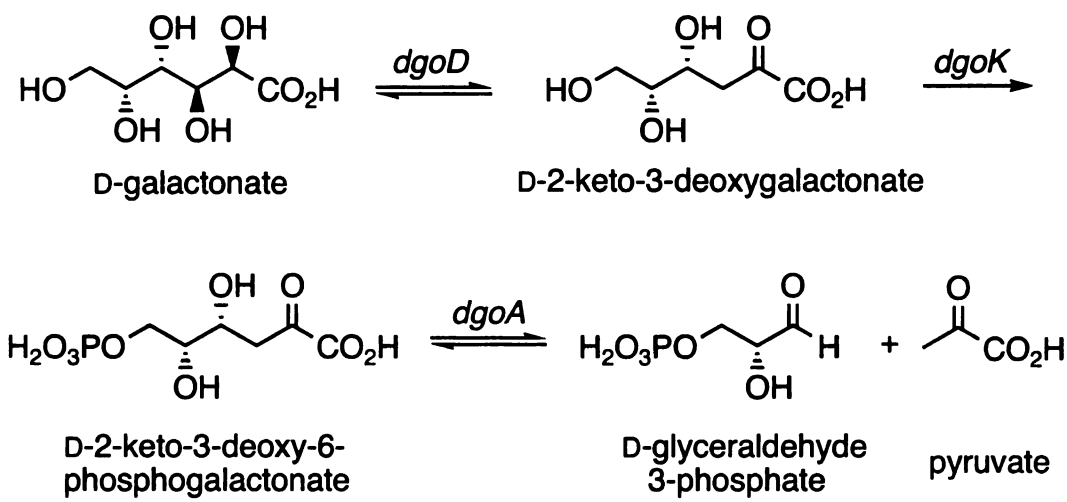

Figure 62. Pathway for D-galactonate catabolism in *E. coli*. Proteins (genes): galatonate permease (*dgoT*); galactonate dehydratase (*dgoD*); 2-keto-3-deoxygalactonate kinase (*dgoK*); 2-keto-3-deoxy-6-phosphogalactonate aldolase (*dgoA*).

KDPG aldolase[33] (2-keto-3-deoxy-6-phosphogluconate aldolase), catalyzes a reaction similar to that catalyzed by KDPGal aldolase (Figure 63a). KDPG aldolase is part of the Entner-Doudoroff pathway, which is an alternative to the Embden-Myerhof-Parnas pathway for glucose catabolism and enables *E. coli* to use gluconic acid as a sole carbon and energy source. KDPG aldolase catalyzes the reversible cleaveage of KDPG

to pyruvate and glyceraldehyde 3-phosphate. Both KDPG aldolase and KDPGal aldolase accept a broad range of short chain unnatural electrophilic aldehydes.[34,35] KDPG aldolase catalyzes the *si*-face addition of pyruvate to an eletrophilic aldehyde to obtain 4-hydroxy-2-ketobutyrates with the *S*-configuration at the newly formed C-4 stereogenic center (Figure 63a,b). By contrast, KDPGal aldolase generates the aldol adducts with the *R*-configuration at the new stereogenic center (Figure 63c).

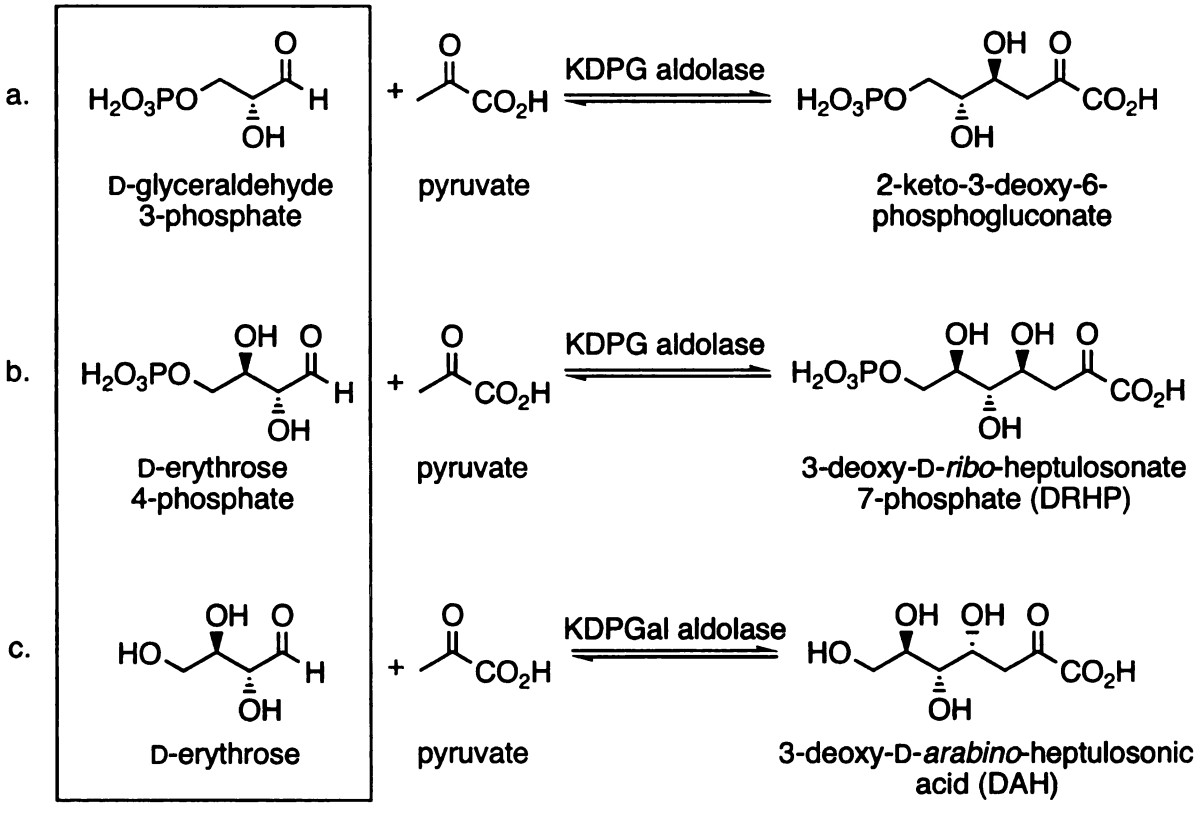

Figure 63. KDPGal aldolase (*dgoA*) and KDPG aldolase (*eda*) catalyzed reactions.

Systematic studies from two research groups have found that KDPG aldolase from *Pseudomonas putida*, *E. coli* and *Zymomonas mobilis* could catalyze the condensation of pyruvate with D-erythrose 4-phosphate.[36] However, the product of this condensation is 3-deoxy-D-*ribo*-heptulosonic acid 7-phosphate (DRHP). DRHP is the

diastereomer of 3-deoxy-D-*arabino*-heptulosonic acid 7-phosphate (DAHP), which is needed in the shikimate pathway (Figure 63). DAHP would be formed in a KDPGal aldolase-catalyzed condensation of pyruvate with D-erythrose 4-phosphate (Figure 63c). D-Erythrose has been previously observed to be a poor substrate for KDPGal aldolase.[34a] Aldose phosphates were known to lead to KDPGal aldolase activities 100-fold higher than with the corresponding aldoses,[34] although there was no direct precedent for KDPGal aldolase-catalyzed condensation of pyruvate with D-erythrose 4-phosphate.

Both KDPG aldolase and KDPGal aldolase belong to the type I aldolase family whose reaction mechanism involves formation of a Schiff base intermediate between a lysine residue and a substrate carbonyl in the active site. The X-ray crystal structure of KDPG aldolase has been solved at 1.95 Å resolution,[37] while the crystal structure of KDPGal aldolase is not currently available. The *E. coli* KDPG aldolase structure indicates that pyruvate underwent a nucleophilic attack with Lys-133, forming a protonated carbinolamine intermediate, a Schiff base precursor, which was stabilized by hydrogen bonding with active site residues Glu-45, Thr-73, Arg-49 and a water molecule. The pyruvate C-3 methyl group was stabilized by Phe-135 through hydrophobic interactions. The Lys-126 residue was also proposed to be the active site of *E. coli* KDPGal aldolase.[38]

Directed evolution of KDPGal aldolase

Expression and purification of *E. coli* KDPGal aldolase. Meloche and O'Connell[39] reported an isolation of KDPGal aldolase from *P. saccarophila* that involved five chromatographic steps with an overall purification yield of 14%. The final KDPGal

aldolase had a specific activity of 130 U/mg. The laborious separation was due to difficulty to achieve complete separation of KDPGal aldolase and KDPG aldolase. Toone and coworkers[34] purified KDPGal aldolase from an *eda*⁻ mutant of *P. cepacia* that was devoid of KDPG aldolase. KDPGal aldolase was purified to a specific activity of 4.2 U/mg with an overall yield of 86% in a single chromatographic step on Sepharose CL-4B derivatized with a Procion Navy H-ER triazine dye. Their attempt to purify *E. coli* KDPGal aldolase from an *eda*⁻ mutant strain DF214 harboring a plasmid pTC190 containing *eda* gene using the same chromatographic column, however, was unsuccessful.

In Toone's experiment, KDPGal aldolase was expressed from the chromosomal *dgoA* gene. In this work, *E. coli* KDPGal aldolase was expressed from a plasmid-localized *dgoA* gene. *E. coli* KDPGal aldolase-encoding *dgoA* gene is localized in the *dgo* cluster at min 83.4 in the *E. coli* chromosome. All the genes involved in D-galactonate catabolism including a regulator protein *dgoR*, 2-keto-3-deoxy-galatonate kinase-encoding *dgoK*, 2-keto-3-deoxy-6-phosphogalatonate aldolase-encoding *dgoA*, D-galatonate dehydratase-encoding *dgoD* and D-galatonate permease-encoding *dgoT* are localized in this cluster sequentially under the control of a single promoter. The *E. coli* *dgoA* gene sequence was obtained from the National Center for Biotechnology Information (NCBI) and sequence errors were corrected according to Babbitt et al.[38] The published *dgoA* gene from NCBI contains a fragment of 1763-nt DNA, which comprises the open reading frames of the 618-nt *dgoA* and the 1149-nt *dgoD* gene. The three nucleotides sequence errors cause a frame shift in the published amino acid sequences.

To explore the catalytic activity of KDPGal aldolase towards phosphorylated D-erythrose (E4P, Figure 58), the 618-nt *E. coli dgoA* was cloned into a cloning vector pCR2.1-TOPO with transcription under the control of a *lac* promoter to prepare plasmid pNR5.223 (Figure 66). *E. coli* AB3248,[40] in which all three DAHP synthase isoenzymes encoded by *aroF*, *aroG* and *aroH* have been inactivated by three successive rounds of random chemical mutagenesis, was transformed with plasmid pNR5.223. Expression of KDPGal aldolase was induced by addition of 0.2 mM isopropyl β–D-thioglucopyranoside (IPTG) in Luria-Bertani (LB) medium containing ampicillin. The specific activity of KDPGal aldolase in crude cell-free extract was 30 U/mg. The cell-free extract, after ammonium sulfate treatment, was applied to a DEAE-cellulose column to afford the partially purified KDPGal aldolase in an overall 4% yield and a final specific activity of 87 U/mg.

Table 7. Purification of *E. coli* KDPGal aldolase.

entry	steps	total protein (mg)	specific activity (U/mg)	total units	purification fold	yield
1	crude extract	1274	30	38661	1.0	100%
2	$(NH_4)_2SO_4$ 25%-65%	630	30	18684	1.0	29%
3	DEAE-cellulose	18	87	1600	2.9	4.1%

Synthesis of 2-keto-3-deoxy-6-phosphogalactonate (KDPGal). KDPGal was chemically synthesized following the synthesis reported by Toone and coworkers (Figure 64).[34b] The synthesis proceeded from commercially available D-galactonate-1,4-lactone. The lactone was treated with a catalytic amount of sulfuric acid in acetone to afford the 5,6-*O*-isopropylidine **16** as the sole product in 90% yield. Compound **16** underwent

β–elimination to yield **17** in 34% yield after treated with 10 equivalents of pyridine and 5 equivalents of acetic anhydride at 50 °C for 48 h. The major byproduct of this reaction was the gluco-epimer **18** (20% yield) presumably arising from the corresponding furan (Figure 65). Selective phosphorylation of the primary alcohol following removal of the isopropylidene was carried out with 1.3 equivalents of dibenzyl-*N*,*N*-diethylphosphoramidite and 1 equivalent of 1*H*-tetrazole in THF at 0 °C. Without purification, the reaction was cooled to –60 °C, and the intermediate was oxidation with 2 equivalents of 85% *m*-CPBA in methylene chloride to afford the phosphate **20** in 37% yield. The reported procedure used two equivalents of 1*H*-tetrazole, however, following the procedure resulted in phosphorylation of both the primary and the secondary alcohols in our hand. Reducing the amount of 1*H*-tetrazole to one equivalent led to the formation of the monophosphorylated product. Phosphorylation of **19** was also attempted with tetrabenzylpyrophosphate (TBPP) in presence of sodium hydride in THF at 0 °C. No phosphorylation was observed and the starting material was recovered. Catalytic hydrogenation removed the benzyl ether phosphate protecting groups and yielded the C-2 acetate-protected KDPGal δ-lactone. After removal of THF, the δ-lactone was dissolved in water and the pH was adjusted to 7.5 with addition of 50 mM aqueous LiOH solution. Simultaneous hydrolysis of the C-2 acetate and δ–lactone were completed after 48 h to afford the KDPGal lithium salt in 70% yield.

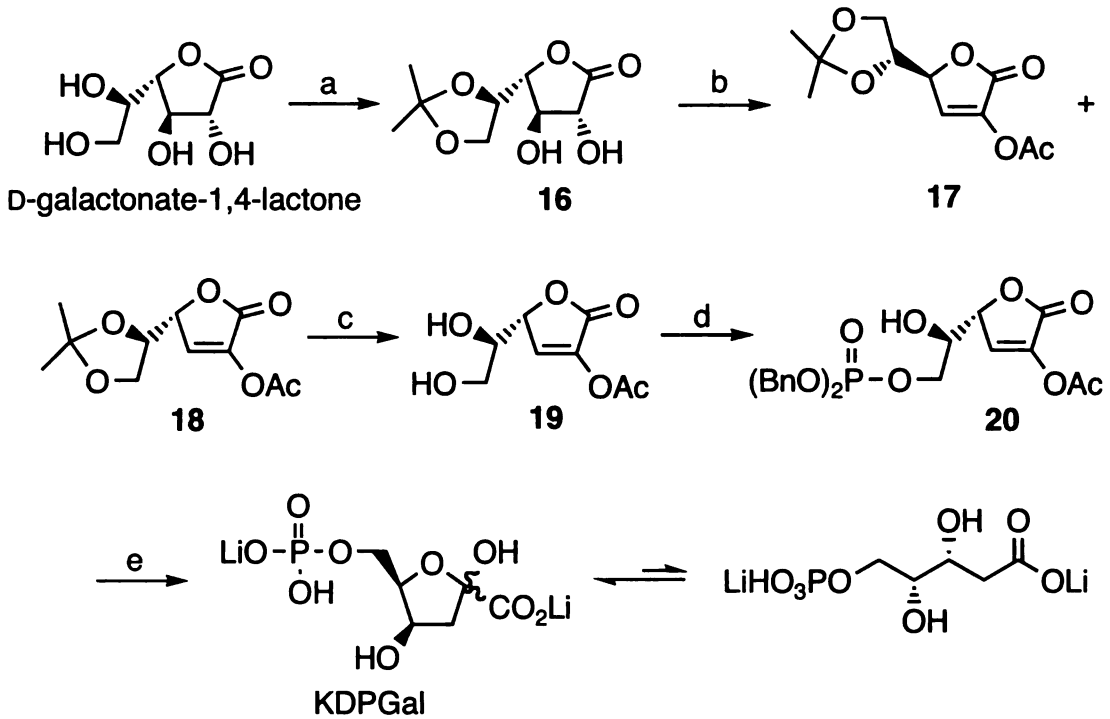

Figure 64. Synthesis of 2-keto-3-deoxy-6-phosphogalactonate. Keys: (a) acetone, H_2SO_4, rt, 4 h, 90%; (b) acetic anhydride, pyridine, CH_2Cl_2, 50 °C, 48 h, 34%; (c) 80% glacial acetic acid, rt, 36 h, 86%; (d) i) Dibenzyl-*N*,*N*-diethylphosphoramidite (DDP), 1*H*-tetrazole, THF; ii) *m*-CPBA, 37%; (e) i) H_2, 10% Pt/C, THF; ii) aqueous 50 mM LiOH, 70%.

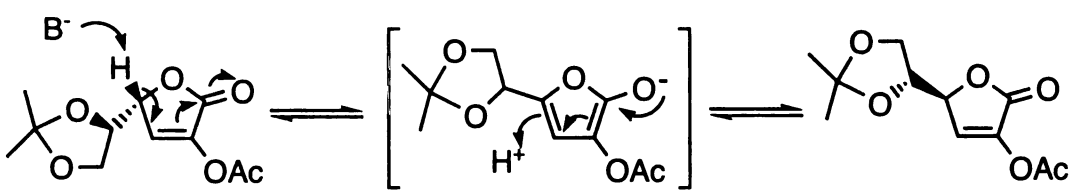

Figure 65. Byproduct formation mechanism in the β-elimination reaction.

Determination of KDPGal aldolase activity. KDPGal aldolase activity was determined by measuring the formation of pyruvate in the KDPGal cleavage reaction.[34b] Formation of pyruvate was monitored by the loss of NADH at 340 nm in the L-lactic dehydrogenase-catalyzed reduction to L-lactic. The assay was carried out in 20 mM KH_2PO_4 buffer (pH 7.5) with NADH, L-lactic dehydrogenase and appropriately diluted cellular lysate. The absorbance at 340 nm was recorded continuously for 1 min after the addition of KDPGal. One unit of KDPGal aldolase catalyzes the loss of one μmol of NADH per minute at 25°C.

Determination of DAHP formation activity of the KDPGal aldolase. DAHP formation activity was measured by coupling product DAHP forward to 3-dehydroshikimate, a chromophore suitable for continuous spectrophotometric assay. The reaction contained 50 mM morpholinepropanesulfonic acid (MOPS) buffer (pH 7.5), 1 mM D-erythrose 4-phosphate, 1 mM pyruvate, 50 μM $CoCl_2$, 10 μM NAD, 1 U of 3-dehydroquinate synthase,[41] 1 U of 3-dehydroquinate dehydratase[42] and cellular lysate. The DAHP formed in the assay reaction was converted to 3-dehydroquinate by 3-dehydroquinate synthase, followed by 3-dehydroquinate dehydratase-catalyzed dehydration to 3-dehydroshikimate whose absorbance at 234 nm was monitored. One unit of DAHP synthase catalyzes the formation of one μmol of 3-dehydroshikimate per minute at 25°C.

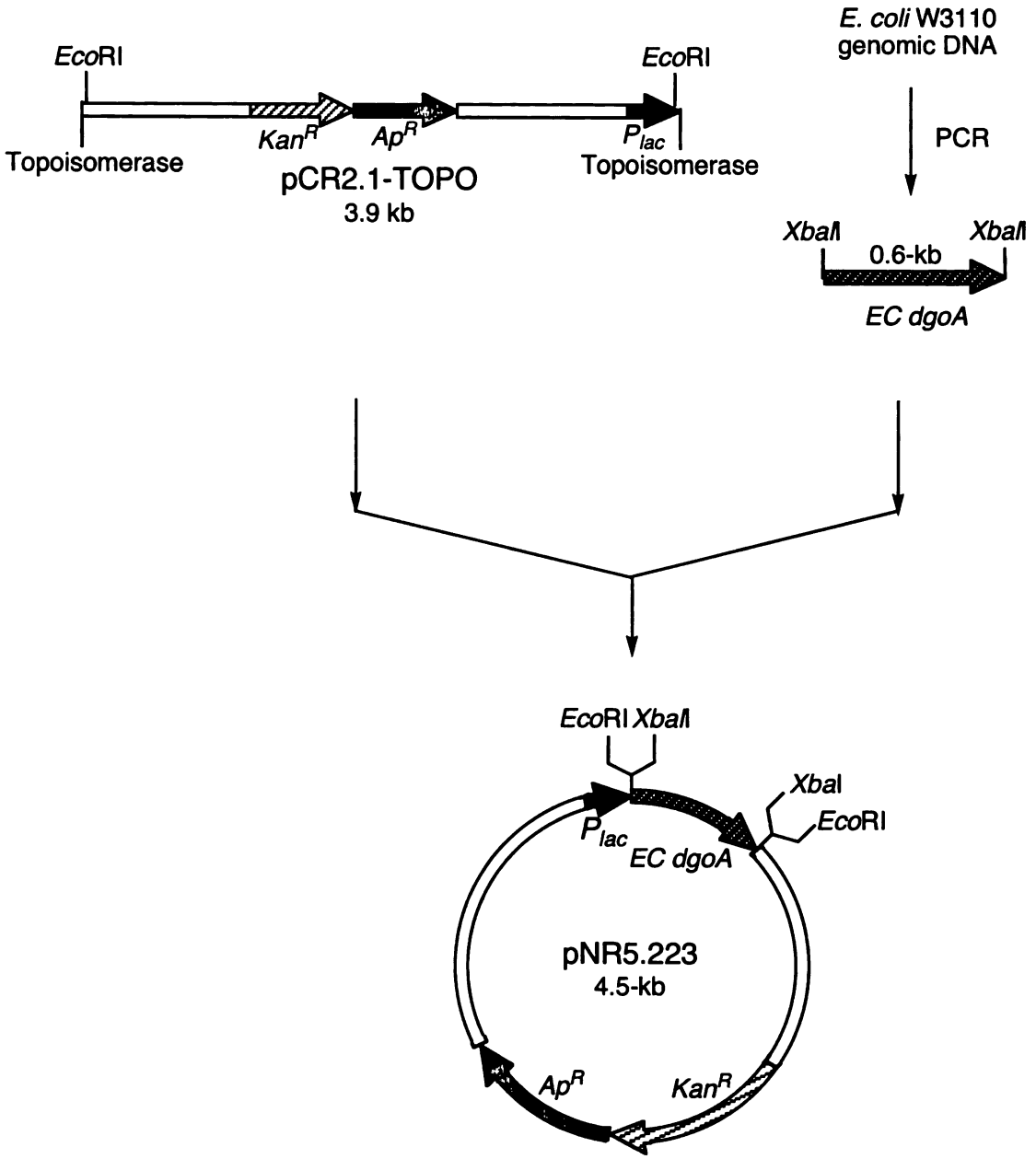

Figure 66. Construction of plasmid pNR5.223.

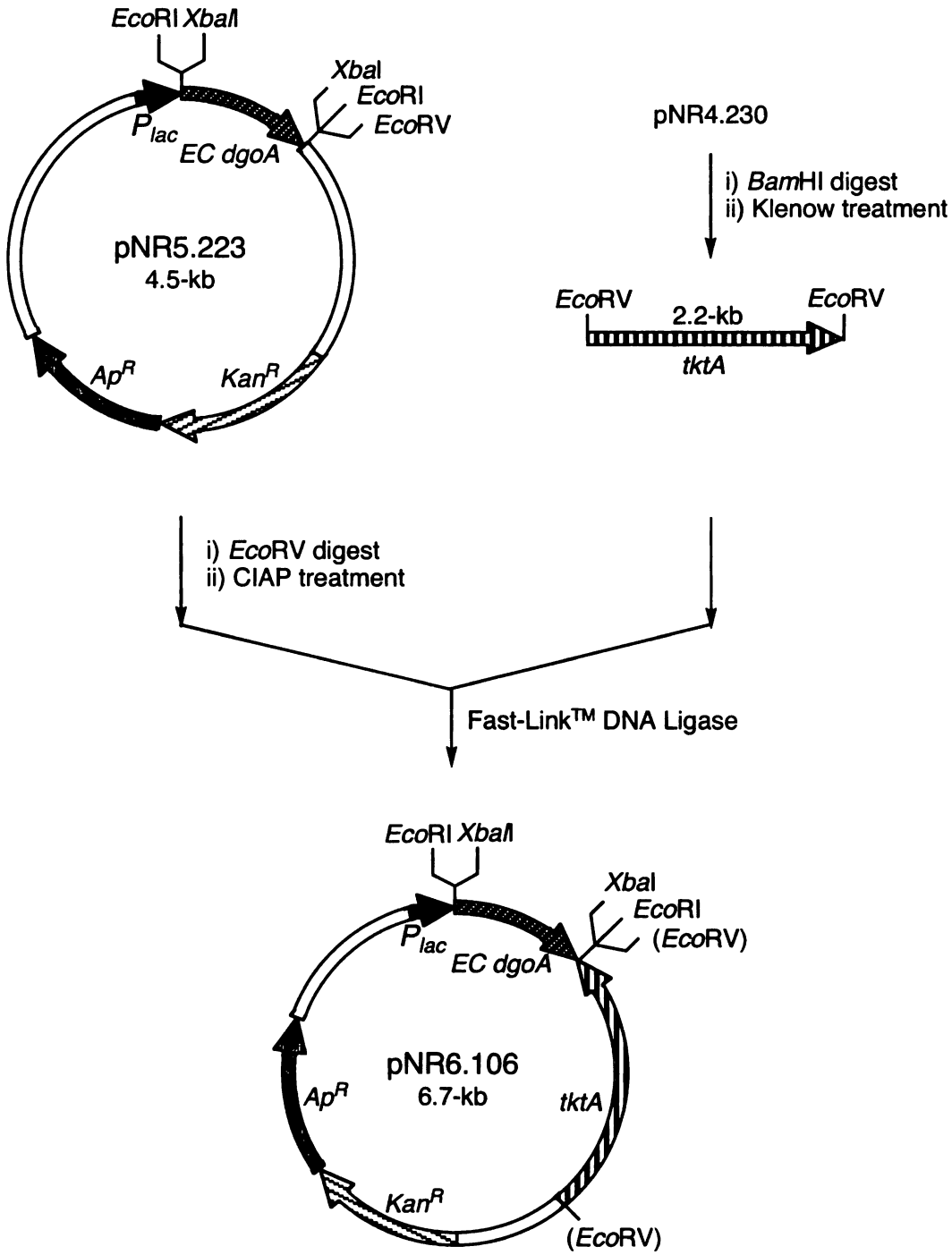

Figure 67. Construction of plasmid pNR6.106.

KDPGal aldolase catalyzes addition of pyruvate with D-erythrose 4-phosphate. The partially purified *E. coli dgoA*-encoded KDPGal aldolase was then incubated with pyruvate, D-erythrose 4-phosphate, 3-dehydroquinate synthase and 3-dehydroquinate dehydratase. Formation of 3-dehydroshikimate in 90% yield based on ^{1}H-NMR analysis established the ability of KDPGal aldolase to catalyze the reaction of pyruvate with D-erythrose 4-phosphate as well as the ability of 3-dehydroquinate synthase to drive this reaction to completion.

With KDPGal aldolase-catalyzed conversion of pyruvate and D-erythrose 4-phosphate established *in vitro*, attention turned to gauging the impact of this activity *in vivo*. *E. coli* AB3248[40] does not have a functional DAHP synthase. *E. coli* AB3248/pNR5.223 can only grow on minimal salts plates without supplementation with aromatic amino acids and aromatic vitamins if the enzyme activity of the plasmid-localized *dgoA*-encoded KDPGal aldolase drives adequate carbon flow into the shikimate pathway. In addition to being an aromatic amino acids auxotroph, *E. coli* AB3248 has acquired numerous side mutations as indicated by the need to supplement its growth with L-histidine, L-isoleucine, L-valine, L-proline and L-arginine in addition to aromatic amino acids and aromatic vitamins. IPTG was added to a final concentration of 0.2 mM to induce *dgoA* expression. The *E. coli* wild-type KDPGal aldolase showed weak *in vivo* activity by enabling *E. coli* AB3248/pNR5.223 to grow on minimal salts plates supplemented with three aromatic amino acids but in the absence of added aromatic vitamins (entry 1, Table 8). *E. coli* AB3248/pNR5.223 was incapable of growing on minimal salts plates without supplementation with all three aromatic amino acids.

Table 8. Effect of expression of wild-type *E. coli* KDPGal aldolase on growth characteristics of *E. coli* strains.

entry	construct	HIVPR[c]	HIVPR/YF[c]	HIVPR/YFW[c]	HIVPR/YFW/vit[c]
1	AB3248/pNR5.223	-[a]	-	+[b]	+
2	AB3248/pNR6.106	-	-	+	+
3	NR1/pNR5.223[d]	-	-	+	+
4	AB3248	-	-	-	+
5	NR1[d]	-	-	-	+

[a] no growth (-), [b] growth (+), [c] Supplements added to M9 medium containing 0.2 mM IPTG includes: H, L-histidine; I, L-isoleucine; V, L-valine; P, L-proline; R, L-arginine; Y, L-tyrosine; F, L-phenylalanine; W, L-tryptophan; vit, *p*-aminobenzoate, *p*-hydroxybenzoate, 2,3-dihydroxybenzoate. [d] L-serine was also added into M9 medium.

D-Erythrose 4-phosphate has never been detected in *E. coli* cytoplasm which suggests it exists at very low concentration. Overexpression of *tktA*-encoded transketolase could increase the availability of E4P. Therefore, the *tktA* was cloned into plasmid pNR5.223 to afford plasmid pNR6.106 (Figure 67). Entry 2 in Table 8 showed *E. coli* AB3248/pNR6.106 had the same growth characteristics as AB3248/pNR5.223.

With expression of KDPGal aldolase in *E. coli* AB3248, DAHP synthase-catalyzed, irreversible condensation of phosphoenolpyruvate and D-erythrose 4-phosphate is being replaced by a reversible condensation of pyruvate and D-erythrose 4-phosphate catalyzed by KDPGal aldolase. Replacement of an irreversible reaction as the first step of shikimate pathway raises concerns as to whether ample carbon flow could be directed into the common pathway. The second enzyme in the shikimate pathway, *aroB*-encoded DHQ synthase, on the other hand, catalyzes an irreversible reaction due to cleavage of a phosphate ester during conversion of DAHP to 3-dehydroquinic acid (Figure 58). Dehydroquinate dehydratase and shikimate dehydrogenase, the next two enzymes in the shikimate pathway after dehydroquinate synthase, both catalyze reversible reactions. Increasing the activity of dehydroquinate synthase might drive the

reversible aldol addition forward and direct more carbon into the common pathway. Snell et al found that incorporation of a second copy of *aroB* into *E. coli* chromosome was sufficient to increase the expression levels to avoid 3-deoxy-D-*arabino*-heptulosonic acid (DAH) accumulation resulted from amplified expression of the first enzyme of the common pathway.[43] *E. coli* NR1 (AB3248*serA::aroB*) was constructed from AB3248 by homologous recombination of *aroB* gene into the *serA* locus. Conditions for the homologous recombination were based on those previously described.[44] The competent *E. coli* AB3248 was transformed with plasmid pKL3.82A, a pMAK705[44a] derivative containing an *aroB* inserted into the *serA* gene. Plasmid pMAK705 contains a temperature-sensitive pSC101 replicon that replicates at 30 °C but is unstable at 44 °C. *E. coli* NR1 was obtained by selecting colonies free of plasmid after homologous recombination induced by heat-shock treatment of AB3248/pKL3.82A. The *serA::aroB* genotype in *E. coli* NR1 was also confirmed by PCR amplification using primers that flanked the *serA* locus and *E. coli* NR1 genomic DNA as a template, a DNA fragment corresponding to the *serA::aroB* locus was obtained.

Due to the inactivation of the *serA* gene, growth of *E. coli* NR1 requires supplementation of L-serine in culture medium (entry 5, Table 8). *E. coli* NR1 was transformed with plasmid pNR5.223 and spread on the same set of minimal salts plates. *E. coli* NR1/pNR5.223 was only capable of growing on minimal salts plates when provided with L-histidine, L-isoleucine, L-valine, L-proline, L-arginine, L-tyrosine, L-phenylalanine, L-tryptophan and L-serine (entry 3, Table 8). Overexpression of *aroB*-encoded DHQ synthase showed no improvement in growth characteristics. The growth

rate of NR1/pNR5.223 was even slower due to the presence of L-serine in the medium that is known to inhibit cell growth.[45]

Besides the requirement for supplementation with L-histidine, L-isoleucine, L-valine, L-proline and L-arginine in its culture medium, *E. coli* AB3248 was later found to be unstable when cultured on minimal salts plates without aromatic amino acid supplementation. Reverants in aromatic amino acids auxotrophy possibly arising by spontaneous mutations were observed repeatedly. Therefore, *E. coli* AB3248 was replaced with use of *E. coli* CB734, which is a stable DAHP synthase auxotroph. The three chromosomal DAHP synthase genes in *E. coli* CB734 have been inactivated by deletion and/or interruption by an antibiotic resistance cassette (C600 *leu thi1 Δ(gal-aroG-nadA)*50 *aroF::Cm*^{R} *ΔaroH::Kan*^{R} *recA1*).[46] Growth of *E. coli* CB734 only requires supplementation with L-leucine in addition to the three aromatic amino acids in minimal salts medium containing glucose.

Selection strategy for directed evolution of KDPGal aldolase. Two strategies for selection of KDPGal aldolase variants with increased activity relative to condensation of pyruvate with D-erythrose 4-phosphate *in vivo* were evaluated. The first strategy involved the conversion of the shikimate pathway metabolite 3-dehydroshikimic acid to protocatechuic acid which could be detected using chromogenic agarose plates containing *p*-toluidine and ferric citrate.[47] The selection has been successfully applied to the isolation of an *aroZ* gene encoding 3-dehydroshikimate dehydratase, which catalyzes the conversion of 3-dehydroshikimic acid to protocatechuic acid, from a *K. pneumoniae* genomic library.[47a] In a preliminary experiment to evaluate the sensitivity of the selection, *E. coli aroE* strain KL7 (AB2834 *serA::aroBaroZ*), which synthesizes

protocatechuic acid due to a chromosomal *aroZ* insert encoding DHS dehydratase was transformed with plasmid pKL4.33 carrying $aroF^{FBR}$ and *serA* genes.[48] The feedback-insensitive DAHP synthase encoded by $aroF^{FBR}$ in plasmid pKL4.33, which should result in increased protocatechuic acid biosynthesis, was used as a positive control. A faint brown color developed around the colonies of KL7/pKL4.33 on the chromogenic plates containing *p*-toluidine, ferric citrate, aromatic amino acids and aromatic vitamins after 30 h incubation at 37 °C. However, it was very difficult to distinguish KL7/pKL4.33 from KL7 based on the faint brown color. Therefore, this strategy was abandoned.

A second selection strategy was then employed that linked the evolved aldolase activity with the survival and growth rate of the DAHP synthase triple auxotroph *E. coli* CB734 in the absence of aromatic amino acid and aromatic vitamin supplementation. *E. coli* CB734 can only grow in minimal salts medium supplemented with both aromatic amino acids and aromatic vitamins. Transforming *E. coli* CB734 with a plasmid contained the wild-type *E. coli dgoA* gene enabled the construct to survive on minimal salts plates supplemented only with aromatic amino acids (entry 2, Table 9). *E. coli* CB734 carrying a mutated *dgoA* gene as a plasmid insert can grow on the minimal salts plates lacking aromatic amino acids supplementation only if the catalytic activity of the KDPGal aldolase variant is sufficient to provide for aromatic amino acid biosynthesis. Given that the evolved activity was more likely to increase incrementally during the course of directed evolution, identification of increased KDPGal aldolase activity relative to condensation of pyruvate with D-erythrose 4-phosphate utilized a stepwise selection that increased in stringency with each round of directed evolution. This entailed sequential omission of L-tryphtophan, L-tyrosine and L-phenylalanine from the minimal

salts medium. Mutant isozymes of DgoA with increased activity were selected on minimal salts medium plates supplemented with only L-tyrosine and L-phenylalanine in the first round. This selection reflects reports that the L-tryptophan requirement in *E. coli* is the smallest among the three aromatic amino acids. In the next round of selection, L-tyrosine supplementation was omitted, and the mutants that could grow on minimal salts plates with only L-phenylalanine supplementation were selected. Eventually, with the increased activity, *E. coli* CB734 carrying a mutant *dgoA* isozyme should be able to grow on minimal medium lacking supplementation with any aromatic amino acids. After that, the stringency of the selection can be further increased by decreasing the concentration of IPTG present in the medium, and by shortening the incubation time, or by using a weaker promoter controlling transcription of mutated, plasmid-localized *dgoA* gene.

Directed evolution of KDPGal aldolase from *E. coli*. Plasmid pNR5.223 is a derivative of a high-copy plasmid pCR2.1-TOPO. Maintaining the high-copy plasmid for *E. coli* CB734 carrying pNR5.223 in minimal salts medium could potentially cause catabolic burden. In addition, transcription of the *dgoA* gene was under the control of a *lac* promoter in pNR5.223. To shorten the selection time, the *E. coli dgoA* gene was then cloned into a medium copy plasmid pTrc99A[49] with transcription controlled by a strong *trc* promoter to give pNR7.088 (Figure 68). Growth of *E. coli* CB734 on glucose-containing minimal salts medium required supplementation with L-phenylalanine, L-tyrosine, L-tryptophan and aromatic vitamins (entry 1, Table 9). *E. coli* CB734/pN7.088 with its plasmid-encoded *E. coli dgoA* was able to biosynthesize its own aromatic vitamins (entry 2, Table 9).

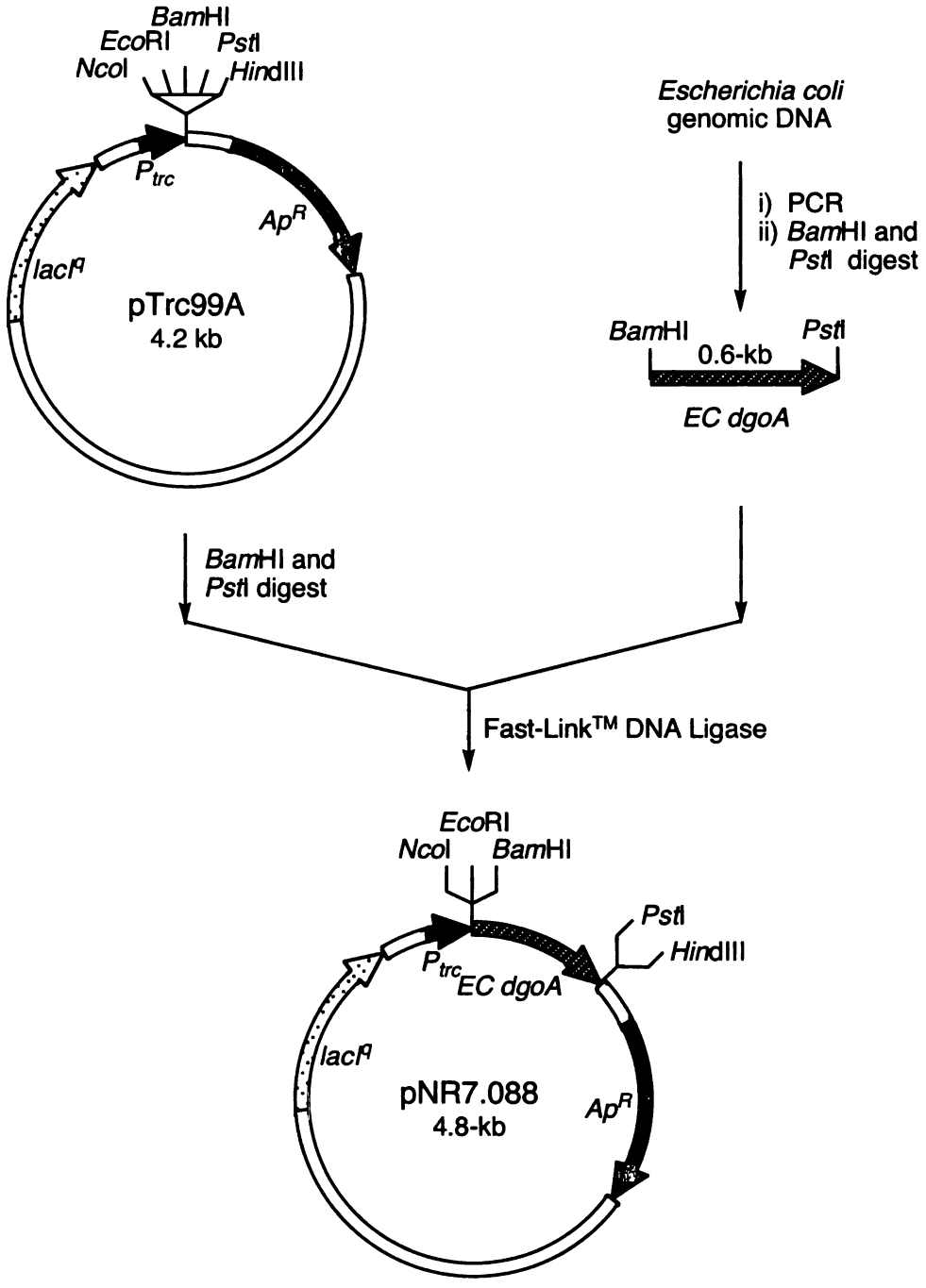

Figure 68. Construction of plasmid pNR7.088.

E. coli dgoA was subjected to two successive rounds of error-prone PCR mutagenesis followed by one round of DNA shuffling. The 0.6-kb wild-type *E. coli dgoA* gene was amplified under error-prone PCR conditions with a controlled mutation rate of 6.6×10^{-3} per nucleotide determined by sequencing 50 randomly selected *dgoA* mutants. The amplification product was purified, digested and cloned into the pTrc99A expression vector to generate the first generation plasmid library (Figure 69). The plasmid library was transformed into competent CB734 cells by electroporation and a library of 1×10^{6} *E. coli* transformants was spread onto minimal salts plates supplemented with L-tyrosine, L-phenylalanine and 0.2 mM IPTG. Colonies appeared on the selection plates after 3 days at 37°C (entry 3, Table 9). From these colonies, a mixture of plasmid (pEC01) from 50 of the largest colonies was prepared. The second round of PCR mutagenesis gave *E. coli* CB734/pEC02 colonies (entry 4, Table 9), whose growth did not require aromatic amino acids supplementation. A mixture of pEC02 plasmids from 50 of the largest colonies was prepared. At this stage, the *in vivo* activity of the mutant KDPGal aldolase was sufficient to compensate for the aromatic amino acids auxotrophy of *E. coli* CB734. The final round of directed evolution involving DNA shuffling gave CB734/pEC03 (entry 5, Table 9) colonies that grew in the absence of aromatic amino acids supplements when evolved KDPGal aldolase expression was reduced by lowering IPTG concentration. After the final round of directed evolution, *dgoA* gene variants from seven of the largest colonies were sequenced and their encoding KDPGal aldolase activities toward DAHP formation were further characterized (Table 10). The evolved KDPGal aldolase showed up to a 6-fold increase in DAHP formation activity as compared to the wild-type KDPGal aldolase.

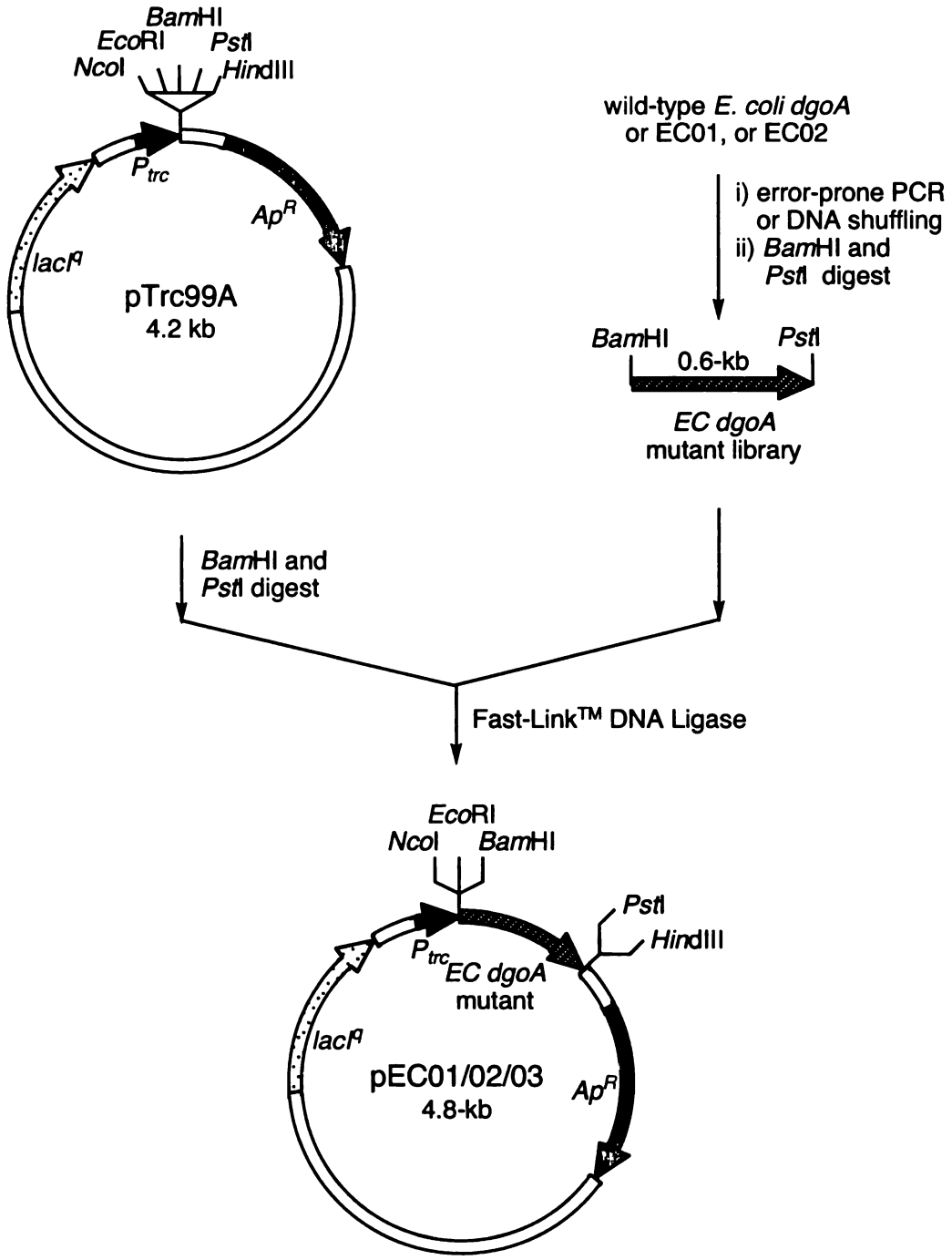

Figure 69. Construction of plasmid libraries of pEC01, pEC02 and pEC03.

Table 9. Directed evolution of *E. coli* KDPGal aldolase.

entry	construct[a]	M9[b]	M9[c]	F[d]	YF[d]	YFW[d]	YFWvit[d]
1	*E. coli* CB734	-[e]	-	-	-	-	+[f]
2	CB734/pNR7.088	-	-	-	-	+	+
3	CB734/pEC01	-	-	-	+	+	+
4	CB734/pEC02	-	+	+	+	+	+
5	CB734/pEC03	+	+	+	+	+	+

[a] All native and evolved *dgoA* genes were inserted into the same plasmid (pTrc99A) with transcription controlled by a *Ptrc* promoter. [b] Contained L-leucine and 0.05 mM IPTG. [c] Contained L-leucine and 0.2 mM IPTG. [d] Supplements added to M9 medium containing L-leucine and 0.2 mM IPTG included: F, L-phenylalanine; Y, L-tyrosine; W, L-tryptophan; vit, *p*-aminobenzoate, *p*-hydroxybenzoate, 2,3-dihydroxybenzoate. [e] no growth (-). [f] growth (+).

Table 10. Mutations and specific activities of *E. coli* KDPGal aldolase variants.

entry	*dgoA*	mutations	DAHP activity[a] (U[b]/mg)
1	*E. coli*	wild-type	0.086
2	EC03-1	F33I, D58N, Q72H, A75V, V85A, V154F	0.56
3	EC03-2	D30G, F33I, D34G, S42T, A75T, V85A, V154F, L179I, A182P	0.30
4	EC03-3	F33I, D34G, K59R, V85A, A111P, G134S, P135L, V154F, P159A	0.56
5	EC03-4	F33I, D34G, S42T, D74N, V85A, A122V, V154F, D167E, A190T	0.32
6	EC03-5	S42T, K59M, V85A, A122V, V154F, D178V	0.37
7	EC03-6	S42T, V85A, H90Y, V154F, L175I	0.32
8	EC03-7	K6N, T17M, V85A, I89T, V154F, S185P	0.29

[a] *E. coli* CB734 was used as host strain for expression of evolved enzymes. [b] One unit of DAHP synthase catalyzes the formation of one μmol of 3-dehydroshikimate per minute at 25°C.

Cloning *dgoA* genes from other bacterial sources. *E. coli* wild-type *dgoA*-encoded KDPGal aldoalse showed weak activity toward accepting D-erythrose 4-phosphate as a substrate. KDPGal aldolases from other bacterial sources might have higher activities for catalyzing the condensation of pyruvate with D-erythrose 4-phosphate. Obtaining *dgoA* genes from other bacteria would also enable a cross-species DNA family shuffling that has been reported to improve enzyme performance rapidly.[50]

Although KDPGal aldolase activities have been identified in *Pseudomonas saccarophila, Pseudomonas cepacia, Caulobacter cresentus*,[51] *Azotobacter vinelandii*,[52] *Rhizobium meliloti*,[53] *Gluconobacter liquefaciens*,[54] and nonpathogenic *Mycobacteria*,[55] none of these *dgoA* gene sequences was known except in *Caulobacter cresentus* in which the genomic sequence has been obtained.[56]

Performing a BLAST (Basic Local Alignment Search Tool) search against *E. coli dgoA* nucleotides sequence in microbial genome database only yielded two possible *dgoA* sequences from *Klebsiella pneumoniae* and *Salmonella typhimurium* LT2. BLAST search against the *E. coli dgoA* protein sequence afforded several more hits including *Caulobacter cresentus* CB15, *Agrobacterium tumefaciens*, *Ralstonia solanacearum*, *Bradyrhizobium japonicum*, *Brucella melitensis* and *Sinorhizobium meliloti*. The genomic DNA of *K. pneumoniae, S. typhimurium* LT2, *A. tumefaciens* and *C. cresentus* CB15 are readily available from the American Type Culture Collection (ATCC). Thus, the open reading frames of the *K. pneumoniae, S. typhimurium* LT2, *A. tumefaciens* and *C. cresentus* CB15 *dgoA* genes were amplified from their respective genomic DNA using PCR and cloned into a medium copy number expression vector pJF118EH with transcription under the control of a P_{tac} promoter to prepare plasmid pNR6.252, pNR7.120, pNR6.300 and pNR7.063, respectively. The native start codon of GTG in *C. cresentus dgoA* was changed into an ATG start codon in plasmid pNR7.063. The corresponding plasmids were transformed into *E. coli* CB734, and in all cases, the KDPGal aldolase activities in crude cell lysates were confirmed and determined (Table 11).

Table 11. KDPGal aldolases from various microorganisms.

entry	*dgoA* source	*dgoA* size (nt)	identity[a] with *E. coli dgoA*	KDPGal cleavage[b]	DAHP formation[b]
1	*Escherichia coli*[c]	618	100%	7.6	0.068
2	*Klebsiella pneumoniae*[d]	618	82%	77	0.29
3	*Salmonella typhimurium*[e]	618	81%	10	0.080
4	*Agrobacterium tumefaciens*[f]	630	54%	4.8	0.30
5	*Caulobacter cresentus*[g]	582	60%	3.6	0.23

[a] Identity is calculated based on nucleotide sequence using the global sequence alignment[57] provided by Biology Workbench.[58] [b] Specific activity is defined as units of enzyme activity per mg of protein in crude cell lysate. One unit of activity = one μmol of KDPGal cleaved or DAHP formed per minute. Crude cell lysatess were prepared from [c] *E. coli* CB734/pNR7.088; [d] *E. coli* CB734/pNR6.252; [e] *E. coli* CB734/pNR7.120; [f] *E. coli* CB734/pNR6.300; [g] *E. coli* CB734/pNR7.063.

Among the five KDPGal aldolases, *K. pneumoniae* and *A. tumefaciens* KDPGal aldolases showed highest activities toward DAHP formation (entries 2 and 4, Table 11). *K. pneumoniae* and *S. typhimurium* LT2 *dgoA* have the highest nucleotide sequence homology of about 81% with the *E. coli dgoA* (entry 2 and 3, Table 11). Family shuffling of all five *dgoA* genes constitutes one option for improving DAHP formation activity. However, a major limitation cited for family shuffling of homologous genes is its reliance on PCR-based assembly of short random fragments generated from homologous genes. This demands a level of sequence identity of more than 70% and 10-15 bp stretches of continuous sequence identity between sequences in order for recombination to occur.[59] Therefore, only *K. pneumoniae* and *S. typhimurium* LT2 KDPGal aldolase were subjected to directed evolution by PCR mutagenesis and DNA shuffling, followed by DNA family shuffling of the most evolved *K. pneumoniae* and *S. typhimurium* KDPGal aldolase mutants with the most evolved *E. coli* KDPGal aldolase mutant.

Directed evolution of KDPGal aldolase from *K. pneumoniae*. Plasmid-encoded *K. pneumoniae dgoA* afforded a 4-fold higher KDPGal aldolase specific activity in *E. coli* CB734/pNR6.252 relative to plasmid-encoded *E. coli dgoA* in *E. coli* CB734/pN7.088 (Table 11). As a result, *E. coli* CB734/pNR6.252 was able to provide for its own aromatic vitamin and L-tryptophan requirements (entry 2, Table 12). *K. pneumoniae dgoA* was subjected to two rounds of error-prone PCR mutagenesis followed by one round of DNA shuffling to combined the beneficial mutations.

The 0.6-kb amplification product from native *K. pneumoniae dgoA* under error-prone conditions was cloned into the pJF118EH expression vector to generate the first generation plasmid library (Figure 70). The plasmid library was electroporated into *E. coli* CB734 and plated out onto minimal salts plates containing L-phenylalanine and 0.2 mM IPTG (entry 3, Table 12). A single colony grew after 48 h incubation at 37°C, and the mutant *dgoA* gene KP01-1 isolated from the plasmid was further amplified under error-prone PCR mutagenesis conditions to yield the second generation mutants KP02 (Figure 70). *E. coli* CB734/pKP02 colonies were able to grow on minimal salts plates without aromatic amino acid supplements (entry 4, Table 12). A library of plasmid pKP02 from 50 of the largest colonies were isolated. For the final round, the mutated *dgoA* genes library of KP02 were shuffled and the resulting CB734/pKP03 colonies could grow in the absence of aromatic amino acids supplements when the evolved KGPGal aldolase expression was reduced by lowering IPTG concentration (entry 5, Table 12). The *dgoA* gene variants from the seven largest colonies in the final round of selection were sequenced and their encoding KDPGal aldolase activities toward DAHP formation were characterized as shown in Table 13.

The most active *K. pneumoniae* mutant (entry 4, Table 13) showed about 4-fold increase in DAHP formation activity as compared to the wild-type counterpart. Two mutants KP03-2 and KP03-5 (entries 3 and 6, Table 13) exhibited lower activity toward DAHP formation. The unexpected reduction in evolved activity might reflect on the *in vitro* instability of some of the *K. pneumoniae* KDPGal aldolase variants.

Table 12. Directed evolution of *K. pneumoniae* KDPGal aldolase.

entry	construct[a]	M9[b]	M9[c]	F[d]	YF[d]	YFW[d]	YFWvit[d]
1	*E. coli* CB734	-[e]	-	-	-	-	+[f]
2	CB734/pNR6.252	-	-	-	+	+	+
3	CB734/pKP01	-	-	+	+	+	+
4	CB734/pKP02	-	+	+	+	+	+
5	CB734/pKP03	+	+	+	+	+	+

[a] All native and evolved *dgoA* genes were inserted into the same plasmid (pJF118EH) with transcription controlled by a P_{tac} promoter. [b] Contained L-leucine and 0.05 mM IPTG. [c] Contained L-leucine and 0.2 mM IPTG. [d] Supplements added to M9 medium containing L-leucine and 0.2 mM IPTG included: F, L-phenylalanine; Y, L-tyrosine; W, L-tryptophan; vit, *p*-aminobenzoate, *p*-hydroxybenzoate, 2,3-dihydroxybenzoate. [e] no growth (-). [f] growth (+).

Table 13. Mutations and specific activities of *K. pneumoniae* KDPGal aldolase variants.

entry	*dgoA*	Mutations	DAHP activity[a] (U[b]/mg)
1	*K. pneumoniae*	wild-type	0.29
2	KP03-1	I10V, V85A, V154F, E187D, F19	0.80
3	KP03-2	I10V, P90L, V85A, P106S, V154F, S185L, F196I	0.15
4	KP03-3	I10V, E71G, V85A, P106S, V154F, E187D, Q191H, F196I	1.30
5	KP03-4	I10V, V85A, V154F, A195T, F196I	0.51
6	KP03-5	I10V, I16V, P70L, V85A, R96Q, P106S, V154F, F196I	0.049
7	KP03-6	I10V, V85A, V154F, F196I	0.66
8	KP03-7	I10V, V85A, P106S, V154F, F196I	0.65

[a] *E. coli* CB734 was used as host strain for expression of evolved enzymes. [b] One unit of DAHP synthase catalyzes the formation of one μmol of 3-dehydroshikimate per minute at 25°C.

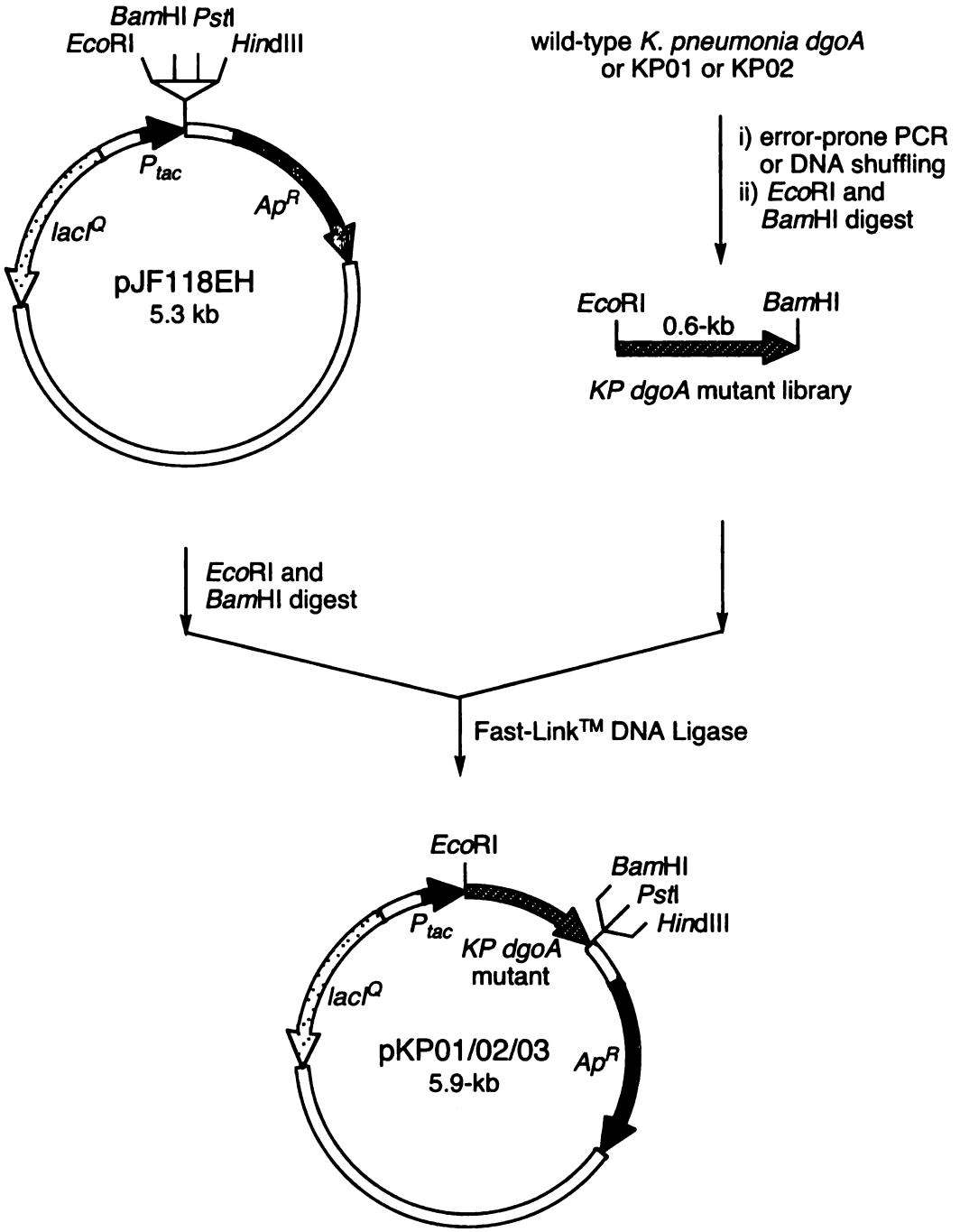

Figure 70. Construction of plasmid libraries of pKP01, pKP02 and pKP03.

Directed evolution of KDPGal Aldolase from *S. typhimurium*. *S. typhimurium dgoA* was subjected two rounds of error-prone PCR mutagenesis and two rounds of DNA shuffling. The plasmid library (Figure 71) from the first round of error-prone PCR mutagenesis was electroporated into *E. coli* CB734 and plated out onto minimal salts plates containing L-tyrosine, L-phenylalanine and 0.2 mM IPTG. *E. coli* CB734/pST01 (entry 3, Table 14) colonies resulted from the first round of PCR mutagenesis performed using wild-type *S. typhimurium dgoA* as template only required L-tyrosine and L-phenylalanine supplementation for growth. The second round of PCR mutagenesis gave *E. coli* CB734/pST02 colonies (entry 4, Table 14) whose growth required only L-phenylalanine supplementation. The third round of mutagenesis involving shuffling gave *E. coli* CB734/pST03 colonies that grew in the absence of aromatic amino acids supplements (entry 5, Table 14). The fourth round of mutagenesis involving shuffling gave CB734/pST04 colonies that grew in minimal salts medium without aromatic amino acids supplementation at reduced KDPGal aldolase expression level by lowering IPTG concentration (entry 6, Table 14). The *dgoA* gene variants from seven largest colonies after the final round of selection were sequenced and their encoding KDPGal aldolase activities toward DAHP formation were characterized (Table 15). All seven evolved KDPGal aldolase showed higher activity toward DAHP formation activity as compared to the wild-type *S. typhimurium* KDPGal aldolase. The most active mutant ST04-5 showed a 15-fold increase in activity.

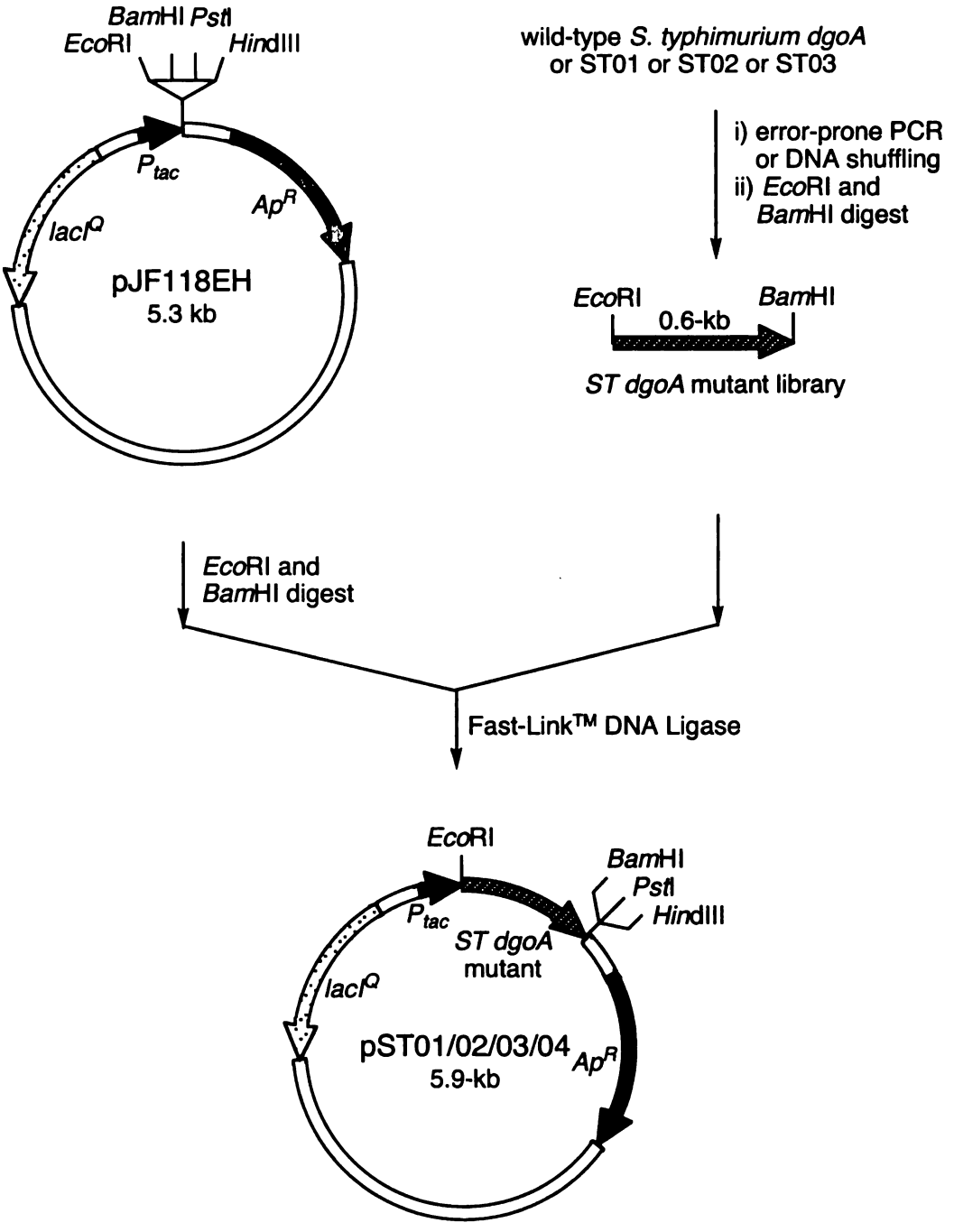

Figure 71. Construction of plasmid libraries of pST01, pST02, pST03 and pST04.

Table 14. Directed evolution of *S. typhimurium* KDPGal aldolase.

entry	construct[a]	M9[b]	M9[c]	F[d]	YF[d]	YFW[d]	YFWvit[d]
1	*E. coli* CB734	-[e]	-	-	-	-	+[f]
2	CB734/pNR7.120	-	-	-	-	+	+
3	CB734/pST01	-	-	-	+	+	+
4	CB734/pST02	-	-	+	+	+	+
5	CB734/pST03	-	+	+	+	+	+
6	CB734/pST04	+	+	+	+	+	+

[a] All native and evolved *dgoA* genes were inserted into the same plasmid (pJF118EH) with transcription controlled by a P_{tac} promoter. [b] Contained L-leucine and 0.05 mM IPTG. [c] Contained L-leucine and 0.2 mM IPTG. [d] Supplements added to M9 medium containing L-leucine and 0.2 mM IPTG included: F, L-phenylalanine; Y, L-tyrosine; W, L-tryptophan; vit, *p*-aminobenzoate, *p*-hydroxybenzoate, 2,3-dihydroxybenzoate. [e] no growth (-). [f] growth (+).

Table 15. Mutations and specific activities of *S. typhimuriume* KDPGal aldolase variants.

entry	*dgoA*	Mutations	DAHP activity[a] (U[b]/mg)
1	*S. typhimurium*	wild-type	0.080
2	ST04-1	V28L, S42T, S50P, P150L, L175S	0.48
3	ST04-2	V28M, S42T, S50P, P150L, D178G, N198K	0.85
4	ST04-3	D20E, V28L, S42T, L175S	0.84
5	ST04-4	V28M, S42T, Q123R, T158M, N161D, D178G	0.54
6	ST04-5	D20E, V28M, S42T, I89T, P150L, D178G	1.24
7	ST04-6	V28M, S42T, S50P, Q164A, L175S, N198K	0.42
8	ST04-7	V28L, S42T, P91Q, P150L, T158M, D178G, N198K	1.04

[a] *E. coli* CB734 was used as host strain for expression of evolved enzymes. [b] One unit of DAHP synthase catalyzes the formation of one μmol of 3-dehydroshikimate per minute at 25°C.

After directed evolution, a total of twenty-one active mutants from *E. coli*, *K. pneumoniae* and *S. typhimurium* mutants were selected for characterization. Each mutant contained 4-9 amino acids substitutions. No insertion or deletion mutants were found. Two amino acids substitutions (V85A, V154F) were observed in all of the seven most active *K. pneumoniae dgoA* and seven most active *E. coli dgoA* mutants. However, these

two mutations were not found in any of the seven most active *S. typhimurium* mutants. Instead, all seven of the most active *S. typhimurium* mutants contained a S42T substitution. EC03-1, the most active evolved *E. coli* KDPGal aldolase, exhibited an 8-fold higher DAHP formation specific activity and a 7-fold reduced KDPGal cleavage specific activity relative to the native *E. coli* KDPGal aldolase (entry 2, Table 16). KP03-3, the most active evolved *K. pneumoniae* KDPGal aldolase, showed a 4-fold higher DAHP formation specific activity and a 30-fold reduced KDPGal cleavage specific activity relative to native *K. pneumoniae* KDPGal aldolase (entry 4, Table 16). ST04-5, the most active evolved *S. typhimurium* KDPGal aldolase, exhibited a 15-fold higher DAHP formation specific activity and a 2-fold reduced KDPGal cleavage specific activity relative to wild-type *S. typhimurium* KDPGal aldolase (entry 6, Table 16).

Table 16. Specific activities of wild-type and evolved KDPGal aldolase isozymes.

entry	enzyme	DAHP assay[a] (U/mg)	KDPGal assay[a] (U/mg)
1	*E. coli* DgoA[b]	0.068	6.7
2	EC03-1[c]	0.56	1.0
3	*K. pneumoniae* DgoA[d]	0.29	77
4	KP03-3[e]	1.30	2.6
5	*S. typhimurium* DgoA[f]	0.080	11
6	ST04-5[g]	1.24	4.8

[a] Specific activity is defined as units of enzyme activity per mg of protein in crude cell lysates. One unit of activity = one μmol of KDPGal cleaved or DAHP formed per minute. Crude cell lysates were prepared from [b] *E. coli* CB734/pNR7.088; [c] *E. coli* CB734/pEC03-1; [d] *E. coli* CB734/pNR6.252; [e] *E. coli* CB734/pKP03-3; [f] *E. coli* CB734/pNR7.120; [g] *E. coli* CB734/pST04-5.

To examine the functioning of the created shikimate pathway variant in intact microbes, growth rates and synthesis of 3-dehydroshikimate were examined. *E. coli* CB734/pEC03-1, *E. coli* CB734/pKP03-3 and *E. coli* CB734/pST04-5 were completely

dependent on plasmid-encoded, evolved DgoA isozymes EC03-1, KPO3-3 and ST04-5, respectively, for the formation of DAHP. *E. coli* CB734/pNR7.126 (Figure 73) relied on plasmid-encoded, feedback-insensitive $AroF^{FBR}$ for DAHP synthase activity. When cultured under identical conditions where growth was dependent on *de novo* synthesis of aromatic amino acids and aromatic vitamins, *E. coli* CB734/pEC03-1, *E. coli* CB734/pKP03-3 and CB734/pST04-5 entered the logarithmic phases of their growths 12 h, 36 h, and 72 h, respectively, later than *E. coli* CB734/pNR7.126 (Figure 72).

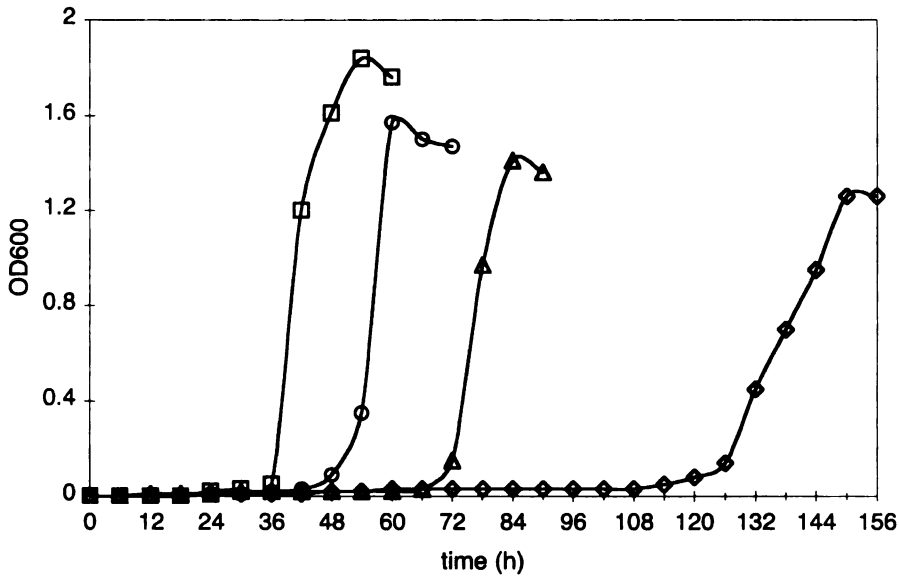

Figure 72. Growth in the absence of aromatic amino acid and aromatic vitamin supplementations in glucose-containing minimal salts medium under shake-flask conditions. *E. coli* CB734/pNR7.126 (squares); *E. coli* CB734/pEC03-1 (circles); *E. coli* CB734/pKP-03-3 (triangles); *E. coli* CB734/pST04-5 (diamonds).

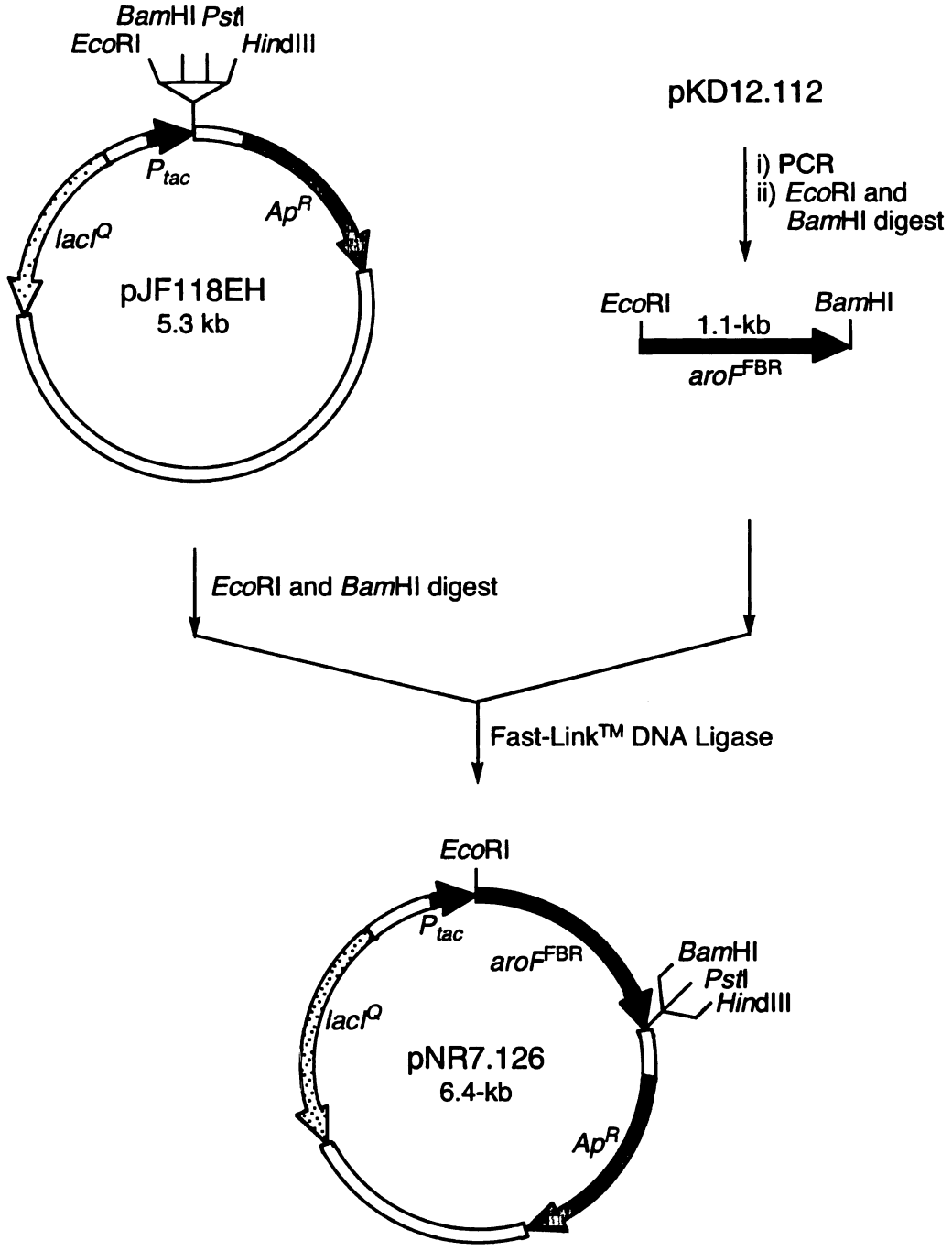

Figure 73. Construction of plasmid pNR7.126.

Synthesis of 3-dehydroshikimic acid via the pyruvate-based shikimate pathway. Use of the pyruvate-based shikimate pathway to synthesize 3-dehydroshikimic acid was examined under fermentor-controlled conditions. 3-Dehydroshikimic acid is the key hydroaromatic intermediate in the biocatalytic conversions of glucose into aromatic bioproducts and a variety of industrial chemicals such as catechol, adipic acid and vanillin (Figure 7, Chapter 1). Carbon flow directed into the shikimate pathway can be conveniently measured by the accumulation of 3-dehydroshikimic acid in the culture supernatants of microbial mutants lacking *aroE*-encoded shikimate dehydrogenase activity.

To genetically engineer the *E. coli* CB734 into a 3-dehydroshikimic acid producing strain, the shikimate dehydrogenase encoded by *aroE* and the newly discovered *ydiB*[60] genes in CB734 need to be inactivated. However, *E. coli* CB734 was not used for fed-batch fermentation of 3-dehydroshikimic acid in this study due to its L-leucine requirement and difficulty in comparing product titer and yield with previously reported 3-dehydroshikimic acid synthesis by constructs based on *E. coli* KL3. Therefore, instead of constructing a CB734*aroEydiB* strain, *E. coli* NR7 was constructed. All three DAHP synthase genes (*aroF, aroG, aroH*) in *E. coli* NR7 were inactivated by site-specific chromosomal insertions carried out in *E. coli* strain KL3 (AB2834 *serA::aroB*).[lf]

The DAHP synthase encoded by *aroF* and *aroH* in *E. coli* CB734 were inactivated by insertion with a chloramphenicol-resistant (Cm^R) gene and a kanamycin-resistance gene (Kan^R), respectively. P1-phage mediated transformation from *E. coli* CB734 could be the simplest way to disrupt the corresponding *aroF* and *aroH* genes in *E.*

coli KL3 directly. Unfortunately, *E. coli* CB734 was found to be a P1 phage resistant strain possibly due to deletion of the *gal* operon in its chromosome. Transforming a plasmid-localized *galE* encoding UDP-galactose-4-epimerase in *E. coli* CB734 failed to reverse the P1 phage resistance phenotype of *E. coli* CB734.

Chromosomal inactivation of DAHP synthase genes *aroF*, *aroG*, *aroH* were then carried out by homologous recombination methods. Special recombinant-proficient *E. coli* hosts lacking exonuclease V of the RecBCD recombination complex are suitable for chromosomal recombination by transforming with linear DNA. Recombination can occur in *recB* or *recC* mutants carrying a suppressor *sbcB* mutation that enhances recombination by the RecF pathway[61] or in *recD* mutants that are recombinase proficient but lack exonuclease V.[62] A simple one-step method applicable to wild-type *E. coli* strain has been developed to use the bacteriophage λ Red recombinase to mediate recombination using linear DNA with short homolog extensions.[63]

To construct *E. coli* NR7, the chloramphenicol-resistant (Cm^R) gene was inserted into *aroF* in a plasmid. The *aroF::Cm*^{R} allele was isolated and transformed into strain JC7623, a hyper-recombinant *recBC sbcBC* strain.[64] Chloramphenicol-resistant transformants JC7623*aroF::Cm*^{R} in which the wild-type *aroF* was exchanged with *aroF::Cm*^{R} allele by double-crossover event were obtained on chloramphenicol plates. P1-phage mediated transduction of JC7623*aroF::Cm*^{R} transferred the *aroF::Cm*^{R} mutation into KL3 to generate *E. coli* KL3*aroF::Cm*^{R}. Similarly, the *aroH::Kan*^{R} mutation was transferred from JC7623*aroH::Kan*^{R} to KL3*aroF::Cm*^{R} to prepare *E. coli* KL3*aroF::Cm*^{R} *aroH::Kan*^{R}. However, attempted transfer of the *aroG::tet* mutation by P1 phage mediated transduction from *JC7623aroG::Tc*^{R} was not successful. The *aroG*

mutation was then generated using the λ Red recombinase method. An *aroG::Tc*^{R} DNA fragment was electroporated into KL3*aroF::Cm*^{R} *aroH::Kan*^{R} carrying a plasmid pKD46 encoding λ Red recombinase. Recombinants were selected for tetracycline resistance (5 μg/mL) at 30°C. Plasmid pKD46 was eliminated by growth at 42°C. Disruption of chromosomal *aroG* was confirmed by PCR from NR7 genomic DNA using a pair of primers flanked the *aroG* locus to amplify a fragment corresponding to the *aroG::tet* allele with correct size. The *E. coli* KL3*aroF::Cm*^{R} *aroG::Tc*^{R} *aroH::Kan*^{R} strain was designated as *E. coli* NR7.

In directed evolution of *E. coli* KDPGal aldolase, *E. coli dgoA* mutants were expressed under the control of a P_{trc} promoter in expression vector pTrc99A, while *K. pneumoniae* and *S. typhimurium dgoA* mutants were expressed under a *tac* promoter in pJF118EH. The *trc* promoter displays a spacing of 17 bp between the –35 and –10 consensus sequences[65a] compared to a spacing of 16 bp between these regions in the *tac* promoter.[65b] Despite the 1 bp difference in spacing, P_{tac} and P_{trc} promoters are virtually of identical strength.[66] However, plasmid pTrc99A does have a smaller size (4.2-kb vs. 5.3-kb in pJF118EH) and an increased plasmid copy number per chromosome (30 vs. 18 in pJF118EH) compared to plasmid pJF118EH. Therefore, the most active evolved *E. coli* mutant EC03-1 was excised from pEC03-1 and cloned into the pJF118EH vector to afford plasmid pNR8.140. Plasmid pNR8.158, pKP03-3serA and pST04-5serA were constructed by inserting a *serA* gene into the plasmids containing the corresponding *dgoA* mutants. Including the *serA* locus on plasmid provides the basis for plasmid maintenance during cultivation in minimal salts medium lacking L-serine supplementation. Furthermore, expression of the *dgoA* mutants in the same plasmid enabled an unbiased

comparison of the *in vivo* activities of the individually evolved KDPGal aldolases in terms of the production of the pyruvate-based shikimate pathway metabolite.

Table 17. Synthesis of 3-dehydroshikimic acid under fermentor-controlled conditions.

entry	construct	genes	DHS[a] (g/L)	DHS (yield[b])
1	NR7/pKP03-3serA	P_{tac}*KP03-3*, *serA*	8.3	5.0%
2	NR7/pNR8.074	P_{tac}*wt-KPdgoA*, *serA*	0	0
3	NR7/pNR8.172	P_{tac}*EC03-1*, *serA*	5.1	2.4%
4	NR7/pNR8.170	P_{tac}*wt-ECdgoA*, *serA*	0	0
5	NR7/pST04-5serA	P_{tac}*ST04-5*, *serA*	6.9	3.3%
6	NR7/pNR8.121	P_{tac}*wt-STdgoA*, *serA*	0.1	0
7	NR7/pNR8.165-2serA	P_{tac}*NR8.165-2*, *serA*	7.4	3.3%
8	NR7/pNR8.165-4serA	P_{tac}*NR8.165-4*, *serA*	9.3	4.6%
9	NR7/pNR8.180	P_{tac}*NR8.165-4*, *serA*, *tktA*	12.4	6.0%
10	NR7/pNR8.182	P_{tac}*aroF*^{FBR}, *serA*	42.7	18%
11	NR7/pNR8.190	P_{T5}*NR8.165-4*, *serA*, *tktA*	10.5	6.5%

[a] DHS: 3-dehydroshikimic acid. [b] yield is calculated as (mol of DHS)/(mol of glucose).

Table 18. Evolved KDPGal aloldase activities towards DAHP formation.

entry	construct	DAHP formation assay (U[a]/mg)			
		12 h	24 h	36 h	48 h
1	NR7/pKP03-3serA	0	0.11	0.02	0.01
3	NR7/pNR8.172	0	0.05	0.05	0.05
5	NR7/ST04-5serA	0	0.30	0.25	0.22
8	NR7/pNR8.165-4serA	0	0.31	0.25	0.19
9	NR7/pNR8.180	0	0.13	0.17	0.15
11	NR7/pNR8.190	0	0.012	0.21	0.25

[a] One unit of DAHP synthase catalyzes the formation of one μmol of 3-dehydroshikimate per minute at 25°C. Isopropyl β-D-thioglucopyranoside (IPTG, 23.8 mg) was added at 12 h and every 6 h after.

E. coli NR7/pKP03-3serA was cultured under glucose-rich conditions at 36°C, 20% air saturation and pH 7.0 in a 2.0-L working volume fermentor, 8.3 g/L of 3-dehydroshikimic acid was produced after 48 h in 5% mol/mol yield from glucose (entry

1, Table 17, Figure 77). In contrast, only trace amount of 3-dehydroshikimic acid was observed in fermentation broth of NR7/pNR8.074 which encoded wild-type *K. pneumoniae dgoA* and *serA* genes (entry 2, Table 17, Figure 78). *E. coli* NR7/pNR8.172 produced 5.1 g/L of 3-dehydroshikimic acid in 2.4% mol/mol yield under the same conditions (entry 3, Table 17, Figure 79), while NR7/pNR8.170, which encoded wild-type *E. coli dgoA* and *serA* genes, produced only trace amount of 3-dehydroshikimic acid (entry 4, Table 17, Figure 80). *E. coli* NR7/pST04-5serA produced 7.1 g/L 3-dehydroshikimic acid in 3.4% yield (entry 5, Table 17, Figure 81). For comparison, NR7/pNR8.121 which encoded the wild-type *S. typhimurium dgoA* gene produced a trace amount of 3-dehydroshikimic acid (entry 6, Table 17, Figure 82).

The evolved KDPGal aldolase specific activities toward catalyzing the condensation of pyruvate and D-erythrose 4-phosphate were measured at 12, 24, 36 and 48 h after inoculation of the culture medium in the fed-batch fermentation runs (Table 18). The evolved DgoA specific activities were stably maintained over the course of fermentation runs except when DgoA mutant KP03-3 was employed. The measured DAHP formation specific activities decreased 11-fold from 0.11 U/mg at 24 h to 0.01 U/mg at 48 h in the fermentation runs of NR7/pKP03-3serA (entry 1, Table 18). However, the specific activities of the mutant KDPGal aldolases showed no apparent correlation with the concentrations of 3-dehydroshikimic acid produced in the fed-batch fermentations. For example, *E. coli* NR7/pKP03-3serA produced higher concentration of 3-dehydroshikimic acid than *E. coli* NR7/pST04-5serA (entry 1 vs. 5, Tables 16), although its DAHP formation specific activities were much lower than the latter (entry 1 vs. 3, Table 18).

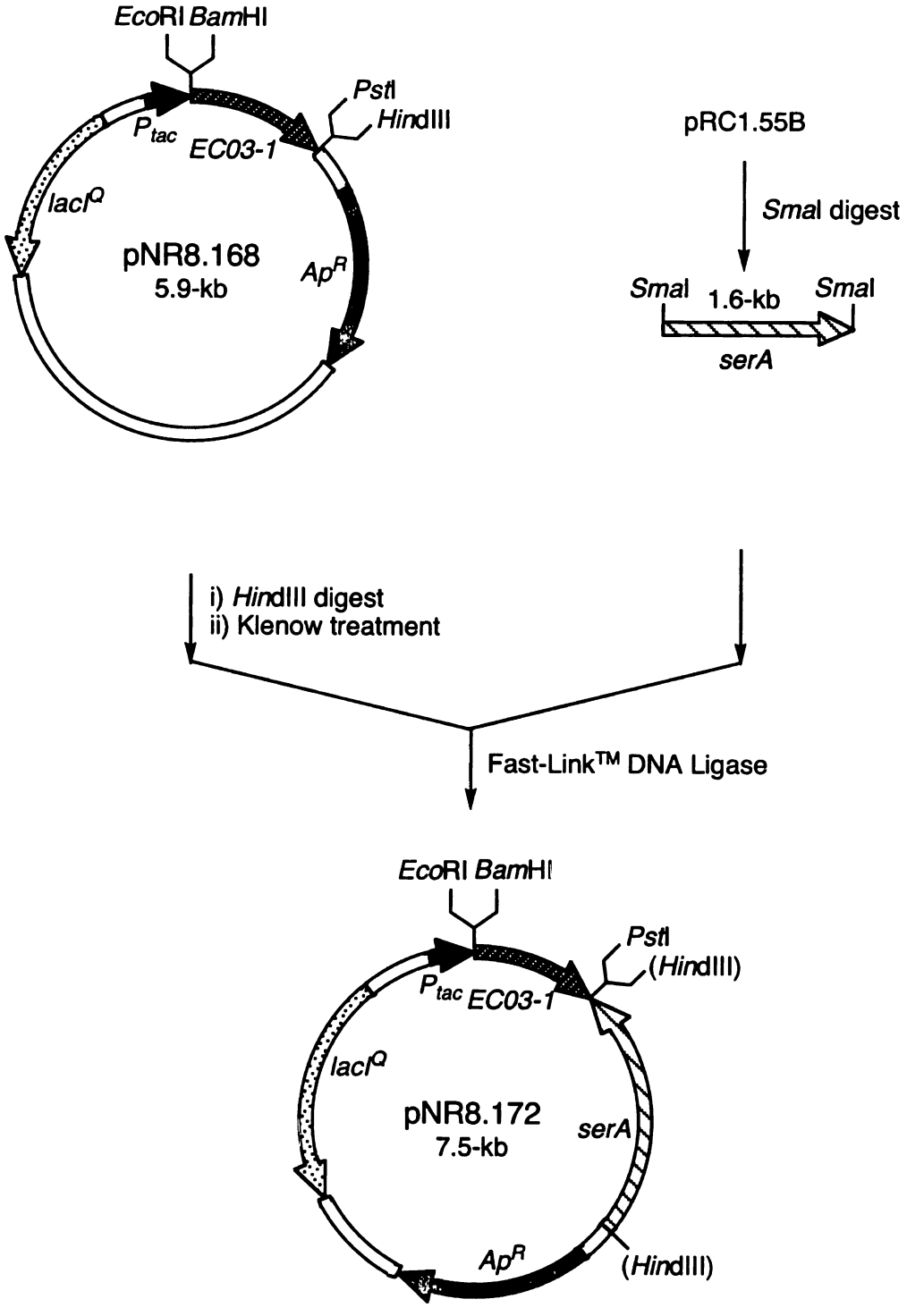

Figure 74. Construction of plasmid pNR8.172.

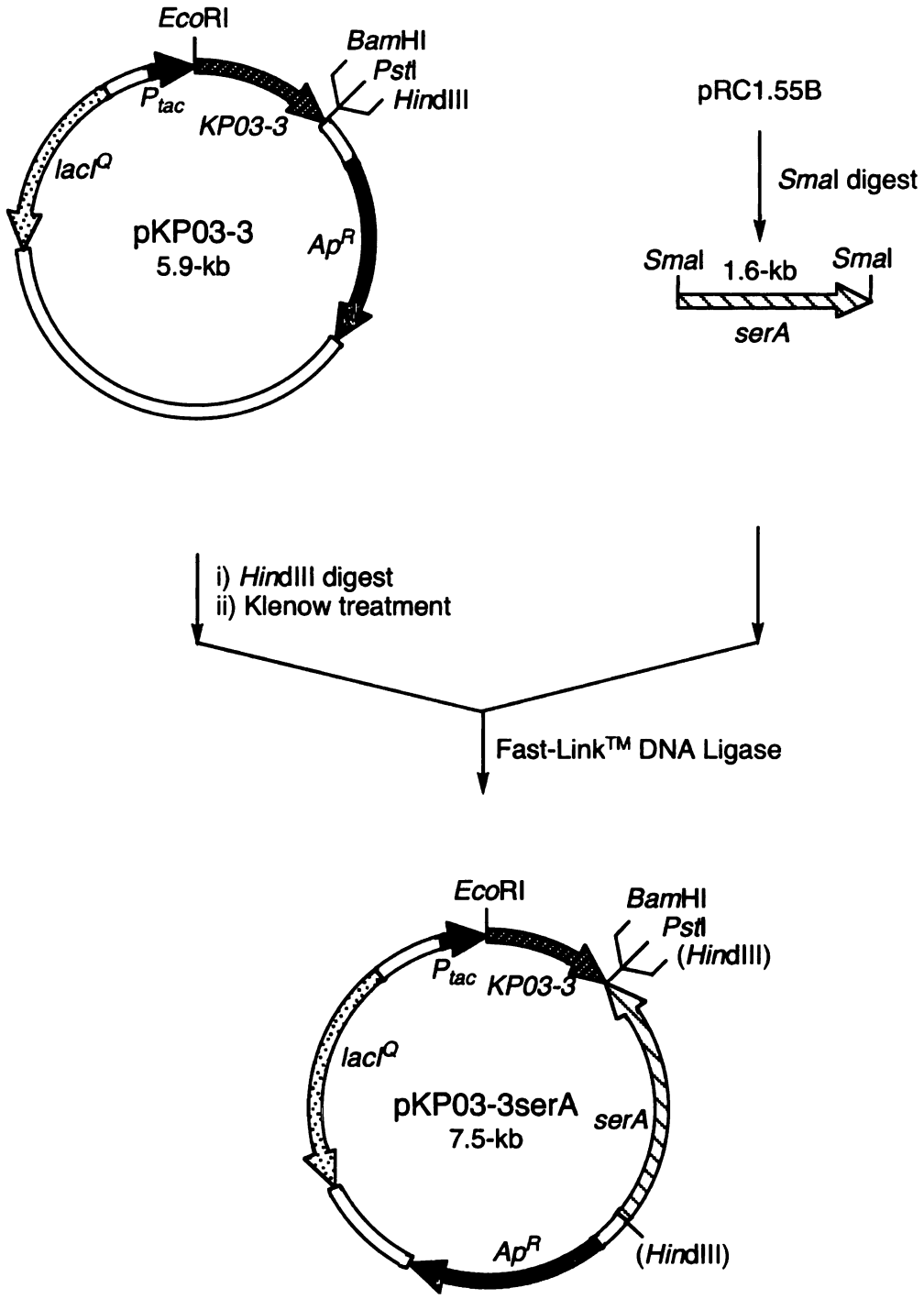

Figure 75. Construction of plasmid pKP03-3serA.

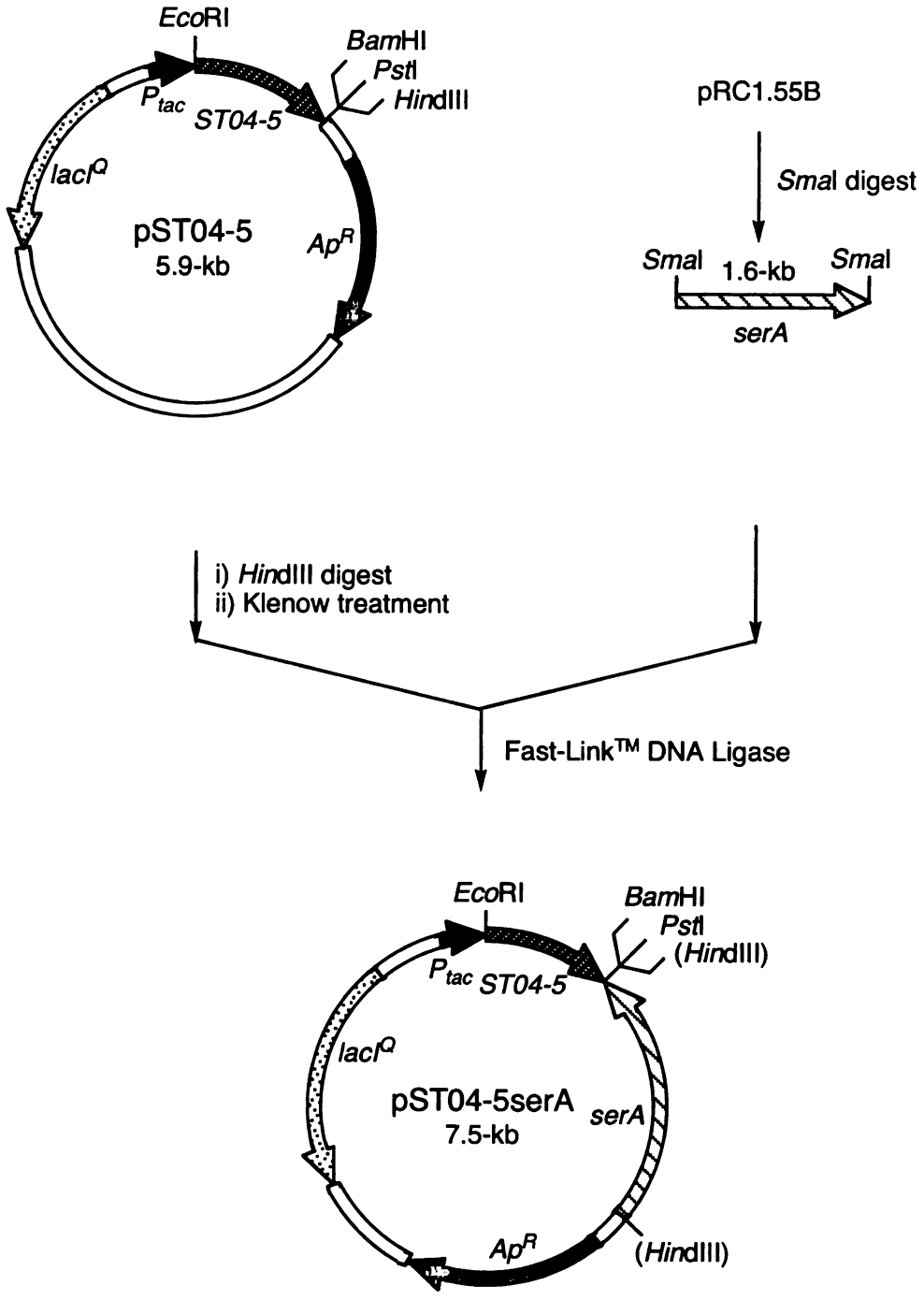

Figure 76. Construction of plasmid pST04-5serA.

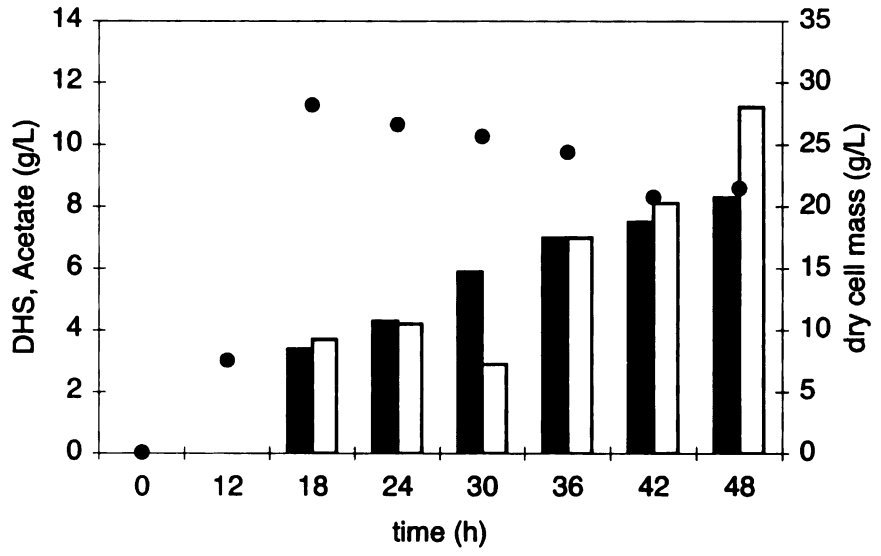

Figure 77. *E. coli* NR7/pKP03-3serA cultured under glucose-rich, fermentor-controlled conditions (36 °C, 20% D. O.). 3-Dehydroshikimic acid (■), acetic acid (□), dry cell mass (●) in g/L.

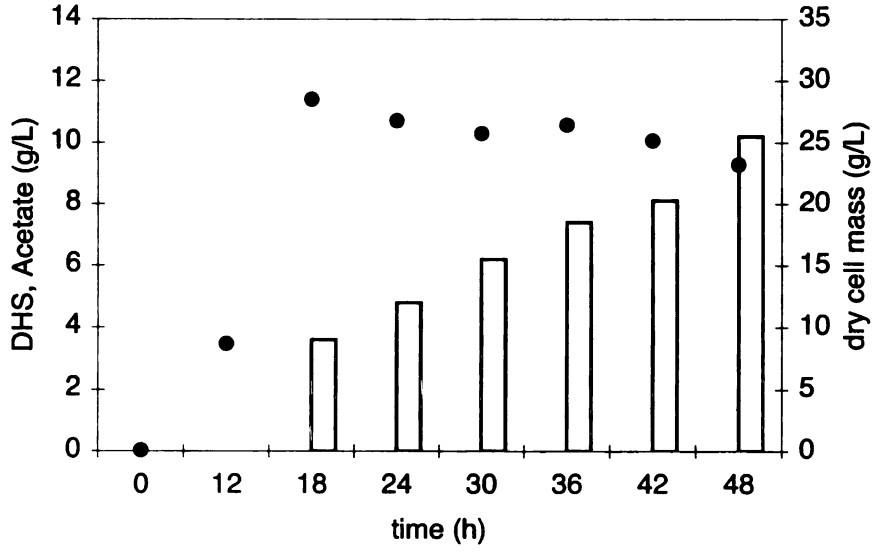

Figure 78. *E. coli* NR7/pNR8.074 cultured under glucose-rich, fermentor-controlled conditions (36 °C, 20% D. O.). 3-Dehydroshikimic acid (■), acetic acid (□), dry cell mass (●) in g/L.

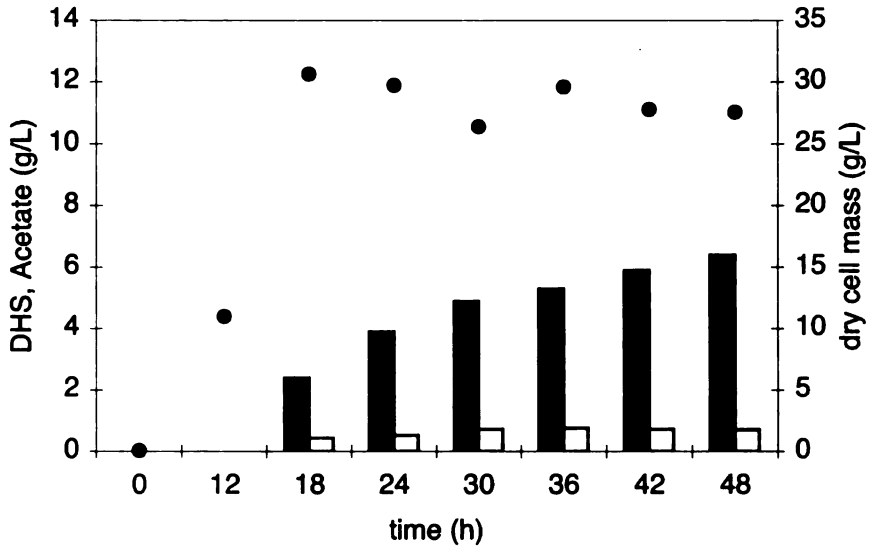

Figure 79. *E. coli* NR7/pNR8.172 cultured under glucose-rich, fermentor-controlled conditions (36 °C, 20% D. O.). 3-Dehydroshikimic acid (■), acetic acid (□), dry cell mass (●) in g/L.

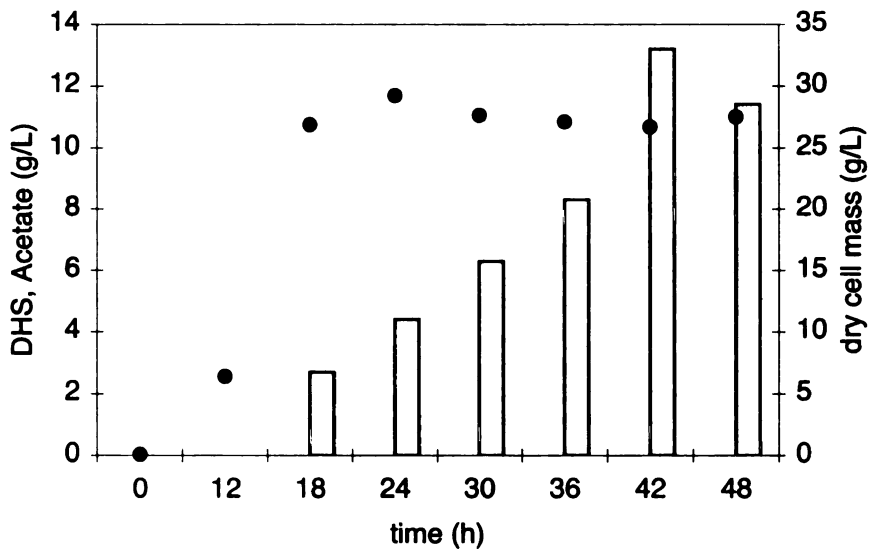

Figure 80. *E. coli* NR7/pNR8.170 cultured under glucose-rich, fermentor-controlled conditions (36 °C, 20% D. O.). 3-Dehydroshikimic acid (■), acetic acid (□), dry cell mass (●) in g/L.

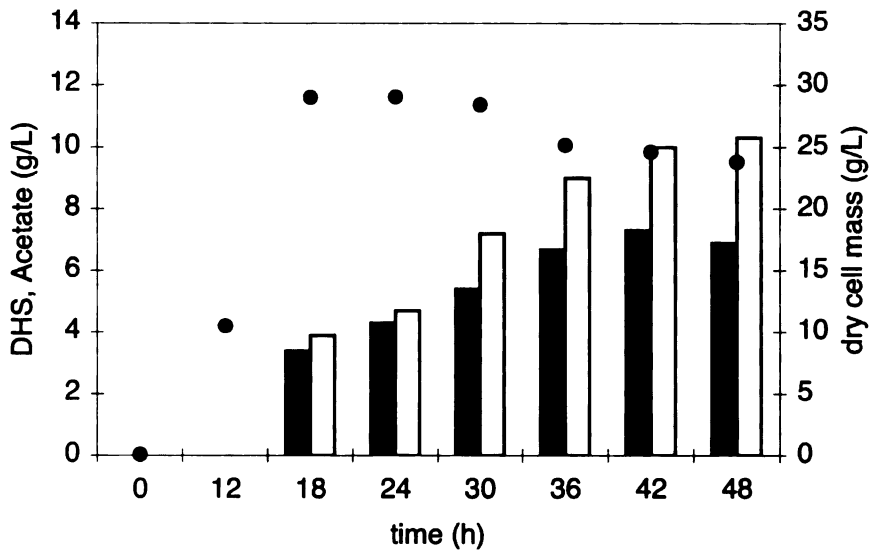

Figure 81. *E. coli* NR7/pST04-5serA cultured under glucose-rich, fermentor-controlled conditions (36 °C, 20% D. O.). 3-Dehydroshikimic acid (■), acetic acid (□), dry cell mass (●) in g/L.

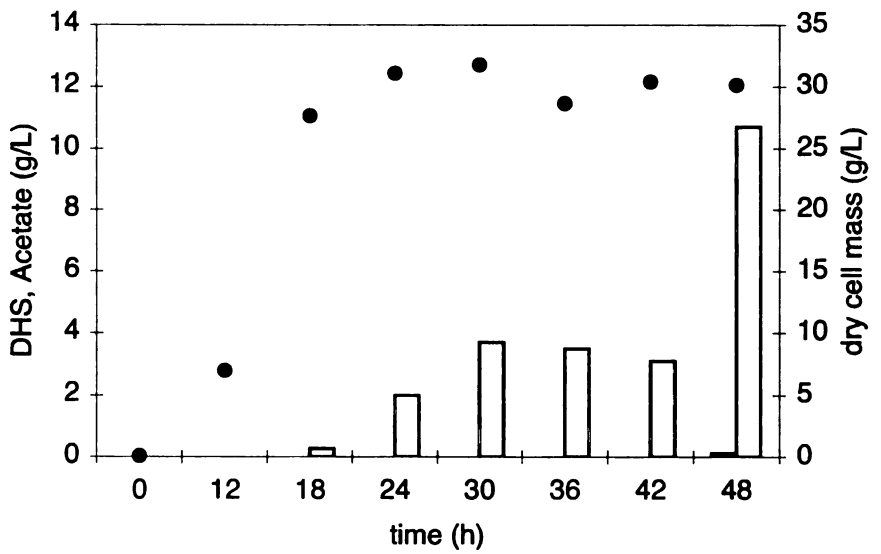

Figure 82. *E. coli* NR7/pNR8.121 cultured under glucose-rich, fermentor-controlled conditions (36 °C, 20% D. O.). 3-Dehydroshikimic acid (■), acetic acid (□), dry cell mass (●) in g/L.

Cross-species DNA shuffling of KP03-3, EC03-1 and ST04-5. DNA shuffling of a family of homologous genes from diverse species creates chimeric hybrids that could lead to a rapid improvement in enzyme activity.[50] To accelerate the evolution process, the three most evolved *dgoA* mutants EC03-1, KP03-3 and ST04-5 from *E. coli*, *K. pneumoniae and S. typhimurium*, respectively, were subjected to DNA family shuffling using the single-stranded DNA shuffling method developed by Zhao and coworkers.[67] Sequencing a small library of mutants (76) obtained from the family shuffling revealed a crossover rate of approximately 1.4 per gene using the published protocol. *E. coli* CB734 was transformed with a plasmid library that contained the chimeric *dgoA* hybrids (NR8.165), and the colonies that showed higher growth rate in the absence of aromatic amino acids supplementation as compared to *E. coli* CB734 carrying plasmid containing the parent gene, *EC03-1*, *KP03-3* or *ST04-5* (colonies appeared after 3 days on minimal salts medium) were selected. The *dgoA* gene hybrids from the five largest colonies that appeared after 2.5 days were sequenced and their encoding KDPGal aldolase activities toward DAHP formation were determined as shown in Table 19.

Table 19. Chimeric *dgoA* genes evolved by cross-species DNA family shuffling.

entry	family shuffling mutants	*dgoA* structure[a]	DAHP formation[b] (U[c]/mg)
1	NR8.165-2	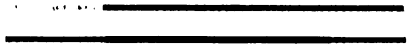	1.31
2	NR8.165-3		0.30
3	NR8.165-4		0.22
4	NR8.165-5		0.10
5	NR8.165-6		0.56

[a] Symbol: —— EC03-1; —— KP03-3; ····· ST04-5.
[b] All *dgoA* mutant were inserted into the same plasmid (pJF118EH) with transcription controlled by a P_{tac} promoter. *E. coli* CB734 was used as host strain for expression of evolved enzymes. [c] One unit of DAHP synthase catalyzes the formation of one μmol of 3-dehydroshikimate per minute at 25°C.

All five mutants were found to be chimeras of genes from the *E. coli*, *K. pneumoniae and S. typhimurium*. Four of them contain two segments resulting from a single crossover event. One mutant, NR8.165-4, contains three segments resulting from two crossovers. It also noteworthy that most crossover events occured in the first 40-80 base pairs area where the three genes have 40-base pairs of nearly identical sequences. Compared with the wild-type *E. coli* KDPGal aldolase, the DgoA mutant NR8.165-4 has a 5-fold increase in k_{cat} and a 5-fold reduction in K_m for D-erythrose 4-phosphate, and thus a 25-fold increase in k_{cat}/K_m (entry 7, Table 20). Both the mutant NR8.165-2 and NR8.165-6 show a decrease in k_{cat}/K_m values relative to their parent enzymes (entries 6 and 8 vs. entries 4 and 5, Table 20). The K_m value ranging from 80 to 157 μM for D-erythrose 4-phosphate of the mutant enzymes is close to the K_m value of *E. coli* native DAHP synthase for D-erythrose 4-phosphate (AroF[68]: K_m = 81.4 μM, k_{cat} = 29.5 s^{-1}; AroG[69]: K_m = 141 μM, k_{cat} = 10.3 s^{-1}; AroH[70]: K_m = 35 μM, k_{cat} = 20.6 s^{-1}). However, the k_{cat} of the mutant DgoAs is still much lower than the k_{cat} of the native DAHP synthases.

Table 20. Kinetic parameters of the wild-type KDPGal aldolases and the evolved variants from cross-species DNA family shuffling.

entry	enzyme[a]	K_m (E4P, μM)	k_{cat} (s^{-1})	k_{cat}/K_m (μM^{-1} s^{-1})
1	wild-type *E. coli* DgoA	571	0.94	1.65×10^{-3}
2	wild-type *K. pneumoniae* DgoA	1507	1.39	3.22×10^{-4}
3	wild-type *S. typhimurium* DgoA	685	0.600	3.76×10^{-3}
4	EC03-1	124	2.49	2.01×10^{-2}
5	ST04-5	119	3.24	2.72×10^{-2}
6	NR8.165-2	157	2.51	1.60×10^{-2}
7	NR8.165-4	115	4.76	4.14×10^{-2}
8	NR8.165-6	80	0.504	6.30×10^{-3}

[a] All wild-type and the evolved KDPGal aldolases were expressed and purified as GST (glutathione S-transferase) fusion proteins.

The two mutants, NR8.165-2 and NR8.165-4 were then selected to evaluate their *in vivo* activities for production of shikimate pathway product 3-dehydroshikimic acid under fermentor-controlled conditions. Plasmids pNR8.165-2serA and pNR8.165-4serA were constructed by inserting a *serA* gene into the plasmids pNR8.165-2 and pNR8.165-4, respectively. *E. coli* NR7/pNR8.165-2serA was cultured under the same set of fermentor-controlled conditions (36 °C, pH 7.0, 20% air saturation) as previously described, 7.4 g/L of 3-dehydroshikimic acid was produced after 48 h in 3.3% mol/mol yield from glucose (entry 7, Table 17). Cultivation of *E. coli* NR7/pNR8.165-4serA under the same conditions led to the accumulation of 9.3 g/L of 3-dehydroshikimic acid after 48 h in 4.6% mol/mol yield (entry 8, Table 17, Figure 83). Increased expression of transketolase in *E. coli* NR7/pNR8.180 resulting from incorporating a *serAtktA* cassette in plasmid pNR8.165-4 afforded 12.4 g/L of 3-dehydroshikimic acid in 6.0% mol/mol yield which represented approximately 33% increase in titer and yield (entry 9 vs. entry 8, Table 17).

The titer and yield of 3-dehydroshikimic acid synthesized by *E. coli* NR7 carrying the evolved *dgoA* is generally low compared with *E. coli* KL3 harboring an feedback-insensitive $aroF^{FBR}$. In order to exclude the possibility that the low titer and yield of the shikimate pathway product are due to difference in host strain, NR7 was transformed with a plasmid pNR8.182 that carries a *serA* gene and a feedback-insensitive $aroF^{FBR}$ with transcription controlled by a P_{tac} promoter (Figure 88). Cultivation of *E. coli* NR7/pNR8.182 under the same fermentor-controlled conditions yielded 43 g/L of 3-dehydroshikimic acid after 48 h in 18% (mol/mol) yield (entry 10, Table 17, Figure 85).

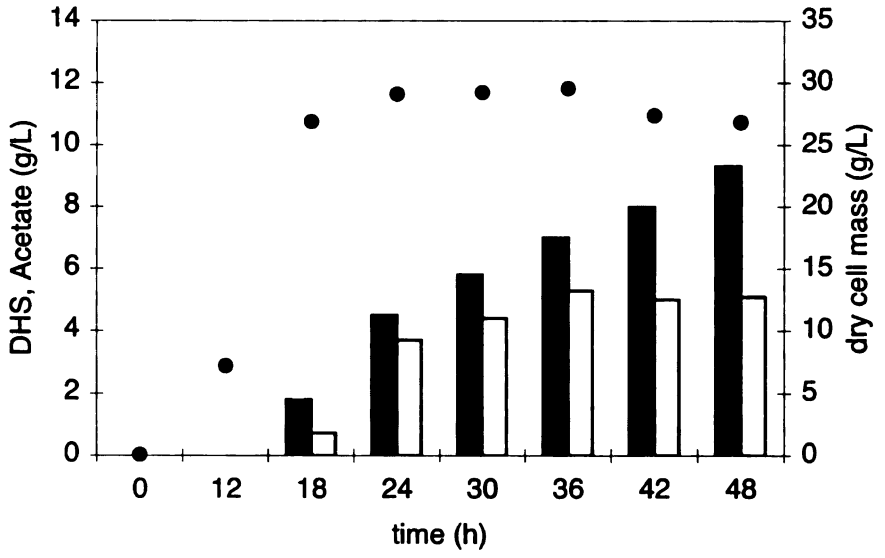

Figure 83. *E. coli* NR7/pNR8.165-4serA cultured under glucose-rich, fermentor-controlled conditions (36 °C, 20% D. O.). 3-Dehydroshikimic acid (■), acetic acid (□), dry cell mass (●) in g/L.

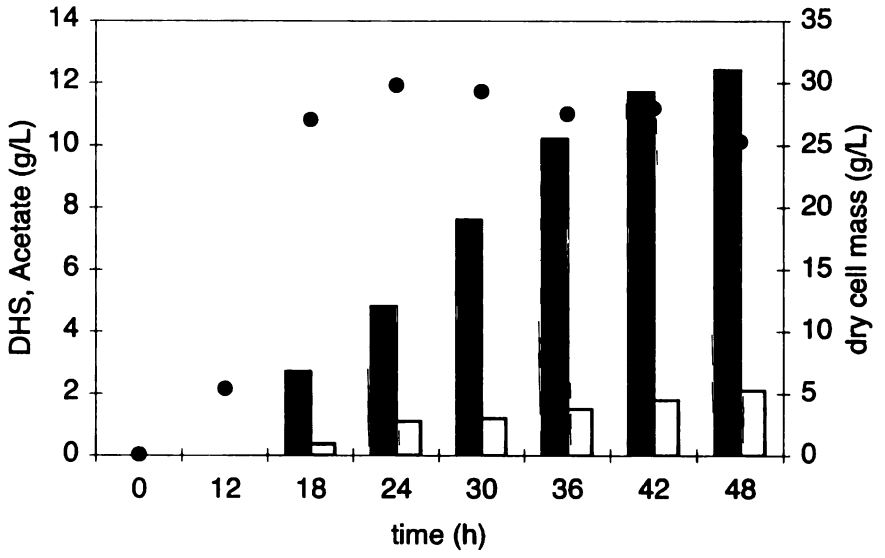

Figure 84. *E. coli* NR7/pNR8.180 cultured under glucose-rich, fermentor-controlled conditions (36 °C, 20% D. O.). 3-Dehydroshikimic acid (■), acetic acid (□), dry cell mass (●) in g/L.

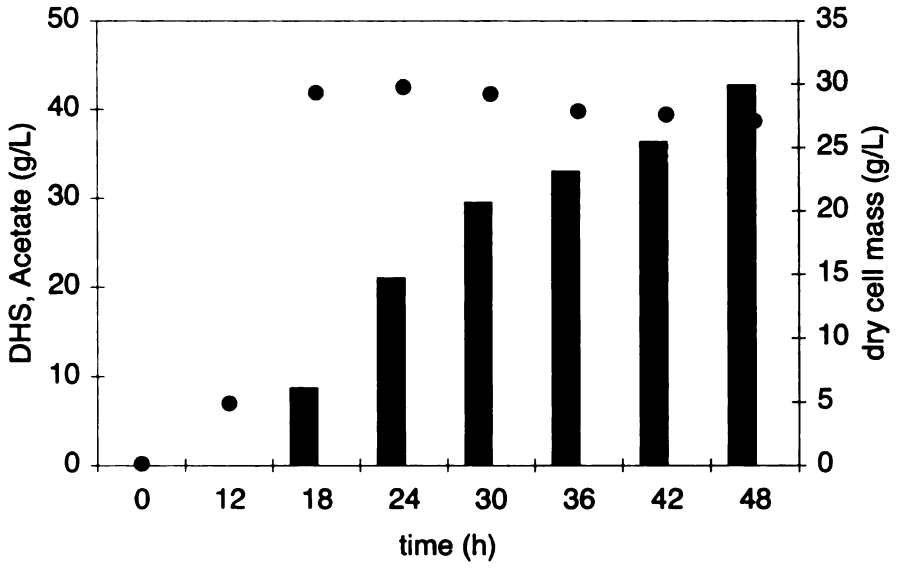

Figure 85. *E. coli* NR7/pNR8.182 cultured under glucose-rich, fermentor-controlled conditions (36 °C, 20% D. O.). 3-Dehydroshikimic acid (■), acetic acid (□), dry cell mass (●) in g/L.

In an effort to increase the specific activity of evolved KDPGal aldolase, plasmid pNR8.190 was constructed in which the transcription of the evolved *dgoA* (*NR8.165-4*) was controlled by a strong P_{T5} promoter (Figure 91). The *tktA* and *serA* genes are also included in the plasmid pNR8.190. *E. coli* NR7/pNR8.190 cultured under the same conditions, however, showed a much slower growth rate and produced 11 g/L of 3-dehydroshikimic acid in 6.5% (mol/mol) yield from glucose after 48 h (entry 11, Table 17). Analysis of the evolved DgoA activity (entry 6, Table 18) indicated no improvement in the specific activity for DAHP formation during the fermentation run.

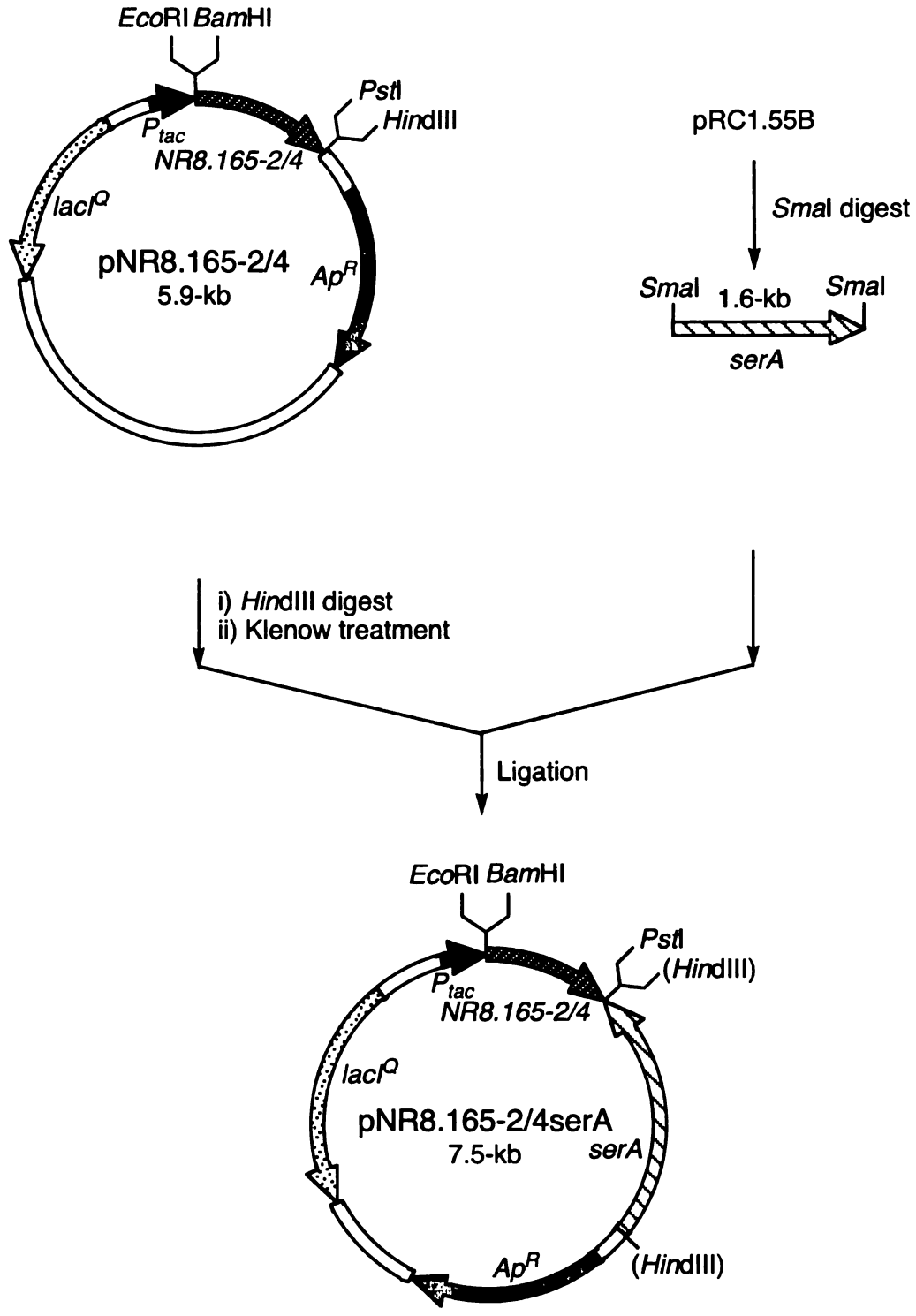

Figure 86. Construction of plasmids pNR8.165-2serA and pNR8.165-4serA.

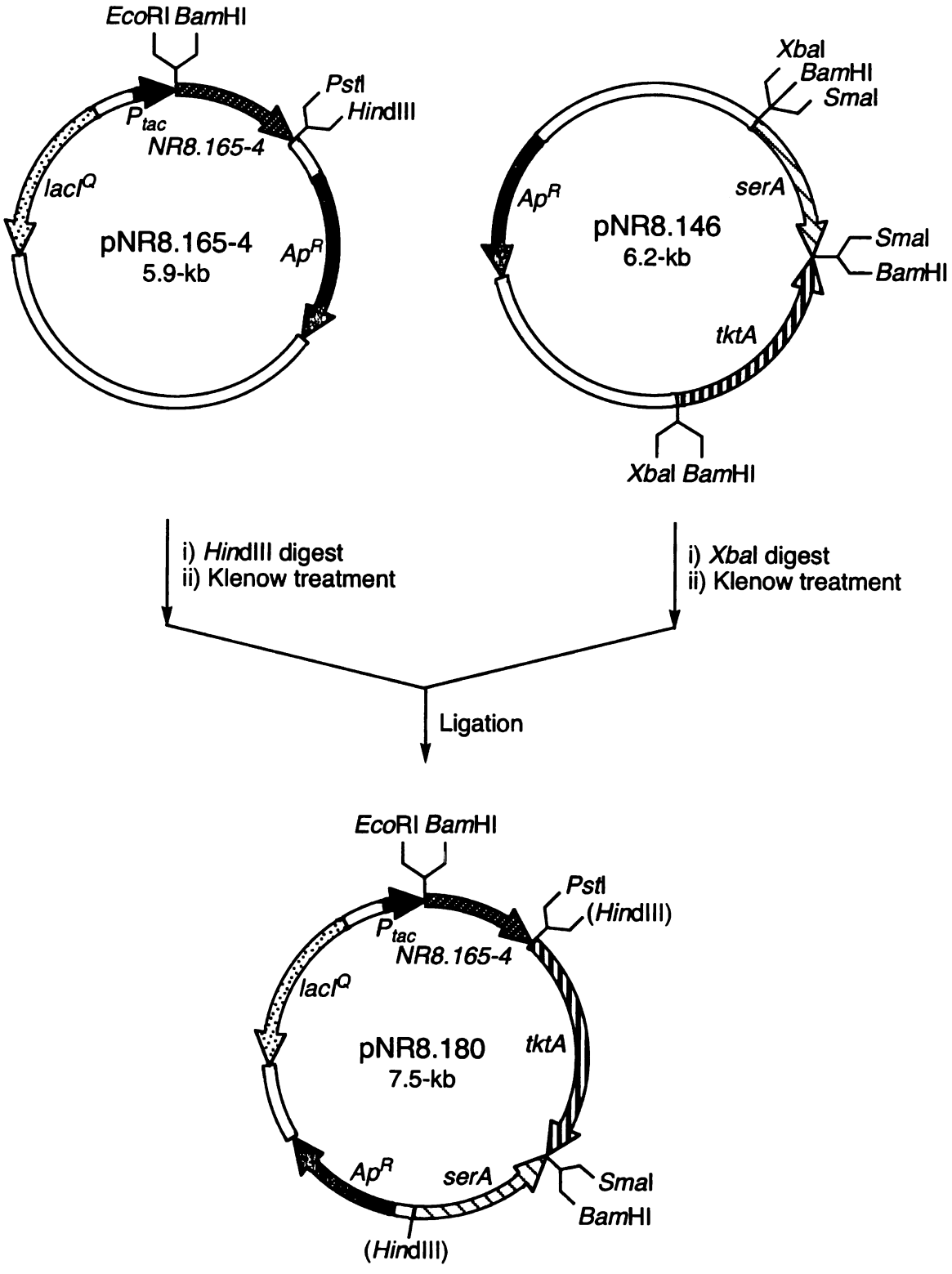

Figure 87. Construction of plasmid pNR8.180.

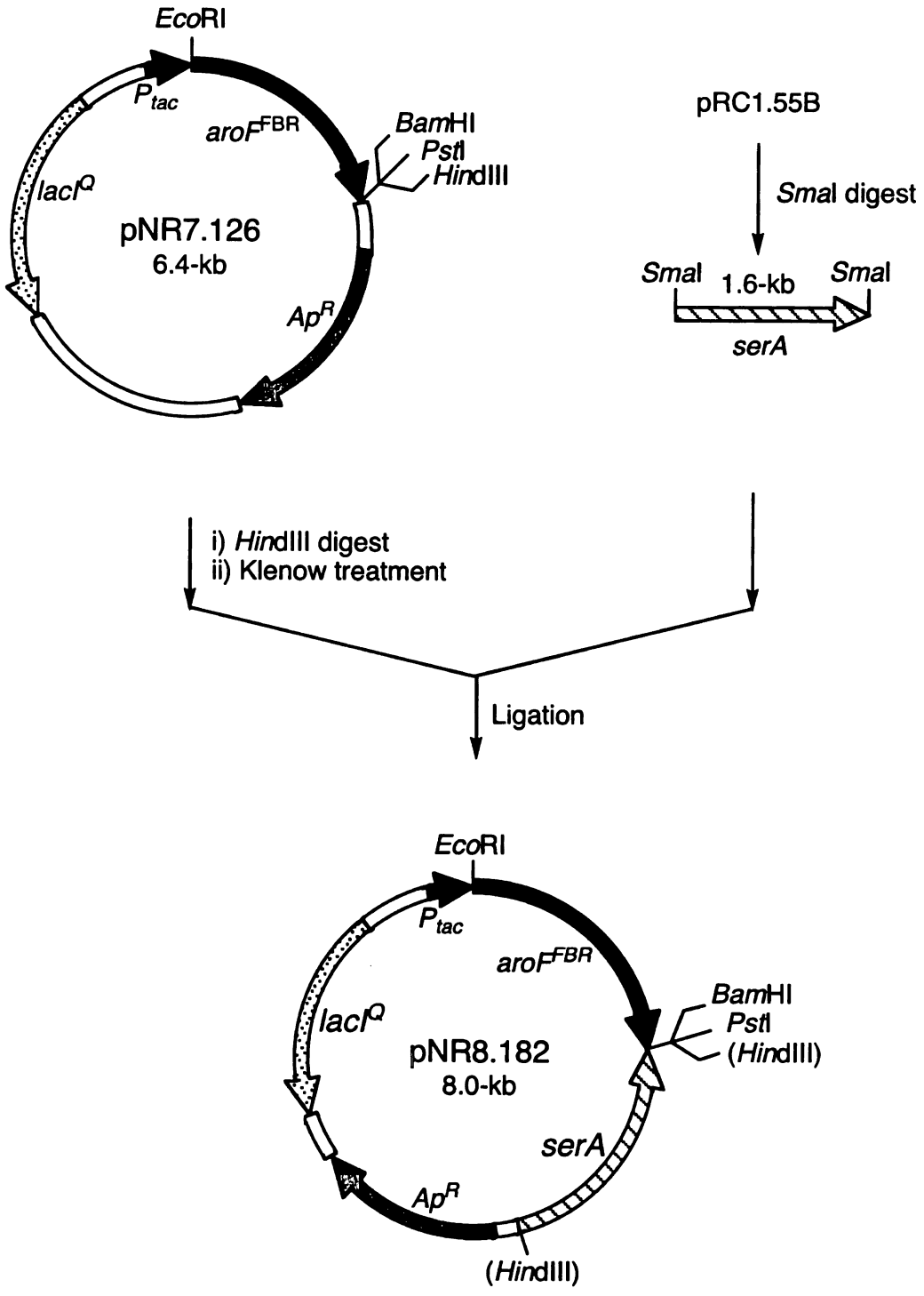

Figure 88. Construction of plasmid pNR8.182.

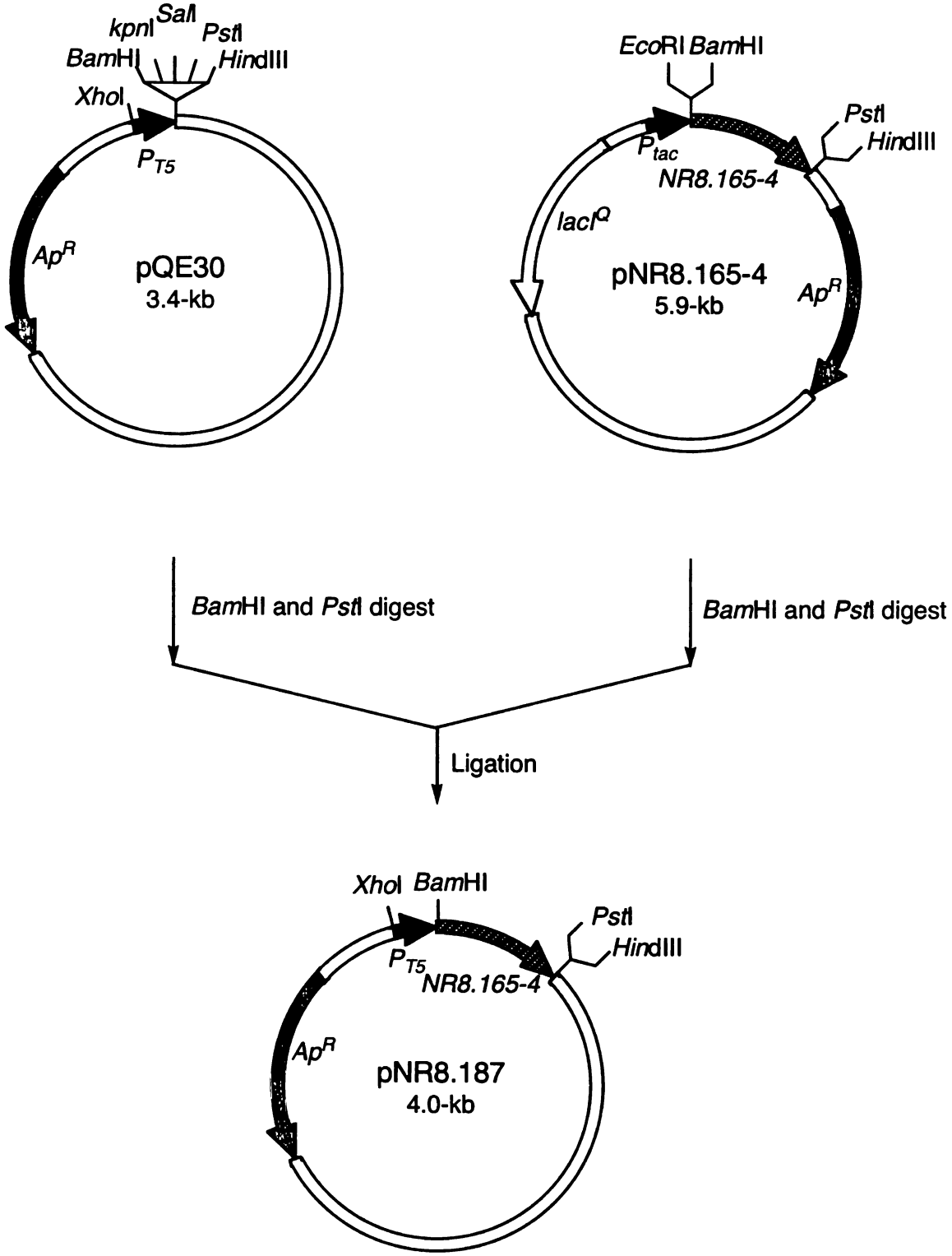

Figure 89. Construction of plasmid pNR8.187.

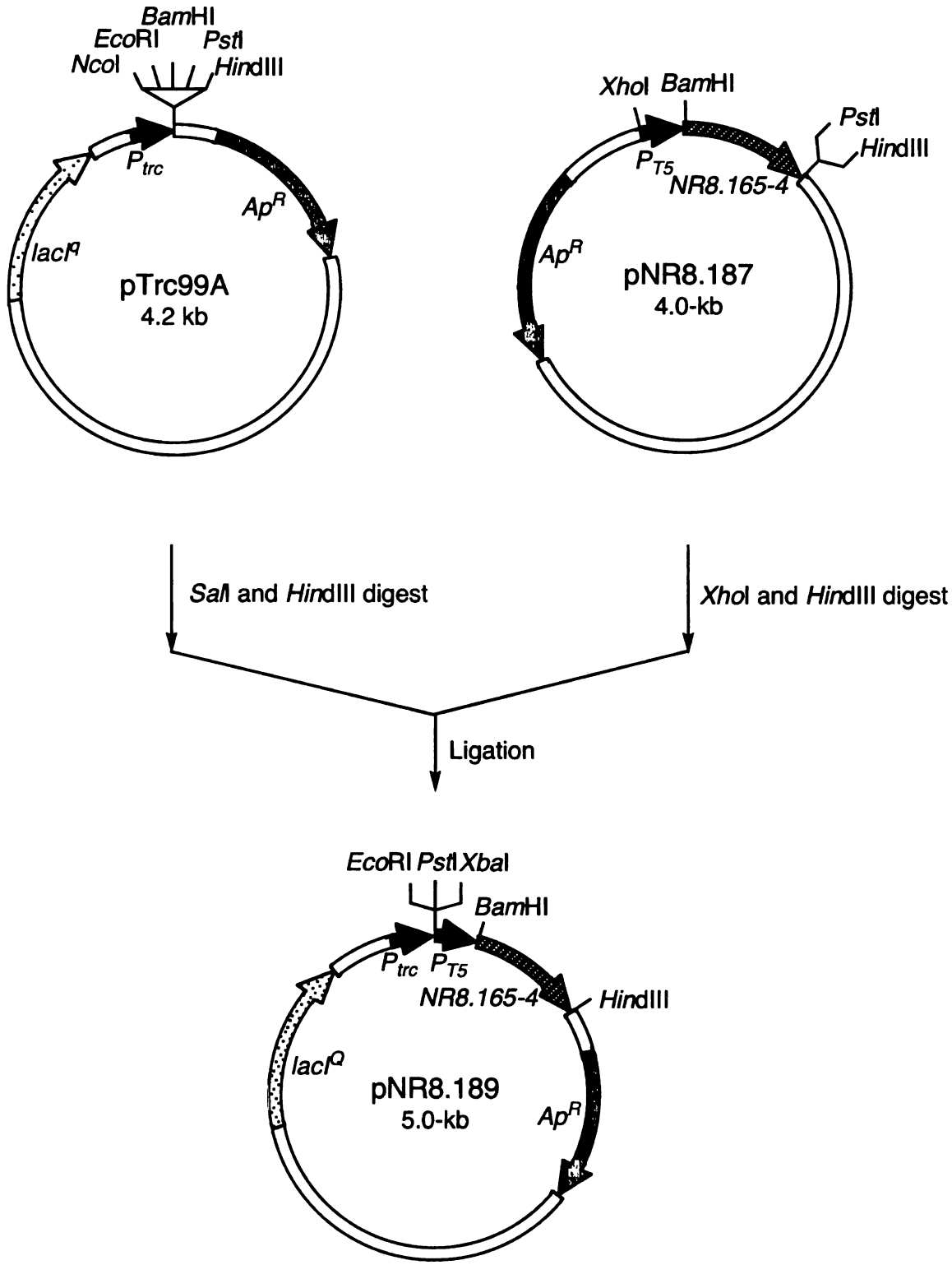

Figure 90. Construction of plasmid pNR8.189.

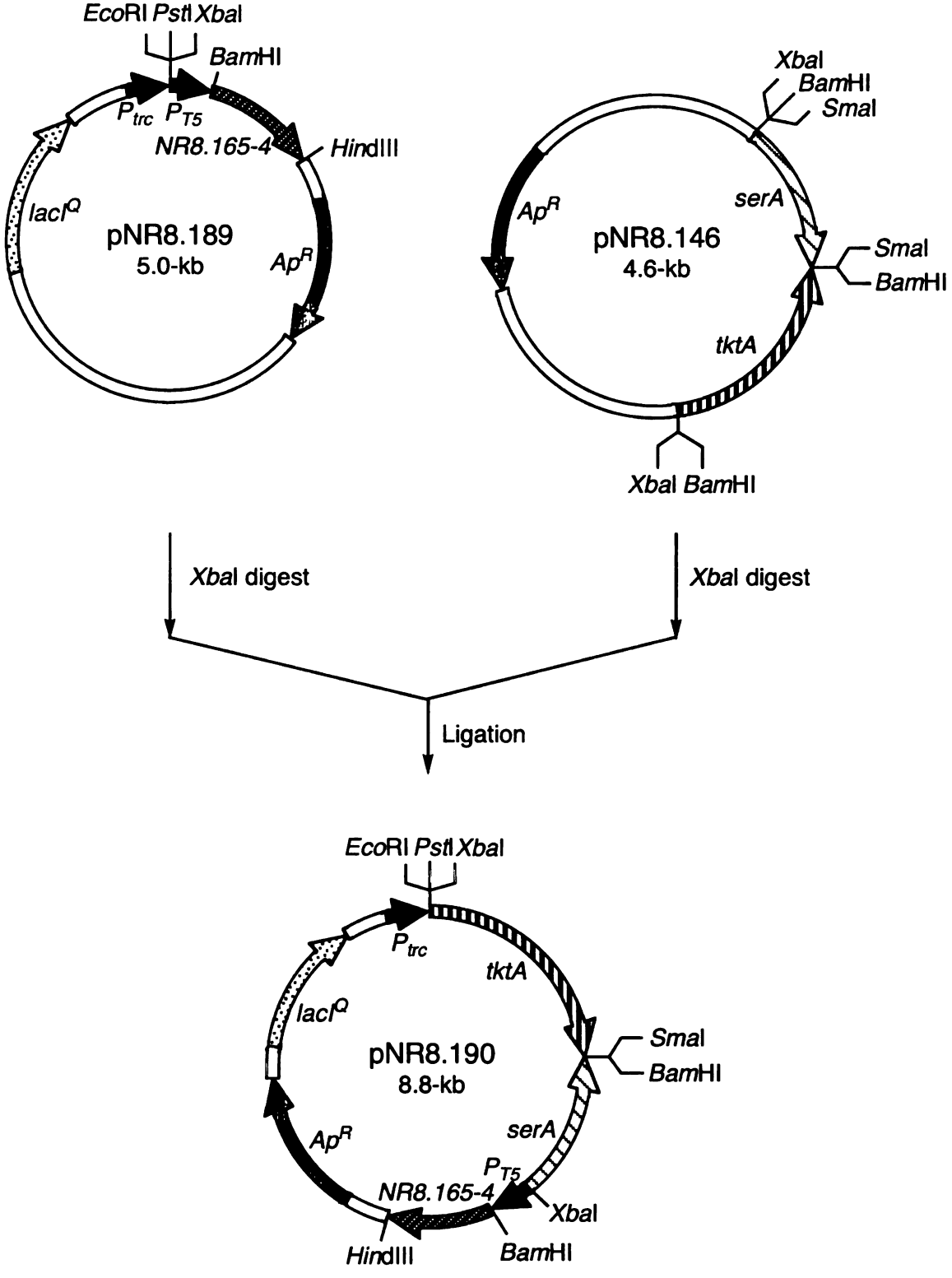

Figure 91. Construction of plasmid pNR8.190.

Discussion

With DAHP formation catalyzed by an evolved KDPGal aldolase, the first reaction in the shikimate pathway can consume the pyruvate byproduct instead of competing for the phosphoenolpyruvate substrate required by PTS-mediated glucose transport. This increases the maximum theoretical yield for shikimate pathway products from 43 to 86% (mol/mol).

To date, the k_{cat}/K_m of the most evolved KDPGal aldolase increased 25-fold relative to the wild-type *E. coli* KDPGal aldolase (entry 7 vs. 1, Table 20). The improvement of catalytic efficiency in the evolved KDPGal aldolase is reflected on both 5-fold higher turnover (k_{cat}) and 5-fold more favorable apparent K_m for D-erythrose 4-phosphate. The low K_m is particularly important to the *in vivo* activity of the evolved KDPGal aldolase due to the fact that the substrate D-erythrose 4-phosphate exists in an undetectable low concentration in the *E. coli* cytoplasm. Previous reports have demonstrated that changing enzyme substrate specificity is generally more difficult than improving the enzyme fitness under various physical environments.[71] Directed evolution of the KDPGal aldolase by 4-5 rounds of PCR mutagenesis and DNA shuffling generated DAHP synthase variants that were capable of replacing wild-type DAHP synthase in the shikimate pathway in *E. coli*. A convenient and reliable selection system that linked the cell viability with the evolved activity enabled the rapid processing of a total of about 10^7 mutants generated in this study.

The DAHP synthase auxotroph *E. coli* NR7 with expression of an evolved KDPGal aldolase could synthesize as much as 9.3 g/L of shikimate pathway product 3-dehydroshikimic acid under fermentor-controlled condition (entry 8, Table 17).

Amplified expression of transketolase in aforementioned construct increased the 3-dehydroshikimic acid production to 12.4 g/L (entry 9, Table 17) under the same cultivation condition. At this stage, the pyruvate-based shikimate pathway does not improve upon the native shikimate pathway that relied on condensation of phosphoenolpyruvate with D-erythrose 4-phosphate as indicated by the 43 g/L of 3-dehydroshikimic acid synthesized by expression of the *aroF*^{FBR}-encoded feedback-insensitive DAHP synthase in NR7. Further improvement of the catalytic activity of KDPGal aldolase might be possible by DNA shuffling of a more genetically diversified pool of KDPGal aldolaseswith the inclusion of *dgoA* sequences from *Agrobacterium tumefaciens* and *Caulobacter cresentus*. New shuffling methods have been developed that require less or no sequence homology as opposed to the method used in this study.[72]

Recently, the *E. coli aroF-* and *aroG*-encoded DAHP synthases were found to form complexes with the *tktA*-encoded transketolase *in vivo*.[73] A plausible D-erythrose 4-phosphate channeling from transketolase to DAHP synthase may occur in such complexes. That might be how nature circumvents the instability of the substrate D-erythrose 4-phosphate. In the pyruvate-based shikimate pathway, it seems unlikely that the native and evolved KDPGal aldolase could form complexes with the transketolase. This might explain the lower concentrations and titers of 3-dehydroshikimic acid synthesized by way of the pyruvate-based shikimate pathway relative to the native shikimate pathway.

Reference

[1] (a) Draths, K. M.; Pompliano, D. L.; Conley, D. L.; Frost, J. W.; Berry, A.; Disbrow, G. L.; Staversky, R. J.; Lievense, J. C. Biocatalytic synthesis of aromatics from D-glucose: the role of transketolase. *J. Am. Chem. Soc.* **1992**, *114*, 3956-3962. (b) Gubler, M., Jetten, M., Lee, S. H., Sinskey, A. J. Cloning of the pyruvate-kinase gene (Pyk) of *Corynebacterium glutamicum* and site-specific inactivation of Pyk in a lysine- producing *Corynebacterium lactofermentum* strain. *Appl. Env. Microbiol.* **1994,** *60*, 2494-2500. (c) Miller, J. E.; Backman, K.C.; O'Conner, M. J.; Hatch, R. T. Production of phenylalanine and organic-acids by phosphoenolpyruvate carboxylase-deficient mutants of *Escherichia coli*. *J. Ind. Microbiol.* **1987,** 2, 143-149. (d) Patnaik, R.; Liao, J. C. Engineering of *Escherichia coli* central metabolism for aromatic metabolite production with near theoretical yield. *Appl. Environ. Microbiol.* **1994,** *60*, 3903-3908. (e) Patnaik, R.; Spitzer, R. G.; Liao, J. C. Pathway engineering for production of aromatics in *Escherichia coli*: confirmation of stoichiometric analysis by independent modulation of AroG, TktA, and Pps activities. *Biotechnol. Bioeng.* **1995**, *46*, 361-370. (f) Li, K.; Mikola, M. R.; Draths, K. M.; Worden, R. M.; Frost, J. W. Fed-batch fermentor synthesis of 3-dehydroshikimic acid using recombinant *Escherichia coli*. *Biotechnol. Bioeng.* **1999**, *64*, 61-73.

[2] (a) Flores, N.; Xiao, J.; Berry, A.; Bolivar, F.; Valle, F. Pathway engineering for the production of aromatic compounds in *Escherichia coli*. *Nat. Biotechnol.* **1996**, *14*, 620-623. (b) Chen, R.; Yap, W. M. G. J.; Postma, P. W.; Bailey, J. E. Comparative studies of *Escherichia coli* strains using different glucose uptake systems: metabolism and energetics. *Biotechnol. Bioeng.* **1997**, *56*, 583-590. (c) Chen, R.; Hatzimanikatis, V.; Yap, W. M. G. J.; Postma, P. W.; Bailey, J. E. Metabolic consequences of phosphotransferase (PTS) mutation in a phenylalanine-producing recombinant *Escherichia coli*. *Biotechnol. Prog.* **1997**, *13*, 768-775. (d) Baez, J. L.; Bolivar, F.; Gosset, G. Determination of 3-deoxy-D-*arabino*-heptulosonate 7-phosphate productivity and yield from glucose in *Escherichia coli* devoid of the glucose phosphotransferase transport system. *Biotechnol. Bioeng.* **2001**, *73*, 530-535. (e) Flores, S.; Gosset, G.; Flores, N.; de Graaf, A. A.; Bolivar, F. Analysis of carbon metabolism in *Escherichia coli* strains with an inactive phosphotransferase system by ^{13}C labeling and NMR spectroscopy. *Metabol. Eng.* **2002**, *4*, 124-137.

[3] (a) Ogino, T.; Garner, C.; Markley, J. L.; Herrmann, K. M. Biosynthesis of aromatic compounds: ^{13}C NMR spectroscopy of whole *Escherichia coli* cells. *Proc. Natl. Acad. Sci. USA* **1982**, *79*, 5828-5832. (b) Weaver, L. M.; Herrmann, K. M. Cloning of an *aroF* allele encoding a tyrosine-insensitive 3-deoxy-D-*aroabino*-heptulosonate 7-phosphate synthase. *J. Bacteriol.* **1990**, *172*, 6581-6584.

[4] (a) Kikuchi, T.; Sotochi, N.; Fukase, K.; Kojima, H.; Kurahashi, O.; Matsui, Y. Aromatic amino acid manufacture enhancement with recombinant microorganism. JP Patent 04248983, 1993. (b) Tonouchi, N.; Kojima, H.; Matsui, H. The use of feedback-insensitive enzymes in the production of aromatic amino acids by fermentation. Eur. Pat. Appl. 488424, 1992.

[5] Ray, J. M.; Yanofsky, C.; Bauerle, R. Mutational analysis of the catalytic and feedback sites of the tryptophan-sensitive 3-deoxy-D-*arabino*-heptulosonate-7- phosphate synthase of *Escherichia coli*. *J. Bacteriol.* **1988**, *170*, 5500-5506.

[6] (a) Draths, K. M.; Frost, J. W. Synthesis using plasmid-based biocatalysis: plasmid assembly and 3-deoxy-D-*arabino*-heptulosonate production. *J. Am. Chem. Soc.* **1990**, *112*, 1657-1659. (b) Frost, J. W. Enhanced production of common aromatic pathway compounds. U.S. Patent 5,168,056, 1992.

[7] (a) Farabaugh, M. M.S. Thesis, Michigan State University, April 1996. (b) Lu, J.-L.; Liao, J. C. Metabolic engineering and control analysis for production of aromatics: role of transaldolase. *Biotechnol. Bioeng.* **1997**, *53*, 132-138.

[8] Walsh, C. T.; Benson, T. E.; Kim, D. H.; Lees, W. J. The versatility of phosphoenolpyruvate and its vinyl ether products in biosynthesis. *Chem. Biol.* **1996**, *3*, 83-91.

[9] Postma, P. W.; Lengeler, J. W.; Jacobson, G. R. Phosphoenolpyruvate:carbohydrate phosphotranferase systems. In *Escherichia coli and Salmonella: Cellular and Molecular Biology, 2nd Ed.*; Neidhardt, F. C., Ed.; ASM Press: Washington, DC, 1996; p. 1149-1174.

[10] PTS-mediated glucose transport is found in microbes such as *E. coli*, *Bacillus subtilis*, and *Streptomyces coelicolor*.

[11] (a) Snoep, J. L.; Arfman, N.; Yomano, L. P.; Fliege, R. K.; Conway, T.; Ingram, L. O. Reconstruction of glucose uptake and phosphorylation in a glucose-negative mutant of *Escherichia coli* by using *Zymomonas mobilis* genes encoding the glucose facilitator protein and glucokinase. *J. Bacteriol.* **1994**, *176*, 2133-2135. (b) Parker, C.; Barnell, W. O.; Snoep, J. L.; Ingram, L. O.; Conway, T. Characterization of the *Zymomonas mobilis* glucose facilitator gene product (*glf*) in recombinant *Escherichia coli*: examination of transport mechanism, kinetics and the role of glucokinase in glucose transport. *Mol. Microbiol.* **1995**, *15*, 795-802. (c) Weisser, P.; Krämer, R.; Sahm, H.; Sprenger, G. A. Functional expression of the glucose transporter of *Zymomonas mobilis* leads to restoration of glucose and fructose uptake in *Escherichia coli* mutants and provides evidence for its facilitator action. *J. Bacteriol.* **1995**, *177*, 3551-3554.

[12] Li, K.; Frost, J. W. Microbial synthesis of 3-dehydroshikimic acid: a comparative analysis of D-xylose, L-arabinose, D-glucose carbon sources. *Biotechnol. Prog.* **1999**, *15*, 876-883.

[13] Li, K.; Frost, J. W. Utilization of succinic acid as a glucose adjunct in fed-batch fermentations: is butane a feedstock option in microbe-catalyzed synthesis. *J. Am. Chem. Soc.* **1999**, *121*, 9461-9462.

[14] Ran, N.; Draths, K. M.; Frost, J. W. Creation of a shikimate pathway variant. *J. Am. Chem. Soc.* **2004**, *126*, 6856-6857.

[15] Lowry, O. H.; Carter, J.; Ward, J. B.; Glaser, L. The effect of carbon and nitrogen sources on the level of metabolic intermediates in *Escherichia coli*. *J. Biol. Chem.* **1971**, *246*, 6511-6521.

[16] (a) Konstantinov, K. B.; Nishio, N.; Yoshida, T. Glucose feeding strategy accounting for the decreasing oxidative capacity of recombinant *Escherichia coli* in fed-batch cultivation of phenylalanine production. *Ferment. Bioeng.* **1990**, *70*, 253-260. (b) Konstantinov, K. B.; Nishio, N.; Seki, T.; Yoshida, T. Physiologically motivated strategies for control of the fed-batch cultivation of recombinant *Escherichia coli* for phenylalanine production. *Ferment. Bioeng.* **1991**, *71*, 350-355.

[17] Tribe, D. E.; Pittard, J. Hyperproduction of tryptophan by *Escherichia coli*: genetic manipulation of the pathways leading to tryptophan formation. *Appl. Environ. Microbiol.* **1979**, *38*, 181-190.

[18] Niersbach, M.; Kreuzaler, F.; Geerse, R. H.; Postma, P. W.; Hirsch, H. J. Cloning and nucleotide sequence of the *Escherichia coli* K-12 *ppsA* gene, encoding PEP synthase. *Mol. Gen. Genetics* **1992**, *231*, 332-336.

[19] Parker, C.; Barnell, W. O.; Snoep, J. L.; Ingram, L. O.; Conway, T. Characterization of the *Zymomonas mobilis* glucose facilitator gene product (*glf*) in recombinant *Escherichia coli*: examination of transport mechanism, kinetics and the role of glucokinase in glucose transport. *Mol. Microbiol.* **1995**, *15*, 795-802.

[20] Saier, M. H. Jr.; Bromberg, F. G.; Roseman, S. Characterization of constitutive galactose permease mutants in *Salmonella typhimurium*. *J. Bacteriol.* **1973**, *113*, 512-514.

[21] Pao, S. S.; Paulsen, I. T.; Saier, M. H. Jr. Major facilitator superfamily. *Microbiol. Mol. Biol. Rev.* **1998**, *62*, 1-34.

[22] (a) Sprenger, G.; Sahm, H.; Karutz, M.; Sonke, T. Microbial preparation of substances from aromatic metabolism/II. WO 98/18937, 1998. (b) Kraemer, M.; Karutz, M.; Sprenger, G.; Sahm, H. Microbial preparation of substances from aromatic metabolism/III. WO 99/55877, 1999. (c) Sprenger, G.; Siewe, R.; Sahm, H.; Karutz, M.; Sonke, T. Microbial preparation of substances from aromatic metabolism/I. U.S. Patent 6,316,232 B1, 2001.

[23] Chandran, S. C.; Yi, J.; Draths, K. M.; von Daeniken, R.; Weber, W.; Frost, J. W. Phosphoenolpyruvate availability and the biosynthesis of shikimic acid. *Biotechnol. Prog.* **2003**, *19*, 808-814.

[24] Shumilin, I. A.; Kretsinger, R. H.; Bauerle, R. H. Crystal structure of phenylalanine-regulated 3-deoxy-D-*arabino*-heptulosonate-7-phosphate synthase from *Escherichia coli*. *Structure* **1999**, *7*, 865-875.

[25] Shumilin, I. A.; Zhao, C.; Bauerla, R.; Krestinger, R. H. Allosteric inhibition of 3-deoxy-D-*arabino*-heptulosonate-7-phosphate synthase alters the coordination of both substrates. *J. Mol. Biol.* **2002**, *320*, 1147-1156.

[26] (a) Deacon, J.; Cooper, R. A. D-Galactonate utilization by Enteric bacteria. *FEBS Lett.* **1977**, *77*, 201-205. (b) Cooper, R. A. The utilization of D-galactonate and D-2-oxo-3-deoxygalactonate by *Escherichia coli* K-12. *Arch. Microbiol.* **1978**, *118*, 199-206.

[27] (a) De Ley, J.; Doudoroff, M. The metabolism of D-galactose in *Pseudomonas saccharophila*. *J. Biol. Chem.* **1957**, *227*, 745-757. (b) Meloche, H. P. Monti, C. T. Bromopyruvate inactivation of 2-keto-3-deoxy-6-phosphogalactonate aldolase of *Pseudomonas saccharophila*. Kinetics and stereochemistry. *Biochem.* **1975**, *14*, 3682-3687. (c) Allenza, P.; Lessie, T. G. *Pseudomonas cepacia* mutants blocked in the Entner-Doudoroff pathway. *J. Bacteriol.* **1982**, *150*, 1340-1347.

[28] Kurn, N.; Contereras, I.; Shapiro; L. Galactose catabolism in *Caulobacter cresentus*. *J. Bacterial.* **1978**, *135*, 517-520.

[29] Wong, T. Y.; Yao, X. The DeLey-Doudoroff pathway of galactose metabolism in *Azotobacter vinelandii*. *Appl. Environ. Microbiol.* **1994**, *60*, 2065-2068.

[30] Arias, A.; Cervenansky, C. Galactose metabolism in *Rhizobium meliloti* L5-30. *J. Bacteriol.* **1986**, *167*, 1092-1094.

[31] Stouthammer, A. H. Glucose and galactose metabolism in *Gluconobacter liquefaciens*. *Biochim. Biophys. Acta* **1961**, *48*, 484-500.

[32] Szumilo, T. Pathway for D-galactonate catabolism in nonpathogenic *Mycobacteria*. *J. Bacteriol.* **1981**, *148*, 368-370.

[33] Conway, T. The Entner-Doudoroff pathway: history, physiology and molecular biology. *FEMS Microbiol. Rev.* **1992**, *9*, 1-27.

[34] (a) Henderson, D. P.; Cotterill, I. C.; Shelton, M. C.; Toone, E. J. 2-Keto-3-deoxy-6-phosphogalactonate aldolase as a catalyst for seteroscontrolled carbon-carbon bond formation. *J. Org. Chem.* **1998**, *63*, 906-907. (b) Cotterill, I. C.; Henderson, D. P.; Shelton, M. C.; Toone, E. J. The synthetic utility of KDPGal aldolase. *J. Mol. Catal. B: Enzym.* **1998**, *5*, 103-111.

[35] Allen, S. T.; Heintzelman, G. R.; Toone, E. J. Pyruvate aldolase as reagents for steterospecific aldol condensation. *J. Org. Chem.* **1992**, *57*, 426-427.

[36] (a) Knappmann, B. R.; Steigel, A.; Kula, M.-R. Investigation of 2-keto-3-deoxy-6-phosphogluconate aldolases from *Zymomonas mobilis* as a catalyst in organic synthesis. *Biotechnol. Appl. Biochem.* **1995**, *22*, 107-120. (b) Shelton, M. C.; Cotterill, I. C.; Novak, S. T. A.; Poonawala, R. M.; Sudarshan, S.; Toone, E. J. 2-Keto-3-deoxy-6-phosphogluconate aldolases as catalysts for stereocontrolled carbon-carbon bond formation. *J. Am. Chem. Soc.* **1996**, *118*, 2117-2125.

[37] Allard, J.; Grochulski, P.; Sygusch, J. Covalent intermediate trapped in 2-keto-3-deoxy-6-phosphogluconate (KDPG) aldolase structure at 1.95 Å resolution. *Proc. Natl. Acad. Sci. USA* **2001**, *98*, 3679-3684.

[38] Babbitt, P. C.; Mrachko, G. T.; Hasson, M. S.; Huisman, G. W.; Kolter, R.; Ringe, D.; Petsko, G. A.; Kenyon, G. L.; Gerlt, J. A. A functionally diverse enzyme superfamily that abstracts the α protons of carboxylic acids. *Science* **1995**, *267*, 1159-1161.

[39] Meloche, H. P.; O'Connell, E. L. 2-Keto-3-deoxygalactonate-6-phosphate aldolase from *Pseudomonas saccharophila. Methods Enzymol.* **1982**, *90*, 263-269.

[40] Zurawski, G.; Gunsalus, R. P.; Brown, K. D.; Yanofsky, C. Structure and regulation of *aroH*, the structural gene for the tryptophan-repressible 3-deoxy-D-*arabino*-heptulosonic acid-7-phosphate synthetase of *Escherichia coli. J. Mol. Biol.* **1981**, *145*, 47-73.

[41] Frost, J. W.; Bender, J. L.; Kadonaga, J. T.; Knowles, J. R. Dehydroquinate synthase from *Escherichia coli*: purification, cloning, and construction of overproducers of the enzyme. *Biochemistry* **1984**, *23*, 4470-4475.

[42] (a) Duncan, K.; Chaudhuri, S.; Campbell, M. S.; Coggins, J. R. The overexpression and complete amino acid sequence of *Escherichia coli* 3-dehydroquinase. *Biochem. J.* **1986**, *238*, 475-483. (b) Chaudhuri, S.; Duncan, K.; Coggins, J. R. 3-Dehydroquinate dehydratase from *Escherichia coli. Methods Enzymol.* **1987**, *142*, 320-324.

[43] Snell, K. D.; Draths, K. M.; Frost, J. W. Synthetic modification of the *Escherichia coli* chromosome: enhancing the biocatalytic conversion of glucose into aromatic chemicals. *J. Am. Chem. Soc.* **1996**, *118*, 5605-5614.

[44] (a) Hamilton, C. M.; Aldea, M.; Washburn, B. K.; Babitzke, P.; Kushner, S. R. New method for genration of deletions and gene replacements in *Escherichia coli. J. Bacteriol.* **1989**, *171*, 4617-4622. (b) Ohya, K.; Beall, D. S.; Mejia, J. P. Shanmugam K. T.; Ingram L. O. Genetic improvement of *Escherichia coli* for ethanol production: Chromosoaml intergration of *Zymomonas mobilis* genes encoding pyruvate decarboxylase and ethanol dehydrogenase II. *Appl. Environ. Microbiol.* **1991**, *57*, 893-900.

[45] Cosloy, S. D. L-Serine-sensitive mutants of *Escherichia coli* K-12. *J. Bacteriol.* **1970**, *103*, 840-841.

[46] *E. coli* CB734 was obtained from Professor Ronald Bauerle (University of Virginia).

[47] (a) Draths, K. M.; Frost, J. W. Environmentally compatible synthesis of catechol from D-glucose. *J. Am. Chem. Soc.* **1995**, *117*, 2395-2400. (b) Parke, D. Application of *p*-toluidine in chromogenic detection of catechol and protocatechuate, diphenolic intermediates in catabolism of aromatic compounds. *Appl. Environ. Microbiol.* **1992**, *58*, 2694.

[48] Li, K.; Frost, J. W. Synthesis of vanillin from D-glucose. *J. Am. Chem. Soc.* **1998**, *120*, 10545-10546.

[49] Amann, E.; Ochs, B.; Abel, K.-J. Tightly regulated *tac* promoter vectors useful for the expression of unfused and fused proteins in *Escherichia coli*. *Gene* **1988**, *69*, 301-315.

[50] Crameri, A.; Raillard, S-A.; Bermudez, E.; Stemmer, W. P. C. DNA shuffling of a family of genes from diverse species accelerates directed evolution. *Nature* **1998**, *391*, 288-291.

[51] Kurn, N.; Contereras, I.; Shapiro; L. Galactose catabolism in *Caulobacter cresentus*. *J. Bacterial.* **1978**, *135*, 517-520.

[52] Wong, T. Y. Yao, X. The DeLey-Doudoroff pathway of galactose metabolism in *Azotobacter vinelandii*. *Appl. Environ. Microbiol.* **1994**, *60*, 2065-2068.

[53] Arias, A.; Cervenansky, C. Galactose metabolism in *Rhizobium meliloti* L5-30. *J. Bacteriol.* **1986**, *167*, 1092-1094.

[54] Stouthammer, A. H. Glucose and galactose metabolism in *Gluconobacter liquefaciens*. *Biochim. Biophys. Acta* **1961**, *48*, 484-500.

[55] Szumilo, T. Pathway for D-galactonate catabolism in nonpathogenic *Mycobacteria*. *J. Bacteriol.* **1981**, *148*, 368-370.

[56] Nierman, W. C.; Feldblyum, T. V.; Paulsen, I. T.; Nelson, K. E.; Eisen, J.; Heidelberg, J. F.; Alley, M.; Ohta, N.; Maddock, J. R.; Potocka, I.; Nelson, W. C.; Newton, A.; Stephens, C.; Phadke, N. D.; Ely, B.; Laub, M. T.; DeBoy, R. T.; Dodson, R. J.; Durkin, A. S.; Gwinn, M. L.; Haft, D. H.; Kolonay, J. F.; Smit, J.; Craven, M.; Khouri, H.; Shetty, J.; Berry, K.; Utterback, T.; Tran, K.; Wolf, A.; Vamathevan, J.; Ermolaeva, M.; White, O.; Salzberg, S. L.; Shapiro, L.; Venter, J. C.; Fraser, C. M. Complete genome sequence of *Caulobacter crescentus*. *Proc. Natl. Acad. Sci. USA* **2001**, *98*, 4136-4141.

[57] (a) Pearson, W. R.; Lipman, D. J. Improved tools for biological sequence comparison.

Proc. Natl Acad. Sci. USA **1988**, *85*, 2444-2448. (b) Pearson, W. R. Rapid and sensitive sequence comparison with FASTP and FASTA. *Methods Enzymol.* **1990**, *83*, 63-98.

[58] http://workbench.sdsc.edu.

[59] Schmidt-Dannert, C. Directed evolution of single proteins, metabolic pathways, and viruses. *Biochemistry* **2001**, *40*, 13125-13136.

[60] Benach, J.; Lee, I.; Edstrom, W.; Kuzin, A. P.; Chiang, Y.; Acton, T. B.; Montelione, G. T.; Hunt, J. F. The 2.3-A crystal structure of the shikimate 5-dehydrogenase orthologue YdiB from *Escherichia coli* suggests a novel catalytic environment for an NAD-dependent dehydrogenase. *J. Biol. Chem.* **2003**, *278*, 19176-19182.

[61] (a) Clark, A.; Sandler, S. J. Homologous genetic recombination: the pieces begin to fall into place. *Crit. Rev. Microbiol.* **1994**, *20*, 125-142. (b) Winans, S. C.; Elledge, S. J.; Krueger, J. H.; Walker, G. C. Site-directed insertion and deletion mutagenesis with cloned fragments in *Escherichia coli*. *J. Bacteriol.* **1985**, *161*, 1219-1221.

[62] (a) Amundsen, S. K.; Taylor, A. F.; Chaudhury, A. M.; Smith, G. R. *recD*: the gene for an essential third subunit of exonuclease V. *Proc. Natl. Acad. Sci. USA* **1986**, *83*, 5558-5562. (b) Biek, D. P.; Cohen, S. N. Identification and characterization of *recD*, a gene affecting plasmid maintenance and recombination in *Escherichia coli*. *J. Bacteriol.* **1986**, *167*, 594-601.

[63] Datsenko, K. A.; Wanner, B. L. One-step inactivation of chromosomal genes in *Escherichia coli* K-12 using PCR products. *Proc. Natl. Acad. Sci. USA* **2000**, *97*, 6640-6645.

[64] Horii, Z. I.; Clark, A. J. Genetic analysis of the *recF* pathway to genetic recombination in *Escherichia coli* K-12: isolation and characterization of mutants. *J. Mol. Biol.* **1973**, *80*, 327-344.

[65] (a) Brosius, J.; Erfle, M.; Storella, J. Spacing of the –10 and –35 regions in the *tac* promoter. *J. Biol. Chem.* **1985**, *260*. 3539-3541. (b) Russel, D. R.; Bennett, G. N. Construction and analysis of *in vivo* activity of *E. coli* promoter hybrids and promoter mutants that alter the –35 and –10 spacing. *Gene* **1982**, *20*, 231-243.

[66] Mulligan, M. E.; Brosius, J. Clure, W. R. Characterization in vitro of the effect of spacer length on the activity of *Escherichia coli* RNA polymerase at the *tac* promoter. *J. Biol. Chem.* **1985**, *260*, 3529-3538.

[67] Zha, W; Zhu, T; Zhao, H. Family shuffling with single-stranded DNA. *Methods Mol. Biol.* **2003**, *231*, 91-97.

[68] Ramilo, C. A.; Evans, J. N. S. Overexpression, purification, and characterization of tyrosine-sensitive 3-deoxy-D-*arabino*-heptulosonic acid 7-phosphate synthase from *Escherichia coli*. *Protein Expres. Purif.* **1997**, *9*, 253-261.

[69] Sheflyan, G. Y.; Howe, D. L.; Wilson, T. L.; Woodard, R. W. Enzymatic synthesis of 3-deoxy-D-*manno*-octulosonate 8-phosphate, 3-deoxy-D-*altro*-octulosonate 8-phosphate, 3,5-dideoxy-D-*gluco*(*manno*)-octulosonate 8-phosphate by 3-deoxy-D-*arabino*-heptulosonate 7-phosphate synthase. *J. Am. Chem. Soc.* **1998**, *120*, 11027-11032.

[70] Akowski, J. P.; Bauerle, R. Steady-state kinetics and inhibitor binding of 3-deoxy-D-*arabino*-heptulosonate-7-phosphate synthase (tryptophan sensitive) from *Escherichia coli*. *Biochemistry* **1997**, *36*, 15817-15822.

[71] (a) Huang, J. K.; Warshel, A. Why ion pair reversal by protein engineering is unlikely to succeed. *Nature* **1988**, *334*, 270-272. (b) Yano, T.; Oue, S.; Kagamiyama, H. Directed evolution of an aspartate aminotransferase with new substrate specificities. *Proc. Natl. Acad. Sci. USA* **1998**, *95*, 5511-5515.

[72] (a) Sieber, V.; Martinez C. A.;, Arnold F. H. Libraries of hybrid proteins from distantly related sequences. *Nat. Biotechnol.* **2001**, *19*, 456-460. (b) Short, J. M. Diversa Corporation. Synthetic ligation assembly in directed evolution. US Patent 6,605,449 B1, 2003.

[73] Frost, J. W. Unpublished result.

CHAPTER FIVE

Experimental

General chemistry

All reactions sensitive to air and moisture were carried out in oven and/or flame dried glassware under positive argon pressure. Air or moisture sensitive reagents and solvents were transferred to reaction flasks fitted with rubber septa via syringes or cannula. Solvents were removed using either a Büchi rotary evaporator at water aspirator pressure or under high vacuum. Hydrogenations were performed on a Parr hydrogenation apparatus under 50 psi of hydrogen at room temperature.

Reagents and solvents

CH_2Cl_2 and benzene were distilled from calcium hydride under nitrogen. CH_3OH was distilled from sodium metal under argon and stored over Linde 4 Å molecular sieves under argon. THF and diethyl ether were distilled under nitrogen from sodium benzophenone ketyl. DMF, DMSO, hexanes and acetone were dried over activated Linde 4 Å molecular sieves under nitrogen. Water was glass distilled and deionized. All reagents and solvents were used as available from commercial sources or purified according to published procedures. Organic solutions of products were dried over anhydrous $MgSO_4$.

Chromatography

Radial chromatography was carried out on a Harrison Associates Chromatotron using 1, 2 or 4 mm layers of silica gel 60 PF_{254} containing gypsum (E. Merck). Silica gel 60 (40-63 μm, E. Merck or Spectrum Chemicals) was used for flash chromatography. Analytical thin-layer chromatography (TLC) utilized precoated plates of silica gel K6F 60A (0.25 mm, Whatman). TLC plates were visualized by immersion in anisaldehyde stain (by volume: 93% ethanol, 3.5% sulfuric acid, 1% acetic acid and 2.5% anisaldehyde) or phosphomolybdic acid stain (7% 12-molybdophosphoric acid in ethanol, w/v) followed by heating.

Spectroscopic and analytical measurements

^1H NMR and ^{13}C NMR spectra were recorded on a Varian VX-300 FT-NMR spectrometer or a Varian VXR-500 FT-NMR spectrometer. Chemical shifts for ^1H NMR spectra were reported in parts per million (ppm) relative to internal tetramethylsilane (Me_4Si, δ = 0.0 ppm) with $CDCl_3$ as the solvent and to internal sodium 3-(trimethylsilyl) propionate-*2,2,3,3-d*$_4$ (TSP, δ 0.0 ppm) when D_2O was the solvent. The following abbreviations are used to describe spin multiplicity: s (singlet), d (doublet), m (unresolved multiplet), dd (doublet of doublets), b (broad). ^{13}C NMR spectra were recorded at 75 MHz on a Varian VX-300 FT-NMR spectrometer or at 125 MHz on a Varian VXR-500 FT-NMR spectrometer. Chemical shifts for ^{13}C NMR spectra were reported (in parts per million) relative to $CDCl_3$ ($CDCl_3$, δ 77.0 ppm) in $CDCl_3$ and to internal standard acetonitrile (CH_3CN, δ 3.69 ppm) or CD_3OD (δ 49.00 ppm) in D_2O. High-resolution fast atom bombardment (FAB) mass spectra for characterization of

synthetic compounds were obtained on a double-focusing Kratos MS50 mass spectrometer at the University of South Carolina. Glycerol was used as the matrix. Fast atom bombardment (FAB(-)) mass spectroscopy for measuring ^{18}O levels in gallic acid reported in Chapter 3 was performed on a JEOL JMS-HX110 mass spectrometer at Michigan State University, and employed glycerol as matrix. Elemental analysis were performed by Atlantic Microlab Inc. (Norcross, GA). UV and visible spectra were recorded on a Perkin-Elmer Lambda 3B spectrometer or a Hewlett Packard 8452A diode array spectrometer.

Microbial strains and plasmids

Plasmid constructions were carried out in *E. coli* DH5α.

Table 21. Microbial strains and plasmids.

strain	characteristics	source
DH5α	*F' φ80lacZΔM15 Δ(lacZYA-argF)U169 deoR recA1 endA1 hsdR17(r_k^-, m_k^+) phoA λ⁻ supE44 thi-1 gyrA96 relA1*	Invitrogen
AB2834	*tsx-352 glnV42 aroE353 malT352 LAM-*	CGSC[1]
AB2848	*tsx-356 glnV42 aroD352 LAM-*	CGSC[1]
QP1.1	AB2848 *serA::aroB*	lab[2]
IT1168	W3110 *ptsG::Tn5*	Kimata[3]
TP2811	*F' xyl argH1 ΔlacX74 aroB ilv4 Δ(ptsH, ptsI, crr)::Kan^R*	Levy[4]
AB3248	*F' aroF363 aroG365 aroH367 proA2 argE3 ilv-7 his-4 lac gal-2 tsx-358 thi*	Zurawski[5]
KL3	AB2834 *serA::aroB*	lab[6]
CB734	C600 *leu thi1 Δ(gal-aroG-nadA)5 0 aroF::cat (Cm^R) ΔaroH::Kan^R recA1*	Bauerle
KL7	AB2834 *serA::aroBaroZ*	lab[7]
JC7623	AB1157 *recC22 recB21 sbcB15 sbcC201*	CGSC[8]
QP1.1*pts*	QP1.1 Δ*ptsHptsIcrr::Kan^R*	Chapter 2
QP1.1*ptsG*	QP1.1 *ptsG::Tn5*	Chapter 2
NR1	AB3248 *serA::aroB*	Chapter 4
NR7	KL3 *aroF::Cm^R aroG::Tc^R aroH::Kan^R*	Chapter 4

plasmid	characteristics	Reference/source
pKD12.112	Ap^R, *aroF*^{FBR}, $P_{tac}P_{aroE}$*aroE*	lab[2]
pKD12.138	Ap^R, *aroF*^{FBR}, *tktA*, $P_{tac}P_{aroE}$*aroE*	lab[9]
pKD15.071	*ppsA*, *aroF*^{FBR}, *tktA*, $P_{tac}P_{aroE}$*aroE*, *serA*	lab
pLZ1.169	Ap^R, *aroF*^{FBR}, P_{tac}*aroE*, *serA*	lab
pKL1.87A	Cm^R, *ppsA*	lab
pSC6.090	*aroF*^{FBR}, $P_{tac}P_{aroE}$*aroE*, *serA*, *tktA*, P_{tac}*glfglk* in pSU18	lab[10]
pKL4.33	Cm^R, *aroF*^{FBR}, *serA* in pSU18	lab[6]
pSU18	Cm^R, P_{lac}*lacZ'*, p15A replicon	Bartolome[11]
pMF51A	Ap^R, *tktA* in pBR325	Farabaugh[12]
pCR2.1-TOPO	Ap^R, Kan^R	Invitrogen
pJF118EH	Ap^R, *lacI*^{Q} in pKK223-3	Fürste[13]
pTrc99A	Ap^R, *lacI*^{Q} in pKK233-2	Amann[14]
pMAK705	Cm^R, *lacZ'*, *ts*-pSC101 replicon	Hamilton[15]
pKL3.82A	*serA::aroB* in pMAK705	lab
p34H	Ap^R	Tsang[16]
pJB14	Ap^R, *aroB* in pKK223-3	Frost[17]
pKD201	*aroD*	Duncan[18]
pKD46	Ap^R, *araC*, $P_{araB}\gamma$, β, *exo*, *ts*-pA101 replicon	CGSC[19]
pRC1.55B	*serA* in pSU18	lab
pSK6.76	Cm^R, P_{tac}*pobA**, *aroZ*, *serA*	lab
pQE30	Ap^R	Qiagen
pGEX-4T-1	Ap^R, *lacI*^{Q}	Amersham
pSK4.203	*serA*, *tktA* in pSU18	lab
pNR4.230	Ap^R, *aroF*^{FBR}, P_{tac}*aroE*, *serA*, *tktA*	Chapter 2
pNR4.272	*ppsA*, *aroF*^{FBR}, P_{tac}*aroE*, *serA*, *tktA*,	Chapter 2
pNR4.276	*ppsA*, P_{tac}*aroE*, *serA*, *tktA*,	Chapter 2
pNR5.223	*ECdgoA* (*wt E. coli*) in pCR2.1	Chapter 4
pNR6.106	*ECdgoA*, *tktA* in pCR2.1	Chapter 4
pNR7.088	*ECdgoA* in pTrc99A	Chapter 4
pNR6.252	*KPdgoA* (*wt K. pneumoniae*) in pJF118EH	Chapter 4
pNR7.120	*STdgoA* (*wt S. typhimurium*) in pJf118EH	Chapter 4
pNR6.300	*ATdgoA* (*wt A. tumefaciens*) in pJF118EH	Chapter 4
pNR7.063	*CCdgoA* (*wt C. cresentus*) in pJF118EH	Chapter 4
pNR7.118	*ECdgoA* (*wt E. coli*) in pJF118EH	Chapter 4
pNR7.126	*aroF*^{FBR} in pJF118EH	Chapter 4
pNR7.288	*aroF::Cm*^{R}, *aroE*, *serA*	Chapter 4
pNR7.260	*aroG* in pSU18	Chapter 4
pNR7.297	*aroG::Tc*^{R} in pSU18	Chapter 4
pNR7.289A	*aroH* in pCR2.1	Chapter 4
pNR7.289B	*aroH* in pTrc99A	Chapter 4
pNR7.290	*aroH::Kan*^{R} in pTrc99A	Chapter 4
pKP03-3serA	P_{tac}*KP03-3*, *serA*	Chapter 4
pNR8.074	P_{tac}*KPdgoA*, *serA*	Chapter 4
pNR8.172	P_{tac}*EC03-1*, *serA*	Chapter 4

pNR8.170	P_{tac}*ECdgoA, serA*	Chapter 4
pST04-5serA	P_{tac}*ST04-5, serA*	Chapter 4
pNR8.121	P_{tac}*STdgoA, serA*	Chapter 4
pNR8.075	P_{trc}*ECdgoA, serA*	Chapter 4
pNR8.158	P_{trc}*EC03-1, serA*	Chapter 4
pNR8.165-2serA	P_{tac}*NR8.165-2, serA*	Chapter 4
pNR8.165-4serA	P_{tac}*NR8.165-4, serA*	Chapter 4
pNR8.180	P_{tac}*NR8.165-4, serA, tktA*	Chapter 4
pNR8.182	P_{tac}*aroF*^{FBR}, *serA*	Chapter 4
pNR8.146	*serAtktA* in p34e	Chapter 4
pNR8.187	*NR8.165-4* in pQE30	Chapter 4
pNR8.189	P_{T5}*NR8.165-4*	Chapter 4
pNR8.190	P_{T5}*NR8.165-4, serA, tktA*	Chapter 4

Storage of microbial strains and plasmids

All bacterial strains were stored at -78 °C in glycerol. Plasmids were transformed into DH5α for long-term storage. Glycerol samples were prepared by adding 0.75 mL of an overnight culture to a sterile vial containing 0.25 mL of 80% (v/v) glycerol. The solution was mixed, left at room temperature for 2 h, and then stored at -78 °C.

Culture medium

All solutions were prepared in distilled, deionized water. LB medium[20] (1 L) contained Bacto tryptone (10 g), Bacto yeast extract (5 g), and NaCl (10 g). L-Broth[20] (1 L) contained Bacto tryptone (10 g), Bacto yeast extract (5 g), NaCl (5 g), glucose (1 g) and $CaCl_2$ (2.5 mM). Soft agar (100 mL) contained Bacto tryptone (1 g), Difco agar (0.55 g), and NaCl (0.5 g). TB medium (1 L) contained tryptone (10 g) and NaCl (5 g). After autoclaving and directly before use, $MgSO_4$ (10 mL of 1 M stock) was added to the TB medium. M9 salts[20] (1 L) contained Na_2HPO_4 (6 g), KH_2PO_4 (3 g), NH_4Cl (1 g), and NaCl (0.5 g). M9 medium contained D-glucose (10 g), $MgSO_4$ (0.12 g), and thiamine (0.001 g) in 1 L of M9 salts. M63 medium (1 L) contained KH_2PO_4 (13.6 g), $(NH_4)_2SO_4$

(2 g), $FeSO_4 \cdot 7\ H_2O$ (0.0005 g), glucose (2 g), $MgSO_4$ (0.12 g) and thiamine (0.001 g). The pH of M63 inorganic salts was adjusted to 7.0 with 1 N KOH before autoclaving. SOC medium (1 L) contained Bacto tryptone (20 g), Bacto yeast extract (5 g), NaCl (10 mL, 1 M), KCl (2.5 mL, 1 M), $MgCl_2$ (10 mL, 1 M), $MgSO_4$ (10 mL, 1 M) and glucose (10 mL, 2 M). 2×YT medium (1 L) contained Bacto tryptone (16 g), yeast extract (10 g) and NaCl (5 g). Solutions of inorganic salts, magnesium salts, and carbon sources were autoclaved separately and then mixed at room temperature. Medium E[21] (1 L) contained $MgSO_4 \cdot H_2O$ (0.2 g), citric acid (2 g), K_2HPO_4 (10 g) and $NaNH_4HPO_4 \cdot H_2O$ (3.5 g). X-Gal indicator plates[22] contained glucose (4 g), lactose (4 g), X-gal (5-bromo-4-chloro-3-indolyl-β-D-galactopyranoside) (1 mL, 3 mg/mL in EtOH:H_2O, 1:1, v/v) in medium E (1 L) with 1.5% (w/v) Difco agar.

Antibiotics were added where appropriate to the following final concentrations unless noted otherwise: chloramphenicol, 20 μg/mL; ampicillin, 50 μg/mL; kanamycin, 50 μg/mL; tetracycline, 12.5 μg/mL; and fosfomycin, 20 μg/mL. Stock solutions of antibiotics were prepared in water with the exceptions of chloramphenicol, which was prepared in 95% ethanol, and tetracycline, which was prepared in 50% aqueous ethanol. L-Phenylalanine, L-tyrosine, L-tryptophan, and L-serine were added to M9 medium where indicated to a final concentration of 0.04 g/L. Aromatic vitamins potassium *p*-aminobenzoate, 2,3-dihydroxybenzoic acid and *p*-hydroxybenzoic acid (0.01 g) were added to a final concentration of 0.01 g/L. Antibiotics, isopropyl β-D-thioglucopyranoside (IPTG), thiamine, and amino acid supplementations were sterilized through 0.22-μm membranes prior to addition to M9 medium. Solid medium was prepared by addition of 1.5% (w/v) Difco agar to the medium.

Fermentation medium (1 L) contained K_2HPO_4 (7.5 g), ammonium iron (III) citrate (0.3 g), citric acid monohydrate (2.1 g), L-phenylalanine (0.7 g), L-tyrosine (0.7 g), and L-tryptophan (0.35 g), and concentrated H_2SO_4 (1.2 mL). The culture medium was adjusted to pH 7.0 by addition of concentrated NH_4OH before autoclaving. The following supplemens were added immediately prior to initiation of the fermentation: glucose (19 to 22 g under glucose-limited conditions or 20 to 24 g under glucose-rich conditions), $MgSO_4$ (0.24 g), aromatic vitamins potassium *p*-aminobenzoate (0.01 g), 2,3-dihydroxybenzoic acid (0.01 g), and *p*-hydroxybenzoic acid (0.01 g), and trace minerals $(NH_4)_6(Mo_7O_{24})\cdot 4\ H_2O$ (0.0037 g), $ZnSO_4\cdot 7\ H_2O$ (0.0029 g), H_3BO_3 (0.0247 g), $CuSO_4\cdot 5\ H_2O$ (0.0025 g), and $MnCl_2\cdot 4\ H_2O$ (0.0158 g). Solutions of D-glucose and $MgSO_4$ were autoclaved separately. Aromatic vitamins and trace minerals were sterilized through 0.22-μm membranes prior to addition to the medium.

Fed-batch fermentation (general)

Fermentations were conducted in a B. Braun M2 culture vessel with a 2 L working capacity. Environmental conditions were supplied by a B. Braun Biostat MD controlled by a DCU-1. Data was acquired on a Dell Optiplex Gs+ 5166M personal computer using B. Braun MFCS/Win software. PID control loops were used to control temperature, pH, and glucose addition. The temperature was maintained at 33 °C or 36 °C as indicated and the pH was maintained at 7.0 by addition of NH_4OH and 2 N H_2SO_4. Glucose was added as a 60% (w/v) solution. Dissolved oxygen (D.O.) was monitored using a Mettler-Toledo 12 mm sterilizable O_2 sensor fitted with an Ingold A-type O_2 permeable membrane. D.O. was maintained at 10% air saturation throughout the course

of the fermentations unless otherwise specified. Antifoam (Sigma 204) was manually pumped into the vessel as needed.

Inoculants were prepared by introduction of a single colony into 5 mL of M9 medium. The culture was grown at 37 °C with agitation at 250 rpm until they were turbid (~18-30 h) and subsequently transferred to 100 mL of M9 medium. Cultures were grown at 37 °C for an additional 12 h. The inoculant (OD_{600} = 1.5-3.0) was then transferred into the fermentor vessel and the batch fermentation was initiated (t = 0 h).

Glucose-limited, fermentor-controlled conditions

The initial glucose concentration in the fermentation medium was 18 to 24 g/L, depending on the strain being examined. Three staged methods were used to maintain D.O. levels at either 10% or 20% air saturation. With the airflow at an initial setting of 0.06 L/L/min, D.O. concentration was maintained by increasing the impeller speed from its initial set point of 50 rpm to a preset maximum of 940 rpm. With the impeller rate constant at 940 rpm, the mass flow controller then maintained D.O. levels by increasing the airflow rate from 0.06 L/L/min to a preset maximum of 1.0 L/L/min. After the preset maxima of 940 rpm and 1.0 L/L/min of airflow were reached, the third stage of the fermentation was initiated in which the D.O. concentration was maintained at 10% or 20% air saturation for the remainder of the run by oxygen sensor-controlled glucose feeding. At the beginning of this stage, the D.O. concentration initially fell below 20% air saturation due to residual initial glucose in the medium. This lasted for up to 30 min before glucose (65% w/v) feeding commenced. The glucose feed PID control parameters were set to 0.0 s (off) for the derivative control (τ_D) and 999.9 s (minimum control action)

for the integral control (τ_I). X_P was set to 950% to achieve a K_c of 0.1. Isopropyl β-D-thiogalactopyranoside (IPTG) was added at concentrations specified every six hours beginning at the third phase of growth.

Glucose-rich, fermentor-controlled conditions

The initial glucose concentration in the fermentation medium was in the range of 20 to 30 g/L. Three staged methods were used to maintain D.O. levels at 20% air saturation during the course of the fermentations. With the airflow at an initial setting of 0.06 L/L/min, D.O. concentration was maintained by increasing the impeller speed from its initial set point of 50 rpm to a preset maximum of 750 rpm. With the impeller rate constant at 750 rpm, the mass flow controller then maintained D.O. levels by increasing the airflow rate from 0.06 L/L/min to a preset maximum of 1.0 L/L/min. After the preset maxima of 750 rpm and 1.0 L/L/min were reached, the third stage of the fermentation was initiated in which glucose (65% w/v) was added to the vessel at a rate sufficient to maintain a glucose concentration in the range of 5 to 30 g/L for the remainder of the run. Airflow was maintained at 1.0 L/L/min, and the impeller was allowed to vary in order to maintain the D.O. level at 10% or 20% air saturation. The impeller speed typically varied from 750 rpm to 1600 rpm during the remainder of the run. Isopropyl β-D-thiogalactopyranoside (IPTG) was added at concentrations specified every six hours beginning at the third phase of growth.

Analysis of fermentation broth

Samples (5 mL) of fermentation broth were taken at the indicated timed intervals. Cell densities were determined by dilution of fermentation broth with water (1:100) followed by measurement of absorption at 600 nm (OD_{600}). Dry cell weight (g/L) was calculated using a conversion coefficient of 0.43 g/L/OD_{600}. The remaining fermentation broth was centrifuged to obtain cell-free broth.

Glucose concentrations in cell-free broth were measured using the Glucose Diagnostic Kit purchased from Sigma. Solute concentrations in the cell-free broth were quantified by ^{1}H NMR. Solutions were concentrated to dryness under reduced pressure, concentrated to dryness one additional time from D_2O, and then redissolved in D_2O containing a known concentration of the sodium salt of 3-(trimethylsilyl)propionic-*2,2,3,3-d*$_4$ acid (TSP, 10 mM). ^{1}H NMR spectra were recorded and concentrations were determined by comparison of integrals corresponding to each compound with the integral corresponding to TSP (δ = 0.00 ppm). A standard concentration curve was determined for each metabolite using solutions of authentic, purified compounds. The following resonances were used to quantify each compound: quinic acid (δ 4.16, m, 1 H); 3-dehydroshikimic acid (δ 4.28, d, 1 H); 3-dehydroquinic acid (δ 4.38, d, 1 H); 3-deoxy-D-*arabino*-heptulosonic acid (δ 1.81, t, 1 H); gallic acid (δ 7.02, s, 2 H) and acetate (δ 1.92, s, 3 H). The precise concentration of each compound was calculated by application of the following formula: $[\text{compound}]_{\text{actual}}$ = response factor × $[\text{compound}]_{\text{NMR}}$. The following response factors were used for each molecule: quinic acid, 0.75; 3-dehydroshikimic acid, 0.95; 3-dehydroquinic acid, 0.89; 3-deoxy-D-*arabino*-heptulosonic acid, 1.22; gallic acid, 1.36.

Genetic manipulations

Recombinant DNA manipulations generally followed methods described by Sambrook et al.[23] Restriction enzymes were purchased from Invitrogen or New England Biolabs. T4 DNA ligase was obtained from Invitrogen. Fast-Link™ DNA Ligation Kit was obtained from Epicentre. Zymoclean Gel DNA Recovery Kit and DNA Clean & Concentrator Kit was obtained from Zymo Research Company. Maxi and Midi Plasmid Purification Kits were obtained from Qiagen. Calf intestinal alkaline phosphatase was obtained from Boehringer Mannheim. Agarose (electrophoresis grade) was obtained from Invitrogen. Phenol was prepared by addition of 0.1 % (w/v) 8-hydroxyquinoline to distilled, liquefied phenol. Extraction with an equal volume of 1 M Tris-HCl (pH 8.0) two times was followed by extraction with 0.1 M Tris-HCl (pH 8.0) until the pH of the aqueous layer was greater than 7.6. Phenol was stored at 4 °C under an equal volume of 0.1 M Tris-HCl (pH 8.0). SEVAG was a mixture of chloroform and isoamyl alcohol (24:1, v/v). TE buffer contained 10 mM Tris-HCl (pH 8.0) and 1 mM Na_2EDTA (pH 8.0). TAE buffer contained 40 mM Tris-acetate (pH 8.0) and 2 mM Na_2EDTA. Endostop solution (10× concentration) contained 50% glycerol (v/v), 0.1 M Na_2EDTA, pH 7.5, 1% sodium dodecyl sulfate (SDS) (w/v), 0.1% bromophenol blue (w/v), and 0.1% xylene cyanole FF (w/v) and was stored at 4 °C. Prior to use, 0.12 mL of DNase-free RNase was added to 1 mL of 10X Endostop solution. DNase-free RNase (10 mg mL^{-1}) was prepared by dissolving RNase in 10 mM Tris-HCl (pH 7.5) and 15 mM NaCl. DNase activity was inactivated by heating the solution at 100 °C for 15 min. Aliquots were stored at -20 °C. PCR amplifications were carried out as described by Sambrook et

al.[23] Standard reaction (0.1 mL) contained 10 mM KCl, 20 mM Tris-HCl (pH 8.8), 10 mM $(NH_4)_2SO_4$, 2 mM $MgSO_4$, 0.1% Triton X-100, dATP (0.2 mM), dCTP (0.2 mM), dGTP (0.2 mM), dTTP (0.2 mM), template DNA, 0.5 μM of each primer, and 2 units of the *Taq* polymerase. Template concentration varied from 0.02 μg to 1.0 μg.

Large scale purification of plasmid DNA

Plasmid DNA was purified on a large scale using a modified alkaline lysis method described by Sambrook et al.[23] In a 2 L Erlenmeyer flask, 500 mL of LB containing the appropriate antibiotics was inoculated from a single colony, and the culture was incubated in a gyratory shaker at 37 °C for 14 h with agitation at 250 rpm. Cells were harvested by centrifugation (4 000*g*, 5 min, 4 °C) and then resuspended in 10 mL of cold GETL solution (50 mM glucose, 20 mM Tris-HCl (pH 8.0), 10 mM Na_2EDTA, pH 8.0) into which lysozyme (5 mg/mL) had been added immediately before use. The suspension was stored at room temperature for 5 min. Addition of 20 mL of 1% sodium dodecyl sulfate (w/v) in 0.2 N NaOH was followed by gentle mixing and storage on ice for 15 min. Fifteen milliliters of an ice-cold solution containing 3 M KOAc (prepared by combining 60 mL of 5 M potassium acetate, 11.5 mL of glacial acetic acid, and 28.5 mL of H_2O) was added. Vigorous shaking resulted in formation of a white precipitate. After the suspension was stored on ice for 10 min, the cellular debris was removed by centrifugation (48 000*g*, 20 min, 4 °C). The supernatant was transferred to two clean centrifuge bottles and isopropanol (0.6 volumes) was added to precipitate the DNA. After the samples were left at room temperature for 15 min, the DNA was

recovered by centrifugation (20 000*g*, 20 min, 4 °C). The DNA pellet was then rinsed with 70% ethanol and dried.

Further purification of the DNA sample involved precipitation with polyethylene glycol (PEG). The isolated DNA was dissolved in TE (3 mL) and transferred to a Corex tube. Cold 5 M LiCl (3 mL) was added and the solution was gently mixed. The sample was then centrifuged (12 000*g*, 10 min, 4 °C) to remove high molecular weight RNA. The clear supernatant was transferred to a clean Corex tube and isopropanol (6 mL) was added followed by gentle mixing. The precipitated DNA was collected by centrifugation (12 000*g*, 10 min, 4 °C). The DNA was then rinsed with 70% ethanol and dried. After re-dissolving the DNA in 0.5 mL of TE containing 20 μg/mL of RNase, the solution was transferred to a 1.5 mL microcentrifuge tube and stored at room temperature for 30 min. DNA was precipitated from solution upon addition of 500 μL of 1.6 M NaCl containing 13% PEG-8000 (w/v) (Sigma). The solution was mixed and centrifuged (microcentrifuge, 10 min, 4 °C) to recover the precipitated DNA. The supernatant was removed, and the DNA was then re-dissolved in 400 μL of TE. The sample was extracted sequentially with phenol (400 μL), phenol and SEVAG (400 μL each), and finally SEVAG (400 μL). Ammonium acetate (10 M, 100 μL) was added to the aqueous DNA solution. After thorough mixing, 95% ethanol (1 mL) was added to precipitate the DNA. The sample was left at room temperature for 5 min and then centrifuged (microcentrifuge, 5 min, 4 °C). The DNA was rinsed with 70% ethanol, dried, and then redissolved in 200-500 μL of TE.

Alternatively, DNA was purified using a Qiagen Maxi Kit or Midi Kit as described by the manufacturer. The purity of DNA isolated by these kits was adequate for DNA sequencing.

Small scale purification of plasmid DNA

An overnight culture (5 mL) of the plasmid-containing strain was grown in LB containing the appropriate antibiotics. Cells from 3 mL of the culture were collected in a 1.5 mL microcentrifuge tube by centrifugation. The resulting cell pellet was liquefied by vortexing (30 sec) and then resuspended in 0.1 mL of cold GETL solution into which lysozyme (5 mg/mL) had been added immediately before use. The solution was stored on ice for 10 min. Addition of 0.2 mL of 1% sodium dodecyl sulfate (w/v) in 0.2 N NaOH was followed by gentle mixing and storage on ice for 5-10 min. To the sample was added 0.15 mL of cold KOAc solution. The solution was shaken vigorously and stored on ice for 5 min before centrifugation (15 min, 4 °C). The supernatant was transferred to another microcentrifuge tube and extracted with equal volumes of phenol and SEVAG (0.2 mL). The aqueous phase (approximately 0.5 mL) was transferred to a fresh microfuge tube, and DNA was precipitated by the addition of 95% ethanol (1 mL). The sample was left at room temperature for 5 min before centrifugation (15 min, room temperature) to collect the DNA. The DNA pellet was rinsed with 70% ethanol, dried, and redissolved in 50 to 100 μL TE. DNA isolated using this method was used for restriction enzyme analysis, although the concentration of DNA could not be accurately determined by spectroscopic methods.

Restriction enzyme digestion of DNA

Restriction enzyme digests were performed in buffers provided by Invitrogen or New England Biolabs. A typical restriction enzyme digest contained 0.8 μg of DNA in 8 μL of TE, 2 μL of restriction enzyme buffer (10× concentration), 1 μL of bovine serum albumin (0.1 mg/mL), 1 μL of restriction enzyme and 8 μL TE. Reactions were incubated at 37 °C for 1 h, terminated by addition of 2.2 μL of 10X Endostop solution and analyzed by agarose gel electrophoresis. When DNA was required for cloning experiments, the digest was terminated by addition of 1 μL of 0.5 M Na_2EDTA (pH 8.0) or by heating at 70 °C for 15 min followed by extraction of the DNA using Zymoclean gel DNA recovery kit.

Determination of DNA concentration

The concentration of DNA in the sample was determined as follows. An aliquot (10 μL) of the DNA was diluted to 1 mL in TE and the absorbance at 260 nm was measured relative to the absorbance of TE. The DNA concentration was calculated based on the fact that the absorbance at 260 nm of 50 μg/mL of double stranded DNA is 1.0.

Agarose gel electrophoresis

Agarose gel typically contained 0.7% agarose (w/v) in TAE buffer. Ethidium bromide (0.5 μg/ml) was added to the agarose to allow visualization of DNA fragments under a UV lamp. Agarose gel was run in the TAE buffer. The size of the DNA fragments were determined using two sets of DNA molecular weight standards: λ DNA digested with *Hin*dIII (23.1-kb, 9.4-kb, 6.6-kb, 4.4-kb, 2.3-kb, 2.0-kb and 0.6-kb) and λ

DNA digested with *Eco*RI and *Hin*dIII (21.2-kb, 5.1-kb, 5.0-kb, 4.3-kb, 3.5-kb, 2.0-kb, 1.9-kb, 1.6-kb, 1.4-kb, 0.9-kb, 0.8-kb and 0.6-kb).

Isolation of DNA from agarose

The band of agarose containing DNA of interest was excised from the gel while visualized with long wavelength UV light. Two methods were used for isolating DNA from agarose gels. The first method used Zymoclean gel DNA recovery kit to isolate DNA from the agarose gel according to the procedure provided by Zymo Research. Alternatively, the agarose gel containing DNA was chopped thoroughly with a razor and then transferred to a 0.5 mL microfuge tube packed tightly with glass wool and having an 18 gauge hole at the bottom. The tube was centrifuged for 5 min using a Beckman microfuge to extrude the DNA solution from the agarose into a second 1.5 mL microfuge tube. The DNA was precipitated using 3 M NaOAc and 95% ethanol as described previously and subsequently redissolved in TE.

Treatment of DNA with Klenow fragment

DNA fragments with recessed 3' termini were modified to DNA fragments with blunt ends by treatment with the Klenow fragment of *E. coli* DNA polymerase I. After restriction digestion (20 μL) of the DNA (0.8-2 μg) was complete, a solution (1 μL) containing each of the four dNTPs was added to a final concentration of 1 mM for each dNTP. Addition of 1-2 units of Klenow fragment was followed by incubation at room temperature for 20-30 min. Since the Klenow fragment works well in the common restriction enzyme buffers, there was generally no need to purify the DNA after

restriction digestion and prior to filling recessed 3' termini. Klenow reactions were quenched by extraction with equal volumes of phenol and SEVAG. DNA was recovered using the Zymoclean gel DNA recovery kit or by precipitation as described previously and subsequently dissolved in TE.

Treatment of vector DNA with calf intestinal alkaline phosphatase

Following restriction enzyme digestion, plasmid vectors were dephosphorylated to prevent self-ligation. Digested vector DNA was dissolved in TE (88 μL). To this sample was added 10 μL of dephosphorylation buffer (10× concentration) and 2 μL of calf intestinal alkaline phosphatase (2 units). The reaction was incubated at 37 °C for 1-2 h. The phosphatase was inactivated by the addition of 1 μL of 0.5 M Na_2EDTA (pH 8.0) followed by heat treatment (70 °C, 15 min). The sample was extracted with phenol and SEVAG (100 μL each) to remove the protein, and the DNA was purified as previously described and subsequently dissolved in TE.

Ligation of DNA

Molar ratios of insert to vector were typically maintained at 3 to 1 for DNA ligations. A typical reaction contained 0.1 μg of vector DNA and 0.05 to 2.0 μg of insert DNA in a total volume of 7 μL. To this was added 2 μL of T4 ligation buffer (5× concentrations) and 1 μL of T4 DNA ligase (2 units). The reaction was incubated at 16 °C for at least 4 h and then used to transform competent cells.

Alternatively, Fast-Link™ DNA Ligation Kit (Epicentre, Madison, WI) was used for ligation of insert DNA with cohesive or blunt ends into predigested vectors with compatible ends according to the protocol provided by Epicentre.

Preparation and transformation of competent *E. coli* cells

Competent cells were prepared according to a procedure modified from Sambrook et al.[23] LB medium (5 mL) containing antibiotics where appropriate, was inoculated with a single colony from a LB plate containing antibiotics where appropriate. The culture was grown at 37 °C with shaking at 250 rpm for 10-12 h. An aliquot (1 mL) from the culture (5 mL) was used to inoculate LB (100 mL) containing the appropriate antibiotics. The culture was grown at 37 °C with shaking at 250 rpm in a NBS series 25 incubator shaker until the optical density at 600 nm was between 0.4 and 0.6. The culture was transferred to a centrifuge bottle that had been sterilized with a 25 % (v/v) bleach solution and rinsed four times with sterile, deionized water. The cells were harvested by centrifugation (4000 *g*, 5 min, 4 °C) and the culture medium was decanted. All subsequent manipulations were carried out on ice. The harvested cells were resuspended in ice-cold 0.9 % NaCl (100 mL), and the cells were collected by centrifugation (4000 *g*, 5 min, 4 °C). The 0.9 % NaCl solution was decanted, the cells were resuspended in ice-cold 100 mM $CaCl_2$ (50 mL) and stored on ice for 30 min. After centrifugation (4000 *g*, 5 min, 4 °C), the cells were resuspended in 4 mL of ice-cold 100 mM $CaCl_2$ containing 15% glycerol (v/v). Aliquots (0.25 mL) of competent cells were added to 1.5 mL microfuge tubes, immediately frozen in liquid nitrogen, and stored at -78 °C.

Frozen competent cells were thawed on ice for 5 min before transformation. A small aliquot (1 to 10 μL) of plasmid DNA or a ligation reaction was added to the thawed competent cells (0.1 mL). The solution was gently mixed by tapping and stored on ice for 30 min. The cells were then heat shocked at 42 °C for 30 seconds and returned to ice briefly (1 min). LB (0.5 mL, no antibiotics) was added to the cells, and the sample was incubated at 37 °C (no agitation) for 1 h. Cells were collected by centrifugation (30 s) in a microcentrifuge. If the transformation was to be plated onto LB plates, 0.5 mL of the culture supernatant was removed, and the cells were resuspended in the remaining 0.1 mL of LB and subsequently spread onto plates containing the appropriate antibiotics. If the transformation was to be plated onto minimal medium plates, the cells were washed twice with a solution of M9 inorganic salts (0.5 mL). After resuspension in a fresh aliquot of M9 salts (0.1 mL), the cells were spread onto a plate. An aliquot of competent cells with no DNA added was also carried through the transformation protocol as a control. These cells were used to check the viability of the competent cells and to verify the absence of growth on selective medium.

Transformations were also performed by electroporation using electrocompetent cells. An aliquot (1 mL) from an overnight culture (5 mL) was used to inoculate 500 mL of 2×YT containing the appropriate antibiotics. The cells were cultured at 37 °C with shaking at 250 rpm. Once an absorbance of 0.6-0.8 at 600 nm was observed, the cells were kept on ice for 10 min and harvested (3 000*g*, 5 min, 4 °C). The cells were gently washed three times with sterile, cold water (450 mL once and 250 mL twice) and then resuspended in 100 mL sterile, ice-cold aqueous 10% glycerol (v/v). After centrifugation (3 000*g*, 5 min, 4 °C), the cells were resuspended in 1.5 mL sterile ice-cold aqueous 10%

glycerol (v/v). Aliquots (0.1 mL) of electrocompetent cells were dispensed into 1.5 mL microfuge tubes, and immediately frozen in liquid nitrogen and stored at –78 °C.

The electroporation was performed in Bio-Rad Gene Pulser cuvettes with an electrode gap of 0.2 cm. The cuvettes were chilled on ice for 5 min prior to use. Electrocompetent cells were thawed in ice for 5 min, and 40 μL of thawed cells was added to the chilled cuvette. To this was added 1-10 μL of plasmid DNA (1 μg mL^{-1}), and the mixture was gently shaken. The Bio-Rad Gene Pulser was set at 2.5 kvolts, 25 μF and 200 Ohms. The outside surface of the cuvette was wiped clean and it was placed in the sample chamber. A single pulse was applied, the cuvette was removed, and 1 mL of freshly prepared SOC was added into it. The contents of the cuvette were transferred to a 15 mL sterile centrifugation tube. The cells were incubated at 37 °C for 1 h with shaking at 250 rpm. The transformed cells were plated in the same manner as in the transformation with chemically competent cells.

Purification of *E. coli* genomic DNA

Genomic DNA was purified using a method modified from Silhavy et al.[24] A single colony of an *E. coli* strain was inoculated into 100 mL of TB medium (500 mL Erlenmeyer flask). The cells were cultured in a gyratory shaker (37 °C, 250 rpm) for 12 h. Centrifugation (4 000*g*, 5 min, 4 °C) of the culture was followed by resuspension of the cell pellet in 5 mL of buffer (50 mM Tris-HCl, 50 mM Na_2EDTA, pH 8.0) and storage at -20 °C for 20 min to freeze the suspension. To the frozen cells was added 0.5 mL of 0.25 M Tris-HCl (pH 8.0) that contained 5 mg of lysozyme. The suspension was thawed at room temperature in a water bath with gentle mixing and then stored on ice for

45 min. The sample was then transferred to a Corex tube. After addition of 1 mL of STEP solution (25 mM Tris-HCl (pH 7.4), 200 mM Na_2EDTA (pH 8.0), 0.5% SDS (w/v), and proteinase K (1 mg mL^{-1}), prepared just before use), the mixture was incubated at 50 °C for at least 1 h with gentle, periodic mixing. The solution was then divided into two Corex tubes, and the contents of each tube were extracted with phenol (4 mL). The organic and aqueous layers were separated by centrifugation (1 000*g*, 15 min, room temperature), and the aqueous layer was transferred to a fresh Corex tube. All transfers of the aqueous layer were carried out using wide bore pipette tips to minimize shearing of the genomic DNA. The contents of each tube were extracted again with a mixture of phenol (3 mL) and SEVAG (3 mL). Extractions with phenol/SEVAG were repeated (approximately 6 times) until the aqueous layer was clear.

Genomic DNA was precipitated by addition of 0.1 volume of 3 M NaOAc (pH 5.2) followed by gentle mixing and addition of 2 volumes of 95% ethanol. Threads of DNA were spooled onto a sealed Pasteur pipette and transferred to a Corex tube that contained 5 mL of 50 mM Tris-HCl (pH 7.5), 1 mM Na_2EDTA (pH 8.0), and 1 mg of RNase. The mixture was stored at 4 °C overnight to allow the DNA to dissolve completely. The solution was then extracted with SEVAG (5 mL) and centrifuged (1 000 *g*, 15 min, room temperature). The aqueous layer was transferred to a fresh Corex tube and the genomic DNA was precipitated as described above. The threads of DNA were spooled onto a Pasteur pipette and redissolved in 2 mL of 50 mM Tris-HCl (pH 7.5) and 1 mM Na_2EDTA (pH 8.0). Genomic DNA was stored at 4 °C.

Alternatively, genomic DNA was purified using a method described by Pitcher et al..[25] A single colony of an *E. coli* strain was inoculated into 20 mL of LB medium. The

cells were culture in a gyratory shaker (37 °C, 250 rpm) overnight, and were subsequently harvested by centrifugation (1 000*g*, 15 min, room temperature). Cell pellet obtained was resuspended into 100 μL of TE and incubated at 37°C for 30 min. Cells were lysed with 0.5 mL 5 M guanidine thiocyanate, 100 mM EDTA and 0.5% (v/v) sarkosyl (GES reagent), which was prepared as follows. Guanidine thiocyanate (60 g), 0.5 M Na_2EDTA, pH 8.0 (20 mL), and deionized water (20 mL) were heated at 65°C with mixing until dissolved. After cooling, 5 mL of 10% v/v sarkosyl were added, the solution was made up to 100 mL with deionized water, filtered through a 0.22-μm membrane and stored at room temperature.

The cell suspension was vortexed briefly and checked for lysis (clear solution) after 5-10 min. The lysate was cooled on ice, and a cold solution of ammonium acetate (7.5 M, 0.25 mL) was added with mixing on ice for 10 min. To this sample, 0.5 mL SEVAG was added and mixed thoroughly. After centrifugation in a 1.5 mL Eppendorf tube (25 000*g*, 10 min, room temperature), the supernatant was transferred to an Eppendorf tube and 0.54 volumes of cold 2-propanol was added. The tubes were inverted for 1 min to mix the solutions and the fibrous DNA precipitate was collected by centrifugation (6 500*g*, 20 sec, room temperature). DNA pellet was washed five times with 70% ethanol and dried in air at room temperature for 20 min. Finaaly, the genomic DNA was redissolved in 100 μL TE.

P1 phage-mediated transduction

Transduction with P1 phage was carried out using a method modified from Miller.[26] P1 phage lysate was prepared by propagation of phage in the donor strain using

the following procedure. Serial dilutions of P1 phage stock (0.1 mL, 10^{-1} to 10^{-5}) in LB were prepared in sterile test tubes (13 × 100 mm). An aliquot (0.1 mL, approximately 5 × 10^8 cells) of an overnight culture of the donor strain was added to each tube. Sterile, molten soft agar (45 °C) was added to each tube. The contents of each tube were mixed and poured immediately onto a pre-warmed (37 °C) L plate and swirled gently to achieve uniform coverage of the plate. After the agar had solidified, the plates were incubated at 37 °C until confluent lysis had occurred (approximately 8 h). Because the multiplicity of infection is critical to phage generation, confluent lysis occurred on only one or two of the plates. To the plates displaying confluent lysis, L-broth (4 mL) was added, and the plates were then stored overnight at 4 °C to allow the phage particles to diffuse into the broth. The L-broth was collected from the plate and vortexed with several milliliters of $CHCl_3$. The solution was centrifuged (2 000*g*, 5 min, room temperature) to separate the layers. Aqueous phage lysate was stored in 1.5 mL microfuge tubes over several drops of $CHCl_3$ at 4 °C.

Infection of the recipient strain with phage lysate proceeded as follows. An overnight culture (2 mL) of the recipient strain was centrifuged (microfuge, 30 sec, 4 °C) and the growth medium was discarded. The cells were resuspended in 1 mL sterile solution containing of 5 mM $CaCl_2$ and 100 mM $MgSO_4$, and shaken (250 rpm) at 37 °C for 15 min to promote aeration of the cells. In the meantime, 0.1 mL serial dilutions (10^0 to 10^{-3}) of phage lysate in LB were prepared in sterile microfuge tubes. An aliquot (0.1 mL) of aerated recipient cells was added to each of the phage dilutions, the samples were gently mixed. and then incubated at 37 °C for 20 min without shaking. Sodium citrate (1 M, 0.2 mL) was added to each sample, and the cells were harvested (microfuge, 30 s,

room temperature) and resuspended in 0.2 mL of LB containing 100 mM sodium citrate. After incubation at 30 °C for 30 min, cells were again harvested (microfuge, 30 sec, room temperature), resuspended in 0.1 mL of growth medium, and plated out onto appropriate agar plates.

Enzyme assays

After collected and resuspended in the proper resuspension buffer, the cells were disrupted by two passages through a French pressure cell (SLM Aminco) at 16000 psi. Cellular debris was removed from the lysate by centrifugation (48 000*g*, 20 min, 4 °C). Protein was quantified using the Bradford dye-binding procedure.[27] A standard curve was prepared using bovine serum albumin. Protein assay solution was purchased from Bio-Rad and used as described by the manufacture.

DAHP synthase assay

DAHP synthase was assayed according to the procedure described by Schoner et al.[28] Harvested cells were resuspended in 50 mM potassium phosphate (pH 6.5) that contained 10 mM PEP and 0.05 mM $CoCl_2$. The cells were disrupted using a French press as described above. Cellular lysate was diluted in a solution of potassium phosphate (50 mM), PEP (0.5 mM), and 1,3-propanediol (250 mM), pH 7.0. A dilute solution of E4P[29] was first concentrated to 12 mM by rotary evaporation and neutralized with 5 M KOH. Two different solutions were prepared and incubated separately at 37 °C for 5 min. The first solution (1 mL) contained E4P (6 mM), PEP (12 mM), ovalbumin (1 mg/mL), and potassium phosphate (25 mM), pH 7.0. The second solution (0.5 mL)

consisted of the diluted lysate. After the two solutions were mixed (time = 0), aliquots (0.15 mL) were removed at timed intervals and quenched with 0.1 mL of 10% trichloroacetic acid (w/v). Precipitated protein was removed by centrifugation, and the DAHP in each sample was quantified using thiobarbituric acid assay[30] as described below.

An aliquot (0.1 mL) of DAHP containing sample was reacted with 0.1 mL of 0.2 M $NaIO_4$ in 8.2 M H_3PO_4 at 37 °C for 5 min. The reaction was quenched by addition of 0.8 M $NaAsO_2$ in 0.5 M Na_2SO_4 and 0.1 M H_2SO_4 (0.5 mL) and vortexed until a dark brown color disappeared. Upon addition of 3 mL of 0.04 M thiobarbituric acid in 0.5 M Na_2SO_4 (pH 7), the sample was heated at 100 °C for 15 min. Samples were cooled (2 min), and the pink chromophore was then extracted into cyclohexanone (4 mL). The aqueous and organic layers were separated by centrifugation (2 000*g*, 15 min, room temperature). The absorbance of the organic layer was recorded at 549 nm (ε = 68,000 M^{-1} cm^{-1}). One unit of DAHP synthase activity was defined as the formation of 1 μmol of DAHP per min at 37 °C.

Shikimate dehydrogenase assay

Shikimate dehydrogenase was assayed using shikimic acid as the substrate according to the procedure described by Chaudhuri et al.[31] Lysate was prepared and protein concentrations were determined as previously mentioned. Cells were harvested and resuspended as a buffer containing Tris-HCl (100 mM, pH 7.5), Na_2EDTA (1 mM) and diethiothreitol (0.4 mM). Cellular lysate was diluted in 100 mM Tris-HCl (pH 9.0). Assays (1 mL) contained Tris-HCl (100 mM), shikimic acid (4 mM), and β-NADP (2

mM) sodium salt. Tris-HCl, shikimic acid, and diluted lysate solutions were mixed, and the spectrophotometer was zeroed. Addition of β-NADP initiated the assay. The formation of NADPH was monitored at 340 nm (ε = 6,220 M^{-1} cm^{-1}) for 60 seconds. One unit of shikimate dehydrogenase activity was defined as the formation of 1 μmol of NADPH per minute at room temperature.

Phosphoenolpyruvate synthase assay

PEP synthase activity was assayed at 30 °C according to the procedure described by Cooper.[32] The reaction (1 mL) contained 100 mM Tris-HCl (pH 8.0), 10 mM $MgCl_2$, 10 mM ATP, 1.25 mM sodium pyruvate and was initiated by addition of cell-free lysate. Aliquots (100 μL) of reaction mixture were removed at 1 min intervals and immediately added to a microcentrifuge tube containing 0.33 mL of an aqueous 0.1% solution of 2,4-dinitrophenylhydrazine and 0.9 mL H_2O. The resulting mixture was incubated at 30 °C for 10 min. Following addition of 1.67 mL of 10% (w/v) NaOH, the mixture was further incubated at 30 °C for 10 min. The disappearance of pyruvate was quantified by measuring the absorbance at 445 nm (ε = 18,000 M^{-1} cm^{-1}). One unit of PEP synthase activity was defined as the consumption of 1 μmol of pyruvate per min at 30 °C.

KDPGal aldolase assay

KDPGal aldolase activity was determined using a coupled enzyme assay previously described by Cotterill et al.[33] The assay solution (1 mL) contained 20 mM KH_2PO_4 (pH 7.5), 0.35 mM NADH, 1 unit of L-lactic dehydrogenase and appropriately diluted cellular lysate (1:10 to 1:50 dilution in 20 mM KH_2PO_4, pH 7.5). The solution

was mixed and pre-incubated for 2 min at room temperature. The reaction was initiated by addition of chemically synthesized KDPGal (16 μL, 100 mg/mL, Li^+ salt). The absorbance at 340 nm was recorded continuously for 1 min. One unit of KDPGal aldolase catalyzes the loss of one μmol of NADH (ε=6,220 M^{-1} cm^{-1}) per minute at 25°C.

DAHP formation assay

DAHP formation activity was measured by coupling product DAHP forward to 3-dehydroshikimate, the formation of which was monitored at OD_{234}. The reaction (1 mL) contained 50 mM morpholinepropanesulfonic acid (MOPS) buffer (pH 7.5), 1 mM D-erythrose 4-phosphate, 1 mM pyruvate, 50 μM $CoCl_2$, 10 μM NAD, 1 unit of 3-dehydroquinate synthase, 1 unit of 3-dehydroquinate dehydratase and cellular lysate. The reaction was initiated by addition of diluted cellular lysate to the assay solution, and the absorbance at 234 nm was monitored continuously for 5 min. One unit of DAHP fomation activity corresponds the formation of one μmol of 3-dehydroshikimate (ε=1.19×10^4 M^{-1} cm^{-1})[34] per minute at 25°C.

CHAPTER TWO

E. coli* QP1.1*pts

E. coli QP1.1*pts* (QP1.1 Δ*ptsHptsIcrr::Kan*^{R}) was made from *E. coli* QP1.1 by P1 phage-mediated transduction using *E. coli* TP2811[4] as donor strain. Colonies were plated on LB plates containing kanamycin. The resulting colonies were screened for the

following growth characteristics: growth on LB plates containing kanamycin; no growth on M9 glucose plates with aromatic amino acids, aromatic vitamins and L-serine.

E. coli QP1.1*ptsG*

E. coli QP1.1*ptsG* was prepared from *E. coli* QP1.1 by P1 phage-mediated transduction using *E. coli* IT1168[3] as donor strain. Colonies were plated on LB plates containing kanamycin (200 mg/L). The resulting colonies were screened for the following growth characteristics: growth on M9 glucose plates with aromatic amino acids, aromatic vitamins and L-serine; blue colonies on X-Gal plates containing glucose and lactose; no growth on M9 glucose plates with aromatic amino acids, and aromatic vitamins; no growth on M9 glucose plates with L-serine s.

pNR4.230.

This 9.5-kb plasmid was created by inserting a 2.2-kb *tktA*-encoding fragment into plasmid pLZ1.169. Plasmid pLZ1.169[35] is a pSU18–based plasmid that encodes $aroF^{FBR}$, $P_{tac}aroE$, *serA* and Ap^R. The 2.2-kb *tktA*-encoding fragment was excised from plasmid pSK4.203[36] by *Bam*HI digestion. Plasmid pLZ1.169 was partially digested with *Bam*HI and ligated to *tktA* to provide the plasmid pNR4.230. The *tktA* gene is transcribed in the same orientation as *serA*.

pNR4.272.

This 11.5-kb plasmid was constructed by ligation of a 3.0-kb *ppsA* gene into pNR4.230. The *ppsA* locus was isolated from pKL1.87A[37] following *Hin*dIII/*Eco*RI

digestion and treatment with Klenow fragment. Plasmid pNR4.230 was digested with *Nco*I and treated with Klenow fragment and calf intestinal alkaline phosphatase. Subsequent ligation of the *ppsA* insert into the 8.5-kb plasmid afforded plasmid pNR4.272. The *ppsA* gene is transcribed in the opposite direction as *serA*.

pNR4.276.

Plasmid pNR4.276 is identical to pNR4.230 except that pNR4.276 does not contain a functional $aroF^{FBR}$ gene. To inactivate the $aroF^{FBR}$ gene of pNR4.230, advantage was taken of a unique *Bgl*II recognition site located internal to the $aroF^{FBR}$ gene. Plasmid pNR4.230 was digested with *Bgl*II, and the overhanging ends were eliminated by treatment with Klenow fragment. Subsequent ligation of the blunt ends created plasmid pNR4.276 with an inactive $aroF^{FBR}$.

Purification of quinic acid fermentation broth

Cells were removed from fermentation broth by centrifugation (4 200*g*, 30 min). and the supernatant containing quinic acid (62.3 g, 0.324 mol) was refluxed for 1 h. The solution was cooled to room temperature, concentrated sulfuric acid was added to a final pH of 2.5. Centrifugation at 13 700*g* for 10 min removed the precipitated proteins. The supernatant was decolorized by stirring with charcoal (Darco® KB-B, 20 g) at room temperature for 2 h, followed by filtration to remove charcoal. The clarified solution was passed through a Dowex 50WX8-200 (H^+) column at 4°C to afford an aqueous solution of quinic acid (61.2 g, 0.318 mol, 98%).

Synthesis of hydroquinone by hypochlorite oxidation of quinic acid

The solution of quinic acid (61.2 g, 0.318 mol, 1120 mL) was stirred at room temperature and separate solutions of ommercial bleach (Clorox®, 1800 mL) and H_2SO_4 (178 mL, 2 M) were added in a 5 L 3-neck round bottom flask dropwise over a period of 1 h. The mixture was stirred for 2 h after the additions were completed, and then isopropanol (130 mL) was added to quench unreacted HOCl. Without further purification, the resulting solution containing 3(*R*),5(*R*)-trihydroxycyclohexanone (44.7 g, 0.306 mol, 96%) was heated to reflux under an argon atmosphere for 10 h. After cooling to room temperature, hydroquinone was extracted into *t*-butyl methyl ether (4×500 mL) and the combined organic phase was dried over $MgSO_4$. The solution was stirred with charcoal (20 g) for 10 min and filtered through a pad of Celite. The Celite was washed with an additional aliquot of *t*-butyl methyl ether (200 mL). The filtrates were then concentrated in vacuo to obtain hydroquinone as a brown solid (29.4 g, 87%). Sublimation of the isolated material yielded hydroquinone as a white solid in 78% overall yield from quinic acid.

3(*R*),5(*R*)-trihydroxycyclohexanone (10)

To a stirred solution of quinic acid (7.0 g, 36.4 mmol) in 50 mL water at room temperature was added commercial bleach (Clorox®, 155 g) and H_2SO_4 (14.6 mL, 2 mol/L) dropwise. The mixture was stirred for 3 h, and isopropanol (8.4 mL) was then added and stirred for an additional 30 min. The resulting solution was neutralized with 10% aqueous Na_2CO_3 and then lyophilized to dryness. The resulting white powder was

stirred in 200 mL acetone for 1 h, and the solution was filtered through a pad of Celite to remove the inorganic salts and concentrated to dryness. Purification by flash chromatography gave the desired product **10** as a white powder (4.02 g, 76%). ^{1}H NMR (D_2O) δ 4.27-4.31 (m, 1H), 4.15 (ddd, J = 8.2, 8.2, 5.1 Hz, 1H), 3.97 (dd, J = 7.5, 2.7 Hz, 1H), 2.75-2.83 (m, 2H), 2.50-2.65 (m, 2H); ^{13}C NMR (D_2O) δ 215.5, 75.7, 71.4 (C2, C6), 48.4, 48.3. HRMS (FAB^+) calcd. for $C_6H_{11}O_4$ ($M+H^+$) 147.0657, found 147.0653. Anal. calcd. for $C_6H_{10}O_4$: C, 49.31: H, 6.90. Found: C, 49.42; H, 6.91.

4,5-*O*-Isopropylidene-4(*S*),5(*R*)-dihydroxy-2-cyclohexene-1-one (13)

A solution of trihydroxycyclohexanone **10** (3.0 g, 20.5 mmol) and TsOH (40 mg, 0.205 mmol) in dry acetone (50 mL) was stirred vigorously under an argon atmosphere at room temperature for 19 h. Removal of the solvent afforded a yellow oil which was purified by flash chromatography to yield 3,4-*O*-isopropylidene-3(*R*),4(*S*),5(*R*)-trihydroxycyclohexanone as white crystals (3.03 g, 79%). ^{1}H NMR ($CDCl_3$) δ 4.70-4.74 (m, 1H), 4.32 (ddd, J = 7.2, 2.1, 2.1 Hz, 1H), 4.24 (dd, J = 6.3, 2.7 Hz, 1H), 2.82 (dd, J = 17.8, 3.9 Hz, 1H), 2.70-2.72 (m, 1H), 2.65-2.66 (m, 1H), 2.46 (m, 1H), 2.24 (b, 1H), 1.45 (s, 3H), 1.37 (s, 3H); ^{13}C NMR ($CDCl_3$) δ 208.0, 108.8, 74.9, 72.2, 68.2, 41.6, 40.1, 26.4, 23.8. HRMS (FAB^+) calcd. for $C_9H_{15}O_4$ ($M+H^+$) 187.0970, found 187.0970. Anal. calcd. for $C_9H_{14}O_4$: C, 58.05; H, 7.58. Found: C, 58.17; H, 7.58.

To a solution of 3,4-*O*-isopropylidene-3(*R*),4(*S*),5(*R*)-trihydroxycyclohexanone (2.0 g, 10.8 mmol) in CH_2Cl_2 (8 mL) at 0 °C was added 4-(dimethylamino) pyridine (20 mmol), diisopropylethylamine (3.75 mL, 21.5 mmol) and acetic anhydride (1.22 mL, 12.9 mmol). After stirring for 3 h at 0 °C, the reaction was washed with saturated

aqueous $NaHCO_3$ (2×20 mL), and the $NaHCO_3$ solution was extracted with CH_2Cl_2 (4×40 ml). The organic layer was dried over $MgSO_4$ and concentrated to dryness to afford a pale yellow solid. Kugelrohr distillation gave **13** (1.65 g, 91%) as a colorless oil which crystallized as a white solid. ^1H NMR ($CDCl_3$) δ 6.65 (dd, J = 10.2, 3.6 Hz, 1H), 6.04 (d, J = 10.2 Hz, 1H), 4.67-4.75 (m, 2H), 2.93 (dd, J = 17.7, 2.7 Hz, 1H), 2.70 (dd, J = 17.7, 3.9 Hz, 1H), 1.39 (s, 3H), 1.38 (s, 3H); ^{13}C NMR δ 195.3, 145.8, 128.8, 109.9, 73.3, 71.0, 38.7, 27.7, 26.5. HRMS (FAB^+) calcd. for $C_9H_{13}O_3$ ($M+H^+$) 169.0865, found 169.0864. Anal. calcd. for $C_9H_{12}O_4$: C, 64.27; H, 7.19. Found: C, 64.07; H, 7.15.

4(*S*),5(*R*)-dihydroxy-2-cyclohexen-1-one (11)

A solution of compound **13** (0.5 g, 2.98 mmol) in CF_3CO_2H/H_2O (2:1, v/v, 25 mL) was stirred at 0°C for 20 min. The organic solvent was removed in vacuo, and the compound was purified by flash chromatography to give **11** (0.16 g, 43%) as a colorless oil, which crystallized into a white solid. ^1H NMR (D_2O) δ 6.97 (m, 1H), 6.11 (m, 1H), 4.69-4.72 (m, 1H), 4.39-4.41 (m, 1H), 2.82 (ddd, J = 17.0, 3.3, 0.8 Hz, 1H), 2.72 (dd, J = 17.0, 5.0 Hz, 1H); ^{13}C NMR (D_2O) δ 204.4, 154.2, 131.5, 72.4, 70.3, 45.6. HRMS (FAB^+) calcd. for $C_6H_8O_3K$ ($M+K^+$) 167.0111, found 167.0108. Anal. calcd. for $C_6H_8O_3$: C, 56.25; H, 6.29. Found: C, 56.38; H, 6.37.

Butane 2,3-bisacetal-protected 1-(hydroxymethyl)-1(*S*),3(*R*),4(*R*),5(*R*)-tetrahydroxycyclohexane (15)

BBA-protected methyl quinate **14**[38] (4.0 g, 12.5 mmol) was dissolved in dry THF (50 mL) at 0 °C, and $LiAlH_4$ (1.42 g, 37.5 mmol) was added in portions. The mixture

was stirred for 1 h at 0 °C and then warmed to room temperature. After 10 h, all of the starting material was consumed. The resulting mixture was cooled to 0 °C and excess hydride was quenched by successive addition of water (1.4 mL), 15% aqueous NaOH (1.4 mL) and water (4.2 mL). Celite (8.0 g) was added, and the slurry was stirred for 2 h. The alumina salt was separated by vacuum filtration through a pad of Celite, and the Celite was washed with hot ethyl acetate (100 mL). The filtrate was then concentrated to dryness and purified by flash chromatogaphy to afford the desired product **15** as a white solid (3.4 g, 93%). ^{1}H NMR ($CDCl_3$) δ 4.26-4.35 (m, 1H), 4.21-4.22 (m, 1H), 3.55 (dd, J=10.2, 2.7 Hz, 1H), 3.46 (d, J=11.0 Hz, 1H), 3.35 (d, J=11.0 Hz, 1H), 3.27 (s, 3H), 3.25 (s, 3H), 3.13 (b, 1H), 2.44 (b, 1H), 2.24 (m, 1H), 1.93-1.98 (m, 1H), 1.38-1.52 (m, 2H), 1.33 (s, 3H), 1.30 (s, 3H); ^{13}C NMR ($CDCl_3$) δ 100.3, 99.7, 74.1, 73.4, 70.4, 69.5, 62.9, 48.0, 47.9, 37.7, 36.0, 17.9, 17.6. HRMS (FAB^+) calcd. for $C_{13}H_{24}O_7Na$ ($M+Na^+$) 315.1420, found 315.1421. Anal. calcd. for $C_{13}H_{24}O_7$: C, 53.41; H, 8.28. Found: C, 52.93; H, 8.19.

Butane 2,3-bisacetal-protected 3(*R*),5(*R*)-trihydroxycyclohexanone (16)

Triol **15** (2.5 g, 8.56 mmol) was dissolved in 50 mL potassium phosphate buffer (0.5 M, pH 7) and the solution was cooled to 0°C. Sodium periodate (2.74 g, 12.8 mmol) was added in portions. After addition was completed, the mixture was brought to room temperature and stirred for 1 h. The aqueous mixture was then extracted with ethyl acetate (4×50 mL), and the combined organic phase was dried with $MgSO_4$, filtered, and concentrated in vacuo. Compound **16** was obtained as a white powder (1.61 g, 72%). ^{1}H NMR ($CDCl_3$) δ 4.23-4.33 (m, 2H), 3.89 (dd, J = 10.2, 2.4 Hz, 1H), 3.31 (s, 3H), 3.24 (s,

3H), 2.63-2.69 (m, 2H), 2.61 (b, 1H), 2.45-2.54 (m, 2H), 1.35 (s, 3H), 1.31 (s, 3H); ^{13}C NMR ($CDCl_3$) δ 205.5, 100.2, 99.2, 72.2, 67.6, 63.2, 48.1, 47.9, 46.2, 44.7, 17.7, 17.5. HRMS (FAB^+) calcd. for $C_{12}H_{20}O_6Na$ ($M+Na^+$) 283.1158, found 283.1156. Anal. calcd. for $C_{12}H_{20}O_6$: C, 55.37; H, 7.74. Found: C, 55.51; H, 7.63.

4(*R*),5(*R*)-dihydroxy-2-cyclohexen-1-one (12)

To a solution of the β-hydroxy ketone **16** (1.01 g, 3.85 mmol) in CH_2Cl_2 (10 mL) at 0 °C was added 4-(dimethylamino) pyridine (9.4 mg, 0.077 mmol), diisopropylethylene (1.34 mL, 7.7 mmol) and acetic anhydride (0.44 mL, 4.6 mmol). After stirring at 0 °C for 6 h, the solution was washed with saturated aqueous $NaHCO_3$ and the aqueous solution was extracted with CH_2Cl_2 (4×40 mL). The organic phase was dried over anhydrous $MgSO_4$ and concentrated to dryness. Flash chromatography afforded butane 2,3-bisacetal-protected 4(*R*),5(*R*)-dihydroxy-2-cyclohexen-1-one as a white solid (0.94 g, 100%). ^1H NMR ($CDCl_3$) δ 6.87 (dd, J = 10.2, 1.8 Hz, 1H), 6.01 (dd, J = 10.2, 2.4 Hz, 1H), 4.51 (m, 1H), 4.00-4.10 (m, 1H), 3.33 (s, 3H), 3.27 (s, 3H), 2.74 (dd, J = 16.2, 4.7 Hz, 1H), 2.49 (dd, J = 16.2, 13.2 Hz, 1H), 1.37 (s, 3H), 1.34 (s, 3H); ^{13}C NMR ($CDCl_3$) δ 196.8, 148.5, 130.1, 100.8, 99.7, 69.2, 68.0, 48.2, 48.1, 42.0, 17.7, 17.6. HRMS (FAB^+) calcd. for $C_{12}H_{19}O_5$ ($M+H^+$) 243.1232, found 243.1222. Anal. calcd. for $C_{12}H_{18}O_5$: C, 59.49; H, 7.49. Found: C, 59.21; H, 7.49.

The butane 2,3-bisacetal-protected 4(*R*),5(*R*)-dihydroxy-2-cyclohexen-1-one (0.344 g, 1.42 mmol) was stirred in a mixture of trifluoroacetic acid (18 mL) and CH_2Cl_2 (2 mL) for 30 min at 0°C. Solvents were removed in vacuo. The residue was azeotroped with toluene (20 mL) and purified by flash chromatography to yield **12** as a white solid

(0.137 g, 75%). ^{1}H NMR (D_2O) δ 7.04 (dd, J = 10.2, 2.4 Hz, 1H), 6.08 (m, 1H), 4.45 (m, 1H), 3.99-4.07 (m, 1H), 2.82 (ddd, J = 16.4, 4.8, 1.2 Hz, 1H), 2.58 (dd, J = 16.4, 11.9 Hz, 1H); ^{13}C NMR (D_2O) δ 204.8, 156.1, 131.4, 74.4, 74.3, 46.5. HRMS (FAB^+) calcd. for $C_6H_8O_3K$ ($M+K^+$) 167.0111, found 167.0112. Anal. calcd. for $C_6H_8O_3$: C, 56.25; H, 6.29. Found: C, 56.22; H, 6.39.

Oxidation of quinic acid by $Ag_3PO_4/K_2S_2O_8$

To a clarified, decolorized, ammonium ion-free fermentation broth containing quinic acid (0.960 g, 5.00 mmol) was added $K_2S_2O_8$ (1.62 g, 6.00 mmol) and Ag_3PO_4 (0.0481 g, 0.115 mmol). The heterogeneous solution was stirred at 50 °C for 4 h and then refluxed for 8 h under an argon atmosphere. After filtration of the crude reaction solution and extraction with EtOAc (3 × 50 mL), the organic layer was dried and concentrated. Purification of the residue by flash chromatography (1:1 EtOAc/hexane, v/v) gave hydroquinone (0.407 g, 74%) as a white solid. The ^{1}H NMR and ^{13}C NMR spectra were identical with those of authentic hydroquinone.

Oxidation of quinic acid by $(NH_4)_2Ce(SO_4)_3$

Ceric ammonium sulfate (7.15 g, 12.0 mmol) was added over a 30 min period to a clarified, decolorized, ammonium ion-free fermentation broth containing quinic acid (0.960 g, 5.00 mmol) at pH 1.5. The solution was then refluxed for 10 h under an argon atmosphere. After the mixture was cooled to room temperature, the resulting solution was filtered to obtain an aqueous solution of hydroquinone, which was then extracted with EtOAc (3 × 50 mL). The combined organic layers were dried and concentrated to a

brown solid, which was purified by flash chromatography (1:1 EtOAc/hexane, v/v) to afford hydroquinone (0.503 g, 91%) as a white solid. The ^{1}H NMR and ^{13}C NMR spectra were identical with those of authentic hydroquinone.

Oxidation of quinic acid by V_2O_5

To a clarified, decolorized, ammonium ion-free fermentation broth containing quinic acid (0.960 g, 5.00 mmol) at pH 1.5 were added V_2O_5 (1.00 g, 5.50 mmol) and H_2SO_4 (7.5 mmol). The solution was stirred at 50 °C for 4 h and then heated to reflux for 8 h under an argon atmosphere. After extraction of the crude reaction solution with EtOAc (3 × 50 mL), the organic layer was dried and concentrated to dryness. Purification by flash chromatography (1:1 EtOAc/hexane, v/v) afforded hydroquinone (0.466 g, 85%) as a white solid.

CHAPTER THREE

Synthesis of [5-^{18}O]-3-dehydroshikimic acid

Methyl [5-^{18}O]-shikimate (22)

(*1S,5R,6S*)-5-Hydroxy-7-oxibicyclo[4,1,0]hept-3-ene-carboxylic acid methyl ester **21** was prepared from shikimic acid in 80% yield, essentially as previously described.[39] To an epoxide **21** (4.24 g, 25.0 mmol) in 32 mL freshly distilled CH_3CN solution was added ^{18}O-labeled H_2O (97% atom, Aldrich, 1.0 g, 49.9 mmol) and

trifluoromethanesulfonic acid solution (0.221 ml, 2.5 mmol in 2 mL CH_3CN) at 0 °C. The cold solution was stirred for 24 h in an ice bath followed by 24 h at room temperature under an argon atmosphere. The product precipitated as white powder after 24 h. Filtration and evaporation the solvent in vacuum afforded the desired product (1.27 g). The remaining filtrate was concentrated to dryness and further purification by reverse phase HPLC gave product **22** (0.50 g) as white powder. The combined yield is 37% (1.77 g). ^{1}H NMR (CD_3OD) δ 6.78 (m, 1H), 4.37 (m, 1H), 3.99 (m, 1H), 3.74 (s, 3H), 3.68 (dd, J = 7.0, 4.3 Hz, 1H), 2.69 (m, 1H), 2.20 (m, 1H); ^{13}C NMR (CD_3OD) δ 168.7, 139.1, 130.2, 72.6, 68.4, 67.3, 52.3, 31.5. HRMS (FAB^+) calcd. for $C_8H_{13}O_4{}^{18}O$ ($M+H^+$) 191.0806, found 191.0809.

[5-^{18}O]-shikimic acid

To the [5-^{18}O]-shikimate (1.77 g, 9.31 mmol) in a THF-H_2O (1:1, v/v, 89 mL) solution was added NaOH (1 M, 10.2 mL, 10.2 mmol). The mixture was stirred at room temperature for 5 h under an argon atmosphere. After the solution was acidified with Dowex 50 (H^+) resin (pre-washed with THF-H_2O, 1:1, v/v), CH_3CN was evaporated in vacuum and the aqueous solution was lyophized to obtain 1.65 g [5-^{18}O]-shikimic acid as a white powder. ^{1}H NMR (D_2O) δ 6.83 (m, 1H), 4.46 (m, 1H), 4.05 (m, 1H), 3.79 (dd, J = 8.0, 4.5 Hz, 1H), 2.75 (m, 1H), 2.24 (m, 1H); ^{13}C NMR (D_2O) δ 173.1, 140.0, 132.7, 73.9, 69.4, 68.6, 33.1. HRMS (FAB^-) calcd. for $C_7H_{10}O_4{}^{18}O$ ($M-H^+$) 175.0493, found 175.0494.

[5-^{18}O]-3-dehydroshikimic acid

Into a 500 mL round bottom flask were placed [5-^{18}O]-shikimic acid (1.64 g, 9.29 mmol), α-ketoglutaric acid (2.71 g, 18.6 mmol), NH_4Cl (1.99 g, 37.2 mmol), dithiothreitol (15.4 mg, 0.1 mmol) and 10 mM potassium phosphate buffer (pH 8.0, 200 mL). The pH of the resulting solution was adjusted to 8.0 with addition of KOH (10 *N*), the solution was degassed with argon under vacuum. $NADP^+$ (71.1 mg, 0.093 mmol), shikimic dehydrogenase (820 units) and L-glutamic dehydrogenase (1640 units) were added to start the reaction. The reaction was stirred for 6 h at room temperature under an argon atmosphere and monitored by TLC (elute solvent, ethyl acetate:acetic acid:methanol:water, 5:1:1:1, v/v/v/v; R_f of DHS = 0.36, shikimic acid = 0.45). After the reaction was completed, the reaction mixture was divided into two portions, each portion (100 mL) was loaded on an anion exchange resin column (Bio-Rad AG-1-X8, acetic form, 80 mL). [5-^{18}O]-DHS was eluted with a gradient solution of H_2O (500 mL) to HOAc:H_2O (7:3, v/v, 500 mL) at 4°C. The fractions containing the product were combined and freeze-dried to give [5-^{18}O]-DHS (1.36 g, 84%) as off-white powder. ^{1}H NMR (D_2O) δ 6.76 (d, J = 3.0 Hz, 1H), 4.28 (d, J = 11.5 Hz, 1H), 4.01 (m, 1H), 3.13 (dd, J = 18.0, 5.8 Hz, 1H), 2.63 (ddd, J = 18.0, 10.0, 3.0 Hz, 1H); ^{13}C NMR (D_2O) δ 204.4, 172.1, 151.6, 133.5, 81.2, 73.5, 36.0. HRMS (FAB^+) calcd. for $C_7H_9O_4{}^{18}O$ ($M+H^+$) 175.0493, found 175.0490.

Oxidation of 3-dehydroshikimic acid to gallic acid

A solution of 3-dehydroshikimic acid (50 mg, 0.29 mmol) and $Cu(OAc)_2 \cdot H_2O$ (128 mg, 0.64 mmol) in 4 mL HOAc/H_2O (3:1) solution was stirred at 40 °C under an argon atmosphere for 24 h. After filtration, the solution was diluted with H_2O (5 mL) and

extracted with EtOAc (10 mL×3). EtOAc layer was dried over Na_2SO_4 and evaporated under reduced pressure. The resulting solid was dissolved into H_2O and purified by reverse phase HPLC. The Reverse phase HPLC purification was performed with an Alltech Econosphere C18 column (250 mm×22 mm). The product was eluted with a gradient solvent of 95:5 A:B (solvent A: H_2O containing 0.05% trifluoroacetic acid, solvent B: acetonitrile) to 70:30 A:B.

Purification of gallic acid

The fermentation broth free of cells (450 mL) was adjusted to pH 2.5 with the addition of concentrated H_2SO_4. Centrifugation at 13 700*g* for 10 min precipitated the proteins. The supernatant (420 mL) was then extracted with diethyl ether (3×250 mL). The ether layer was filtered through a short pad of silica gel and dried over Na_2SO_4. Diethyl ether was evaporated under reduced pressure and the residue was redissolved into H_2O (4 mL). Purification using reverse phase HPLC afforded gallic acid (46.2 mg, 25%) as white powder. ^1H NMR (D_2O) δ 7.13 (s, 2H); ^{13}C NMR (D_2O) δ 173.0, 147.3, 140.9, 123.8, 112.9. HRMS (FAB^-) calcd. for $C_7H_5O_5$ ($M\text{-}H^+$) 169.0137, found 169.0141; HRMS (FAB^-) calcd. for $C_7H_5O_4{}^{18}O$ ($M\text{-}H^+$) 171.0179, found 171.0181.

Air Oxidation of [5-^{18}O]-enriched 3-dehydroshikimic acid

Air oxidation of 3-dehydroshikimic acid was performed as described previously.[7] [5-^{18}O]-Enriched DHS (0.25 g, 1.45 mmol) was dissolved in 7.5 ml 1 M $Na_{1.5}H_{1.5}PO_4$ (equivmolar mixture of 1 M Na_2HPO_4 and 1 M NaH_2PO_4). The solution was adjusted to pH 6.6 then stirred open to the atmosphere at 40°C. After 48 h, the solution was acidified

to pH 3.0 and extracted with EtOAc. The organic solvent was dried over Na_2SO_4 and evaporated to dryness under reduced pressure. Purification of the crude product by the reverse phase HPLC yielded gallic acid (32.2 mg, 13.0%).

Isolation of [5-^{18}O]-enriched 3-dehydroshikimic acid from fermentation broth

Liquid-liquid continuous extraction was used isolate the [5-^{18}O]-enriched 3-dehydroshikimic acid from KL3/pRC1.55B fermentation broth. Cells were removed from the fermentation broth by centrifugation (4 200*g*, 30 min). The fermentation broth (200 mL) was adjusted to pH 2.5 with addition of concentrated H_2SO_4, centrifuge at 13 700*g* for 10 min precipitated proteins. The supernatant was extracted with EtOAc (400 mL) using a continuous extractor for 5 h. The EtOAc solution was passed through a pad of charcoal and dried over $MgSO_4$. The solution (50 mL) was taken out and concentrated to dryness to obtain 3-dehydroshikimic acid (50 mg). Oxidation with $Cu(OAc)_2$ followed by reverse phase HPLC purification isolated gallic acid (35 mg).

CHAPTER FOUR

***E. coli* NR1**

E. coli NR1 was prepared by homologous recombination of a *serA::aroB* cassette into the *serA* locus of *E. coli* AB3248.[5] Localization of the *serA* gene in plasmid pMAK705[15] followed by insertion of the *aroB* cassette into an *Eco*RI site internal to *serA* yielded plasmid pKL3.82A.[6]

Conditions for homologous recombination were based on those previously described.[15] Competent *E. coli* AB3248 was transformed with plasmid pKL3.82A. Following heat-shock treatment, cells were incubated in LB at 44 °C for 1 h and subsequently plated onto LB plates containing chloramphenicol. Plates were incubated at 44 °C for approximately 20 h before colonies appeared. The resulting cointegrates were inoculated into 5 mL of LB containing no antibiotics, and the cells were grown at 30 °C for 12 h to allow excision of the plasmid from the genome. Cultures were diluted (1:20000) in LB without antibiotics, and two more cycles of growth at 30 °C for 12 h were carried out to enrich cultures for more rapidly growing cells that had lost the temperature-sensitive replicon. Cultures were then diluted (1:20000) into LB and grown at 44 °C for 12 h to promote plasmid loss from the cells. Serial dilutions of each culture were spread onto LB plates and incubated at 30 °C overnight. The resulting colonies were screened on multiple plates to select for recombined ones. *E. coli* NR1 was isolated based on the following growth characteristics: growth on M9 containing L-histidine, L-isoleucine, L-valine, L-proline, L-arginine, L-tyrosine, L-phenylalanine, L-tryptophan, aromatic vitamins and L-serine; no growth on M9 containing L-histidine, L-isoleucine, L-valine, L-proline, L-arginine, L-tyrosine, L-phenylalanine, L-tryptophan and aromatic vitamins; and no growth on LB containing Cm. The *serA::aroB* genotype was also verified by size analysis of the DNA fragment amplified by PCR of chromosomal DNA using the following primers flanked the *serA* gene: 5'-ATGGCAAAGGTATCGCTGGA and 5'-GGAATTAGTACAGCAGACGG. Genomic DNA from *E. coli* NR1 afforded a PCR fragment of 3.0-kb where *E. coli* AB3248 genomic DNA afforded a PCR fragment of 1.3-kb.

E. coli **NR7**

Disruption of the *aroF*, *aroG* and *aroH* genes in *E. coli* KL3 proceeded as follows. Plasmid pNR7.288 was digested with *Eco*RI to liberate the insertionally inactivated *E. coli aroF* gene. The purified fragment (*aroF::Cm*^{R}) was electroporated into the hyper-recombinant *E. coli* strain JC7623.[8] Chloramphenicol resistant colonies were selected on LB plates containing 20 μg/mL chloramphenicol, and the genotype was verified by size analysis of the DNA fragment amplified by PCR of chromosomal DNA using the following primers: 5'-GGAATTCGCATAAACAGGATCGCCATCA and 5'-CTGGATCCTTAAGCCACGCGAGCCGT. The *aroF::Cm*^{R} mutation was then transferred from JC7623*aroF::Cm*^{R} to *E. coli* KL3 by P1 phage -mediated transduction to afford KL3*aroF::Cm*^{R}.

Similarly, the *aroH::Kan*^{R} DNA fragment was excised from plasmid pNR7.290 by digestion with *Xba*I and *Hin*dIII and subsequently electroporated into JC7623. The JC7623*aroH::Kan*^{R} candidates were selected on LB plates containing 50 μg/mL kanamycin. The correct genotype was verified by PCR analysis of chromosomal DNA using the following primers: 5'-TCCGTACTGCGCGTATTGAGA and 5'-AGAGGCGAGTTTTTCGACCA. P1 phage mediated transduction was employed to transfer the *aroH::Kan*^{R} mutation into KL3*aroF::Cm*^{R} to produce NR3 (KL3*aroF::Cm*^{R} *aroH::Kan*^{R}).

The *aroG* mutation was generated by the methods described by Datsenko et al.[19] Plasmid pNR7.297 was digested with *Kpn*I and *Pst*I to liberate an *aroG::Tc*^{R} DNA fragment, and the purified DNA was electrporated into NR3/pKD46. Recombinants were

selected for tetracycline resistance (5 μg/mL) at 30°C. Plasmid pKD46 was eliminated by growth at 42°C. Disruption of *aroG* was confirmed by PCR analysis using the following primers: 5'-GCAGCATTGTGCCGCCAGAA and 5'-GTGCGCTGGT-GAAATATCTT. The KL3*aroF::Cm*^{R} *aroH::Kan*^{R} *aroG::Tc*^{R} strain was designated as *E. coli* NR7.

pNR5.223.

A 0.6-kb fragment encoding the *E. coli dgoA* gene and its ribosomal binding site was amplified from *E. coli* W3110 genomic DNA using *Taq* polymerase and the following primers containing *X b a*I recognition sequences: 5'-GCTCTAGATGCAGTGGCAAACTAAACT and 5'-GACTCTAGATCATTGCACT-GCCTCTCGAT. The PCR fragment was combined with pCR2.1-TOPO to afford the 4.5-kb plasmid pNR5.223. Transcription of *dgoA* is in the same orientation as the P_{lac} promoter.

pNR6.106.

This 6.7-kb plasmid was constructed by inserting *tktA* into plasmid pNR5.223. The 2.2-kb *tktA* fragment was liberated from pNR4.230 by digestion with *Eco*RV. Plasmid pNR5.223 was digested with *Eco*RV and ligated to the *tktA* fragment to provide the plasmid pNR6.106. The *tktA* gene is transcribed in the opposite direction as *dgoA*.

pNR7.088.

A 0.6-kb fragment encoding the *E. coli dgoA* gene and its ribosomal binding site was amplified from *E. coli* W3110 genomic DNA using *Pfu* polymerase and the following primers: 5'-GACGGATCCTATAAGGAGCATCGCTCATG and 5'-GAAGCTGCAGTCATTGCACTGCCTCTCGAT. Localization of the amplified *dgoA* as a *Bam*HI-*Pst*I fragment into the corresponding sites of pTrc99A afforded the 4.8-kb plasmid pNR7.088. The *dgoA* locus is oriented in the same direction as the P_{trc} promoter.

pNR6.252.

This 5.9-kb plasmid contains the *K. pneumoniae dgoA* gene located behind the P_{tac} promoter of pJF118EH. A 0.6-kb DNA fragment encoding the *dgoA* gene and its native ribosomal binding site was amplified from *Klebsiella pneumoniae subsp. pneumoniae* genomic DNA (ATCC 700721D) using the following primers: 5'-GACAGGAATAAGGAGCATCG and 5'-GGAGGTAAACGGTACGTGGT. The resulting PCR fragment was combined with pCR2.1-TOPO to afford pNR6.223B. The 0.6-kb locus was then excised from pNR6.223B by *Eco*RI digestion and subsequently ligated with pJF118EH which had been previously treated with *Eco*RI to afford pNR6.252. The *dgoA* gene is transcribed in the same orientation as the *tac* promoter.

pNR6.300.

This 5.9-kb plasmid was created to express *Agrobacterium tumefaciens dgoA* gene from the P_{tac} promoter. The *dgoA* gene and its native ribosomal binding site was amplified from *Agrobacterium tumefaciens* genomic DNA (ATCC 33970D) using the

following primers: 5'-CAGAATTCATGCGTATTCCCTTCCCTTC and 5'-AGGGATCCTTATCCTCCGA-TGGCTGCAT. The amplified 0.63-kb DNA fragment was digested with *Eco*RI and *Bam*HI and ligated into the pJF118EH predigested with *Eco*RI and *Bam*HI to provide the plasmid pNR6.300. The *dgoA* gene is transcribed in the same orientation as the P_{tac} promoter.

pNR7.063.

This 5.9-kb plasmid was created to express the *Caulobacter cresentus* CB15 *dgoA* gene from the *tac* promoter. The *dgoA* gene and its native ribosomal binding site was amplified from *Caulobacter cresentus* CB15 genomic DNA (ATCC 19089D) using the following primers: 5'-CAGAATTCATGAACCGCACTCCCCTGC and 5'-AGGGATCCTCAGCCATGCCAGGCGGC. The amplified 0.58-kb DNA fragment was digested with *Eco*RI and *Bam*HI and ligated into pJF118EH predigested with *Eco*RI and *Bam*HI to provide the plasmid pNR7.063. The *dgoA* gene is transcribed in the same orientation as the P_{tac} promoter.

pNR7.118.

A 0.6-kb *E. coli dgoA* locus was excised from pNR7.088 by digestion with *Bam*HI and *Pst*I. Ligation of the DNA fragment to pJF118EH which was previously digested with *Bam*HI and *Pst*I afforded plasmid pNR7.118. The *dgoA* gene is transcribed in the same orientation as the P_{tac} promoter.

pNR7.120.

This 5.9-kb plasmid contained *Salmonella typhimurium dgoA* gene located behind the *tac* promoter of pJF118EH. The 0.6-kb *dgoA* open reading frame with its ribosomal binding site was amplified from *Salmonella choleraesuis subsp. choleraesuis serotype typhimurium* LT2 genomic DNA (ATCC 700720D) using the following primers: 5'-GGCTGGAATAAGGAGCATCG and 5'-GGAGGTAAACGGTACGTGGT. The resulting PCR fragment was combined with pCR2.1-TOPO vector to afford pNR6.230. The 0.6-kb *dgoA* locus was then excised from pNR6.230 by *Eco*RI digestion. Ligation to the *Eco*RI site of vector pJF118EH afforded plasmid pNR7.120. The *dgoA* gene is transcribed in the same orientation as the P_{tac} promoter.

pNR7.126.

This 6.4-kb plasmid was constructed by ligating the *aroF*^{FBR} gene with its native ribosomal binding site into the *Eco*RI site of pJF118EH. The *aroF*^{FBR} gene was amplified by PCR from pKD12.112[2] using the following primers: 5'-GGAATTCGCATAAACAG-GATCGCCATCA and 5'-CTGGATCCTTAAGCCACGCGAGCCGT. The *aroF*^{FBR} gene is transcribed in the same orientation as the P_{tac} promoter.

pNR7.288.

A 0.8-kb Cm^R gene was amplified from pSU19 using *Pfu* polymerase and the following primers: 5'-CGGGATCCTTGGCGAAAATGAGACGTTG and 5'-GCGGATCCAAATTACGCCCCGCCCT. The PCR fragment was digested with *Bam*HI and subsequently ligated into the *Bgl*II site internal to the *aroF*^{FBR} gene of pKD12.112 to

produce plasmid pNR7.288. The Cm^R gene is transcribed in the opposite orientation as $aroF^{FBR}$.

pNR7.297.

A 1.3-kb fragment containing the *aroG* gene was amplified from *E. coli* W3110 genomic DNA using the following primers: 5'-GTGGATCCTTAATCCG-TTCATAGTGTAAA and 5'-TGGGATCCATGAGAAAGCCGACTGCAA. The amplified PCR fragment was ligated into the *Bam*HI site of pSU18 to create pNR7.260. The *aroG* gene is transcribed in the opposite orientation as the P_{lac} promoter. Ligation of a Tc^R-encoding fragment of DNA obtained by digestion of vector pBR322 with *Ssp*I and *Ava*I into the *Mfe*I site internal to the *aroG* gene in pNR7.260 resulted in plasmid pNR7.297. Transcription of Tc^R is in the opposite orientation as *aroG*.

pNR7.290.

A 1.3-kb fragment encoding the *aroH* gene was amplified from *E. coli* W3110 genomic DNA using the following primers: 5'-GTTCGTCAGTGCAGGATGGA and 5'-GTTCAGGCGTGAGTTTTCTGCT. The PCR product was ligated into pCR2.1-TOPO to afford plasmid pNR7.289A. The *aroH* gene was then excised from pNR7.289A by digestion with *Hin*dIII and *Xba*I and the fragment was subsequently ligated to pTrc99A which had been digested with *Hin*dIII and *Xba*I to afford the 5.5-kb plasmid pNR7.289B. The *aroH* gene is oriented in the same direction as the P_{trc} promoter. A 1.3-kb Kan^R gene was excised from plasmid pKAD62A by digestion with *Pst*I and cloned into the *Pst*I site

internal to the *aroH* gene in pNR7.289B to afford pNR7.290. The Kan^R gene is transcribed in the opposite orientation as the *aroH*.

pNR8.074.

A 1.6-kb *serA* gene was excised from plasmid pRC1.55B[40] by digestion with *Sma*I. Ligation of the *serA* locus to plasmid pNR6.252 which had been digested with *Hin*dIII and treatment with Klenow fragment afforded the 7.5-kb plasmid pNR8.074. The *serA* gene is transcribed in the same orientation as the *dgoA*.

pNR8.075.

The 1.6-kb *serA* gene was excised from plasmid pRC1.55B by digestion with *Sma*I. Ligation of the *serA* locus to plasmid pNR7.088 which had been digested with *Hin*dIII and treatment with Klenow fragment afforded the 6.8-kb plasmid pNR8.075. The *serA* gene is transcribed in the same orientation as the *dgoA*.

pNR8.158.

This 7.5-kb plasmid was created by ligation of a 1.6-kb fragment encoding *serA* excised from pRC1.55B by digestion with *Sma*I into pNR8.140. Plasmid pNR8.140, which contains the evolved *E. coli dgoA* gene *EC03-1* located behind the P_{tac} promoter of pJF118EH, was digested with *Hin*dIII and the overhanging ends were eliminated by treatment with Klenow fragment. Subsequent ligation of *serA* into pNR8.140 afforded plasmid pNR8.158. The transcription of *serA* is in the opposite direction as the *EC03-1*.

pKP03-1serA.

This 7.5-kb plasmid was constructed by ligation of the 1.6-kb *serA* gene into pKP03-3, which contains an evolved *K. pneumoniae dgoA* gene *KP03-3* located behind the *tac* promoter of pJF118EH. Plasmid pKP03-3 was digested with *Hin*dIII, and the overhanging ends were eliminated by treatment with Klenow fragment. The *serA* locus was isolated by digestion of pRC1.55B with *Sma*I. Ligation of the *serA* gene into pKP03-3 yielded the plasmid pKP03-3serA in which the *serA* gene is transcribed in the opposite direction as the *KP03-3*.

pST04-5serA.

This 7.5-kb plasmid was constructed by ligation of the 1.6-kb *serA* gene into pST04-5, which contains an evolved *S. typhimurium dgoA* gene *ST04-5* located behind the P_{tac} promoter of pJF118EH. Plasmid pST04-5 was digested with *Hin*dIII, and the overhanging ends were eliminated by treatment with Klenow fragment. The *serA* locus was isolated by digestion of pRC1.55B with *Sma*I. Subsequent ligation of *serA* into pST04-5 created the plasmid pST04-5serA in which the *serA* gene is transcribed in the opposite direction as the *ST04-5*.

pNR8.165-4serA.

This 7.5-kb plasmid was constructed by ligation of the 1.6-kb *serA* gene into pNR8.165-4, which contains an evolved *dgoA* gene *NR8.165-4* obtained from cross-species DNA family shuffling. Plasmid pNR8.165-4 was digested with *Hin*dIII, and the overhanging ends were eliminated by treatment with Klenow fragment. Ligation of a

serA locus isolated by digestion of pRC1.55B with *Sma*I into pNR8.165-4 afforded pNR8.165-4serA. The *serA* gene is transcribed in the opposite direction as *NR8.165-4.*

pNR8.146.

A 1.6-kb fragment encoding *serA* gene was excised from pRC1.55B by digestion with *Sma*I. Ligation of the *serA* fragment into the *Sma*I site of plasmid p34e afforded the plasmid pNR8.123. The 2.2-kb fragment encoding *tktA* was isolated from plasmid pNR4.230 by digestion with *Bam*HI. Plasmid pNR8.123 was partially digested with *Bam*HI and ligated to the *tktA* fragment to provide plasmid pNR8.146. The *tktA* is transcribed in the opposite direction as the *serA*.

pNR8.180.

This 9.7-kb plasmid was constructed by inserting the *tktAserA* cassette into the plasmid pNR8.165-4 containing the evolved *dgoA* gene *NR8.165-4*. The *tktAserA* fragment was liberated from plasmid pNR8.146 by digestion with *Xba*I and treated with Klenow fragment. The *tktAserA* cassette was ligated into plasmid pNR8.165-4 that was previously digested with *Hin*dIII and treated with Klenow fragment to afford the plasmid pNR8.180.

pNR8.182.

This 8.0-kb plasmid was created by ligation of a 1.6-kb *Sma*I fragment encoding *serA* obtained from pRC1.55B into plasmid pNR7.126 previously digested with *Hin*dIII

and treated with Klenow fragment. The *serA* gene is transcribed in the opposite orientation as *aroF*^{FBR}.

pNR8.187.

This 4.0-kb plasmid was constructed by inserting the evolved *dgoA* gene *NR8.165-4* into the *Bam*HI-*Pst*I site of expression vector pQE30. The *NR8.165-4* locus was excised from plasmid pNR8.165-4 by digestion with *Bam*HI and *Pst*I. The *NR8.165-4* locus is transcribed in the same orientation as the external P_{T5} promoter.

pNR8.189.

This 5.0-kb plasmid was constructed by ligating the P_{T5}*NR8.165-4* fragment into expression vector pTrc99A. The P_{T5}*NR8.165-4* fragment was excised from plasmid pNR8.180 by digestion with *Xho*I and *Hin*dIII. Subsequent ligation of P_{T5}*NR8.165-4* into the *Sal*I-*Hin*dIII site of pTrc99A yielded the plasmid pNR8.189 in which the *NR8.165-4* is transcribed in the same orientation as *trc* promoter.

pNR8.190.

This 8.8-kb plasmid was created by ligating a *Xba*I fragment containing the *tktAserA* cassette isolated from pNR8.146 into the *Xba*I site of plasmid pNR8.189. The *tktA* gene is transcribed in the same orientation as the P_{T5}*NR8.165-4*.

Purification of KDPGal aldolase from *E. coli*

E. coli AB3248/pNR5.223 was grown in 4×1 L of LB medium containing 50 μg/mL ampicillin at 37°C. When the OD_{600} reached 0.5, IPTG was added to a final concentration of 0.2 mM. The cells were grown for an additional 6 h and collected by centrifugation (4 200*g*, 10 min). The cells were washed with 0.9% NaCl and resuspended in 20 mM KH_2PO_4, pH 6.5 containing 1 mM phenylmethyl sulfonyl fluoride (PMSF). Disruption of the cells was achieved by two passages through a French pressure cell (16000 psi). Cellular debris was removed by centrifugation (48 000*g*, 20 min). Crude cell-free lysate was first treated with 2% protamine sulfate (0.2 volumes) for 15 minutes at room temperature and then centrifuged (31 000*g*, 30 min). The supernatant was made to 25% saturation with addition of solid $(NH_4)_2SO_4$, and precipitated proteins were removed by centrifugation (31 000*g*, 30 min). The resulting supernatant was then made to 65% saturation with addition of solid $(NH_4)_2SO_4$. Proteins were precipitated by centrifugation (31 000*g*, 30 min) and resuspended into KH_2PO_4 buffer (20 mM, pH 6.5) and dialyzed overnight against the same buffer. The protein was then applied to a DEAE-cellulose (2.5 cm × 12 cm) column previously equilibrated with buffer B (20 mM KH_2PO_4, 50 mM KCl, pH 7.5). The column was washed with buffer B until the OD_{280} of the column eluent was below 0.2. The column was then eluted with a linear gradient of 300 mL of buffer B and 300 mL of buffer C (20 mM KH_2PO_4, 400 mM KCl, pH 7.5) at 4°C. Fractions containing KDPGal aldolase were concentrated, dialyzed, frozen in liquid nitrogen and stored at –80°C (87 units/mg).

In-vitro biosynthesis of 3-dehydroshikimate

D-Erythrose 4-phosphate (0.45 mL, 12 mM, pH 7.0), sodium pyruvate (0.054 mL, 100 mM, pH 7.0), $CoCl_2$ (0.027 mL, 10 mM), NAD (0.054 mL, 1 mM), 3-dehydroquinate synthase[17] (2 units) and 3-dehydroquinate dehydratase[41] (2 units) were incubated with KDPGal aldolase (100 units, 87 units/mg) at room temperature for 2 h. Protein was subsequently removed from the solution by ultrafiltration through a Millipore PM-10 membrane. 3-Dehydroshikimate was formed in 90% yield as quantified by ^1H NMR analysis.

Error-prone PCR

Random mutagenesis of the *dgoA* gene used methods described by Cadwell and Joyce[42] at a mutation rate of 6.6×10^{-3} per nucleotide. PCR was performed in a 100 μL reaction mixture containing 20 mM Tris-HCl (pH 8.4), 50 mM KCl, 7 mM $MgCl_2$, 0.5 mM $MnCl_2$, 0.2 mM dATP, 0.2 mM dGTP, 1.0 mM dCTP, 1.0 mM dTTP, 5 U *Taq* polymerase, 10 ng of *dgoA* template and 50 pmol of primers. The 0.6-kb *dgoA* template was digested from plasmid and purified by agarose gel electrophoresis. Wild-type *K. pneumoniae dgoA* template was excised from pNR6.252 by digestion with *Eco*RI, and the wild-type *E. coli dgoA* template was excised from pNR7.088 by digestion with *Bam*HI and *Pst*I. The primers used for PCR were 5'-GGAATTCGACAGGAAT-AAGGAGCATCG and 5'-GACGGATCCTCATTTCACTGCCTCTCGAT for *K. pneumoniae dgoA* and *S. typhimurium dgoAs*. And 5'-GACGGATCCTATAAGGA-GCATCGCTCATG and 5'-GAAGCTGCAGTCATTGC-ACTGCCTCTCGAT for *E. coli dgoA*. Conditions for PCR were as follows: one cycle at 94°C for 4 min followed by

22 cycles of 94°C for 45 sec, 45°C for 45 sec, 72°C for 45 sec, followed by one cycle at 25°C for 10 min.

DNA Shuffling

DNA shuffling followed the protocol of Stemmer[43] as modified by Zhao and Arnold.[44] The 0.6-kb *dgoA* gene of interest was amplified using *Pfu* polymerase under standard PCR conditions and purified through the DNA Clean and Concentrator kit. The purified PCR product was incubated with DNase I in a 50 μL reaction that contained 5 μg DNA, 50 mM Tris-HCl (pH 8.0), 10 mM $MnCl_2$, and 0.05 U of DNase I for 10 min at 15°C. The reaction was stopped by addition of 15 μL EDTA (100 mM, pH 8.0). Fragments of 20 to 80 bps were purified from a 2.0% low melting point agarose gel using DE81 ion-exchange paper as previously described.[45] The purified DNA fragments were dissolved into 30 μL sterile water.

DNA fragments were reassembled by PCR without primers in a 50 μL reaction containing 20 mM Tris-HCl (pH 8.4), 50 mM KCl, 2 mM $MgCl_2$, 0.2 mM of each dNTP, 10 μL of DE81 purified DNA fragments and 2.5 U of *Taq* polymerase. PCR was conducted as follows: one cycle at 94°C for 1 min followed by 45 cycles at 94°C for 30 sec, 50°C for 30 sec, 72°C for 30 sec, followed by one cycle at 72°C for 5 min and one cycle at 25°C for 5 min. The 0.6-kb full-length *dgoA* gene was reassembled by PCR with the same forward and reverse primers as reported in error-prone PCR section in a 100 μL reaction containing 20 mM Tris-HCl (pH 8.4), 50 mM KCl, 2 mM $MgCl_2$, 0.2 mM of each dNTP, 50 pmol of each primer, 5 U of *Taq* polymerase and 5 μL of PCR reaction solution from the PCR reaction without primers.

Directed Evolution of KDPGal Aldolase (DgoA)

Selection medium consisted of Na_2HPO_4 (6 g/L), KH_2PO_4 (3 g/L), NH_4Cl (1g/L), NaCl (0.5 g/L), glucose (4 g/L), $MgSO_4$ (0.12 g/L), thiamine (6 mg/L), L-leucine (25 mg/L), nicotinic acid (6 mg/L). IPTG was added to a final concentration of 0.2 mM or 0.05 mM as indicated. L-Phenylalanine (40 mg/L), L-tyrosine (40 mg/L) and L-tryptophan (40 mg/L) were added as indicated. Solid medium was prepared by addition of 1.5% (w/v) Difco agar to medium solution.

Directed evolution of KDPGal aldolase from *K. pneumoniae*

The native *K. pneumoniae dgoA* gene from plasmid pNR6.252 was amplified under error-prone PCR conditions with the following primers: 5'-GGAATTCGACAGGAATAAGGAGCATCG and 5'-GACGGATCCTCATTTCA-CTGCCTCTCGAT. The 0.6-kb amplification product was purified through the DNA Clean and Concentrator kit, digested with *Eco*RI and *Bam*HI, and cloned into the *Eco*RI-*Bam*HI restriction site of pJF118EH to generate the first generation plasmid library. The plasmid library was electroporated into CB734 and a library of 1×10^6 of colonies were plated out onto minimal salts plates containing L-phenylalanine and 0.2 mM IPTG. A single colony grew after 48 h incubation at 37°C, and the plasmid carrying the first generation mutant, KP01-1, was isolated from the colony. For the second generation, the *dgoA* fragment from KP01-1 was amplified under error-prone PCR conditions and cloned as described above, followed by transformation into CB734. A library of 6×10^5 colonies were spread onto minimal salts plates containing 0.2 mM IPTG. After 4 days incubation

at 37°C, fifty of the largest colonies were inoculated into a single test tube and the plasmids were isolated as a mixture, which was designated as pKP02-mix. For the third round, the mutated *dgoA* genes KP02 were shuffled and subsequently ligated with predigested plasmid pJF118EH and transformed into *E. coli* CB734. A library of 3×10^4 colonies were spread on minimal salts plates with 0.05 mM IPTG. After 3 days at 37°C, the seven largest colonies were picked and their plasmids were isolated for characterization. The seven evolved *dgoA* genes contained in these plasmids were designated *KP03-1~KP03-7.*

Directed evolution of KDPGal aldolase from *E. coli*

The *dgoA* gene encoding the native *E. coli* KDPGal aldolase in plasmid pNR7.088 was amplified under error-prone PCR conditions using the following primers: 5'-GACGGATCCTATAAGGAGCATCGCTCATG and 5'-GAAGCTGCAGTCATTG-CACTGCCTCTCGAT. The 0.6-kb *E. coli dgoA* amplification product was purified, digested with *Bam*HI and *Pst*I, and cloned into the *Bam*HI-*Pst*I restriction sites of pTrc99A to generate the first generation plasmid library. The plasmid library was transformed into competent CB734 cells by electroporation and a library of 1×10^6 colonies was spread onto minimal salts plates containing L-tyrosine, L-phenylalanine and 0.2 mM IPTG. After incubation at 37°C for 3 days, 50 of the largest colonies were inoculated into a single tube and a mixture of plasmids designated pEC01-mix was purified. For the second round of selection, the *dgoA* fragments from the pEC01-mix were amplified under error-prone PCR conditions and cloned into pTrc99A as described above. A library of 1×10^6 colonies were spread onto minimal salts plates containing 0.2

mM IPTG. After 4 days of incubation, fifty of the largest colonies were inoculated into a single tube and a mixture of plasmids designated as pEC02-mix was purified. For the third round, the mutated *dgoA* genes EC02-mix were shuffled and cloned into pTrc99A. A library of 3×10^5 colonies were spread onto minimal salts plates containing 0.05 mM IPTG. After 3 days incubation at 37°C, the seven largest colonies were selected and their plasmids were isolated for characterization. The seven evolved *dgoA* genes contained in these plasmids were designated *EC03-1~EC03-7.*

Directed evolution of KDPGal aldolase from *S. typhimurium*

The *dgoA* gene encoding the native *S. typhimurium* KDPGal aldolase in plasmid pNR7.120 was amplified under mutagenic PCR conditions using the following primers: 5'-GGAATTCGACAGGAATAAGGAGCATCG and 5'-GACGGATCCTCATTTCAC-TGCCTCTCGAT. The 0.6-kb *S. typhimurium dgoA* amplification product was digested with *Eco*RI and *Bam*HI, and cloned into the *Eco*RI-*Bam*HI restriction site of pJF118EH. A library of 1×10^5 colonies were plated on minimal salts plates with supplement of L-tyrosine and L-phenylalanine and 0.2 mM IPTG in the first round of selection. Twenty colonies were selected after incubation at 37°C for 48 h, and a plasmids mix designated pST01-mix was prepared. For the second round of mutagenesis, the *dgoA* fragment from pST01-mix was amplified under error-prone PCR conditions and cloned into pJF118EH as described previously. A library of 1×10^6 CB734 containing the second-generation plasmid were spread onto minimal salts plates containing L-phenylalanine and 0.2 mM IPTG, four colonies appeared after 3 days of incubation and a plasmid mixture designated pST02-mix was purified. For the third round of mutagenesis, the *dgoA* fragments were

amplified from pST02-mix under mutagenic PCR conditions and cloned into pJF118EH. A library of 1×10^6 colonies were spread onto minimal salts plates containing only 0.2 mM IPTG, thirty colonies were selected after 5 days of incubation at 37 °C. For the fourth round of mutagenesis, the 0.6-kb fragments encoding the mutant *dgoA* were amplified from the pST03-mix, the fragments were shuffled and cloned into pJF118EH. A library of 4×10^4 colonies were spread onto minimal salts plates containing 0.05 mM IPTG. After incubation at 37°C for 4 days, the seven most active mutants were selected and their plasmids were isolated for characterization. The seven evolved *dgoA* genes contained in these plasmids were designated as *ST04-1~ST04-7.*

DNA shuffling of the evolved *dgoA* genes *EC03-1*, *KP03-3* and *ST04-5*

Single-stranded DNA shuffling was performed following the protocol developed by Zhao and coworkers.[46] The 0.6-kb *dgoA* genes encoding the most evolved KDPGal aldolases EC03-1, KP03-3 and ST04-5 with one of the two DNA strands phosphorylated at 5'-terminus were amplified using *Pfu/Taq* (1:1) DNA polymerase under standard PCR conditions. The *dgoA* fragment *EC03-1* was amplified from plasmid pEC03-1 using the following primers: 5'-phosphate-GACGGATCCTATAAGGAGCATCGCTCATG and 5'- GAAGCTGCAGTCATTGCACTGCCTCTCGAT. THE *dgoA* fragments *KP03-3* and *ST04-5* were amplified from plasmids pKP03-3 and pST04-5, respectively, using the following primers: 5'-GACGGATCCTATAAGGAGCATCGCTCATG and 5'-phosphate-GAAGCTGCAGTCATTGCACTGCCTCTCGAT. The amplified *dgoA* fragments were purified using the DNA Clean and Concentrator kit. Single-stranded DNA templates were prepared by λ exonuclease digestion in a 50 μL reaction that

contained 3 μg PCR product, 5 μL 10× λ exonuclease reaction buffer and 10 U of λ exonuclease. The reaction mixture was incubated at 37 °C for 1 h, and the single stranded DNA products were separated by gel electrophoresis and purified using the DNA Clean and Concentrator kit. The purified three single-stranded DNA products were mixed in molar ratio of *EC03-1*:*KP03-3*:*ST04-5* (2:1:1), followed by random fragmentation with DNase I. Fragmentation of the purified PCR product with DNase I was carried out in a 50 μL reaction that contained 0.5 μg single-stranded DNA, 5 μL 50 mM Tris-HCl (pH 7.4), and 0.1 U of DNase I. The reaction was incubated at 15°C for 12 min, then was stopped by heat-shock at 90 °C for 10 min. Single-stranded DNA fragments were purified through a Centri-step-20 column (Princeton Separations, Inc.) following the manufacturer's protocol.

DNA fragments were reassembled by PCR without primers in a 20 μL reaction containing 20 mM Tris-HCl (pH 8.4), 50 mM KCl, 2 mM $MgCl_2$, 0.2 mM each of dNTP, 15 μL of purified single-stranded DNA fragments and 0.5 U of *Taq* polymerase. PCR was conducted as follows: one cycle at 96°C for 3 min followed by 40 cycles at 94°C for 30 sec, at 55°C for 1 min, at 72°C for 1 min + 5 sec/cycle, followed by one cycl at 72°C for 7 min and one cycle at 25°C for 10 min. The full-length chimeric *dgoA* genes were reassembled in a 100 μL reaction that contained 1 μL of the assembly reaction solution, 20 mM Tris-HCl (pH 8.4), 50 mM KCl, 2 mM $MgCl_2$, 0.2 mM each dNTPs, 2.5 U of *Pfu*/*Taq* (1:1) DNA polymerase mixture and 50 pmol each of the following primers: 5'-GACGGATCCTATAAGGAGCATCGCTCATG and 5'-GAAGCTGCAGTCATTGCA-CTGCCTCTCGAT. PCR reaction was conducted as follows: one cycle at 96°C for 2 min followed by 10 cycles at 94°C for 30 sec, at 55°C for 30 sec, at 72°C for 45 sec,

followed by 14 cycle at 94°C for 30 sec, at 55°C for 30 sec, at 72°C for 45 sec + 20 sec/cycle, and finally one cycle at 72°C for 7 min followed by one cycle at 25°C for 10 min.

Determination of K_m and k_{cat}

The native *E. coli dgoA* gene and the evolved *EC03-1* were amplified from plasmid pNR7.088 and pEC03-1, respectively, under standard PCR condition using the following primers: 5'-CGCGGATCCCAGTGGCAAACTAAACTC and 5'-TCTCCCGGGTCATTGCACTGCCTCTCG. The native *K. pneumoniae dgoA* gene was amplified from pNR6.252 with the following primers: 5'-CGCGGATCCATGCAGTGGCAAACTAAC and 5'- TCTCCCGGGTCATTGCACT-GCCTCTCG. The native *S. typhimurium dgoA* geneand the evolved *ST04-5* were amplified from plasmid pNR7.120 and pST04-5, respectively, with the following primers: 5'-CGCGGATCCATGCAGTGGCAAACTAAT and 5'-TCTCCCGGGTCATTGCACT-GCCTCTCG. The *NR8.164-2* was amplified from plasmid pNR8.165-2 with the following primers: 5'-CGCGGATCCATGCAGTGGCAAACTAAT and 5'-TCTCCCGGGTCATTGCA-CTGCCTCTCG. The evolved *dgoA* gene *NR8.165-4* was amplified from plasmid pNR8.165-4 using the following primers: 5'-CGCGGATCCCAGTGGCAAAC-TAAACTC and 5'-TCTCCCGGGTCATTGCACTGCCTCTCG. The evolved *dgoA* gene *NR8.16564* was amplified from plasmid pNR8.165-6 using the following primers: 5'-CGCGGATCCATGCAGTGGCAAACTAAC and 5'-TCTCCCGGGTCATTGC-ACTGCCTCTCG. The PCR products were digested with *Bam*HI and *Sma*I and ligated

into pGEX-4T-1 (Amersham Bioscience) previously digested with *Bam*HI and *Sma*I. The native and evolved KDPGal aldolases were produced as N-terminal fusions with glutathione *S*-transferase. Cultures of *E. coli* CB734 possessing the pGEX-4T-1-*dgoA* construct were cultured in 1 L of 2×YT medium containing ampicillin at 50 μg/mL. Expression was induced by addition of IPTG to a final concentration of 1 mM when the culture reached an optical density of 0.6 at 600 nm. The culture was incubated an additional 4 h prior to harvest. *E. coli* cells were recovered by centrifugation at 4 000*g* for 20 min, and the pellets were washed once with 0.9% saline and resuspended into 30 mL PBS buffer (1.4 mM NaCl, 27 mM KCl, 101 mM Na_2PO_4, 18 mM KH_2PO_4, pH 7.3) containing 1 mM PMSF (phenylmethyl sulfonyl fluoride). The cells were lysed by two passages through a French pressure cell at 16,000 psi and the cell debris was removed by centrifugation at 48 000*g* for 20 min at 4 °C. The GST-DgoA fusion protein was purified using glutathione-Sepharose 4B resin column provided in Bulk GST Purification Modules (Amersham Bioscience) following the manufacturer's protocol.

Kinetic parameters for the wild type and evolved DgoA proteins were determined by measuring DAHP formation activity with concentration of D-erythrose 4-phosphhate ranging from 50 μM to 2 mM with a constant pyruvate concentration of 2 mM using the DAHP formation assay discussed previously. The K_m and k_{cat} were derived using the non-linear regression program of Prism 4 (GraphPad Software, San Diego, CA) based on the Michaelis-Menton model equation. The resulting curves represent best-fit values for the data. The proteins were assayed side by side under identical conditions.

Reference

[1] Pittard, J.; Wallace, B. J. Distribution and function of genes concerned with aromatic biosynthesis in *Escherichia coli*. *J. Bacteriol.* **1966**, *91*, 1494-1508.

[2] Draths, K. M.; Knop, D. R.; Frost, K. M. Shikimic acid and quinic acid: replacing isolation from plant sources with recombinant biocatalysis. *J. Am Chem. Soc.* **1999**, *121*, 1603-1604.

[3] Kimata, K.; Takahashi, H.; Inada, T.; Postma, P.; Aiba, H. cAMP receptor protein-cAMP plays a crucial role in glucose-lactose diauxie by activating the major glucose transporter gene in *E. coli*. *Proc. Natl. Acad. Sci. USA* **1997**, *94*, 12914-12919.

[4] Levy, S.; Zeng, G.; Danchin, A. Cyclic AMP synthesis in *Escherichia coli* strains bearing known deletions in the *pts* phosphotransferase operon. *Gene* **1990**, *86*, 27-33.

[5] Zurawski, G.; Gunsalus, R. P.; Brown, K. D.; Yanofsky, C. Structure and regulation of *aroH*, the structural gene for the tryptophan-repressible 3-deoxy-D-*arabino*-heptulosonic acid-7-phosphate synthetase of *Escherichia coli*. *J. Mol. Biol.* **1981**, *145*, 47-73.

[6] Li, K.; Mikola, M. R.; Draths, K. M.; Worden, R. M.; Frost, J. W. Fed-batch fermentor synthesis of 3-dehydroshikimic acid using recombinant *Escherichia coli*. *Biotechnol. Bioeng.* **1999**, *64*, 61-73.

[7] Kambourakis, S.; Draths, K. M.; Frost, J. W. Synthesis of gallic acid and pyrogallol from glucose: replacing natural product isolation with microbial catalysis. *J. Am. Chem. Soc.* **2000**, *122*, 9042-9043.

[8] Horii, Z. I.; Clark, A. J. Genetic analysis of the *recF* pathway to genetic recombination in *Escherichia coli* K-12: isolation and characterization of mutants. *J. Mol. Biol.* **1973**, *80*, 327-344.

[9] Ran, N.; Knop, D. R.; Draths, K. M.; Frost, J. W. Benzene-free synthesis of hydroquinone. *J. Am. Chem. Soc.* **2001**, *123*, 10927-10934.

[10] Chandran, S. C.; Yi, J.; Draths, K. M.; von Daeniken, R.; Weber, W.; Frost, J. W. Phosphoenolpyruvate availability and the biosynthesis of shikimic acid. *Biotechnol. Prog.* **2003**, *19*, 808-814.

[11] Bartolome, B.; Jubete, Y.; Martinez, E.; de la Cruz, F. Construction and properties of a family of pACYC184-derived cloning vectors compatible with pBR322 and its derivatives. *Gene* **1991**, *102*, 75-78.

[12] Farabaugh, M. A. M.S. Thesis, Michigan State University, 1996.

[13] Fürste, J. P.; Pansegrau, W.; Frank, R.; Blocker, H.; Scholz, P.; Bagdasarian, M.; Lanka, E. Molecular cloning of the plasmid Rp4 primase region in a multi-host-range P_{tac} expression vector. *Gene* **1986**, *48*, 119-131.

[14] Amann, E.; Ochs, B.; Abel, K.-J. Tightly regulated *tac* promoter vectors useful for the expression of unfused and fused proteins in *Escherichia coli*. *Gene* **1988**, *69*, 301-315.

[15] Hamilton, C. M.; Aldea, M.; Washburn, B. K.; Babitke, P.; Kushner, S. R. New method for generation of deletions and gene replacements in *Escherichia coli*. *J. Bacteriol.* **1989**, *171*, 4617-4622.

[16] Tsang, T.; Copeland, V.; Bowden, G. T. A set of cassette cloning vectors for rapid and versatile adaptation of restriction fragments. *BioTechniques* **1991**, *10*, 330.

[17] Frost, J. W.; Bender, J. L.; Kadonaga, J. T.; Knowles, J. R. Dehydroquinate synthase: purification, cloning, and the construction of *E. coli* overproducers of the enzyme. *Biochemistry* **1984**, *23*, 4470-4475.

[18] Duncan, K.; Chaudhuri, S.; Campbell, M. S.; Coggins, J. R. The overexpression and complete amino acid sequence of *Escherichia coli* 3-dehydroquinase. *Biochem. J.* **1986**, *238*, 475-483.

[19] Datsenko, K. A.; Wanner, B. L. One-step inactivation of chromosomal genes in *Escherichia coli* K-12 using PCR products. *Proc. Natl. Acad. Sci. USA* **2000**, *97*, 6640-6645.

[20] Miller, J. H. *Experiments in Molecular Genetics*; Cold Spring Harbor Laboratory: Plainview, NY, 1972.

[21] Vogel, H. J.; Bonner, D. M. Acetylornithinase of *Escherichia coli*: partial purification and some properties. *J. Biol. Chem.* **1956**, *218*, 97-106.

[22] Donnelly, M. I.; Sanville-Millard, C.; Chatterjee; R. Method for construction of bacterial strains with increased succinic acid production. U.S. Patent 6,159,738, 2000.

[23] Sambrook, J.; Russell, D. W. *Molecular Cloning: A Laboratory Manual*; Cold Spring Harbor Laboratory Press: Cold Spring Harbor, NY, 2001.

[24] Silhavy, T. J.; Berman, M. L.; Enquist, L. W. *Experiments with Gene Fusions*; Cold Spring Harbor Laboratory: Plainview, NY, 1984.

[25] Pitcher, D. G.; Saunders, N. A.; Owen, R. J. Rapid extraction of bacterial genomic DNA with guanidium thiocyanate. *Lett. Appl. Microbiol.* **1989**, *8*, 151-156.

[26] Miller, J. H. *A Short Course in Bacterial Genetics*; Cold Spring Harbor Laboratory: Plainview, NY, 1992.

[27] Bradford, M. M. A rapid and sensitive method for the quantitation of microgram quantities of protein utilizing the principle of protein-dye binding. *Anal. Biochem.* **1976**, *72*, 248-254.

[28] Schoner, R.; Herrmann, K. M. 3-Deoxy-D-*arabinose*-heptulosonate 7-phosphate synthase. Purification, properties, and kinetics of the tyrosine-sensitive isoenzyme from *Escherichia coli*. *J. Biol. Chem.* **1976**, *251*, 5440-5447.

[29] Sieben, A. S.; Perlin, A. S.; Simpson, F. J. An improved preparative method for D-erythrose 4-phosphate. *Can. J Biochem.* **1966**, *44*, 663-9.

[30] Gollub, E.; Zalkin, H.; Sprinson, D. B. Assay for 3-deoxy-D-*arabinose*-heptulosonate acid 7-phosphate synthase. *Methods Enzymol.* **1970**, *17A*, 349-350.

[31] Chaudhuri, S.; Anton, I. A.; Coggins, J. R. Shikimate dehydrogenase from *Escherichia coli*. *Methods Enzymol.* **1987**, *142*, 315-319.

[32] Cooper, R. A. Phosphoenolpyruvate synthetase. *Methods Enzymol.* **1969**, *13*, 309-314.

[33] Cotterill, I. C.; Henderson, D. P.; Shelton, M. C.; Toone, E. J. The synthetic utility of KDPGal aldolase. *J. Mol. Catal. B: Enzym.* **1998**, *5*, 103-111.

[34] Chaudhuri, S.; Duncan, K.; Coggins, J. R. 3-Dehydroquinate dehydratase from *Escherichia coli*. *Methods Enzymol.* **1987**, *142*, 320-324.

[35] Zhu, L.; Frost, J. W. Unpublished result.

[36] Kambourakis, S. Doctorate Dissertation, Michigan State University, 2000.

[37] Yi, J.; Li, K.; Draths, K. M.; Frost, J. W. Modulation of phosphoenolpyruvate synthase expression increases shikimate pathway product yields in *E. coli*. *Biotechnol. Prog.* **2002**, *18*, 1141-1148.

[38] Montchamp, J.-L.; Tian, F.; Hart, M. E.; Frost, J. W. 2,3-Butane bisacetal protection of vicinal diequatorial diols. *J. Org. Chem.* **1996**, *61*, 3897-3899.

[39] Tan, D. S.; Foley, M. A.; Stockwell, B. R.; Shair, M. D.; Schreiber, S. L. Synthesis and preliminary evaluation of a library of polycyclic small molecules for use in chemical genetic assays. *J. Am. Chem. Soc.* **1999**, *121*, 9073-9087.

[40] Yi, J.; Draths, K. M.; Li, K.; Frost, J. W. Altered glucose transport and shikimate pathway product yields in *E. coli*. *Biotechnol. Prog.* **2003**, *19*, 1450-1459.

[41] Chaudhuri, S.; Duncan, K.; Coggins, J. R. 3-Dehydroquinate dehydratase from *Escherichia coli*. *Methods Enzymol.* **1987**, *142*, 320-4.

[42] (a) Cadwell, R. C.; Joyce, G. F. Randomization of genes by PCR mutagenesis. *PCR Methods Appl.* **1992**, *2*, 28-33. (b) Leung, D. W.; Chen, E.; Goeddel, D. V. A method for random mutagenesis of a defined DNA fragment using a modified polymerase chain reaction. *BioTechniques* **1989**, *1*, 11-15.

[43] (a) Stemmer, W. P. C. DNA shuffling by random fragmentation and reassembly: *in vitro* recombination for molecular evolution. *Proc. Natl. Acad. Sci. USA* **1994**, *91*, 10747-10751. (b) Stemmer, W. P. C. Rapid evolution of a protein *in vitro* by DNA shuffling. *Nature* **1994**, *370*, 389-391.

[44] Zhao, H.; Arnold, F. H. Optimization of shuffling for high fidelity recombination. *Nucleic Acids Res.* **1997**, *25*, 1307-1308.

[45] Dretzen, G.; Bellard, M.; Sassone-Corsi, P.; Chambon, P. A reliable method for the recovery of DNA fragments from agarose and acrylamide gels. *Anal. Biochem.* **1981**, *112*, 295-298.

[46] Zha, W.; Zhu, T.; Zhao, H. Family shuffling with single-stranded DNA. *Methods Mol. Biol.* **2003**, *231*, 91-97.